

**REGIOSELECTIVE FUNCTIONALIZATIONS OF HETEROCYCLES AND
APPLICATIONS IN METHODOLOGY, MEDICINAL CHEMISTRY, AND NATURAL
PRODUCT SYNTHESIS**

by

Kara M. George Rosenker

B.S., Juniata College, 2008

Submitted to the Graduate Faculty of
The Kenneth P. Dietrich School of Arts and Sciences in partial fulfillment
of the requirements for the degree of
Doctor of Philosophy

University of Pittsburgh

2013

UNIVERSITY OF PITTSBURGH
THE KENNETH P. DIETRICH SCHOOL OF ARTS AND SCIENCES

This dissertation was presented

by

Kara M. George Rosenker

It was defended on

November 7, 2013

and approved by

Dennis P. Curran, Distinguished Service Professor of Chemistry and Bayer Professor,

Department of Chemistry

Paul E. Floreancig, Professor, Department of Chemistry

Qiming Jane Wang, Associate Professor, Department of Pharmacology and Chemical Biology

Dissertation Advisor: Peter Wipf, Distinguished University Professor, Department of

Chemistry

Copyright © by Kara M. George Rosenker

2013

**REGIOSELECTIVE FUNCTIONALIZATIONS OF HETEROCYCLES AND
APPLICATIONS IN METHODOLOGY, MEDICINAL CHEMISTRY, AND
NATURAL PRODUCT SYNTHESIS**

Kara M. George Rosenker, PhD

University of Pittsburgh, 2013

The first two sections of this dissertation describe the development of a regioselective palladium-catalyzed cross-coupling strategy to access highly functionalized heterocycles. This method was successfully applied to 2,4,7-trichloroquinazoline, allowing for the efficient synthesis of quinazolines bearing functionality in specific positions of the heterocyclic ring. The strategy was also extended to 1,3,6-trichloroquinoline for the synthesis and scale-up of a promising 3-aminoisoquinolin-1(2*H*)-one inhibitor of the dual-specificity phosphatase Cdc25B.

The third section of this dissertation describes the design and synthesis of novel thieno[3,2-*d*]pyrimidine- and thieno[3,2-*c*]pyridine-based analogs for the inhibition of protein kinase D. A small library of analogs was prepared to assess the structure-activity relationship, and one analog was tested *in vivo*.

The fourth section of this dissertation discusses the investigation of an unusual alkene isomerization process, which occurred during the ring-closing metathesis for the preparation of a tricyclic isoindolinone scaffold. The final section of this thesis details our work towards the synthesis of *Stemona* alkaloids. In particular, a second-generation approach to sessilifoliamide was achieved.

TABLE OF CONTENTS

| | |
|--|-----------|
| ACKNOWLEDGEMENTS | XX |
| 1.0 REGIOSELECTIVE PALLADIUM-CATALYZED CROSS-COUPPLING OF 2,4,7-TRICHLOROQUINAZOLINE..... | 1 |
| 1.1 INTRODUCTION | 1 |
| 1.2 RESULTS AND DISCUSSION..... | 6 |
| 1.3 BIOLOGICAL ACTIVITY | 16 |
| 1.4 CONCLUSION..... | 17 |
| 2.0 REGIOSELECTIVE CROSS-COUPPLING REACTIONS OF 1,3,6-TRICHLOROISOQUINOLINE: SYNTHESIS OF A DUAL-SPECIFICITY PHOSPHATASE CDC25B INHIBITOR | 18 |
| 2.1 INTRODUCTION | 18 |
| 2.1.1 Biological Significance of Cdc25..... | 18 |
| 2.1.2 Synthesis and Biological Evaluation of 3-Aminoisoquinolin-1(2<i>H</i>)-one Inhibitors of Cdc25B: Previous Work in the Wipf Group..... | 21 |
| 2.2 RESULTS AND DISCUSSION..... | 27 |
| 2.2.1 Application of a Regioselective Cross-Coupling Strategy for the Synthesis and Scale-up of Lead Structure 2-15..... | 27 |
| 2.2.2 Biological Activity | 32 |

| | | |
|-------|--|----|
| 2.3 | CONCLUSION | 33 |
| 3.0 | INHIBITORS OF PROTEIN KINASE D: SYNTHESIS AND STRUCTURE- ACTIVITY RELATIONSHIP..... | 34 |
| 3.1 | INTRODUCTION | 34 |
| 3.1.1 | Protein Kinase D as a Potential New Target for Cancer Therapy | 34 |
| 3.1.2 | Chemical Inhibitors of PKD: Old and New | 36 |
| 3.1.3 | Structure-Activity Relationship of CID755673: Previous Work in the Wipf Group..... | 39 |
| 3.2 | RESULTS AND DISCUSSION..... | 44 |
| 3.2.1 | Synthesis of Thieno[3,2- <i>d</i>]pyrimidine-Based Analogs | 46 |
| 3.2.2 | Synthesis of Thieno[3,2- <i>b</i>]pyridine-Based Analogs..... | 51 |
| 3.2.3 | Biological Activity of Analogs | 54 |
| 3.3 | CONCLUSION | 57 |
| 4.0 | INVESTIGATION OF AN ALKENE ISOMERIZATION REACTION DURING THE PREPARATION OF TRICYCLIC ISOINDOLINONES..... | 59 |
| 4.1 | INTRODUCTION | 59 |
| 4.2 | RESULTS AND DISCUSSION..... | 63 |
| 4.3 | CONCLUSION | 66 |
| 5.0 | PROGRESS TOWARD THE SYNTHESIS OF SESSILIFOLIAMIDE C | 67 |
| 5.1 | INTRODUCTION | 67 |
| 5.1.1 | Introduction to <i>Stemona</i> Alkaloids..... | 67 |
| 5.1.2 | Total Synthesis of (-)-Sessilifoliamide C in the Wipf Group | 69 |
| 5.1.3 | Total Synthesis of <i>epi</i> -Sessilifoliamide J and Sessilifoliamide J..... | 73 |

| | | |
|-------|--|-----|
| 5.2 | RESULTS AND DISCUSSION..... | 76 |
| 5.2.1 | Second Generation Approach: Mitsunobu Reaction and Addition of <i>in situ</i> Generated Organoalanes to Acyliminium Ions | 76 |
| 5.2.2 | Third Generation Approach: Alkylation and Addition of <i>in situ</i> Generated Organoalanes to Acyliminium Ions Bearing a Chiral Auxiliary | 80 |
| 5.2.3 | Fourth Generation Approach: Transannular Ring Closure..... | 84 |
| 5.3 | CONCLUSION | 93 |
| 6.0 | EXPERIMENTAL PART..... | 94 |
| 6.1 | GENERAL EXPERIMENTAL..... | 94 |
| 6.2 | CHAPTER 1 EXPERIMENTAL PART | 95 |
| 6.3 | CHAPTER 2 EXPERIMENTAL PART | 123 |
| 6.4 | CHAPTER 3 EXPERIMENTAL PART | 129 |
| 6.4.1 | Thieno[3,2- <i>d</i>]pyrimidine-Based Inhibitors | 129 |
| 6.4.2 | Thieno[3,2- <i>b</i>]-Based Inhibitors | 141 |
| 6.5 | CHAPTER 4 EXPERIMENTAL PART | 149 |
| 6.6 | CHAPTER 5 EXPERIMENTAL PART | 152 |
| 6.6.1 | Second Generation Approach | 152 |
| 6.6.2 | Third Generation Approach | 164 |
| 6.6.3 | Fourth Generation Approach | 178 |
| | APPENDIX A | 184 |
| | BIBLIOGRAPHY | 201 |

LIST OF TABLES

| | |
|---|-----|
| Table 1. Selective Suzuki coupling at the C-4 position. | 8 |
| Table 2. Selective Suzuki coupling at the C-2 position. | 8 |
| Table 3. Selective Suzuki reaction at the C-2 position. | 13 |
| Table 4. Palladium-catalyzed, copper(I)-mediated coupling at the C-4 position. | 14 |
| Table 5. Suzuki reaction at the C-7 position. | 15 |
| Table 6. Synthesis of 3-amino-1,2-dihydro-1-isoquinolinone with various amines and the <i>in vitro</i> inhibitory activity against Cdc25B. | 22 |
| Table 7. <i>In vitro</i> Cdc25B inhibitory activity of C-6 functionalized isoquinolinone analogs. | 27 |
| Table 8. PKD inhibitory activity of CID755673 and zone I analogs. | 40 |
| Table 9. PKD inhibitory activity of CID755673 and zone II-IV analogs. | 41 |
| Table 10. PKD inhibitory activity of kb-NB142-70 and zone I-IV analogs. | 43 |
| Table 11. Chemical structures and PKD1 inhibitory activities of the thieno[3,2- <i>d</i>]pyrimidine and thieno[3,2- <i>b</i>] analogs. | 55 |
| Table 12. Optimization of the macrolactamization of 5-83 to provide lactam 5-82 | 88 |
| Table 13. Iodocyclization of lactam 5-82 | 90 |
| Table 14. Optimization of the intramolecular nucleophilic cyclization of β -alkynylamide 5-82 | 92 |
| Table 15. Crystal data and structure refinement for 1-24b | 185 |

| | |
|--|-----|
| Table 16. Atomic coordinates ($\times 10^4$) and equivalent isotropic displacement parameters ($\text{\AA}^2 \times 10^3$) for 1-24b | 185 |
| Table 17. Bond lengths (\AA) and angles ($^\circ$) for 1-24b | 186 |
| Table 18. Anisotropic displacement parameters ($\text{\AA}^2 \times 10^3$) for 1-24b | 190 |
| Table 19. Hydrogen coordinates ($\times 10^4$) and isotropic displacement parameters ($\text{\AA}^2 \times 10^3$) for 1-24b | 190 |
| Table 20. Crystal data and structure refinement for kmg-NB4-23 | 191 |
| Table 21. Atomic coordinates ($\times 10^4$) and equivalent isotropic displacement parameters ($\text{\AA}^2 \times 10^3$) for kmg-NB4-23 | 192 |
| Table 22. Bond lengths (\AA) and angles ($^\circ$) for kmg-NB4-23 | 192 |
| Table 23. Anisotropic displacement parameters ($\text{\AA}^2 \times 10^3$) for kmg-NB4-23 | 194 |
| Table 24. Hydrogen coordinates ($\times 10^4$) and isotropic displacement parameters ($\text{\AA}^2 \times 10^3$) for kmg-NB4-23 | 195 |
| Table 25. Sample and crystal data for 5-82 | 195 |
| Table 26. Data collection and structure refinement for 5-82 | 196 |
| Table 27. Atomic coordinates and equivalent isotropic atomic displacement parameters (\AA^2) for 5-82 | 196 |
| Table 28. Bond lengths (\AA) for 5-82 | 197 |
| Table 29. Bond angles ($^\circ$) for 5-82 | 198 |
| Table 30. Torsion angles ($^\circ$) for 5-82 | 199 |
| Table 31. Anisotropic atomic displacement parameters (\AA^2) for 5-82 | 199 |
| Table 32. Hydrogen atomic coordinates and isotropic atomic displacement parameters (\AA^2) for 5-82 | 200 |

LIST OF FIGURES

| | |
|---|----|
| Figure 1. Quinazoline derivatives designed as LXR modulators. | 2 |
| Figure 2. Quinazoline-based drugs approved for clinical use..... | 2 |
| Figure 3. Carbon-chlorine BDE's of quinazoline using G3B3 (bold) and B3LYP (parentheses); energies in kcal/mol. | 6 |
| Figure 4. X-Ray crystal structure of 1-24b (Appendix A.1)..... | 16 |
| Figure 5. CDC25 phosphatases control mammalian cell-cycle progression..... | 19 |
| Figure 6. Known inhibitors of Cdc25 phosphatases. | 20 |
| Figure 7. HTS hit for Cdc25B inhibition. | 21 |
| Figure 8. Chemical structures of phosphine ligands used for the Buchwald-Hartwig amination reactions of 2-20 | 29 |
| Figure 9. Major PKD signaling pathways..... | 35 |
| Figure 10. PKD inhibitors staurosporine, Gö6976 , K252a , and resveratrol; and PKD activator suramin..... | 37 |
| Figure 11. Recent PKD inhibitors from the research and patent literature..... | 39 |
| Figure 12. Major structural zones dissected for SAR analysis. | 40 |
| Figure 13. Chemical structure lead compound kb-NB142-70 and four analogs. | 44 |
| Figure 14. Zone I modification of the lead compounds to install a pyrimidine moiety. | 45 |

| | |
|---|-----|
| Figure 15. Effect of kmg-NB4-23 (KMG) on PC3 s.c. tumor xenografts in nude mice and the structure of PX-866 | 57 |
| Figure 16. Isoindolinone natural products and pharmaceuticals. | 60 |
| Figure 17. Relative energies of alkene isomers based on RB3LYP/6-311G* calculations with MacSpartan '06. | 62 |
| Figure 18. Classification of <i>Stemona</i> alkaloids into eight groups. | 68 |
| Figure 19. X-Ray crystal structure of 1-24b | 184 |
| Figure 20. X-Ray crystal structure of kmg-NB4-23 | 191 |
| Figure 21. X-Ray structure of 5-82 | 195 |

LIST OF SCHEMES

| | |
|---|----|
| Scheme 1. Regioselective palladium-catalyzed alkylations of 2,4-dichloroquinazoline (1-6) with trialkylalanes. | 3 |
| Scheme 2. Regioselective Sonagashira cross-coupling reactions of 2,4-dichloroquinazoline (1-6). | 3 |
| Scheme 3. Stille coupling of 2,4-dichloroquinazoline 1-10 with arylstannane 1-12 | 3 |
| Scheme 4. Regioselective palladium-catalyzed alkylation of 6-bromo-2,4-dichloroquinazoline (1-13) with alkylalanes. | 4 |
| Scheme 5. Sonagashira cross-coupling reaction of 6-bromo-2,4-dichloroquinazoline (1-13). | 4 |
| Scheme 6. Regioselective Suzuki-Miyaura cross-coupling reactions of 4,7-dichloro-2-(2-methylprop-1-enyl)-6-nitroquinazoline (1-18). | 5 |
| Scheme 7. Selective cross-coupling strategy to minimize synthetic steps and maximize diversity in quinazolines 1-24 | 7 |
| Scheme 8. Alternative strategy to selective cross-couplings reactions. | 9 |
| Scheme 9. Synthesis of thioether 1-26a | 10 |
| Scheme 10. Alternative route to selective cross-coupling reactions. | 10 |
| Scheme 11. Mechanism of palladium-catalyzed, copper-mediated cross-coupling of heteroaryl thioethers with boronic acids. | 11 |
| Scheme 12. Synthesis of fused tetracyclic analog 2-8 | 23 |

| | |
|--|----|
| Scheme 13. Synthesis of 4-substituted isoquinolinone 2-10 | 24 |
| Scheme 14. Initial synthetic strategies to functionalize the 6-position of isoquinolinone..... | 25 |
| Scheme 15. Synthetic strategy to obtain functionalized isoquinolines 2-18a-g (n.d.= not determined). | 26 |
| Scheme 16. Initial synthetic route for the synthesis of inhibitor 2-15 | 28 |
| Scheme 17. Attempted synthesis of thioether 2-21 | 29 |
| Scheme 18. Alternative route to 2-15 | 30 |
| Scheme 19. Attempted synthesis of isoquinolinone 2-22 | 30 |
| Scheme 20. Regioselective palladium-catalyzed cross-coupling strategy to synthesize 2-15 | 32 |
| Scheme 21. Bioisosteric replacement of aromatic CH with N to yield clinical candidate 3-5 | 45 |
| Scheme 22. Retrosynthetic approach to thieno[3,2- <i>d</i>]pyrimidine analogs 3-6 | 46 |
| Scheme 23. Attempted synthesis of 3-16 | 47 |
| Scheme 24. Regioselective metalation at positions C-6 and C-7. | 48 |
| Scheme 25. Synthesis of thieno[3,2- <i>d</i>]pyrimidine analog kmg-NB4-23 | 49 |
| Scheme 26. Synthesis of thieno[3,2- <i>d</i>]pyrimidine analogs kmg-NB4-69A and kmg-NB4-77A3 | 50 |
| Scheme 27. Conversion of kmg-NB4-69A/77A3 to 3-22 in the presence of MeOH..... | 50 |
| Scheme 28. Synthesis of C-4 protected thieno[3,2- <i>d</i>]pyrimidine analogs kmg-NB5-13C and kmg-NB5-15A | 51 |
| Scheme 29. Retrosynthetic strategy to access thieno[3,2- <i>b</i>]pyridine analogs 3-23 | 52 |
| Scheme 30. Attempted synthesis of thieno[3,2- <i>b</i>]pyridine analogs. | 52 |
| Scheme 31. Revised synthetic approach to thieno[3,2- <i>b</i>]pyridine analogs. | 53 |
| Scheme 32. Revised synthesis of thieno[3,2- <i>b</i>]pyridine analogs. | 54 |

| | |
|--|----|
| Scheme 33. Wipf group approach to isoindolinones and strategy for the preparation of a library of tricyclic isoindolinone amino alcohols (4-5)..... | 60 |
| Scheme 34. Synthesis of isomerized azepinoisoindolinone 4-10 and epoxide 4-11 | 61 |
| Scheme 35. Ring-closing metathesis of diene 4-8 in the absence of Ti(O <i>i</i> -Pr) ₄ and hydroxyepoxide 4-17 | 63 |
| Scheme 36. Preparation and RCM reaction in the presence of Ti(O <i>i</i> -Pr) ₄ of bis-terminal diene 4-18 | 63 |
| Scheme 37. RCM reaction in the absence of Ti(O <i>i</i> -Pr) ₄ of bis-terminal diene 4-18 and epoxide formation..... | 64 |
| Scheme 38. RCM reaction of 4-8 in the presence of Ti(O <i>i</i> -Pr) ₄ under an atmosphere of ethylene. | 65 |
| Scheme 39. Oxidative cyclization of Cbz-L-tyrosine and the conserved hydroindole core found in stenine and tuberostemonine..... | 69 |
| Scheme 40. Biosynthetic hypothesis based on the structural similarities between parvistemoline and sessilifoliamides. | 70 |
| Scheme 41. Retrosynthetic approach for sessilifoliamide C. | 71 |
| Scheme 42. Preparation of vinylpyrrolidinone 5-19 | 71 |
| Scheme 43. Preparation of iodide fragment 5-15 | 72 |
| Scheme 44. Synthesis of key intermediate 5-12 | 72 |
| Scheme 45. Synthesis of sessilifoliamide C via a novel [3,3]-sigmatropic Claisen rearrangement strategy..... | 73 |
| Scheme 46. Asymmetric total synthesis of 9- <i>epi</i> -sessilifoliamide J and (–)-sessilifoliamide J. . | 74 |
| Scheme 47. Total synthesis of (–)-sessilifoliamide J..... | 75 |

| | |
|---|----|
| Scheme 48. Second-generation retrosynthetic analysis to intermediate 5-12 | 76 |
| Scheme 49. Catalytic enantioselective Mukaiyama aldol additions using chiral Ti(IV) complex 5-49 | 77 |
| Scheme 50. Racemic synthesis of alcohol 5-51 | 78 |
| Scheme 51. Addition of hexenylalane to the <i>in situ</i> generated iminium ion of 5-52 | 79 |
| Scheme 52. Vinyl alane addition to 5-55 | 79 |
| Scheme 53. Revised retrosynthesis of key intermediate 5-12 using a chiral auxiliary (R*). | 81 |
| Scheme 54. Model system for the asymmetric vinyl alane addition to pivaloate 5-62 | 81 |
| Scheme 55. Synthesis of chiral <i>N</i> -acyliminium precursor 5-69 and vinyl alane addition. | 82 |
| Scheme 56. Synthesis of chiral <i>N</i> -acyliminium precursor 5-74 and vinyl alane addition. | 83 |
| Scheme 57. Chiral induction via a chelated <i>N</i> -acyliminium ion of 5-78 | 84 |
| Scheme 58. Revised retrosynthetic strategy featuring a novel transannular ring closure to construct the pyrrolo[1,2- <i>a</i>]azepine core. | 85 |
| Scheme 59. Synthesis of requisite amino acid 5-83 | 86 |
| Scheme 60. Lactamization of 5-83 and the X-ray structure of 5-82 | 87 |
| Scheme 61. Electrophilic cyclization of acyclic alkynylamides to access γ -iodo lactams..... | 89 |
| Scheme 62. Gold-catalyzed cyclization reaction of bispropargylic amide 5-96 | 90 |
| Scheme 63. Electrophilic cyclization of 5-82 | 91 |
| Scheme 64. Intramolecular cyclization of β -alkynylamides to γ -alkylidene- γ -butyrolactams.... | 91 |
| Scheme 65. Attempts to functionalize a mixture of enamides 5-101 and 5-98 | 93 |

LIST OF ABBREVIATIONS

| | | |
|--------------------|-------|--|
| Ac | | acetyl |
| ATR | | attenuated total reflectance |
| aq | | aqueous |
| BDE | | bond dissociation energy |
| BINAP | | 2,2'bis(diphenylphosphino)-1,1'-binaphthyl |
| BRSM | | based on recovered starting material |
| Bn | | benzyl |
| Boc | | <i>tert</i> -butyloxycarbonyl |
| BOP | | (benzotriazol-1-yloxy)tris(dimethylamino)phosphonium hexafluorophosphate |
| Bu | | butyl |
| calcd | | calculated |
| CaMK | | calcium/calmodulin-dependent kinase |
| cat | | catalytic |
| Cbz | | benzyloxycarbonyl |
| Cdc25 | | cell division cycle 25 |
| CDK | | cyclin-dependent kinase |
| conc | | concentrated |
| Cp | | cyclopentadienyl |
| CuTC | | copper(I) thiophene-2-carboxylate |
| Cy | | cyclohexyl |
| CyPF- <i>t</i> -Bu | | (2 <i>R</i>)-1[(1 <i>R</i>)-[bis(1,1-dimethylethyl)phosphine]ethyl]-2-(dicyclohexylphosphino)ferrocene |
| DAG | | diacylglycerol |

dba.....dibenzylideneacetone
 DBADdi-*tert*-butyl azodicarboxylate
 DBU1,8-diazabicyclo[5.4.0]undec-7-ene
 DCCdicyclohexylcarbodiimide
 DIPEA.....*N,N*-diisopropylethylamine
 DMADdimethyl acetylenedicarboxylate
 DMAP4-dimethylaminopyridine
 DMSOdimethylsulfoxide
 DME.....1,2-dimethoxyethane
 DMF*N,N*-dimethylformamide
 DMPDess-Martin periodinane
 DPPAdiphenylphosphoryl azide
 dppp.....1,3-bis(diphenylphosphino)propane
dr.....diastereomeric ratio
 EDCI1-ethyl-3-(3-dimethylaminopropyl) carbodiimide
eeenantiomeric excess
 EI.....electron impact
 ESI.....electrospray ionization
 Et.....ethyl
 equivequivalent(s)
erenantiomeric ratio
 FMOfrontier molecular orbital
 FDPPpentafluorophenyl diphenylphosphinate
 HATU1-[bis(dimethylamino)methylene]-1*H*-1,2,3-triazolo[4,5-*b*]pyridinium 3-oxid
 hexafluorophosphate
 HOAt.....1-hydroxy-7-azabenzotriazole
 HOBt.....1-hydroxybenzotriazole
 HPLChigh performance liquid chromatography
 HRMShigh resolution mass spectroscopy
 HWEHorner-Wadsworth-Emmons
 IR.....infrared spectroscopy

kcalkilocalorie
KHMDSpotassium bis(trimethylsilyl)amide
LAHlithium aluminum hydride
LUMO.....lowest unoccupied molecular orbital
m-CPBA.....3-chloroperoxybenzoic acid
Memethyl
MOM.....methoxymethyl
mpmelting point
NMRnuclear magnetic resonance
NMO*N*-methylmorpholine oxide
MWI.....microwave irradiation
PGprotecting group
PHpleckstrin homology
PKC.....protein kinase C
PKD.....protein kinase D
p-Tol.....*para*-toluene
PTSA.....*para*-toluene sulfonic acid
quant.....quantitative
RCM.....ring closing metathesis
rtroom temperature
SAR.....structure-activity relationship
satsaturated
SFCsupercritical fluid chromatography
SM.....starting material
TBAFtetrabutylammonium fluoride
TBAItetrabutylammonium iodide
TBDPS*tert*-butyldiphenylsilyl
TBS*tert*-butyldimethylsilyl
TEA.....triethylamine
TFA.....trifluoroacetic acid
TGN*trans* golgi network

THFtetrahydrofuran
TLCthin layer chromatography
TMP2,2,6,6-tetramethylpiperidine
Ts.....*p*-toluenesulfonyl
Xantphos4,5-bis(diphenylphosphino)-9,9-dimethylxanthene

ACKNOWLEDGEMENTS

First and foremost I would like to thank Professor Peter Wipf for providing me with the opportunity to work in his laboratory. I am very grateful for the invaluable training that I have received during my time in his group. I would also like to express my appreciation to Professors Dennis Curran, Paul Floreancig, Q. Jane Wang, and Xinyu Liu for serving on my various committees. Additionally, I would like to acknowledge the National Institutes of Health, University of Pittsburgh, and ACS Division of Medicinal Chemistry for their financial support.

I would also like to thank all of the Wipf group members, both past and present, for their support and friendships over the years. In particular, I would like to thank Chenbo Wang for guiding me during my early years of graduate school and remaining a source of advice and encouragement throughout my graduate career.

I would also like to express my gratitude to my family for their unconditional love and support during my graduate studies. Lastly, I would like to thank my husband, Christopher Rosenker, for his unwavering encouragement, advice, and knowledge both in life and chemistry.

1.0 REGIOSELECTIVE PALLADIUM-CATALYZED CROSS-COUPLING OF 2,4,7-TRICHLOROQUINAZOLINE

1.1 INTRODUCTION

Palladium-catalyzed cross-coupling reactions represent a powerful and popular method for the formation of highly substituted heterocycles.¹ The regioselective activation of polyhalogenated heteroaromatics in cross-coupling reactions has been extensively studied¹ and provides a versatile method for incorporating substituents in specific positions of the heterocyclic scaffold. One heterocyclic scaffold in particular, quinazoline, is a component of a variety of biologically active compounds, including potent tyrosine kinase inhibitors,² antibacterial,³ and anticancer agents.⁴ Tri-substituted quinazoline derivatives **1-1** and **1-2** (Figure 1) have been prepared as part of a series of liver X receptor (LXR) modulators for the treatment of atherosclerosis.⁵ Several approved drugs also contain the quinazoline moiety⁶ including Erlotinib (**1-3**),⁷ used to treat several types of tumors, Gefitinib (**1-4**),⁸ an epidermal growth factor receptor inhibitor approved for the treatment of non-small cell lung cancer, and Prazosin (**1-5**),⁹ an α -adrenergic receptor blocker (Figure 2).

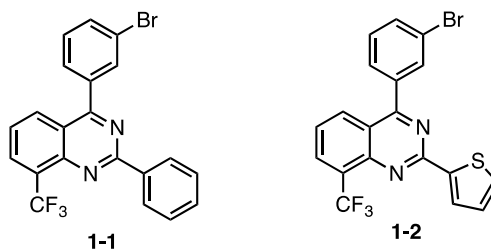


Figure 1. Quinazoline derivatives designed as LXR modulators.

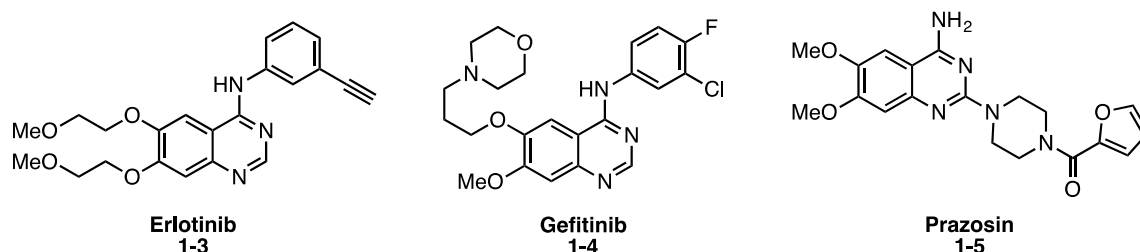
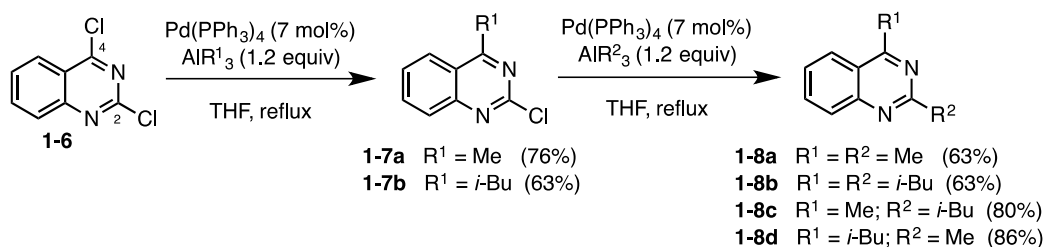
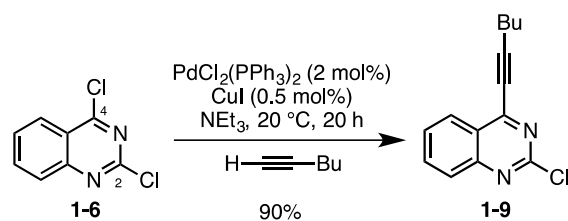


Figure 2. Quinazoline-based drugs approved for clinical use.

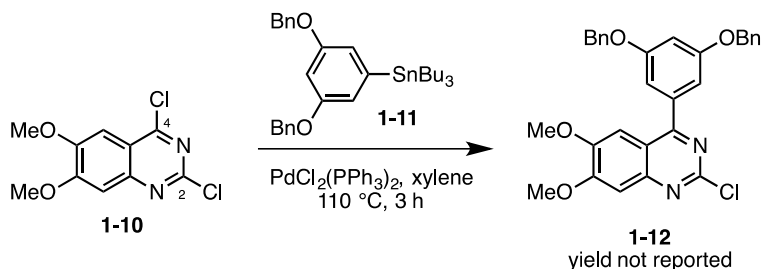
The regioselectivity for palladium-catalyzed alkylation¹⁰, alkynylation,¹¹ and arylation¹² of 2,4-dichloroquinazolines **1-6** and **1-10** have been explored. Selective Stille coupling¹³ of the C-4 position using trimethyl- or triisobutylalanes in the presence of catalytic amounts of Pd(PPh)₄ was reported to proceed in good yields, with only a small amount (<10%) of the 2,4-dialkylated quinazoline being detected (Scheme 1).¹⁰ Subjecting C-4 alkylated products **1-7a** and **1-7b** to a second equivalent of either alane worked equally well and provided the corresponding bis-coupled products **1-8a-d** (Scheme 1).¹⁰ Analogously, the palladium-catalyzed Sonagashira cross-coupling reaction of **1-6** gave excellent selectivity for the C-4 coupled product **1-9** (Scheme 2).¹¹ Although the Stille coupling of 2,4-dichloroquinazoline **1-10** with arylstannane **1-11** has been reported to provide C-2 coupled product **1-12**, the yields and selectivity are not disclosed (Scheme 3).¹²



Scheme 1. Regioselective palladium-catalyzed alkylations of 2,4-dichloroquinazoline (**1-6**) with trialkylalanes.¹⁰



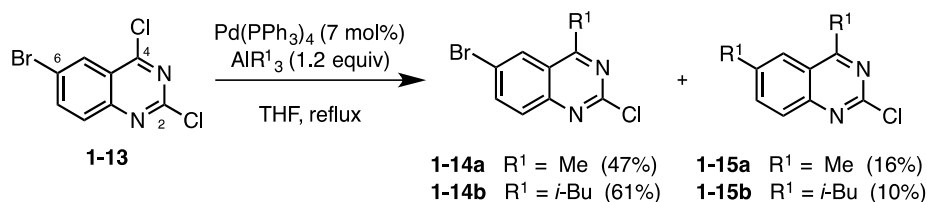
Scheme 2. Regioselective Sonagashira cross-coupling reactions of 2,4-dichloroquinazoline (**1-6**).¹¹



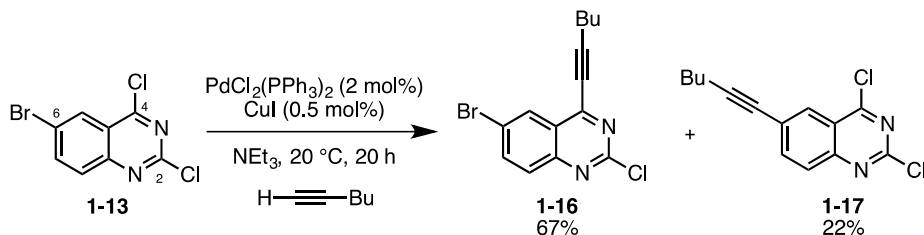
Scheme 3. Stille coupling of 2,4-dichloroquinazoline **1-10** with arylstannane **1-11**.¹²

In addition to selective couplings involving 2,4-dichloroquinazolines (**1-6** and **1-10**), attempts to achieve monosubstitution of more highly halogenated quinazolines under palladium-catalyzed conditions have also been explored. Alkylation of 6-bromo-2,4-dichloroquinazoline (**1-13**) using trimethylalane, in a similar manner to that reported in Scheme 1, provided a 3:1 mixture of **1-14a** and **1-15a**, with the major product resulting from substitution at the C-4 position (Scheme 4).^{10b} An improved selectivity of 6:1 in favor of monoalkylated product **1-14b**

was observed when triisobutyl alane was employed. The Sonagashira cross-coupling reactions of 6-bromo-2,4-dichloroquinazoline (**1-13**) was also plagued by a lack of regioselectivity (Scheme 5), yielding a 3:1 mixture of C-4 and C-6 monosubstituted products **1-16** and **1-17**, respectively.¹¹ Prior to the disclosure of our work discussed in this thesis, the sequential Suzuki-Miyaura cross-coupling¹⁴ of polyhalogenated quinazolines had not been disclosed.



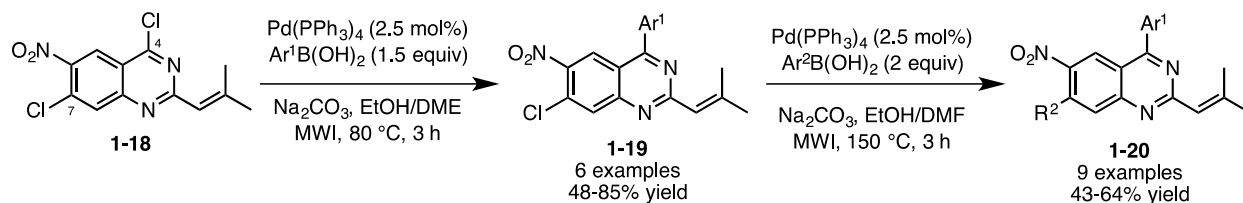
Scheme 4. Regioselective palladium-catalyzed alkylation of 6-bromo-2,4-dichloroquinazoline (**1-13**) with alkylalanes.^{10b}



Scheme 5. Sonagashira cross-coupling reaction of 6-bromo-2,4-dichloroquinazoline (**1-13**).¹¹

Since the 2010 publication of our work detailed in this thesis,¹⁵ the regioselective Suzuki-Miyaura reaction of 4,7-dichloroquinazoline **1-18** was reported (Scheme 6).¹⁶ Vanelle and co-workers achieved selective cross-coupling of the C-4 position by using 1.5 equivalents of boronic acid in the presence of $\text{Pd(PPh}_3)_4$. The reactions were carried out at 80 °C under microwave irradiation with DME/EtOH (9:1) as a solvent to furnish monocoupled products **1-19**. The solubility properties of **1-19** under their original conditions prevented efficient coupling at

C-7. The solvent mixture was changed to DMF/EtOH (9:1) resulting in the successful coupling **1-19** to provide 4,7-diarylquinazolines **1-20** in modest to good yields (Scheme 6).



Scheme 6. Regioselective Suzuki-Miyaura cross-coupling reactions of 4,7-dichloro-2-(2-methylprop-1-enyl)-6-nitroquinazoline (**1-18**).¹⁶

The regioselectivity of the abovementioned palladium-catalyzed cross-coupling reactions of polyhalogenated quinazoline is well supported by computational studies by Houk and co-workers.¹⁷ In general, the oxidative insertion step is considered to be the selectivity determining step in the overall cross-coupling process. The factors controlling the regioselectivity during the oxidative addition include both the energy to distort reactants to the transition state geometry, a factor related to the bond dissociation energy (BDE), and the interaction between these distorted reactants, which is governed by the frontier molecular orbital (FMO) interactions.¹⁷⁻¹⁸ In order to develop a predictive model for determining the reactivity in sequential cross-coupling reactions, the C-Cl BDEs of quinazoline were explored using B3LYP¹⁹ and G3B3²⁰ calculations (Figure 3).¹⁷

It was determined that the lowest carbon-chlorine BDE exists at the C-4 position with a value of 92 kcal/mol, followed by the C-2 position at 95 kcal/mol (Figure 3). All of the positions on the phenyl ring were reported to have similar BDEs and were 5-6 kcal/mol higher in energy than the BDE of the C-2 position. Based on these calculated BDEs, the trend for reactivity, and hence regioselectivity, was shown to be in good agreement with the abovementioned

experimental data (Scheme 1–Scheme 6), supporting the utility of BDE calculations as a useful tool for predicting the relative reactivity of polyhalogenated quinazolines. The exception to this trend is the Sonagashira coupling of 6-bromo-2,4-dichloroquinazoline **1-13** (Scheme 5) where the BDE of the carbon-chlorine bond at the C-4 position (85 kcal/mol) is actually larger than that of the carbon-bromine bond at the C-6 position (83 kcal/mol). The selectivity of this coupling reaction is thought to be governed by the FMO interactions between the distorted reactants, which evidently favors coupling with the stronger carbon-chlorine bond at position C-4.¹⁷

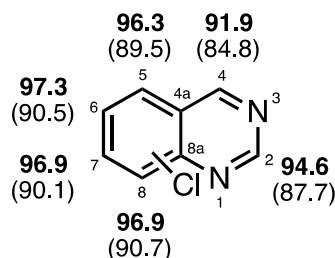
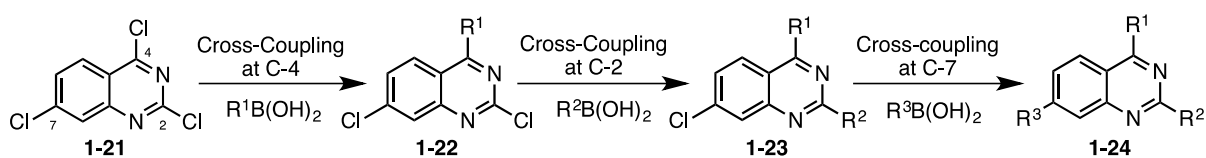


Figure 3. Carbon-chlorine BDE's of quinazoline using G3B3 (bold) and B3LYP (parentheses); energies in kcal/mol.¹⁷

1.2 RESULTS AND DISCUSSION

Our initial goal for this project was to achieve regioselective cross-coupling of 2,4,7-trichloroquinazoline **1-21**²¹ by consecutive Suzuki-Miyaura reactions (Scheme 7). At the outset of this project, the regioselective Suzuki-Miyaura cross-coupling reactions of polyhalogenated quinazolines had not been reported, although the analogous reactions of the polyhalogenated parent heterocycle, pyrimidine, had been extensively studied.¹ Based upon the calculated carbon-chlorine BDEs of quinazoline (Figure 3),¹⁷ we envisioned the first coupling reaction to

take place at the most electrophilic C-4 position, followed by substitutions at the C-2 and C-7 positions, respectively. Initial coupling reactions at the C-4 position under standard Suzuki-Miyaura coupling conditions provided the desired products **1-22a-c** in good yields (Table 1, entries 1-3). However, the reactions alkyl-substituted boronic acids in the C-4 coupling reactions proved to be low-yielding due to competitive hydrolysis at that site (Table 1, entries 4 and 5). Nonetheless, subsequent coupling at the C-2 position under both conventional heating and microwave heating provided the desired bis-coupled products **1-23a-e** in good to modest yields (Table 2). It was evident from these data that attenuation of the reactivity of position C-4 was required to achieve selective coupling of C-4 with optimal yields while avoiding hydrolysis.



Scheme 7. Selective cross-coupling strategy to minimize synthetic steps and maximize diversity in quinazolines **1-24**.

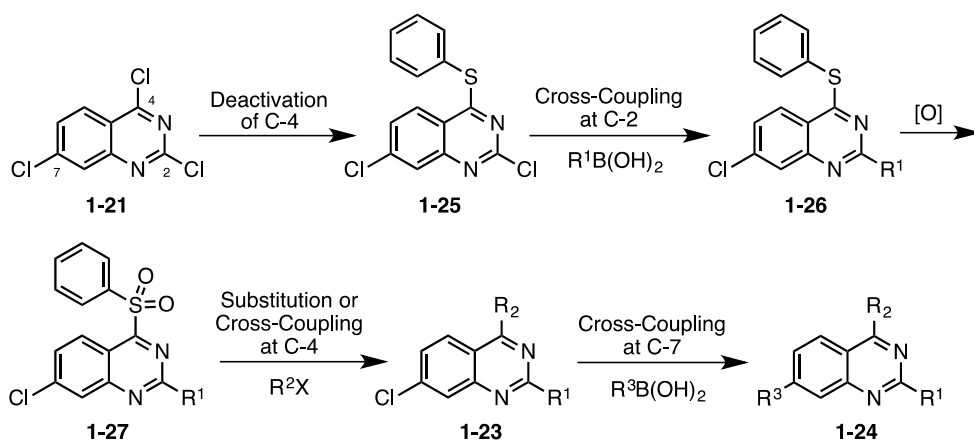
Table 1. Selective Suzuki coupling at the C-4 position.

| entry | R ¹ | temp, time | yield | compound |
|-------|----------------|--------------|-------|--------------|
| 1 | | 80 °C, 16 h | 86% | 1-22a |
| 2 | | reflux, 18 h | 70% | 1-22b |
| 3 | | reflux, 12 h | 71% | 1-22c |
| 4 | | 80 °C, 36 h | 49% | 1-22d |
| 5 | | reflux, 21 h | 33% | 1-22e |

Table 2. Selective Suzuki coupling at the C-2 position.

| entry | R ¹ | R ² | temp, time | yield | compound |
|-------|----------------|----------------|---------------------|-------|--------------|
| 1 | | | reflux, 22 h | 85% | 1-23a |
| 2 | | | reflux, 15 h | 61% | 1-23b |
| 3 | | | 75 °C, 24 h | 45% | 1-23c |
| 4 | | | MWI, 130 °C, 30 min | 79% | 1-23a |
| 5 | | | MWI, 120 °C, 40 min | 75% | 1-23d |

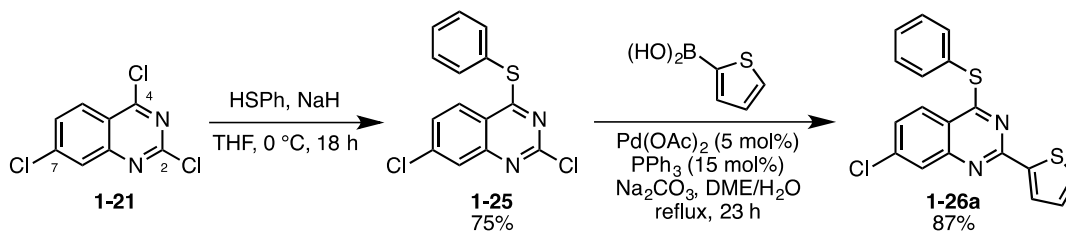
To circumvent the problem with competitive C-4 hydrolysis, the reactions were carried out under anhydrous conditions. Unfortunately, the reaction was either sluggish or did not progress under these conditions. At this stage a new route was designed in which the C-4 position would be temporarily deactivated by a thioether, followed by a regioselective cross-coupling at the C-2 position (Scheme 8). The C-4 position would then be functionalized via sulfur oxidation and either substitution or cross-coupling of the resulting sulfone to provide compounds of type **1-23**. A final Suzuki reaction at the remaining C-7 position would provide tri-functionalized quinazoline target compounds **1-24**.



Scheme 8. Alternative strategy to selective cross-couplings reactions.

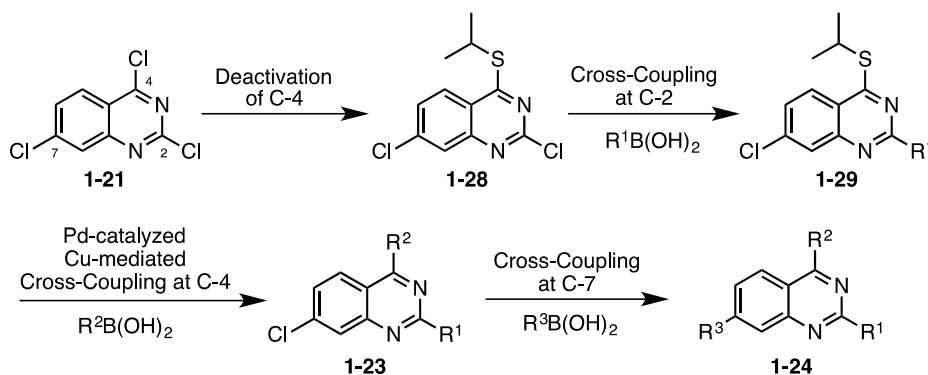
Thioether **1-25** was accessed by treatment of **1-21**²¹ with 1.05 equiv of thiophenol and NaH (Scheme 9). Substitution occurred exclusively at the more electrophilic C-4 position. Subsequent regioselective C-2 cross-coupling of **1-25** with thiophene-2-boronic acid proceeded in good yield in the presence of 5 mol% Pd(OAc)₂ and 15 mol% PPh₃ in refluxing DME to furnish product **1-26a**. Attempts to oxidize **1-26a** to the corresponding sulfone using Oxone® gave no reaction, while treatment with *m*-CPBA or Na₂WO₄ and H₂O₂ led to hydrolysis at

position C-4. Hydrolysis at the C-4 position is likely a result of initial formation of the sulfone, which activates the C-4 position allowing for hydrolysis during the basic aqueous workup.



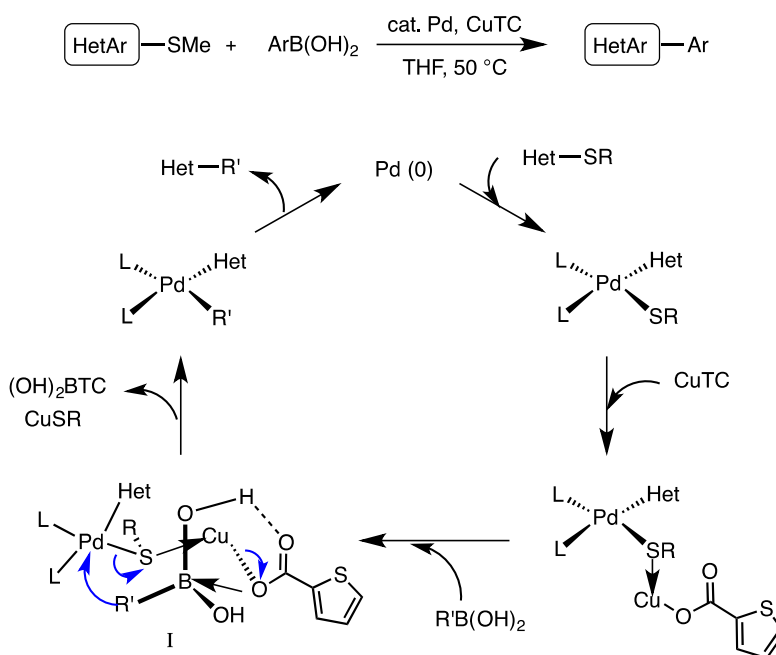
Scheme 9. Synthesis of thioether **1-26a**.

At this point, hydrolysis at position C-4 was still a major problem and an alternative route was designed. This route would also feature the deactivation of the C-4 position by a thioether followed by regioselective coupling at C-2 (Scheme 10). This strategy would rely on the palladium-catalyzed, copper(I)-mediated cross-coupling method developed by Liebeskind and co-workers²² to functionalize the C-4 position. This approach would avoid activation and subsequent hydrolysis of the C-4 position, and provide compounds of type **1-23**. The 2,4-disubstituted quinazolines (**1-23**) would then undergo a Suzuki-Miyaura reaction to provide trifunctionalized quinazoline targets **1-24**.



Scheme 10. Alternative route to selective cross-coupling reactions.

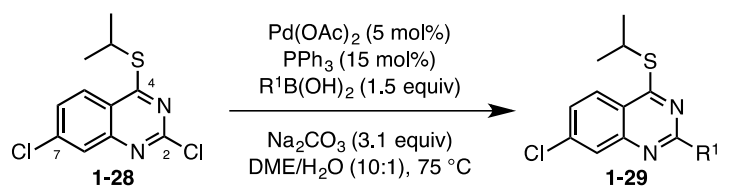
The key step in this approach employs on the palladium-catalyzed, copper (I)-thiophene-2-carboxylate (CuTC) mediated, base-free coupling method developed by Liebeskind.²² This group reported the efficient coupling of a range of thioether heteroaromatics to a variety of boronic acids within 18 h at 50 °C in THF in the presence of stoichiometric CuTC. The proposed mechanism of this transformation relies on CuTC to facilitate the baseless transmetalation of $\text{ArB}(\text{OH})_2$ by simultaneously polarizing the Pd–S bond while activating the trivalent boron (Scheme 11, intermediate I). This desulfative coupling method has been successfully employed by Guillaumet and co-workers to achieve the regioselective cross-coupling of 2,4-dichloropyrido[3,2-d]pyrimidine and other heterocycles.²³

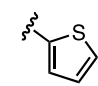
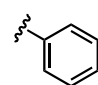
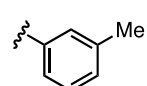
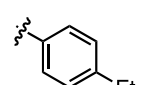
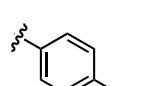
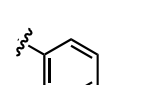
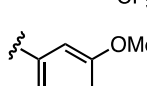
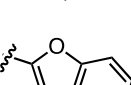
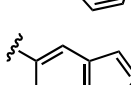
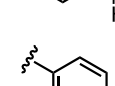


Scheme 11. Mechanism of palladium-catalyzed, copper-mediated cross-coupling of heteroaryl thioethers with boronic acids.²²

Thioether **1-28** was accessed by treatment of **1-21**²¹ with 1.05 equiv of isopropyl mercaptan and NaH. Substitution occurred exclusively at the more electrophilic C-4 position. Subsequent regioselective C-2 arylation of **1-28** proceeded in excellent yields with most arylboronic acids in the presence of 5 mol% Pd(OAc)₂ and 15 mol% PPh₃ at 75 °C, furnishing products **1-29a-g** (Table 3, entries 1-7). In the case of oxygen- and nitrogen-containing heterocyclic nucleophiles, slightly lower yields were obtained (Table 3, entries 8-10). This is presumably due to the electron-poor nature of heteroarylboronic acids, which undergo transmetalation at a slower rate. Additionally, electron-poor boronic acids are susceptible to homocoupling and metal-catalyzed protodeboronation.²⁴ The lower reactivity of these reagents is further supported by the need for prolonged reaction times and excess boronic acid (1.5 equiv) to ensure complete consumption of starting material.

Table 3. Selective Suzuki reaction at the C-2 position.¹⁵



| entry | R ¹ | time (h) | yield | compound |
|-------|---|----------|-------|--------------|
| 1 |  | 24 | 99% | 1-29a |
| 2 |  | 33 | 92% | 1-29b |
| 3 |  | 36 | 90% | 1-29c |
| 4 |  | 33 | 95% | 1-29d |
| 5 |  | 25 | 93% | 1-29e |
| 6 |  | 13 | 89% | 1-29f |
| 7 |  | 17 | 89% | 1-29g |
| 8 |  | 33 | 79% | 1-29h |
| 9 |  | 48 | 66% | 1-29i |
| 10 |  | 48 | 53% | 1-29k |

Stage 2 functionalization at the C-4 position was performed using the palladium-catalyzed, copper(I)-mediated desulfurative coupling conditions reported by Liebeskind and co-workers.²² These reactions were carried out in the presence of excess CuTC and boronic acid.

All desulfitative arylations were achieved with complete selectivity for the C-4 position and in excellent yields (Table 4). Notably, unprotected 5-indoleboronic acid provided **1-23o** in good yield despite the lower reactivity of unprotected *N*-heteroarylboronic acids in cross-coupling reactions (Table 4, entry 8).²⁴

Table 4. Palladium-catalyzed, copper(I)-mediated coupling at the C-4 position.¹⁵

| entry | R ¹ | R ² | time (h) | yield | compound |
|-------|----------------|----------------|----------|-------|--------------|
| 1 | | | 26 | 89% | 1-23f |
| 2 | | | 22 | 83% | 1-23g |
| 3 | | | 19 | 89% | 1-23h |
| 4 | | | 19 | 87% | 1-23i |
| 5 | | | 19 | 86% | 1-23k |
| 6 | | | 27 | 91% | 1-23m |
| 7 | | | 13 | 97% | 1-23n |
| 8 | | | 48 | 66% | 1-23o |

The third and final cross-coupling reaction was initially carried out using the conditions reported in Table 3 (Table 5, entry 1). Incomplete consumption of starting material resulted, and attempts to facilitate complete conversion of starting material using elevated temperatures and increasing the equivalents of boronic acid gave a 1:1 mixture of starting material and product (Table 5, entry 2). In order to ensure the complete consumption of starting material, 10 mol% Pd(OAc)₂, 30 mol% PPh₃, and 4.0 equiv of boronic acid were used. These conditions resulted in successful cross-coupling at the C-7 position in good yields for both aryl- and heteroarylboronic acids (Table 5, entries 3-5). The regioselectivity of these cross-coupling reactions was confirmed by X-ray analysis of **1-24b** (Figure 4) and is in agreement with the predicted order of coupling as calculated by Houk.¹⁸

Table 5. Suzuki reaction at the C-7 position.¹⁵

| entry | R ¹ | R ² | R ³ | time (h) | yield | compound |
|----------------|----------------|----------------|----------------|----------|------------------|--------------|
| 1 ^a | | | | 29 | SM (93%) | 1-24a |
| 2 ^b | | | | 24 | SM:product (1:1) | 1-24a |
| 3 ^c | | | | 34 | 81% | 1-24b |
| 4 ^c | | | | 22 | 86% | 1-24c |
| 5 ^c | | | | 34 | 66% | 1-24d |

^a R³B(OH)₂, 1.5 equiv; Na₂CO₃, 3.1 equiv; Pd(OAc)₂, 0.05 equiv; PPh₃, 0.15 equiv; DME/H₂O, 75 °C
^b R³B(OH)₂, 2.0 equiv; Na₂CO₃, 3.1 equiv; Pd(OAc)₂, 0.05 equiv; PPh₃, 0.15 equiv; DME/H₂O, reflux
^c R³B(OH)₂, 4.0 equiv; Na₂CO₃, 6.2 equiv; Pd(OAc)₂, 0.10 equiv; PPh₃, 0.30 equiv; DME/H₂O, reflux

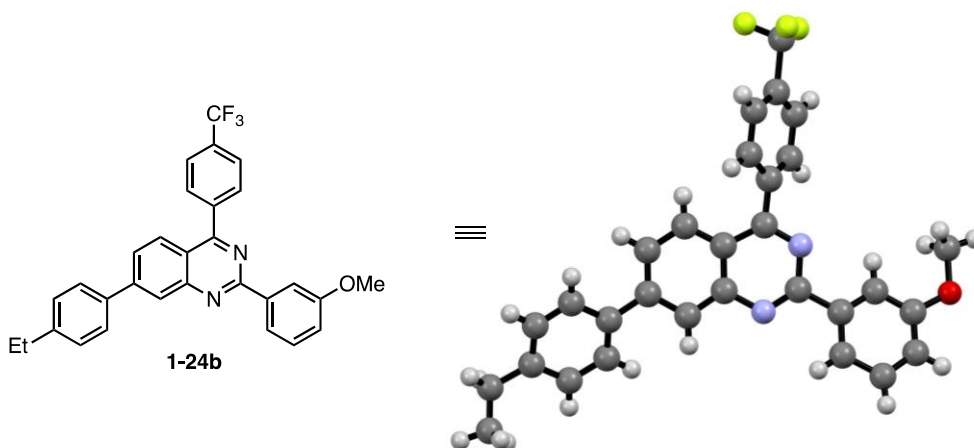


Figure 4. X-Ray crystal structure of **1-24b** (Appendix A.1).

1.3 BIOLOGICAL ACTIVITY

A selection of fourteen substituted quinazolines was deposited in the PubChem database. Five of these compounds were tested against 88 protein targets in 92 primary assays and 24 confirmatory assays, yielding one active compound (**1-23a**). Compound **1-23a** was identified as a weak agonist of mouse 5-hydroxytryptamine (serotonin) receptor 2A (HTR2A) and showed 17.4% activation at 7.6 μM . Due to the structural similarity of these substituted quinazolines to known liver X receptor (LXR) modulators **1-1** and **1-2** (Figure 1), we submitted these compounds to our collaborators²⁵ to evaluate their effect on the activation of LXRs. Human H4 neuroglioma cells were treated with each compound at 10 μM . Three of the compounds (**1-24b–d**) resulted in upregulation of gene expression relative to the vehicle (DMSO); however, they were significantly less effective than the positive control.²⁵

1.4 CONCLUSION

We have demonstrated that temporary deactivation of the C-4 position of 2,4,7-trichloroquinazoline by substitution of the chlorine atom with isopropyl mercaptan allowed for the regioselective palladium-catalyzed cross-coupling at the C-2 position in 2,7-dichloroquinazoline (**1-28**). Subsequent palladium-catalyzed, copper(I)-mediated desulfitative coupling at the C-4 position, followed by the final palladium-catalyzed cross-coupling at the C-7 position, allowed for convenient access to the desired tricarbosubstituted quinazolines.¹⁵ This simple and efficient sequential coupling route to highly substituted quinazolines showcases the utility of regioselective palladium-catalyzed cross-coupling reactions for the preparation of focused libraries of kinase inhibitors.²⁶

2.0 REGIOSELECTIVE CROSS-COUPPLING REACTIONS OF 1,3,6-TRICHLOROISOQUINOLINE: SYNTHESIS OF A DUAL-SPECIFICITY PHOSPHATASE CDC25B INHIBITOR

2.1 INTRODUCTION

2.1.1 Biological Significance of Cdc25

The cell division cycle 25 (Cdc25) dual specificity phosphatases, a subclass of protein tyrosine phosphatases, play an essential role in the regulation of the mammalian cell cycle. Cdc25s dephosphorylate and subsequently activate cyclin-dependent kinase (CDK) complexes, making their regulation of critical importance in controlling cell proliferation. These protein kinases serve as key activators of the CDK complexes and are also crucial components in cell cycle checkpoints that prevent CDK activation following DNA damage (Figure 5).²⁷ There are three human Cdc25 isoforms, Cdc25A, Cdc25B, and Cdc25C. The over-expression of one isoform in particular, Cdc25B, enables the bypass of normal cell cycle checkpoints and has been linked to a variety of human cancers.^{27a,28} As a result, Cdc25B has become an attractive target for the development of anticancer therapeutics.^{27b,29}

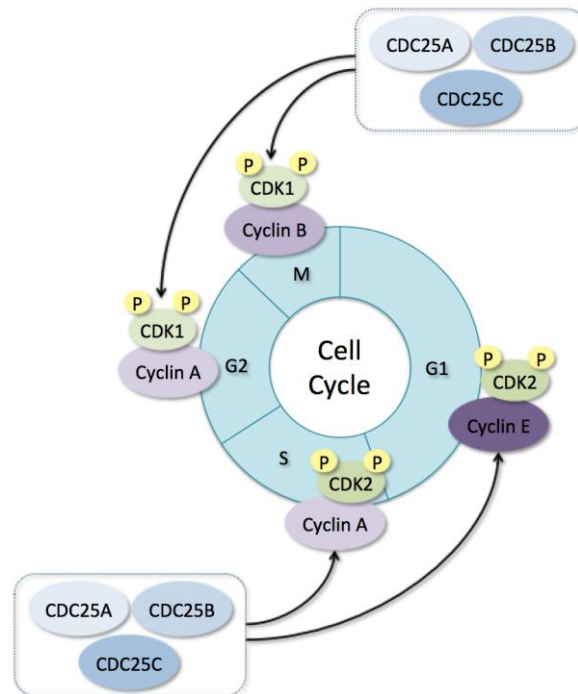


Figure 5. CDC25 phosphatases control mammalian cell-cycle progression.³⁰

The structures of the catalytic domains of the Cdc25 isoforms have been solved by X-ray crystallography³¹ and contain the signature active site sequence, HCX₅R, common to all protein tyrosine kinases.³² The catalytic sequence forms a loop that is positioned above a long α -helix. This positioning creates a unique dipole environment in which the catalytic cysteine exists as a thiolate with a pK_a of 5.6-6.3 (*ca.* 8.0 for free cysteine).³³ This unusually low pK_a of the active site cysteine renders it highly susceptible to covalent modifications and oxidation by reactive oxygen species (ROS).³⁴ Additionally, the active site pocket is surprisingly shallow with no apparent groove for binding proteins or small molecules.³²

The inherent features of the Cdc25 active site pose a formidable challenge for inhibitor development. Numerous promising advancements have been made, but a clinically active candidate in this field has yet to emerge.^{27b,29} The majority of Cdc25 inhibitors fall into six

distinct classes, which were previously designated and reviewed by Wipf and Lazo.^{29b} These classes include, but are not limited to: (1) natural products dysidolides and dnacins; (2) hydrophobic acids SC- $\alpha\alpha\delta 9$; (3) quinones and vitamin K analogs menadione and DA3003-1; (4) electrophiles such as fascaplysin; (5) phosphate surrogates such as the xenicane diterpenoids; and (6) peptides and peptide analogs (Figure 6).

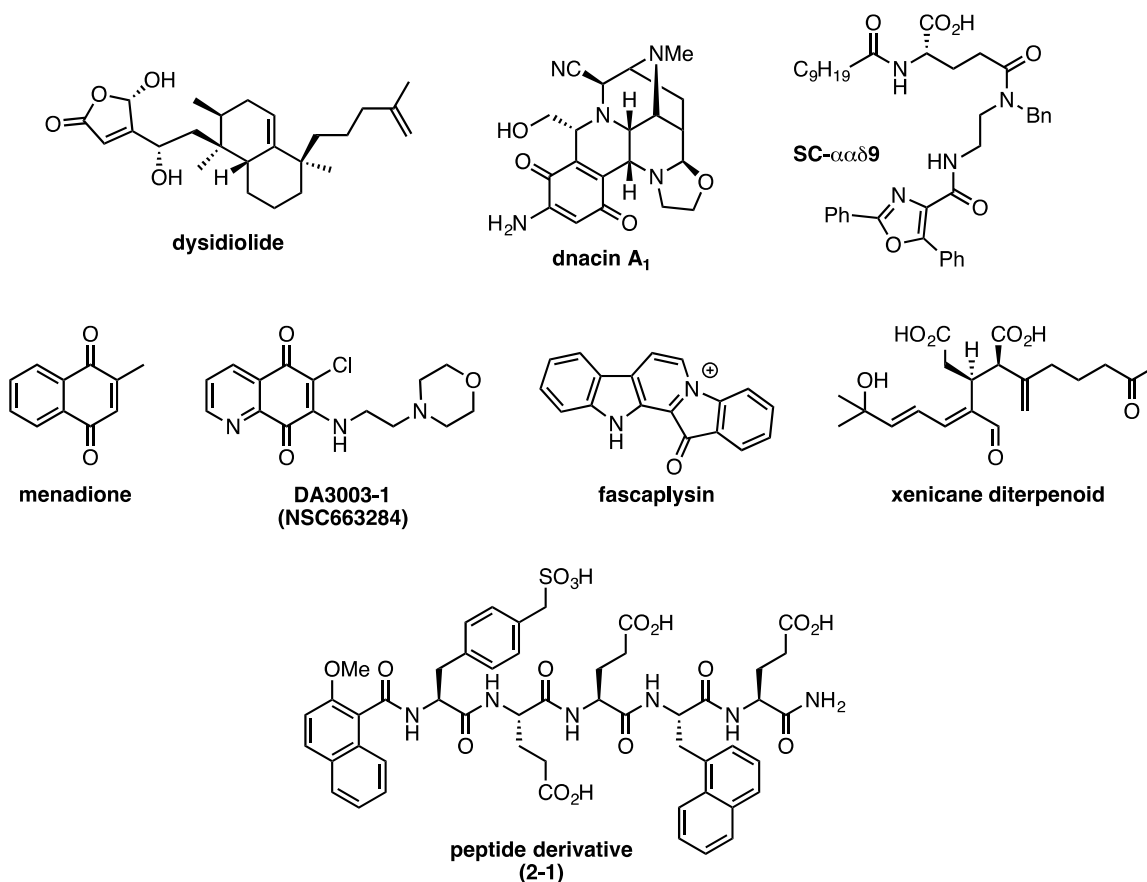


Figure 6. Known inhibitors of Cdc25 phosphatases.

2.1.2 Synthesis and Biological Evaluation of 3-Aminoisoquinolin-1(2H)-one Inhibitors of Cdc25B: Previous Work in the Wipf Group

Although non-quinoid compounds have attracted attention as inhibitors of Cdc25, quinone-type compounds still represent the majority of the known inhibitors of Cdc25. As part of a high-throughput screening (HTS) effort, Wipf and co-workers identified the 3-amino-1,2-dihydro-1-isoquinolinone (**2-2**) scaffold as a promising non-quinoid pharmacophore for Cdc25B inhibition (Figure 7).³⁵ These heterocycles were not extensively characterized chemically and biologically;³⁶ therefore, a medicinal chemistry program to investigate structure-activity relationships (SARs) in this series was initiated by our group.

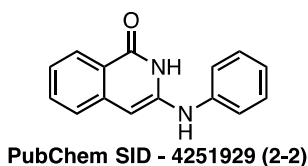
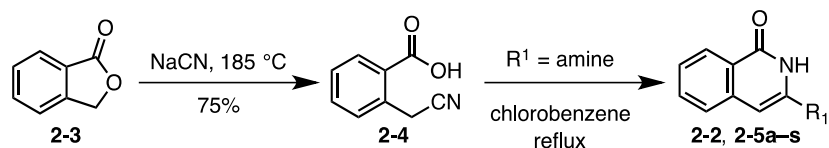


Figure 7. HTS hit for Cdc25B inhibition.

The synthesis of the initial HTS hit **2-2** began with the preparation of 2-cyanomethylbenzoic acid **2-4**, which was readily available from the nucleophilic opening of phthalide **2-3** with sodium cyanide at 185 °C (Table 6).³⁷ Subsequent treatment of the acid with aniline in chlorobenzene at reflux afforded target compound **2-2** in 58% yield (Table 6, entry 1).³⁶ The rapid construction of the isoquinolinone core enabled the synthesis of a variety of derivatives (**2-5a-s**) by modification of the amine used in the condensation reaction (Table 6, entries 2-19). The wide range of yields (25-82%) was attributed to the low solubility of some of

the products in 2-propanol and methanol, which were used in the streamlined purification process.

Table 6. Synthesis of 3-amino-1,2-dihydro-1-isoquinolinone with various amines and the *in vitro* inhibitory activity against Cdc25B.³⁸



| entry | R ¹ | yield (%) | <i>In vitro</i> Cdc25B IC ₅₀ (μM) ^a | compound |
|-------|--------------------------------------|-----------|--|-------------|
| 1 | aniline | 58 | 0.74 ± 0.10 | 2-2 |
| 2 | 2-chloroaniline | 55 | 4.19 ± 0.49 | 2-5a |
| 3 | 4-methylaniline | 69 | 0.77 ± 0.17 | 2-5b |
| 4 | 2-fluoroaniline | 48 | 1.85 ± 0.07 | 2-5c |
| 5 | 4-fluoroaniline | 81 | 0.83 ± 0.11 | 2-5d |
| 6 | <i>p</i> -anisidine | 45 | 13.63 ± 2.79 | 2-5e |
| 7 | 2,5-dimethoxyaniline | 59 | 5.25 ± 0.62 | 2-5f |
| 8 | 2-aminophenol | 35 | 1.21 ± 0.20 | 2-5g |
| 9 | 4-aminoethylbenzene | 62 | 10.75 ± 0.75 | 2-5h |
| 10 | 2-phenylaniline | 45 | 2.57 ± 0.32 | 2-5i |
| 11 | benzyl amine | 60 | 0.85 ± 0.17 | 2-5k |
| 12 | 4-methoxybenzylamine | 70 | 0.77 ± 0.11 | 2-5l |
| 13 | <i>N</i> -methylbenzylamine | 76 | 1.55 ± 0.32 | 2-5m |
| 14 | 2-bromo- <i>N</i> -methylbenzylamine | 82 | 3.80 ± 0.68 | 2-5n |
| 15 | 1,2,4-triazole-3-amino | 74 | 4.48 ± 1.37 | 2-5o |
| 16 | 2-aminopyridine | 53 | 3.31 ± 0.55 | 2-5p |
| 17 | piperidine | 60 | 2.31 ± 0.39 | 2-5q |
| 18 | morpholine | 75 | 3.37 ± 0.30 | 2-5r |
| 19 | 6-amino-1-hexanol | 25 | 0.64 ± 0.16 | 2-5s |

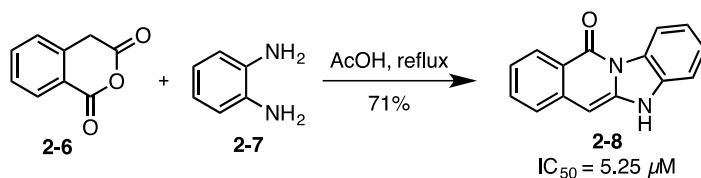
^a Histidine₆-tagged recombinant Cdc25B was assayed *in vitro* with 7-10 concentrations of each compound and with the artificial substrate *O*-methylfluorescein phosphate as previously described.^{35,39} Each IC₅₀ was calculated as the mean ± standard deviation, *n* = 3.

Initial insight into the substituent effects of these compounds was determined base on the biological evaluation of **2-5a–s** by Johnston and co-workers.³⁸ The parent hit **2-2** showed good activity with an IC₅₀ value of 740 nM (Table 6, entry 1). Substitution on the aniline ring gave analogs with comparable or diminished IC₅₀ values (Table 6, entries 2-10). Specifically, *ortho*-

substituted anilines gave analogs with reduced inhibitory activity, while the *para*-methyl and *para*-fluoro anilines were well tolerated. The aniline moiety was also replaced by benzyl amine to afford **2-5k** and the methoxy substituted **2-5l**, which possessed comparable inhibitory activities to the parent hit (Table 6, entries 1, 11, and 12). The corresponding *N*-alkylated derivatives were less active (Table 6, entries 13 and 14).

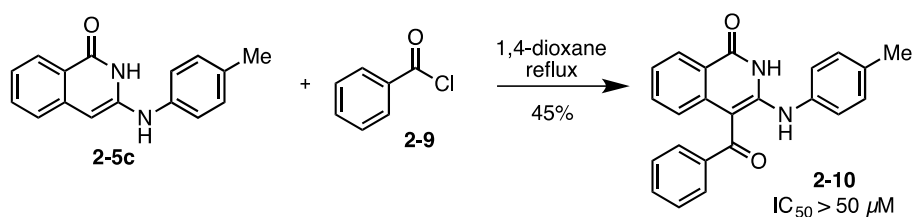
Heterocyclic amines as R¹ groups in the 3-position were also explored (Table 6, entries 15-18). However, both the triazole (**2-5o**) and the pyridine (**2-5p**) showed only modest activity with IC₅₀ values of 4.48 μM and 3.31 μM, respectively. The fully saturated piperidine (**2-5q**) and morpholine (**2-5r**) derivatives were also less active than the parent compound **2-2**, although the hexanol analog **2-5s** showed slightly improved activity with an IC₅₀ of 640 nM (Table 6, entry 19).

To further evaluate the structural requirements for Cdc25B inhibition, and to restrict the rotational flexibility of the R¹ amino substituent in the 3-position of the isoquinolinone **2-2**, the fused tetracyclic analog was synthesized (Scheme 12). The synthesis of **2-8** was accomplished in 71% yield by heating homophthalic anhydride **2-6** at reflux with *ortho*-phenylenediamine **2-7** in acetic acid.⁴⁰ The loss in inhibitory activity of **2-8** (IC₅₀ = 5.25 μM) suggested that a planar orientation of the tetracycle was detrimental for target inhibition, and the hydrogen-bond donor at the 2-position of the isoquinolinone may be required for activity.



Scheme 12. Synthesis of fused tetracyclic analog **2-8**.³⁸

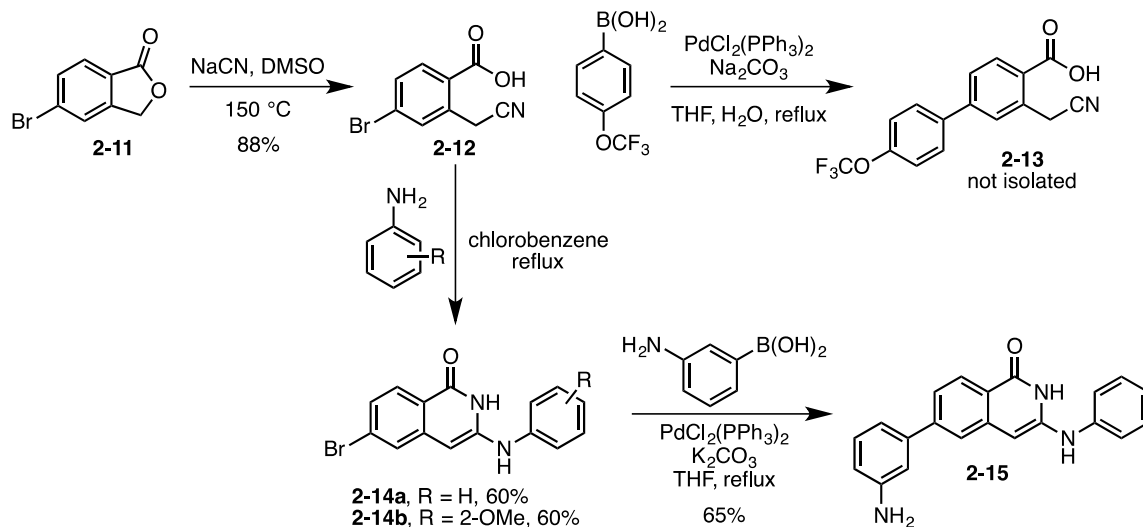
A unique chemical characteristic of the isoquinolinone core structure is its high nucleophilicity at the 4-position. This “enamine-like” position can react with suitable electrophiles,^{36,41} which provides an opportunity for further structural diversification. Although substitution at this position was not exploited extensively, the acylated analog **2-10** was synthesized in 45% yield by treatment of isoquinolinone **2-5c** with benzoyl chloride in dioxane (Scheme 13). Substitution at this position proved to be detrimental to the inhibitory activity ($IC_{50} > 50 \mu M$).



Scheme 13. Synthesis of 4-substituted isoquinolinone **2-10**.³⁸

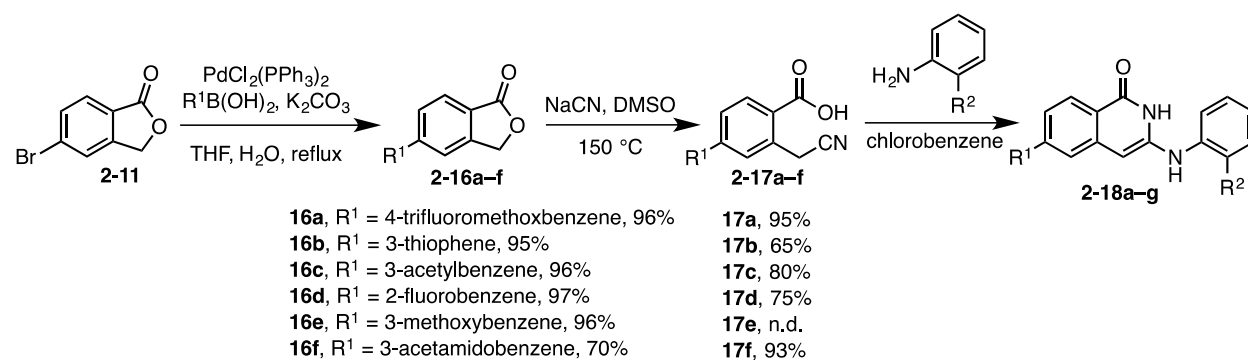
After exploring variations of the 3-amino side chain, the next focus was on the functionalization of the 6-position of the arene ring of the isoquinolinone (Scheme 14). Opening of lactone **2-11** with neat NaCN according to the protocol used in the conversion of **2-3** to **2-4** resulted in the decomposition of the starting material. Employing DMSO as a solvent provided a good yield of the desired 5-bromo-2-cyanomethylbenzoic acid **2-12**, which was then exposed to Suzuki coupling conditions. This approach was not an effective method for library construction due to the difficulty in monitoring the reaction progress and purifying the product mixtures. The use of **2-14a** and **2-14b** as coupling components was explored, and although the Suzuki reaction was successful in the case of **2-14a** to provide **2-15**, this strategy was not employed for library

synthesis due to the potential contamination of the products with trace amounts of palladium in the last step of the synthesis.



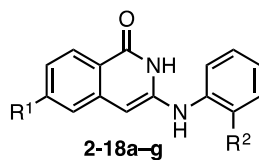
Scheme 14. Initial synthetic strategies to functionalize the 6-position of isoquinolinone.³⁸

Wipf and co-workers developed a modified protocol to introduce various substituents at the 5-position of 5-bromophthalide **2-11** prior to lactone opening (Scheme 15). Suzuki coupling of **2-11** with commercially available electron-rich and -poor boronic acids proved to be a successful strategy to afford the substituted phthalides **2-16a–f** in high yields (Scheme 15). Subsequent exposure of **2-16a–f** to NaCN in DMSO resulted in the desired benzoic acids **2-17a–f**. These benzoic acid derivatives were then treated with aniline or *o*-anisidine and heated to reflux in chlorobenzene to afford isoquinolinones **2-18a–g**.



Scheme 15. Synthetic strategy to obtain functionalized isoquinolines **2-18a-g** (n.d.= not determined).³⁸

The biological activity of analogs **2-18a-g** was carried out by our collaborators³⁸ and is summarized in Table 7. Interestingly, isoquinolinones with R¹ being a *meta*-substituted arene showed the best activity (Table 7, entries 4-8). Their IC₅₀ values ranged from 0.22–2.7 μM and were comparable or higher than the activity found for the initial hit **2-2** (IC₅₀ = 0.74 μM). The most potent compound was the 3-acetamidobenzene substituted analog **2-18e**, which was three-fold more potent than **2-2**. Other substituted arenes, such as 3-acetylbenzene **2-18f** and 3-methoxybenzene **2-18g**, showed comparable activity to **2-2**. The 4-trifluoromethoxybenzene analog **2-18a**, as well as the 2-fluorobenzene (**2-18c**), thiophene (**2-18d**), 3-aminobenzene (**2-15**), and bromide (**2-14a**) analogs also possessed significant, low micromolar inhibitory activities. We only briefly explored the SAR of the R² group in analogs **2-18a-g**, and found that the addition of a methoxy group in the 2-position of the aniline (i.e. **2-18a**) decreased the IC₅₀ ca. five-fold over the R²-unsubstituted **2-18b**.

Table 7. *In vitro* Cdc25B inhibitory activity of C-6 functionalized isoquinolinone analogs.³⁸

| entry | R ¹ | R ² | <i>In vitro</i> Cdc25B IC ₅₀ (μM) ^a | compound |
|-------|--------------------------|----------------|--|--------------|
| 1 | 4-trifluoromethylbenzene | OMe | 2.48 ± 0.33 | 2-18a |
| 2 | 4-trifluoromethylbenzene | H | 12.19 (1) | 2-18b |
| 3 | 2-fluorobenzene | H | 1.77 ± 0.41 | 2-18c |
| 4 | 3-thiophene | H | 1.20 (1) | 2-18d |
| 5 | 3-acetamidobenzene | H | 0.22 ± 0.04 | 2-18e |
| 6 | 3-acetylbenzene | H | 0.87 ± 0.12 | 2-18f |
| 7 | 3-methoxybenzene | H | 0.75 (1) | 2-18g |
| 8 | 3-aminobenzene | H | 2.70 ± 1.70 | 2-15 |
| 9 | Br | H | 1.16 ± 0.44 | 2-14a |

^a Histidine₆-tagged recombinant Cdc25B was assayed *in vitro* with 7-10 concentrations of each compound and with the artificial substrate *O*-methylfluorescein phosphate as previously described.^{35,39} Each IC₅₀ was calculated as the mean ± standard deviation, *n* = 3 unless noted with parenthesis, which indicates an *n* = 1.

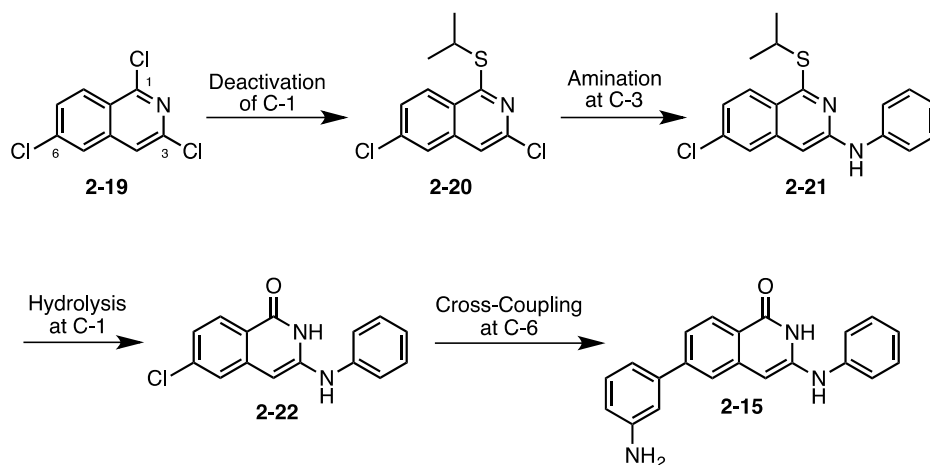
2.2 RESULTS AND DISCUSSION

2.2.1 Application of a Regioselective Cross-Coupling Strategy for the Synthesis and Scale-up of Lead Structure 2-15

As a representative example for the 6-(3-aminophenyl)isoquinolin-1(2*H*)-one series, analog **2-15**, which was computationally predicted to have a favorable aqueous solubility of 2.5 mg/mL, was further investigated. This lead molecule was found to lack the ability to generate reactive oxygen species (ROS), a common issue leading to artifacts in phosphatase assays.⁴² Compound **2-15** was also 6-fold less active *in vitro* against human PTP1B (IC₅₀ = 15.3 μM), demonstrating modest selectivity for Cdc25B. This promising data led us to explore an alternative synthetic

route to access **2-15** in larger quantities for *in vivo* studies. This new route would allow for the application and expansion of the aforementioned regioselective cross-coupling method developed in our lab and others.^{15,23a}

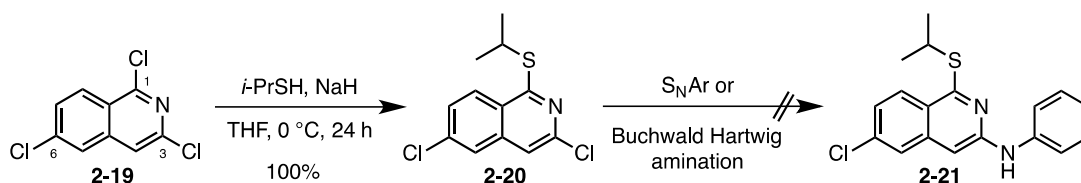
Beginning with 1,3,6-trichloroisoquinoline (**2-19**), we envisioned deactivation of the most active C-1 position with the introduction of isopropyl mercaptan, followed by a regioselective amination reaction at the C-3 position (Scheme 16). At this point, hydrolysis at the C-1 position would allow for the removal of the thioether moiety and generation of the desired isoquinolinone core. A final Suzuki cross-coupling reaction at the remaining C-6 position with 3-aminophenylboronic acid would provide the desired compound, **2-15**.



Scheme 16. Initial synthetic route for the synthesis of inhibitor **2-15**.

Thioether **2-20** was accessed by treatment of **2-19** with 1.1 equiv of isopropyl mercaptan and NaH (Scheme 17). Subsequent regioselective nucleophilic substitution at the C-3 position with aniline in refluxing EtOH or diglyme gave no reaction. Efforts to facilitate the substitution by treatment of aniline with NaH prior to addition to **2-20** did not provide the desired product. Instead, analysis of the crude reaction mixture indicated that substitution of the isopropyl

thioether moiety with aniline had occurred in preference of chloride displacement at position C-3. In order to circumvent this problem, palladium-catalyzed Buchwald-Hartwig coupling reactions were explored. Reactions employing either Pd₂(dba)₃ or Pd(OAc)₂, in combination with phosphine ligands DavePhos, PPh₃, or (±)-BINAP (Figure 8), resulted in no reaction and starting material was recovered.



Scheme 17. Attempted synthesis of thioether **2-21**.

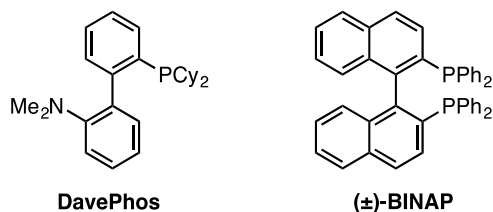
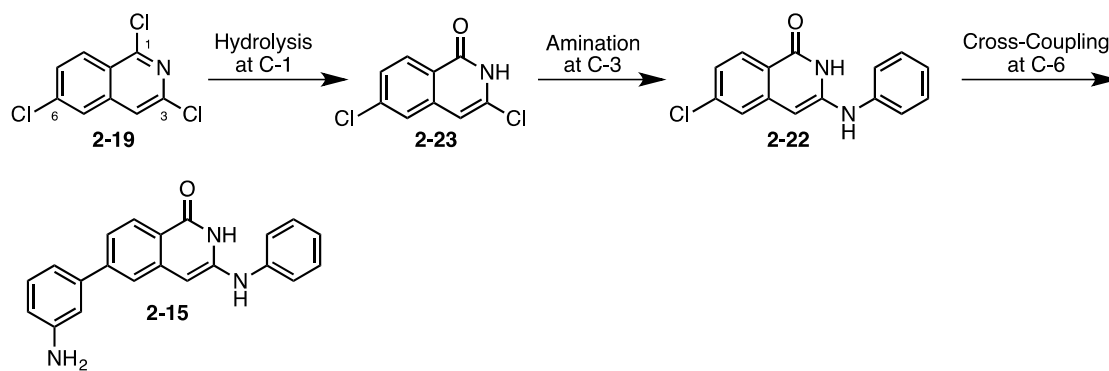


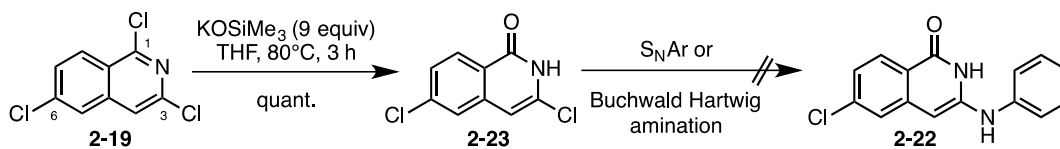
Figure 8. Chemical structures of phosphine ligands used for the Buchwald-Hartwig amination reactions of **2-20**.

At this point we revised our synthetic approach to begin with hydrolysis at position C-1, followed by selective amination at the C-3 position, and final Suzuki coupling at the C-6 position (Scheme 18). With the reactivity of the C-1 site attenuated by formation of the isoquinolinone moiety, chloride displacement at position C-3 should proceed without competitive substitution at C-1.



Scheme 18. Alternative route to **2-15**.

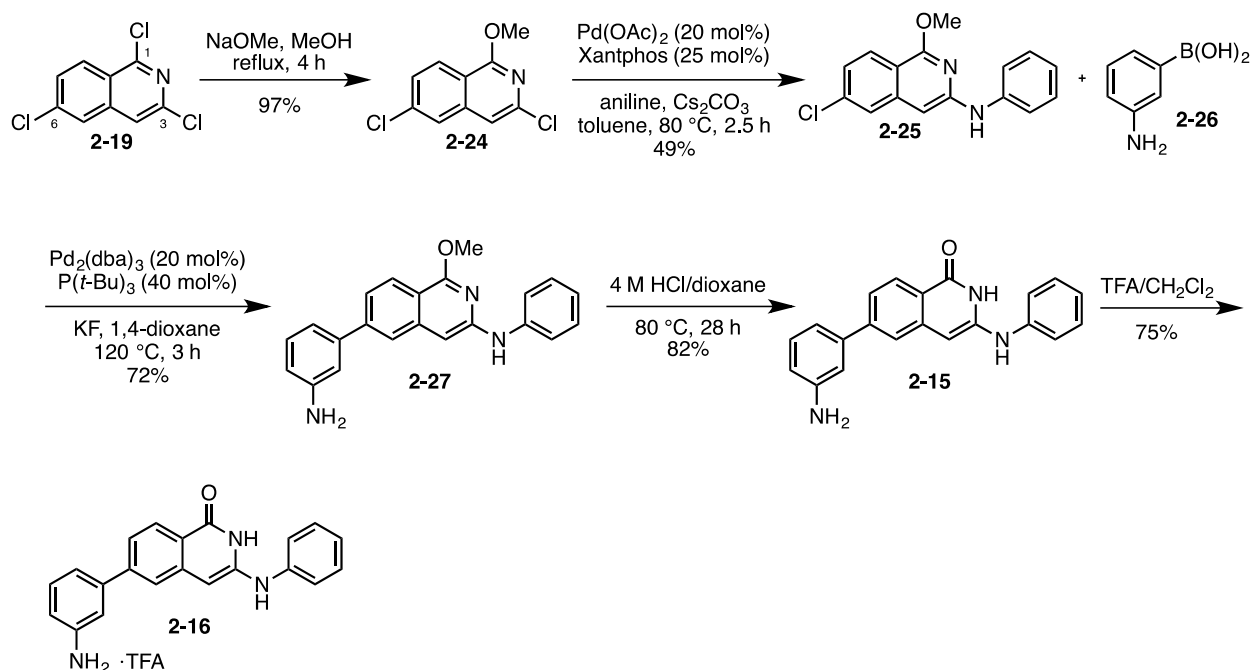
Hydrolysis at the C-1 position using excess KOSiMe_3 furnished the desired product **2-23** in quantitative yield (Scheme 19). Regioselective amination of the C-3 position via nucleophilic substitution with aniline, both in the presence and absence of NaH , resulted in complete recovery of starting material. Buchwald-Hartwig coupling reactions were also explored, but as with the thioether derivative **2-20**, attempts to use either $\text{Pd}_2(\text{dba})_3$ or $\text{Pd}(\text{OAc})_2$, in combination with phosphine ligands DavePhos, PPh_3 , or (\pm) -BINAP resulted in no reaction. It was suspected that both substrates **2-20** and **2-23** were incompatible with the Buchwald-Hartwig amination conditions due to the formation of palladium metal (Pd^0) after prolonged exposure to the reaction conditions.



Scheme 19. Attempted synthesis of isoquinolinone **2-22**.

In order to avoid this problem, the most electrophilic C-1 position of 1,3,6-trichloroisoquinoline (**2-19**) was protected as methyl ether **2-24** (Scheme 20). As with **2-20** and

2-23, introduction of aniline via nucleophilic substitution in the presence of NaH resulted in displacement of the C-1 methyl ether, rather than the chloride at the C-3 position. In contrast to **2-20** and **2-23**, subjection of **2-24** to Buchwald-Hartwig amination reactions furnished the desired product **2-25**; however, optimization of the reaction conditions required the screening of several catalyst systems. The best ratio of the desired to isomeric coupled products was achieved using Pd(OAc)₂ and Xantphos. Under these conditions, the desired compound **2-25** was isolated in 49% yield (57% BRSM), and only 23% (27% BRSM) of the undesired C-6 coupled product was observed. The Suzuki cross-coupling reaction at position C-6 was successful in a sealed tube at 120 °C in the presence of Pd₂(dba)₃ and P(*t*-Bu)₃. With **2-27** in hand, the final demethylation proceeded smoothly in 4 M HCl in 1,4-dioxane at 80 °C to afford 0.450 g of target compound **2-15** (Scheme 20). The TFA salt **2-16** was prepared by treatment of a suspension of **2-15** in CH₂Cl₂ with TFA at room temperature. The identity of **2-16** was confirmed based on the downfield shifts of the *ortho* and *meta* carbons of the aniline ring in the ¹³C NMR spectra from from 112.6, 114.0, and 114.9 to 116.4, 117.7, and 119.9, respectively. Additionally, an upfield shift from 148.7 to 143.7 ppm was observed for carbon directly attached to the amine. The TFA salt was prepared **2-16** to enhance the solubility of **2-15** for *in vivo* studies, and was soluble up to 4.4 mg/mL when formulated with 20% (w/v) Solutol® HS 15 in H₂O.



Scheme 20. Regioselective palladium-catalyzed cross-coupling strategy to synthesize **2-15**.

2.2.2 Biological Activity

Prior to *in vivo* studies, a confirmative *in vitro* assay was performed by Prof. Lazo and co-workers³⁸ using the material from our revised route. The average IC_{50} over 4 days was $2.7 \mu\text{M}$, which is in good agreement with the inhibitor obtained from the previous route.³⁸ With the inhibitory activity confirmed, *in vivo* studies were carried out by Prof. Eiseman et al.⁴³ on mice bearing MDA-MB-231 xenografts with 45 mg/kg (iv) **2-16**. Unfortunately, **2-16** has no effect on tumor size over 15 days of administration and peak tumor concentrations were reached at *ca.* 10 min.⁴³ The pharmacokinetic data indicated a maximum plasma concentration of **2-16** observed at *ca.* 15 min.⁴³ Plasma disappearance of **2-16** was rapid and accompanied by the appearance of a metabolite; and neither **2-16**, nor the metabolite, was detectable beyond 24 h.⁴³ Additionally,

the highest tissue concentration in the kidney and liver was observed at the earliest time point sampled (*ca.* 5 min).⁴³

2.3 CONCLUSION

3-Aminoisoquinolines were identified as attractive new scaffolds for the discovery of non-quinoid dual-specificity phosphatase inhibitors devoid of ROS-generating side effects. We successfully applied a regioselective cross-coupling method¹⁵ in the scale-up of the representative 2.7 μM Cdc25B inhibitor **2-15**. Our preliminary biological studies indicate that **2-15** inhibits the *in vitro* dephosphorylation of Cdk1 by Cdc25B in the absence of ROS production and prevents cell proliferation during mitosis. Unfortunately, **2-15** was rapidly metabolized *in vivo*, limiting the therapeutic potential of this compound.

3.0 INHIBITORS OF PROTEIN KINASE D: SYNTHESIS AND STRUCTURE- ACTIVITY RELATIONSHIP

3.1 INTRODUCTION

3.1.1 Protein Kinase D as a Potential New Target for Cancer Therapy

Protein Kinase D (PKD) constitutes a novel family of serine/threonine kinases and diacylglycerol (DAG) receptors that have emerged as key regulators of multiple cancer-promoting pathways (Figure 9).⁴⁴ PKD is classified as a subfamily of the Ca^{2+} /calmodulin-dependent kinase superfamily and three PKD isoforms have been identified to date: PKD1 (formerly PKC μ),⁴⁵ PKD2,⁴⁶ and PKD3 (formerly PKC ν).⁴⁷ All three PKD isoforms possess a highly homologous sequence and share a distinct structure that includes a catalytic domain, a pleckstrin homology (PH) domain that mediates protein-protein interactions and PKD autoinhibition, and an *N*-terminal cysteine-rich DAG/phorbol ester binding domain (C1 domain).

The activation of PKD and the regulatory mechanisms that control PKD activity have been well documented.^{44,48} Interaction of DAG-responsive protein kinase C (PKC) with the PH domain of PKD results in transphosphorylation of the conserved Ser⁷⁴⁴ and Ser⁷⁴⁸ within the activation loop,⁴⁹ and subsequent autophosphorylation at multiple sites, including Ser⁹¹⁶, results in full activation PKD.⁵⁰ PKD is also capable of shuttling between different subcellular

compartments as a result of spatial regulation by DAG or phorbol esters.^{48a,b,51} The fundamental PKD function in cells is therefore reliant upon this canonical DAG/PKC/PKD pathway.

PKD has been implicated in a variety of cellular processes, including cell proliferation, cell survival through oxidative stress-induced activation of nuclear factor-kappaB (NF-κB) signaling,⁵² gene expression by regulation of class IIa histone deacetylases (HDAC),⁵³ protein trafficking,⁵⁴ cell motility,⁵⁵ and immune responses⁵⁶ due to its central position in the signal transduction pathway (Figure 9). Studies assessing the expression levels of all three isoforms of PKD have shown that PKD is dysregulated in several cancer types, including breast, prostate, and gastric cancer.⁵⁷ PKD also plays an active role in pathological processes such as cardiac hypertrophy,⁵⁸ angiogenesis,⁵⁹ and tumor cell proliferation and metastasis.⁶⁰ This ubiquitous role of PKD renders this class of kinases an attractive therapeutic target for drug development.^{44a}

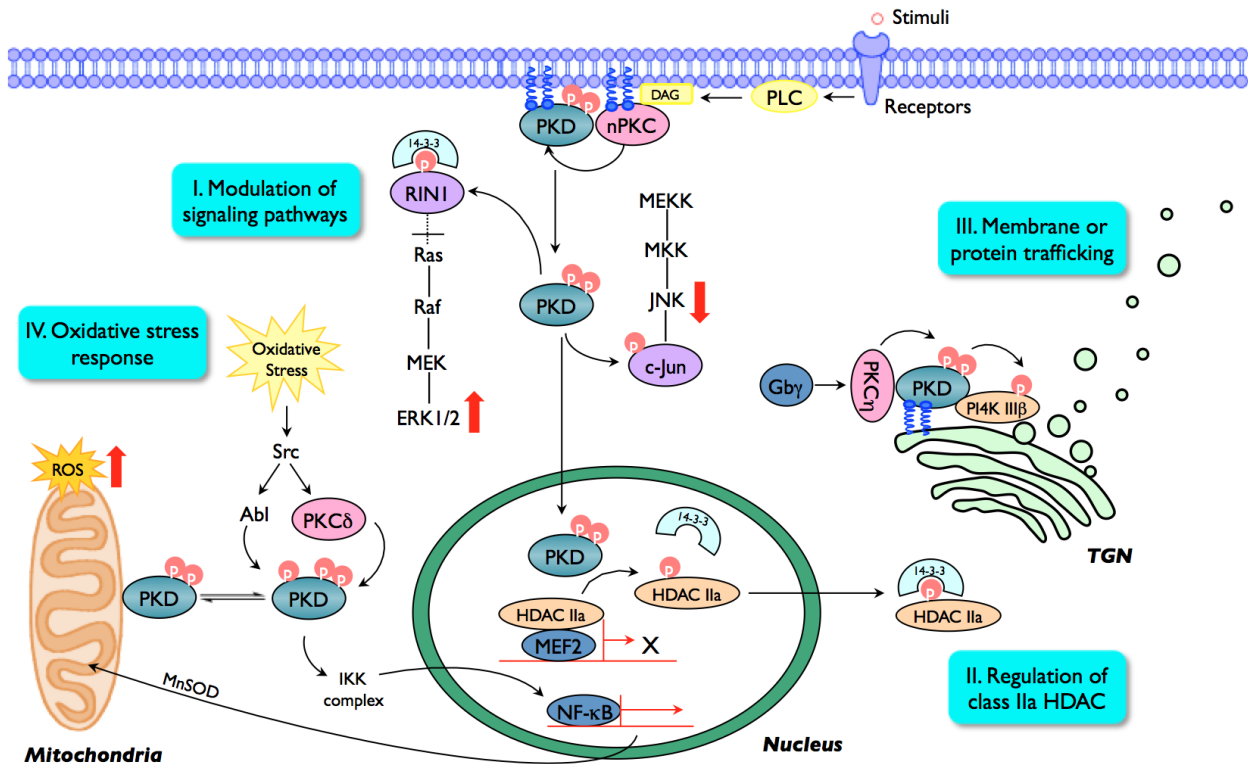


Figure 9. Major PKD signaling pathways.⁶¹

3.1.2 Chemical Inhibitors of PKD: Old and New

Extensive analysis of the role of PKD in biological processes has been hampered by the lack of a three-dimensional (3D) structure of PKD, which prohibits the use of structure-based drug design. Additionally, early inhibitors of PKD were not selective. Among the early inhibitors of PKD were the ATP competitive pan-kinase inhibitor staurosporine and staurosporine related analogs such as K252a (Figure 10). These analogs showed IC₅₀ values in the low nanomolar range but lacked the requisite kinase specificity necessary to interrogate PKD in cells.⁶² Indolocarbazole Gö697 also inhibits PKD with an IC₅₀ *ca.* 20 nM; and, although it is foremost a classical PKC inhibitor, it is commonly used to inhibit PKD in various cellular contexts.⁶²⁻⁶³

Resveratrol, a common antioxidant and chemopreventive agent, has also been reported to inhibit PKD (Figure 10).⁶⁴ Resveratrol is not selective for PKD and high micromolar concentrations of resveratrol are necessary for inhibition of PKD. Nonetheless, resveratrol has shown potent antitumor activity in multiple animal models and it is possible that part of its effectiveness is due to PKD inhibition.^{64c} In contrast to the aforementioned inhibitors, the hexasulfonated naphthylurea, suramin, has been shown to be a novel and effective *activator* of PKD. Suramin has proved to be a valuable tool for dissecting the activities of different PKC isozymes, but it is also plagued by promiscuous kinase inhibition thereby limiting its effectiveness to probe PKD function in relevant biological environments.⁶⁵

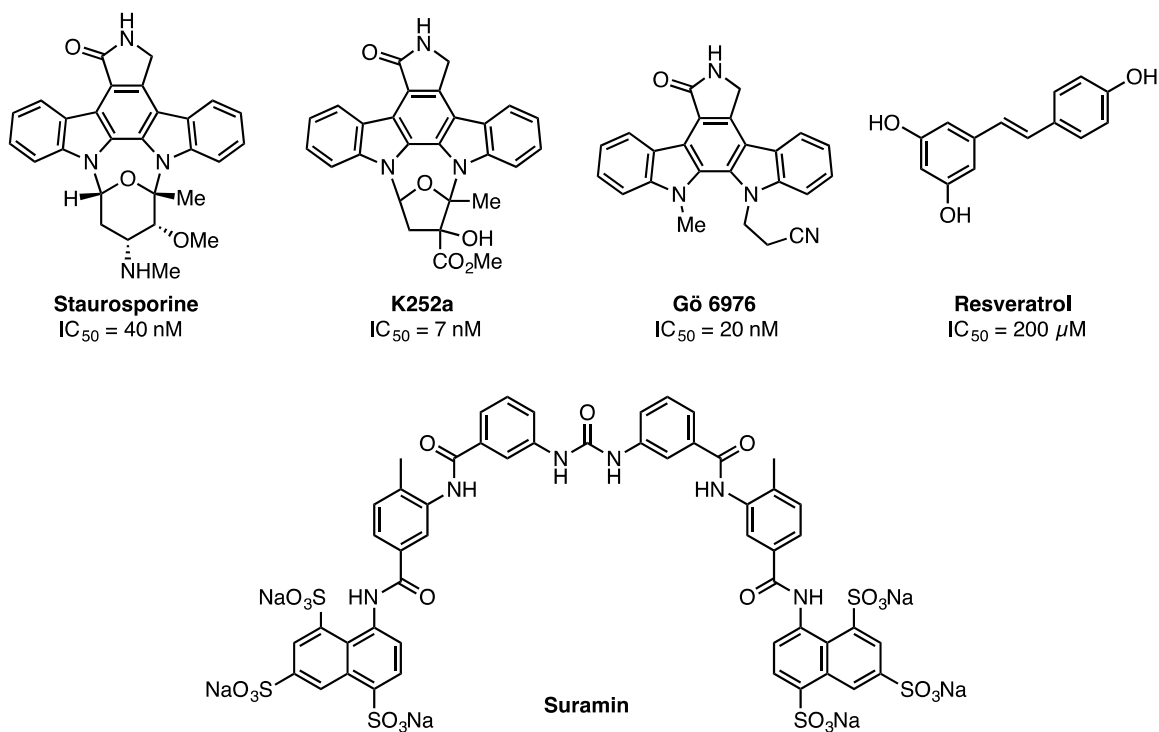


Figure 10. PKD inhibitors staurosporine, Gö6976, K252a, and resveratrol; and PKD activator suramin.

A major advance in this area was the identification and characterization of **CID755673** by Wipf and co-workers (Figure 11).⁶⁶ **CID755673** inhibited all PKD isoforms with an IC_{50} of 200-300 nM and showed specificity toward PKD over several related kinases. Notably, **CID755673** was not competitive with ATP for enzyme inhibition, suggesting an alternate binding site on the enzyme. Due to the highly conserved nature of ATP-binding domains among kinases, this alternative binding mode may account for the selectivity of **CID755673** for PKD compared to other protein kinases. Additionally, **CID755673** effectively blocked PKD-mediated cell functions and inhibited novel tumor-promoting functions of PKD in prostate cancer cells.⁶⁶⁻⁶⁷

Since the disclosure of **CID755673**, promising ATP-competitive inhibitors continue to emerge in the literature.^{58b,68} The novel 2,6-naphthyridine **3-1** was identified by a high

throughput screen (HTS) as a dual PKC/PKD inhibitor (Figure 11).^{68e} Modification of this hit in an effort to reduce the off-target effects and improve PKD selectivity led to a series of amidobipyridyl-based analogs.^{68f} **BPKDi** (Figure 11) was identified from this series as a potent and selective pan-PKD inhibitor with single-digit nanomolar IC₅₀ values and caused substantial inhibition of PKD1 signal-dependent phosphorylation and increased nuclear retention of class HDAC4 and HDAC5 in cardiomyocytes.^{58b}

The ATP-competitive, pan-PKD inhibitor **CRT0066101** was also reported to inhibit all isoforms of PKD with single-digit nanomolar IC₅₀ values (Figure 11).^{68a,68c} While **CRT0066101** was shown to block cell proliferation, induce apoptosis, and reduce the viability of pancreatic cancer cells both *in vitro* and *in vivo*, the most attractive features of **CRT0066101** are its reported orally availability and efficacy *in vivo*.^{68a,68c} Pyrazine benzamide **CRT5** inhibited PKD with an IC₅₀ value of 1.5 nM and suppressed VEGF-induced endothelial cell migration, proliferation, and tubulogenesis.⁶⁹ Lastly, a novel 3,5-diarylazole **3-2** (Figure 11) that was identified in a HTS showed moderate kinase inhibition and led to a series of promising benzamide analogs.^{68d} One analog in particular, **3-3** (Figure 11), inhibited all PKD isoforms with low nanomolar IC₅₀ values and had modest preference for PKD1 inhibition versus PKD2 and PKD3, respectively. Furthermore, **3-3** possessed high selectivity for PKD against a panel of other kinases and pharmacokinetic studies in rats.^{68d}

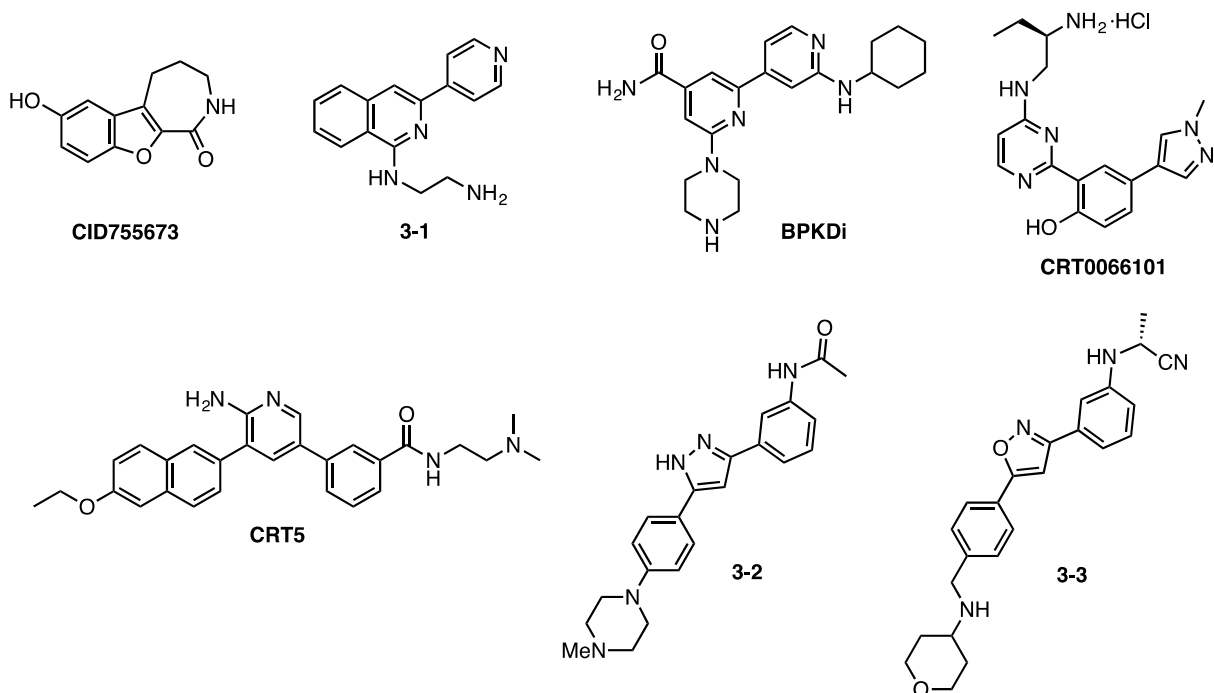


Figure 11. Recent PKD inhibitors from the research and patent literature.

3.1.3 Structure-Activity Relationship of CID755673: Previous Work in the Wipf Group

Despite the high specificity of **CID755673** and its potent *in vitro* inhibition of PKD, its cellular activity was relatively weak ($EC_{50} = 11.8 \mu\text{M}$).⁶⁶⁻⁶⁷ Recent evidence also suggests additional targets of **CID755673**,⁷⁰ but since this structure is not competitive with ATP for PKD inhibition, it represents an orthogonal approach to gain further understanding of the structure and function of PKD. In an effort to enhance the selectivity and potency for potential *in vivo* applications, Wipf and co-workers probed the SAR for **CID755673** by modification of the core structure as well as the side chains. To guide the design of these structural analogs and elucidate SAR, the parent compound CID755673 was dissected into four major structural zones (Figure 12).^{67,71}

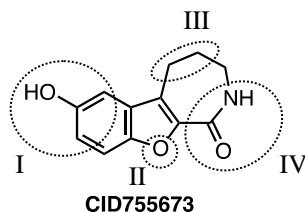
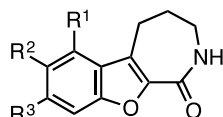


Figure 12. Major structural zones dissected for SAR analysis.

Zone I was modified to include functionalization of the aryl moiety and substitutions on the phenolic hydroxyl group (Table 8). Most of the zone I derivatives were less active than **CID755673**. Specifically, carbon substituents *ortho* to the phenol and *O*-acylations and silylations were detrimental to *in vitro* activity (Table 8, entries 4, 5, and 9), however *ortho*-halogenation and *O*-methylation and allylation were well tolerated (Table 8, entries 2, 3, and 6-8).

Table 8. PKD inhibitory activity of **CID755673** and zone I analogs.^{71b}

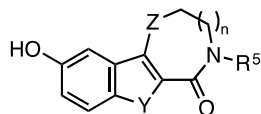


| Entry | Compound | Structure | | | IC ₅₀ | |
|-------|--------------------|----------------|----------------|----------------|--------------------------------|------------------------------------|
| | | R ¹ | R ² | R ³ | IMAP-FP PKD1 (μM) ^a | Radiometric PKD1 (μM) ^b |
| 1 | CID755673 | H | OH | H | 0.64 ± 0.03 | 0.182 ± 0.02 (<i>n</i> = 5) |
| 2 | kb-NB77-56 | H | OMe | H | 2.4 ± 0.14 | 2.39 (<i>n</i> = 1) |
| 3 | kb-NB77-84 | H | OAllyl | H | 2.6 ± 0.2 | 1.23 (<i>n</i> = 1) |
| 4 | kb-NB123-36 | H | OAc | H | 84.89 ± 3.21 | n.d. |
| 5 | kb-NB77-77 | H | OTBS | H | not inhibitory | n.d. |
| 6 | kb-NB77-88 | Cl | OH | H | 1.4 ± 0.1 | 0.892 (<i>n</i> = 1) |
| 7 | kb-NB96-21 | F | OH | H | 1.3 ± 0.05 | 0.238 (<i>n</i> = 1) |
| 8 | kb-NB96-43 | Cl | OH | Cl | not inhibitory | n.d. |
| 9 | kb-NB96-02 | Allyl | OH | H | 2.4 ± 0.3 | 1.58 (<i>n</i> = 1) |

^a PKD1 IC₅₀ was determined using an automated, HTS formatted IMAP-based PKD Fluorescence Polarization (FP) assay as previously described.⁶⁶ Each IC₅₀ was calculated as the mean ± SEM of at least three independent experiments with triplicate determinations at each concentration in each experiment; *n* = number of independent experiments. ^b PKD1 IC₅₀ was determined using a radiometric kinase activity assay as previously described.⁶⁶ Each IC₅₀ was calculated as the mean ± SEM with triplicate determinations at each concentration in each experiment; *n* = number of independent experiments.

In zone II, the replacement of the oxygen in the parent compound **CID755673** with sulfur resulted in enhanced activity, but replacement with nitrogen was associated with a loss of activity (Table 9, entries 2 and 3). In zone III, the ring size was altered by addition or removal of methylene groups and substitution at the benzylic position. Decreasing or increasing the azepinone ring size, although tolerated, resulted in reduced inhibitory activity relative to **CID755673** (Table 9, entries 7 and 8). All modifications of the azepinone moiety at the 5-position (Z), with the exception of thioether insertion, yielded analogs with reduced inhibitory activity (Table 9, entries 3-6). All modifications to zone IV, which included functional group interconversions and replacement of the amide moiety, did not enhance the inhibitory activity (Table 9, entries 9 and 10).

Table 9. PKD inhibitory activity of **CID755673** and zone II-IV analogs.^{71b}



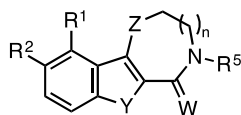
| Entry | Compound | Structure | | | | IC ₅₀ | |
|-------|---------------------|----------------|---|---|-----------------|--------------------------------|------------------------------------|
| | | R ⁵ | n | Y | Z | IMAP-FP PKD1 (μM) ^a | Radiometric PKD1 (μM) ^b |
| 1 | CID755673 | H | 1 | O | CH ₂ | 0.64 ± 0.03 | 0.182 ± 0.02 (n = 5) |
| 2 | kb-NB123-57 | H | 1 | N | CH ₂ | 2.14 ± 0.12 | 0.130 ± 0.01 (n = 3) |
| 3 | kb-NB142-70 | H | 1 | S | S | 0.71 ± 0.02 | 0.0283 ± 0.002 (n = 3) |
| 4 | kb-NB123-63 | H | 1 | O | C=O | 14.93 ± 1.17 | 0.850 ± 0.11 (n = 2) |
| 5 | kb-NB123-89 | H | 1 | O | CHOH | 24.09 ± 0.71 | 1.23 ± 0.21 (n = 2) |
| 6 | kb-NB142-05 | H | 1 | O | C=NNHPh | 21.70 ± 0.52 | 1.13 (n = 1) |
| 7 | kb-NB123-23A | H | 0 | O | CH ₂ | 12.6 ± 1.3 | 1.4 (n = 1) |
| 8 | kb-NB96-53 | H | 2 | O | CH ₂ | 8.3 ± 0.6 | 1.03 (n = 1) |
| 9 | kb-NB142-25 | Me | 1 | O | CH ₂ | n.d. | 4.02 ± 1.09 (n = 2) |
| 10 | kb-NB165-15 | | | | | n.d. | not inhibitory |

^a PKD1 IC₅₀ was determined using an automated, HTS formatted IMAP-based PKD Fluorescence Polarization (FP) assay as previously described.⁶⁶ Each IC₅₀ was calculated as the mean ± SEM of at least three independent experiments with triplicate determinations at each concentration in each experiment; *n* = number of independent experiments. ^b PKD1 IC₅₀ was determined using a radiometric kinase activity assay as previously described.⁶⁶ Each IC₅₀ was calculated as the mean ± SEM with triplicate determinations at each concentration in each experiment; *n* = number of independent experiments.

At this stage, benzothienothiazepinone **kb-NB142-70** emerged as the lead compound with *ca.* 7-fold increase in potency toward PKD1 with IC₅₀ values of 28.3 nM. This increased potency was further confirmed in cell-based assays for which the IC₅₀ was 2.2 μM, a 5-fold improvement over **CID755673** (IC₅₀ = 11.8 μM). At this point, further modifications to this lead compound according to the pharmacophore zones in Figure 12 were explored to elucidate essential SAR (Table 10).

Masking the hydroxyl group as methoxy analog **kb-NB165-09** was only slightly detrimental to PKD inhibition, while the benzyl derivative **kb-NB123-66** resulted in complete loss of inhibitory activity (Table 10, entries 3 and 4). Replacement of the hydroxyl moiety with the corresponding azide resulted in comparable *in vitro* and cellular activities (Table 10, entry 5). Iodination at R¹ was also well tolerated with an *in vitro* IC₅₀ of 114 nM (Table 10, entry 6). These data suggest that while the zone 1 binding pocket may be sterically restricting, the hydrogen-bond donor capability of the lead structure is not necessary for inhibitory activity.

Zone II and III modifications explored sulfur oxidations, thiazepinone ring enlargement, and opening of the thiazepinone ring. While sulfur oxidations provided analogs with significantly reduced inhibitory activity, increasing the azepinone ring size had only minor effects (Table 10, entries 7-9). The open chain analog did not show any PKD1 inhibition and implies that the zone III binding pocket may require the rigidity of the ring for optimal binding interactions (Table 10, entry 12). Finally, functional group interconversions and replacement of the amide moiety in zone IV did not enhance the inhibitory activity (Table 10, entries 10 and 11).

Table 10. PKD inhibitory activity of **kb-NB142-70** and zone I-IV analogs.^{71b}

| Entry | Compound | Structure | | | | | | | IC ₅₀ | |
|-------|--------------------|----------------|----------------|----------------|---|----------------|-----|-----------------|------------------------------------|---------------------------------|
| | | R ¹ | R ² | R ⁵ | n | W | Y | Z | Radiometric PKD1 (μM) ^a | Cellular PKD1 (μM) ^b |
| 1 | CID755673 | H | OH | H | 1 | O | O | CH ₂ | 0.182 ± 0.02 (n = 5) | 11.8 ± 4.0 (n = 3) |
| 2 | kb-NB142-70 | H | OH | H | 1 | O | S | S | 0.0283 ± 0.002 (n = 3) | 2.2 ± 0.6 (n = 3) |
| 3 | kb-NB165-09 | H | OMe | H | 1 | O | S | S | 0.0825 ± 0.005 (n = 4) | 3.1 ± 0.5 (n = 3) |
| 4 | kb-NB123-66 | H | OBn | H | 1 | O | S | S | not inhibitory | n.d. |
| 5 | mcf-292-08 | H | N ₃ | H | 1 | O | S | S | 0.0749 ± 0.01 (n = 5) | 2.2 ± 0.2 (n = 3) |
| 6 | kb-NB165-31 | I | OH | H | 1 | O | S | S | 0.114 ± 0.02 (n = 5) | 8.6 ± 2.0 (n = 3) |
| 7 | kb-NB184-25 | H | OMe | H | 1 | O | S=O | S | 1.08 (n = 1) | n.d. |
| 8 | kb-NB184-45 | H | OMe | H | 1 | O | S | S=O | not inhibitory | n.d. |
| 9 | kb-NB165-92 | H | OH | H | 2 | O | S | S | 0.111 ± 0.006 (n = 3) | 2.6 ± 0.7 (n = 2) |
| 10 | kb-NB165-17 | H | OH | Me | 1 | O | S | S | 0.450 ± 0.05 (n = 2) | n.d. |
| 11 | kb-NB165-83 | H | OH | H | 1 | H ₂ | S | S | 16.4 (n = 1) | n.d. |
| 12 | kb-NB184-80 | | | | | | | | not inhibitory | n.d. |

^a PKD1 IC₅₀ was determined using a radiometric kinase activity assay as previously described.⁶⁶ Each IC₅₀ was calculated as the mean ± SEM with triplicate determinations at each concentration in each experiment; *n* = number of independent experiments. ^b Cellular IC₅₀ was determined by densitometry analysis of Western blotting data for PKD1 autophosphorylation at S⁹¹⁶ in LNCaP cells as previously described.⁶⁷ Each IC₅₀ was calculated as the mean ± SEM of at least three independent experiments; *n* = number of independent experiments.

After initial activity screening of all of the derivatives (*ca.* 50), Wipf and co-workers identified five analogs that were of equal or greater potency compared to the parent compound **CID755678** (Figure 13). These five analogs were subjected to further analysis and each of the analogs demonstrated increased inhibition of PMA-induced autophosphorylation of PKD1, caused a dramatic arrest in cell proliferation, and inhibited cell migration and invasion.⁶⁷ From these experiments, **kb-NB142-70** and **kb-NB165-09** were identified to be the most potent and specific analogs both *in vitro* and in cells.

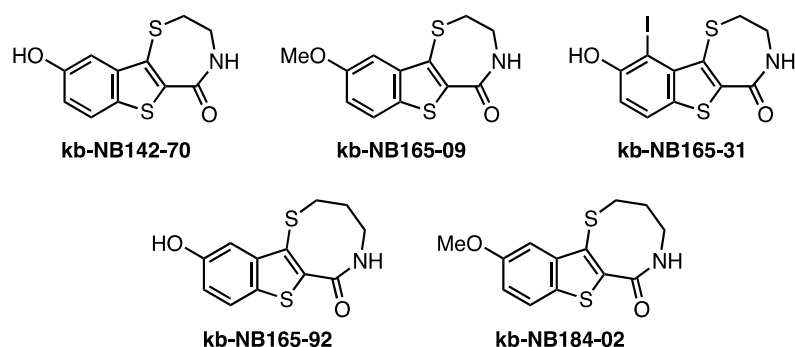


Figure 13. Chemical structure lead compound **kb-NB142-70** and four analogs.

The *in vivo* efficacy and pharmacokinetics of **kb-NB142-70** and **kb-NB165-09** were examined.⁷² The phenolic derivative, **kb-NB142-70**, was rapidly metabolized, with peak tumor concentrations of 11.8 nmol/g obtained at 5 min, and a plasma half-life of 6 min. The major metabolite of **kb-NB142-70** was identified by LC/MS-MS to be an *O*-glucuronide. The methoxy analog, **kb-NB165-09**, which featured protection of the major site of metabolism, showed a maximum tumor concentration of 8.0 nmol and a 2.3-fold increase in the plasma half-life from 6 to 14 min. Metabolite studies of **kb-NB165-09** did not reveal **kb-NB142-70** as a metabolite, suggesting that the methoxy group diverts metabolism from glucuronidation to primarily oxidation. Based on these data, the therapeutic potential of **kb-NB142-70** and **kb-169-05** is limited.

3.2 RESULTS AND DISCUSSION

With rapid metabolism being a major roadblock in tuning the efficacy of **kb-NB142-70** and **kb-NB165-09** *in vivo*, we envisioned a zone I modification to install a heteroaryl moiety in place of the aryl group (Figure 14). The replacement of an aryl group with a heteroaryl group is a

classical bioisosteric replacement used to enhance the physical properties and metabolic stability of a drug.⁷³ The incorporation of heterocyclic moieties serves to replace the site of metabolism, decrease the basicity of the ring, and lower the LogD.

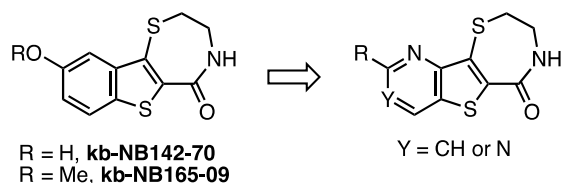
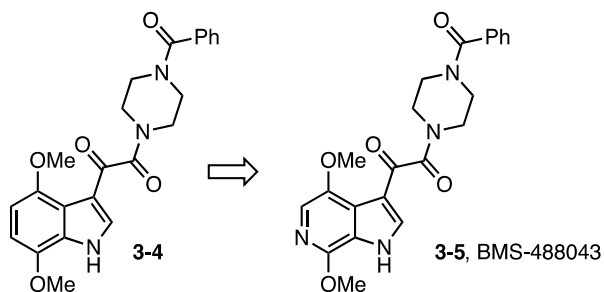


Figure 14. Zone I modification of the lead compounds to install a pyrimidine moiety.

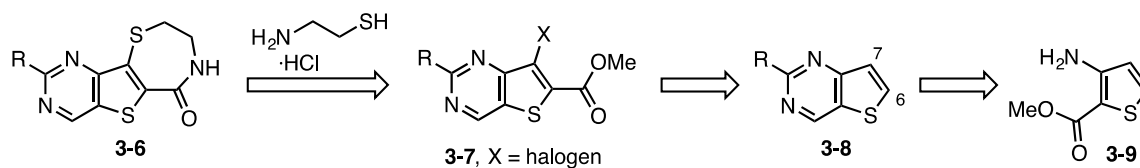
This strategy has been successfully implemented to improve the metabolic profiles in the development of several clinical candidates.⁷³ An example of this was reported by Kadow and co-workers for a series of HIV-1 inhibitors.⁷⁴ Indole **3-4** was a potent antiviral agent, but suffered from rapid metabolism via *O*-demethylation (Scheme 21). Systematic replacement of the aromatic CH sites with N yielded analog **3-5**, which possessed improved aqueous solubility and eliminated the potential for quinone formation in the event of demethylation (Scheme 21).⁷⁴ Analog **3-5** was advanced to clinical trials for the inhibition of HIV-1 in human subjects.⁷⁴



Scheme 21. Bioisosteric replacement of aromatic CH with N to yield clinical candidate **3-5**.

3.2.1 Synthesis of Thieno[3,2-*d*]pyrimidine-Based Analogs

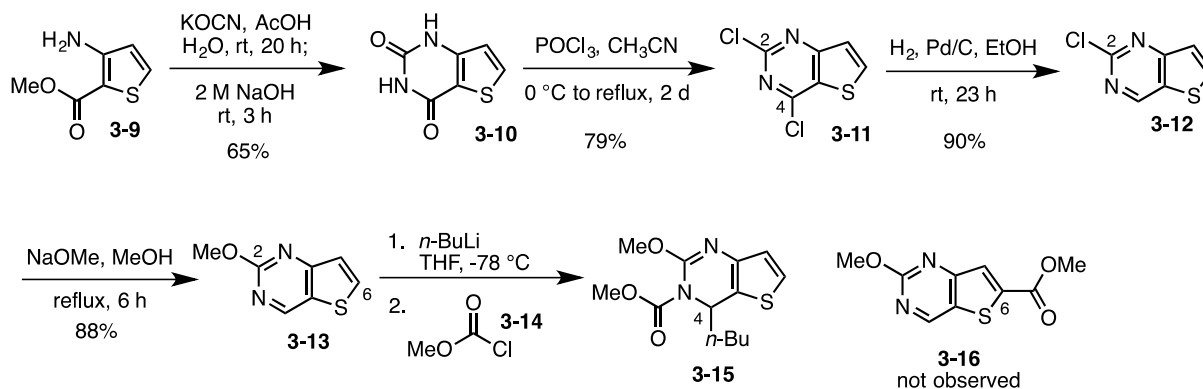
Our synthetic approach to the thieno-[3,2-*d*]pyrimidine-containing analogs **3-6** would feature formation of the thiazepinone moiety via one-pot nucleophilic displacement-condensation reaction of **3-7** with cysteamine hydrochloride (Scheme 22). We envisioned a directed metalation of **3-8** at the C-6 position and trapping with a suitable electrophile would install the requisite ester. Regioselective halogenation at position C-7 would provide access to **3-7**. Precursor **3-8** would be readily prepared by pyridimine formation of commercially available 3-aminothiophene-2-carboxylate (**3-9**).



Scheme 22. Retrosynthetic approach to thieno[3,2-*d*]pyrimidine analogs **3-6**.

Synthesis of the requisite cyclization precursor **3-7** began with thiophene **3-9** (Scheme 23). Formation of the pyrimidine moiety using potassium cyanate, followed by chlorination with POCl_3 gave dichloride **3-11**.⁷⁵ Palladium-catalyzed regioselective dechlorination of **3-11** in the presence of Na_2CO_3 occurred exclusively at the C-4 position,⁷⁶ and substitution of the remaining C-2 chloride with methoxide provided **3-13** in 79% yield over the two steps. At this point we envisioned elaboration of the thiophene C-6 position to be achieved via directed lithiation using *n*-butyllithium, followed by quenching with methylchloroformate (**3-14**). Unfortunately, subjecting of **3-13** to these conditions did not give the desired C-6 functionalized product **3-16**. Rather, analysis of the crude reaction mixture by ^1H NMR indicated nucleophilic addition of the

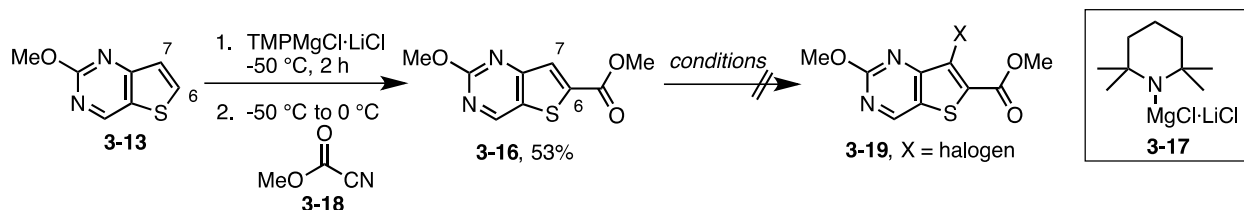
base at the C-4 position (**3-15**). This result is well documented in the literature, and is due to the electrophilic nature of the ring, which can readily undergo addition at position C-4.⁷⁷ Direct functionalization of these pyrimidine-containing systems by lithiation is indeed difficult and often requires low temperature or the use of less nucleophilic bases.^{77a,b}



Scheme 23. Attempted synthesis of **3-16**.

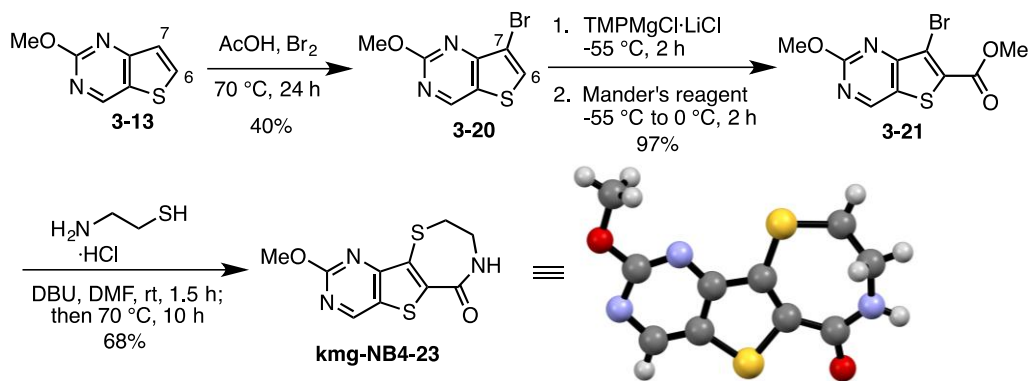
In light of this result, we sought to avoid the use of strong nucleophilic bases, such as *n*-BuLi, and instead use the mixed lithium and magnesium base, TMPMgCl·LiCl (**3-17**), reported by Knochel and co-workers.⁷⁸ Treatment of **3-13** with freshly prepared TMPMgCl·LiCl^{78d} and subsequent quenching with Mander's reagent (**3-18**), resulted in exclusive regioselective metalation at the C-6 position to provide target compound **3-16** in 53% yield (Scheme 24). With the desired methyl ester in hand, the selective halogenation at position C-7 was explored. Attempts to introduce a halogen atom using directed metalation at position C-7 and quenching with I₂ or I(CH₂)₂I resulted in no reaction in cases where *s*-butyllithium was used and both C-4 and C-7 halogenated products were observed in the case of TMPMgCl·LiCl. Electrophilic halogenation of **3-16** using *N*-bromosuccinimide, *N*-chlorosuccinimide, or bromine under a variety of different solvent and temperature conditions gave no reaction; and, in all cases starting

material was recovered. The lack of reactivity at the C-7 position is presumably a result of the presence of the methyl ester at position C-6, which deactivates the C-7 position towards electrophilic attack.



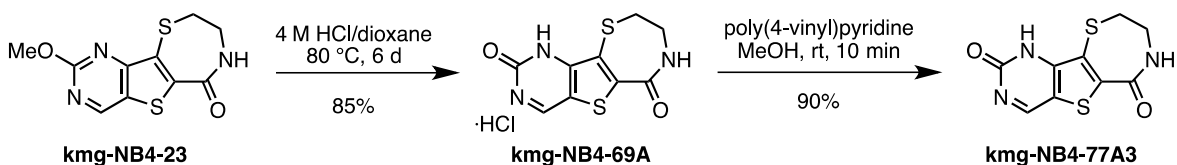
Scheme 24. Regioselective metalation at positions C-6 and C-7.

In order to circumvent this problem, we explored the halogenation of **3-13** prior to the installation of the methyl ester (Scheme 25). Electrophilic bromination of **3-13** using Br₂ in AcOH⁷⁹ gave the desired C-7 brominated compound **3-20** in modest yield. Functionalization of position C-6 under Knochel's conditions,^{78a-c} as in Scheme 24, gave the required cyclization precursor **3-21** in excellent yield. Formation of the thiazepinone moiety was achieved by a one-pot nucleophilic displacement-condensation reaction of **3-21** with cysteamine hydrochloride and provided the desired methoxy analog **kmg-NB4-23** in good yields. A crystal structure of **kmg-NB4-23** was obtained and confirms the regioselectivities of the synthetic sequence (Scheme 25, Appendix A.2). This structure has been deposited at the Cambridge Crystallographic Data Centre and allocated the deposition number CCDC 822403.



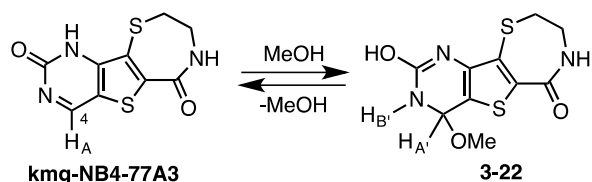
Scheme 25. Synthesis of thieno[3,2-*d*]pyrimidine analog **kmg-NB4-23**.

At this point, all that remained was *O*-demethylation of **kmg-NB4-23** to arrive at **kmg-NB4-69A**. This seemingly trivial transformation could not be affected under a variety of demethylation conditions. Treatment of **kmg-NB4-23** with BBr_3 or NaI in AcOH at elevated temperatures resulted in quantitative recovery of starting material. In contrast, both concentrated aqueous HCl and HI provided complete consumption of starting material; however, the desired product was not detected. Treatment of **kmg-NB4-23** with 33% HBr in AcOH under reflux conditions did provide the desired product **kmg-NB4-69A**, however the reaction was low-yielding and irreproducible. From these data, it was clear that reactivity could only be affected under strongly acidic conditions, but that aqueous reaction and workup conditions must be avoided. Therefore, **kmg-NB4-23** was subjected to 4 M HCl in 1,4-dioxane. Gratifyingly, we observed complete conversion of the starting material to the desired product **kmg-NB4-69A** after 6 days (Scheme 26). The product from this reaction was isolated as the hydrochloride salt and could be readily converted to the free base upon treatment with poly(4-vinyl)pyridine (Scheme 26). As in the case of **kmg-NB4-69A**, it was imperative that aqueous reaction and workup conditions be avoided for the formation of the free base.



Scheme 26. Synthesis of thieno[3,2-*d*]pyrimidine analogs **kmg-NB4-69A** and **kmg-NB4-77A3**.

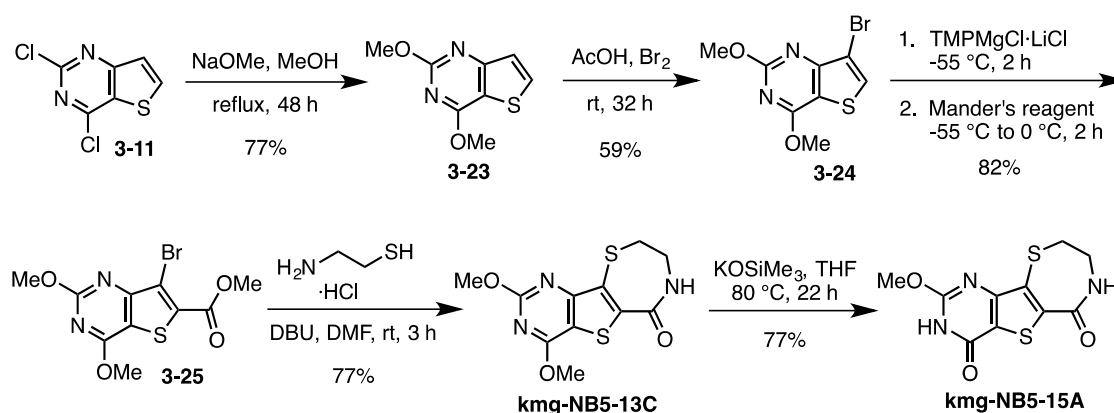
An interesting observation was noted regarding the stability of compounds **kmg-NB4-69A** and **-77A3**. After treatment with methanol, a *ca.* 2:1 ratio of **kmg-NB4-69A/77A3** and **3-22** was observed by ^1H NMR (Scheme 27). The structure of **3-22** was proposed based on the diagnostic $-\text{OCH}_3$ peak at 3.10 ppm, a pair of doublets at 8.20 and 5.74 ppm ($\text{H}_{\text{B}'}$ and $\text{H}_{\text{A}'}$, respectively). This structure was further supported by observing that **3-22** is converted to **kmg-NB4-69A/77A3** upon removal of methanol. To confirm this hypothesis, **kmg-NB4-69A/77A3** was dissolved in $\text{DMSO-}d_6$ and $\text{MeOD-}d_4$ was added. The ^1H NMR revealed a *ca.* 2:1 mixture of **kmg-NB4-69A/77A3** and **3-22**, which supports our hypothesis that **kmg-NB4-69A/77A3** can be converted to **3-22** in the presence of methanol. Similarly, it has been reported that the recrystallization of 2-pyrimidinones from methanol results in the formation of the corresponding methanol adducts, which readily lose methanol upon warming.⁸⁰



Scheme 27. Conversion of **kmg-NB4-69A/77A3** to **3-22** in the presence of MeOH.

Since the C-4 position was susceptible to nucleophilic attack, we decided to synthesize analogs that featured protection at this site. To this end, we utilized dichloropyrimidine **3-11** as

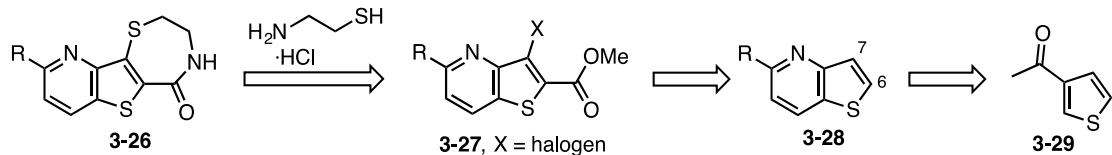
the common intermediate. Similarly to the above synthetic sequence, **3-11** was treated with NaOMe at reflux to provide dimethoxypyrimidine **3-23**, followed by regioselective functionalization to provide **3-25** (Scheme 28). Treatment of **3-25** with cysteamine hydrochloride provided the desired C-4 protected analog **kmg-NB5-13C**. Selective methyl deprotection of the C-4 position provided **kmg-NB5-15A**. Attempts to obtain the corresponding dihydroxypyrimidine were unsuccessful.



Scheme 28. Synthesis of C-4 protected thieno[3,2-*d*]pyrimidine analogs **kmg-NB5-13C** and **kmg-NB5-15A**.

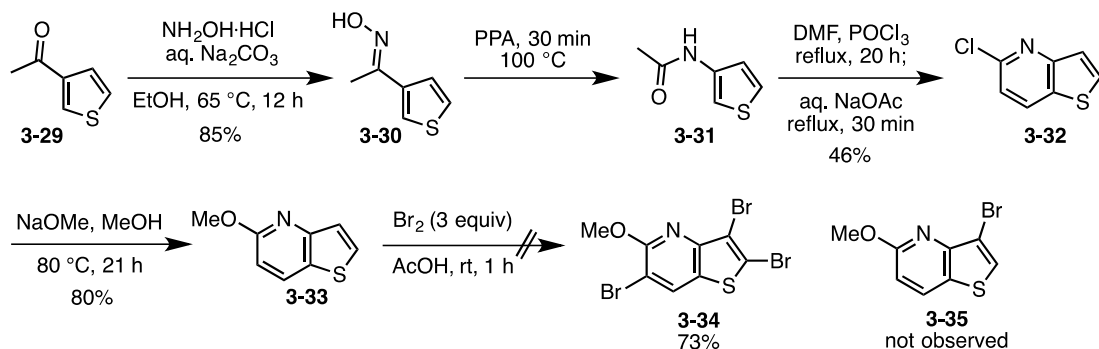
3.2.2 Synthesis of Thieno[3,2-*b*]pyridine-Based Analogs

In an attempt to gain further insight into the SAR and metabolic stability, we sought an additional modification to zone I by introducing the pyridine moiety (Scheme 29). Our synthetic strategy to access the thieno[3,2-*b*]pyridine-based analogs was analogous to the route employed for the thieno[3,2-*d*]pyrimidine series. We envisioned the last step to be thiazepinone ring formation via intermediate ester **3-27**. Ester **3-27** would arise from regioselective functionalization of the thieno[3,2-*b*]pyridine core (**3-28**). The core would be synthesized from commercially available 3-acetylthiophene **3-29** according to literature protocol (Scheme 29).⁸¹



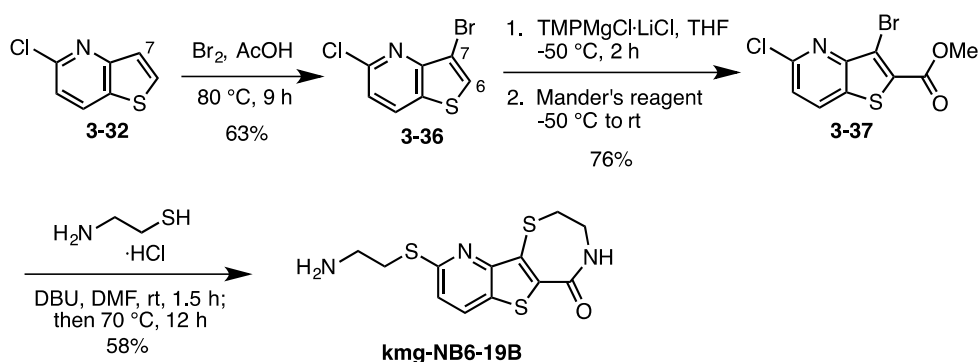
Scheme 29. Retrosynthetic strategy to access thieno[3,2-*b*]pyridine analogs **3-23**.

Beginning with 3-acetylthiophene **3-29**, oxime **3-30** was obtained using standard conditions using hydroxylamine hydrochloride.⁸² Beckmann rearrangement⁸³ of **3-30** furnished 3-acetamidothiophene **3-31**, which was subjected to Vilsmeier reagent⁸⁴ in order to generate the desired thieno[3,2-*b*]pyridine core (**3-32**).⁸¹ Chloride displacement using refluxing NaOMe provided the desired precursor for regioselective functionalization. We envisioned regioselective bromination to occur under the same conditions as in the case of the thieno[3,2-*d*]pyrimidine series. Treatment of **3-33** with Br₂ and AcOH at room temperature resulted in complete consumption of starting material after 1 h. Unfortunately, the undesired tribrominated product **3-34** was isolated in 73% yield. It was apparent that the 2-methoxypyridine **3-33** was much more activated toward electrophilic additions than the corresponding 2-methoxypyrimidine **3-13**.



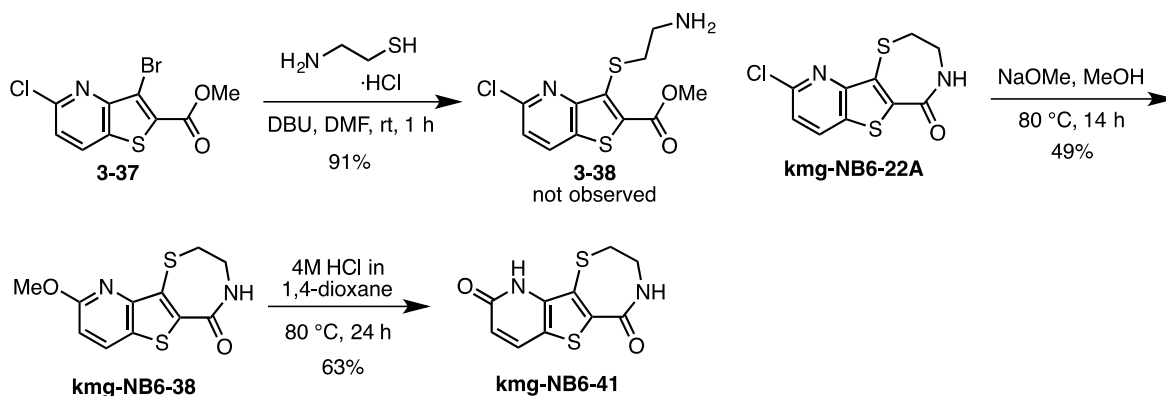
Scheme 30. Attempted synthesis of thieno[3,2-*b*]pyridine analogs.

To circumvent this issue, we subjected chloropyridine **3-32** to the bromination conditions prior to treatment with NaOMe (Scheme 31). This strategy provided the desired mono-brominated product **3-36** in good yield. Regioselective metalation of **3-36** at position C-6 and subsequent trapping with Mander's reagent⁸⁵ afforded the cyclization precursor **3-37** in 76% yield with exclusive selectivity. Thiazepinone formation under the previously reported conditions (Scheme 25) using excess cysteamine hydrochloride gave the unexpected thioether **kmg-NB6-19B**.



Scheme 31. Revised synthetic approach to thieno[3,2-*b*]pyridine analogs.

To avoid the displacement of both halogens during thiazepinone formation, the reaction was performed in a step-wise manner (Scheme 32). Serendipitously, treatment of **3-37** with 1.5 equivalents of cysteamine hydrochloride at room temperature did not provide the expected product **3-38**, but rather the thiazepinone **kmg-NB6-22A** in excellent yield. Methoxide displacement and subsequent methyl deprotection provided target analogs **kmg-NB6-38** and **kmg-NB6-41**, respectively (Scheme 32).

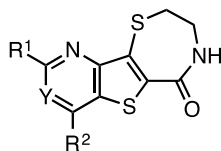


Scheme 32. Revised synthesis of thieno[3,2-*b*]pyridine analogs.

3.2.3 Biological Activity of Analogs

The *in vitro* and cellular PKD inhibitory activities of these novel thieno[3,2-*d*]pyrimidine- and thieno[3,2-*b*]pyridine-based analogs were determined and the results are summarized in Table 11.^{71,86} Methoxy analog **kmg-NB4-23** was a potent pan-PKD inhibitor with nanomolar IC₅₀ values, which is only a slight decrease in activity compared to the parent compound **kb-NB165-09** (Table 11, entry 1). In contrast, **kmg-NB4-69A** had only weak inhibitory activity against PKD1 and the corresponding free base **kmg-NB4-77A3** was inactive towards inhibition of PKD1 (Table 11, entries 2 and 3). The lack of activity of the hydroxy analogs is presumably due to the instability of this compound towards nucleophilic addition at the C-4 position, as noted in section 3.2.1. Unfortunately, all but two compounds in the thieno[3,2-*b*]pyridine series lacked PKD inhibitory activity. Analogs **kmg-NB6-19B** and **kmg-NB6-38** showed good activities in the radiometric kinase assay; however, both compounds were inactive in the corresponding cellular assays.

Table 11. Chemical structures and PKD1 inhibitory activities of the thieno[3,2-*d*]pyrimidine and thieno[3,2-*b*] analogs.^{71b,86}



| Entry | Compound | Structure | | | % PKD activity at (1 μ M) | IC ₅₀ | |
|----------------|---------------------|---|----------------|----|-------------------------------|--|---------------------------------------|
| | | R ¹ | R ² | Y | | Radiometric PKD1 (μ M) ^a | Cellular PKD1 (μ M) ^b |
| 1 | kmg-NB4-23 | OMe | H | N | n.d. | 0.124 \pm 0.031 (<i>n</i> = 4) | 6.8 \pm 1.3 (<i>n</i> = 3) |
| 2 ^c | kmg-NB4-69A | OH | H | N | n.d. | 25.3 (<i>n</i> = 1) | n.d. |
| 3 | kmg-NB4-77A3 | OH | H | N | n.d. | not inhibitory | n.d. |
| 4 | kmg-NB5-13C | OMe | OMe | N | n.d. | >30 (<i>n</i> = 2) | n.d. |
| 5 | kmg-NB5-15A | OMe | OH | N | n.d. | >30 (<i>n</i> = 2) | n.d. |
| 6 | kmg-NB6-19B | -S(CH ₂) ₂ NH ₂ | H | CH | 46.3 \pm 0.7 | 0.453 \pm 0.013 (<i>n</i> = 3) | >50 |
| 7 | kmg-NB6-22A | Cl | H | CH | 70.7 \pm 8.8 | n.d. | n.d. |
| 8 | kmg-NB6-38 | OMe | H | CH | 33.2 \pm 2.5 | 0.234 \pm 0.015 (<i>n</i> = 3) | > 50 |
| 9 | kmg-NB6-41 | OH | H | CH | 97.1 \pm 1.7 | n.d. | n.d. |

^a PKD1 IC₅₀ was determined using a radiometric kinase activity assay as previously described.⁶⁶ Each IC₅₀ was calculated as the mean \pm SEM with triplicate determinations at each concentration in each experiment; *n* = number of independent experiments. ^b Cellular IC₅₀ was determined by densitometry analysis of Western blotting data for PKD1 autophosphorylation at S⁹¹⁶ in LNCaP cells as previously described.⁶⁷ Each IC₅₀ was calculated as the mean \pm SEM of at least three independent experiments; *n* = number of independent experiments. ^c HCl salt.

From these studies, **kmg-NB4-23** emerged as the most potent compound. This analog not only validates our design, but also suggests that the zone I binding pocket is tolerant to a decrease in electron density in the aryl region. Despite the decrease in activity on going from *in vitro* to cellular assays, the cellular activity was promising for further biological testing. The low aqueous solubility posed a significant challenge and led us to explore injectable formulations of **kmg-NB4-23**. The concentration of the formulations was determined by UV-Vis using a standard curve. We first tried the mixed organic/aqueous formulations such as Solutol® HS 15, Cremaphor® EL, Povidone®, DMSO, NMP, and MMS-350. The solubility in each of these formulations was <0.2 mg/mL. We also tried to solubilize **kmg-NB4-23** via cyclodextrin complexation using β -cyclodextrin and hydroxypropyl- β -cyclodextrin. The highest concentration

obtained was <0.4 mg/mL, which prevented the evaluation of the pharmacokinetics, efficacy, and metabolism of this compound.

Although this compound could not be formulated for intravenous administration, it was administered to nude mice bearing s.c. prostate cancer (PC3) xenografts via oral gavage to determine *in vivo* efficacy.⁸⁶ Preliminary data demonstrate that when mice are treated with **kmg-NB4-23** alone there is a decrease in the mean tumor weight and volume; although, the differences were not statistically relevant (Figure 15).⁸⁶ In contrast, when mice were treated with a combination of **kmg-NB4-23** and **PX-866**,^{26c} a known pan-PI3K tumor growth inhibitor, an apparent additive effect is observed.⁸⁶ These data are preliminary and must be confirmed prior to moving forward with this class of inhibitors.

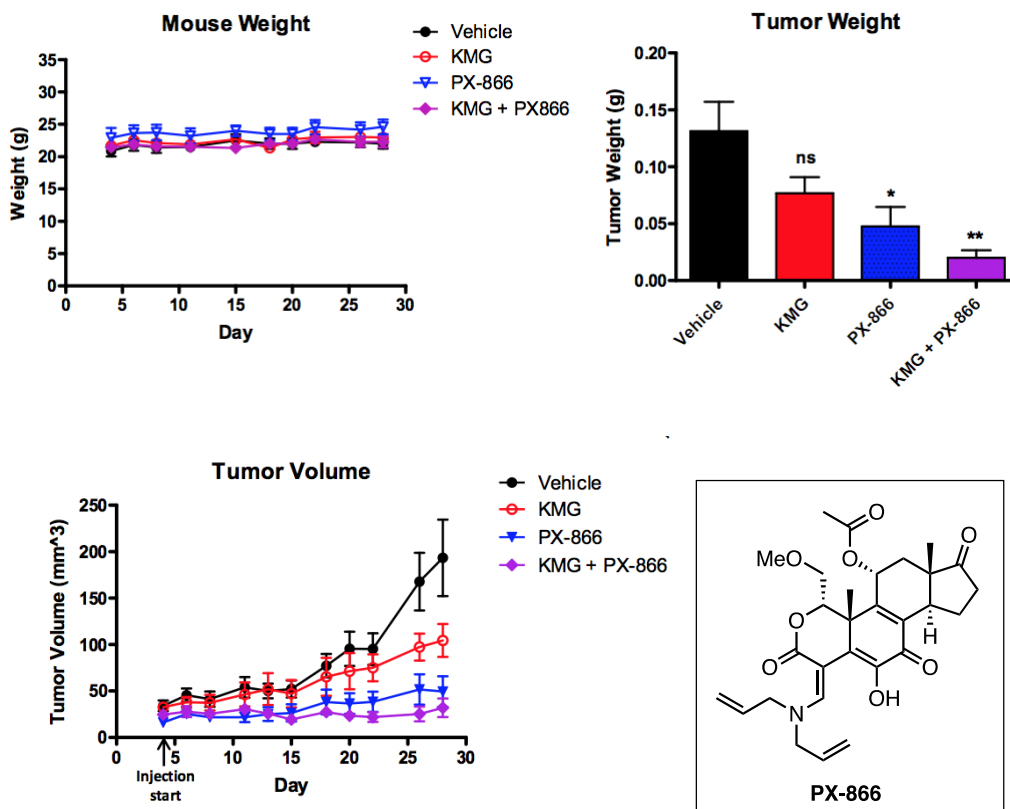


Figure 15. Effect of **kmg-NB4-23** (KMG) on PC3 s.c. tumor xenografts in nude mice and the structure of **PX-866**.⁸⁶

3.3 CONCLUSION

A series of thieno[3,2-*d*]pyrimidine- and thieno[3,2-*b*]pyridine-based inhibitors were successfully synthesized to probe the effects of the incorporation of heteroaryl moieties.⁷¹ One promising analog, **kmg-NB4-23**, was a potent pan-PKD inhibitor with an IC_{50} of 124 nM. This result validates our inhibitor design and shows that a decrease in the electron density of the heterocyclic scaffold is well tolerated in the zone 1 binding pocket. Although the limited aqueous solubility prevented the evaluation of the pharmacokinetic and metabolism data, the

compound was administered to nude mice bearing s.c. prostate cancer (PC3) xenografts via oral gavage to determine *in vivo* efficacy.⁸⁶ These data are preliminary, but do indicate that **kmg-NB4-23** may be capable of reducing tumor growth when used alone or in combination with the known inhibitor **PX-866**.

4.0 INVESTIGATION OF AN ALKENE ISOMERIZATION REACTION DURING THE PREPARATION OF TRICYCLIC ISOINDOLINONES

4.1 INTRODUCTION

Isoindolinones have demonstrated a variety of pharmacological activities including anti-inflammatory,⁸⁷ antihypertensive,⁸⁸ vasodilatory,⁸⁹ antipsychotic,⁹⁰ and anticancer effects.⁹¹ These heterocycles also represent a common scaffold seen in many natural products such as magallanesine,⁹² lennoxamine,⁹³ and clitocybin A,⁹⁴ as well as drug candidates such as pagoclone (Figure 16).⁹⁵ A variety of approaches for the preparation of these biologically relevant heterocycles have been explored.⁹⁶ The Wipf group has reported a synthetic approach to isoindolinones via the addition of functionalized alkenylalanines to phthalimide and succinamide derived *N*-acyliminium ions (Scheme 33).⁹⁷ This method is highly amenable to chemical library synthesis due to the commercial availability or ease of preparation of the starting materials, as well as the opportunities for further functionalization of the scaffold. Of particular interest to the Wipf group was the ring closing metathesis of the alkene addition product (**4-3**) which affords structurally novel tricyclic isoindolinones containing a newly formed seven-membered ring (**4-4**) (Scheme 33).⁹⁷ This concept was further developed toward a library synthesis of novel tricyclic isoindolinone amino alcohols **4-5** (Scheme 33). During the preparation of this library, a unique alkene isomerization was observed by our group.

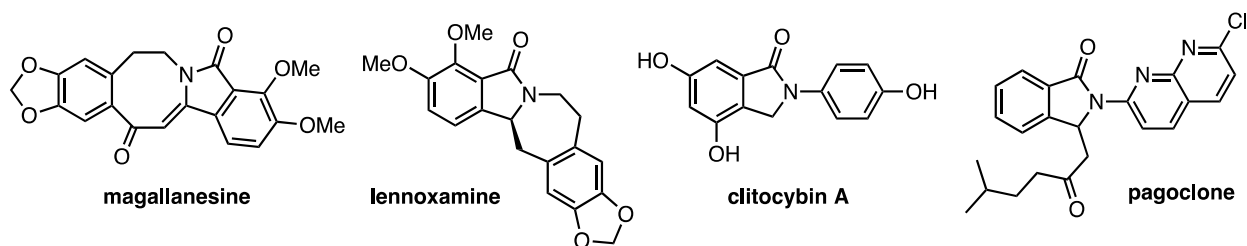
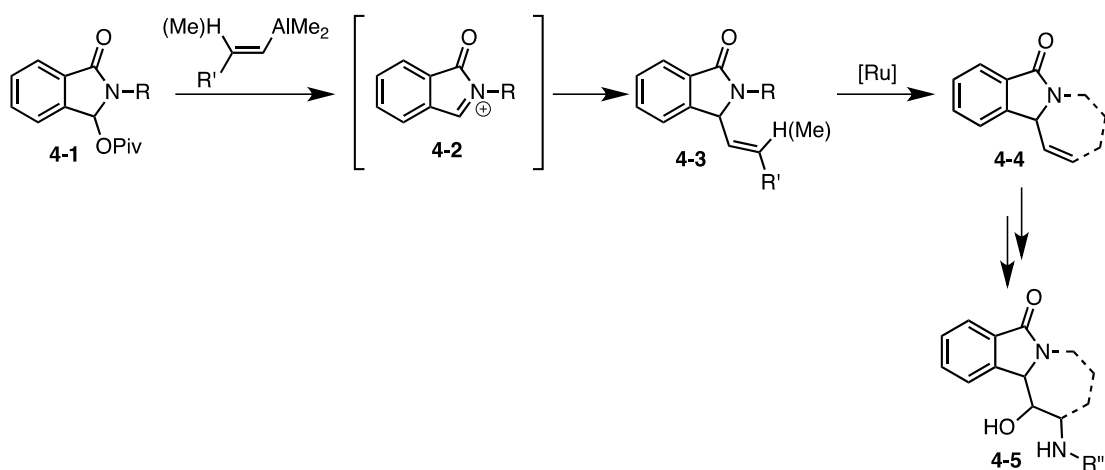


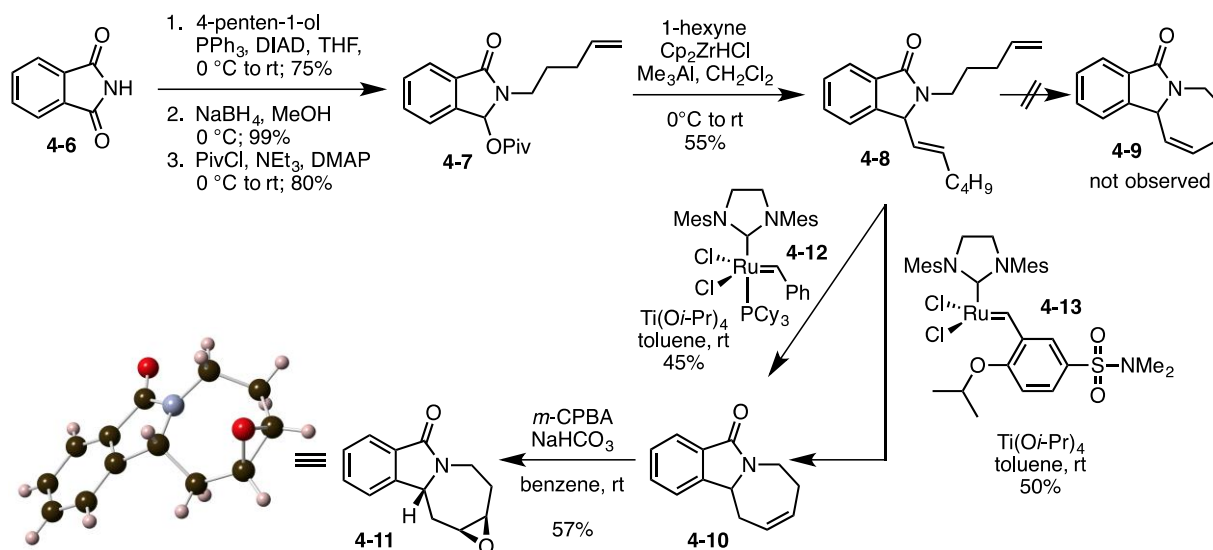
Figure 16. Isoindolinone natural products and pharmaceuticals.⁹⁸



Scheme 33. Wipf group approach to isoindolinones⁹⁷ and strategy for the preparation of a library of tricyclic isoindolinone amino alcohols (**4-5**).⁹⁸

Preparation of the library began with *N*-alkylation of phthalimide (**4-6**) with 4-penten-1-ol under Mitsunobu conditions. Subsequent NaBH₄ reduction and protection of the intermediate hemiaminal as the pivaloate provided alkene **4-7** in 59% overall yield (Scheme 34). Hydrozirconation-transmetalation of 1-hexyne generated the alkenylalane *in situ*, which reacted with the *N*-acyliminium ion of **4-7** to afford diene **4-8**.^{97,99} Ring-closing metathesis of **4-8** using Grubbs 2nd generation catalyst **4-12**^{90b} was carried out in the presence of 1 equiv of Ti(O*i*-Pr)₄ at room temperature.¹⁰⁰ Surprisingly, the alkene-isomerized homoallylic amide **4-10** was isolated rather than the expected allylic amide **4-9** (Scheme 34). To explore the reproducibility of this

result, the RCM was carried out using Zhan catalyst-1B (**4-13**).¹⁰¹ The alkene-isomerized product **4-10** was isolated in 50% yield. Epoxidation of **4-10** using NaHCO₃-buffered *meta*-chloroperbenzoic acid (*m*-CPBA) afforded epoxide **4-11** in 57% yield. X-ray analysis of **4-11** confirmed the formation of the alkene-isomerized product **4-10** (Scheme 34).



Scheme 34. Synthesis of isomerized azepinoisoindolinone **4-10** and epoxide **4-11**.⁹⁸

The unexpected formation of isomerization product **4-10** under the aforementioned metathesis conditions could be explained by a ruthenium-catalyzed double bond isomerization.¹⁰² The release of ring strain can only be partially responsible for this isomerization process since the analysis of the 5 possible alkene isomers of **4-9** using DFT calculations indicated a decrease in relative energy from **4-9** to **4-10**, while other isomers were even lower in energy (**4-14–16**) (Figure 17).

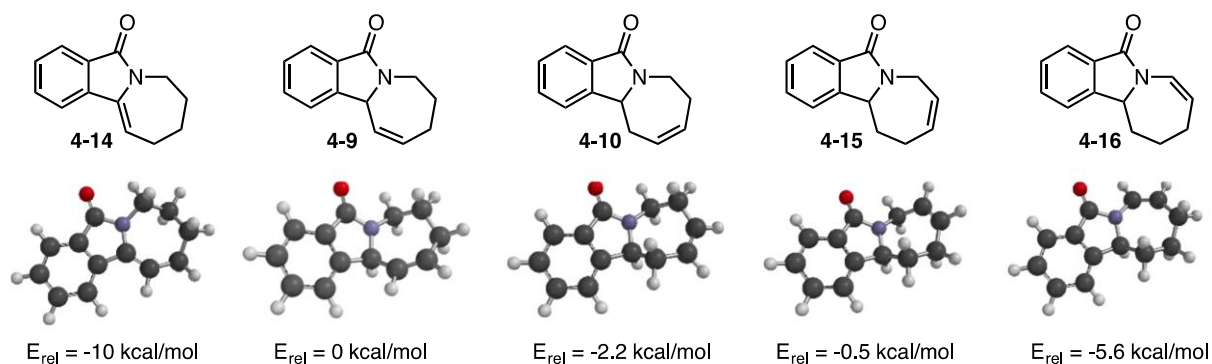
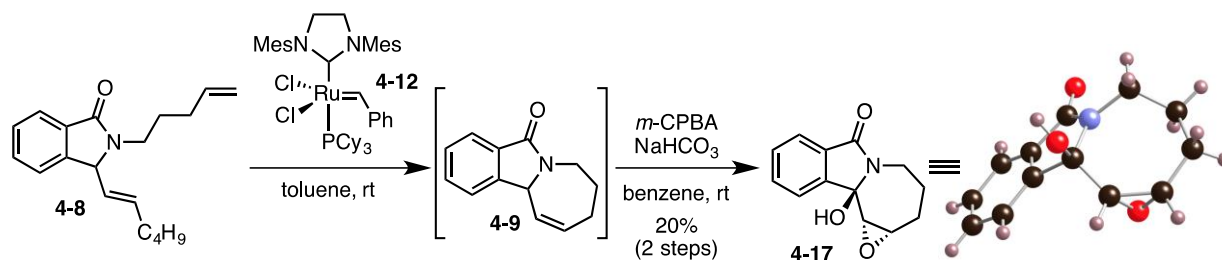


Figure 17. Relative energies of alkene isomers based on RB3LYP/6-311G* calculations with MacSpartan '06.⁹⁸

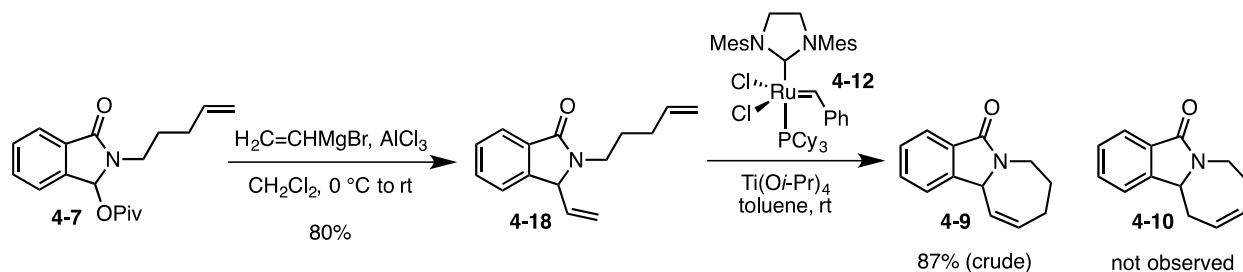
To further investigate the factors influencing the alkene isomerization process, Wipf and co-workers conducted the ring-closing metathesis in the absence of $\text{Ti}(\text{O}i\text{-Pr})_4$ (Scheme 2). The resulting product was quite unstable and was therefore immediately subjected to *m*-CPBA epoxidation conditions to provide **4-17** in modest yields. The structure of **4-17** was assigned by X-ray analysis (Scheme 35) and implies the intermediate presence of the expected RCM product **4-9**. The isolation of **4-17**, and the absence of significant quantities of **4-11**, suggests the chelating additive $\text{Ti}(\text{O}i\text{-Pr})_4$ is the primary factor responsible for the isomerization of **4-9** to **4-10** in Scheme 34. The ability of $\text{Ti}(\text{O}i\text{-Pr})_4$ to induce alkene isomerization during the RCM reaction is noteworthy. Although there are a number of additives known to decrease the rate of isomerization in RCM,¹⁰³ we are unaware of a previous report on an alkene isomerization-promoting effect of an additive in this reaction.



Scheme 35. Ring-closing metathesis of diene **4-8** in the absence of $\text{Ti}(\text{O}i\text{-Pr})_4$ and hydroxyepoxide **4-17**.⁹⁸

4.2 RESULTS AND DISCUSSION

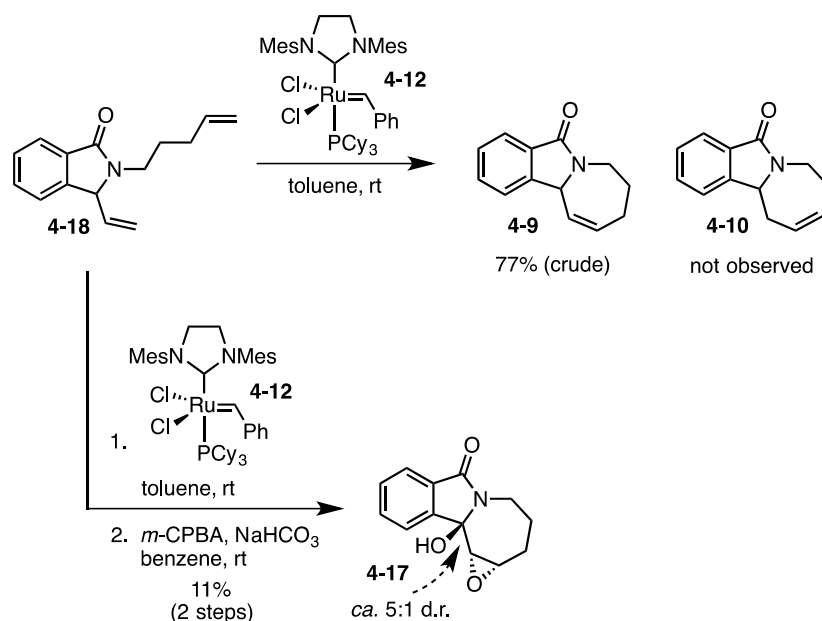
To further investigate the factors influencing the alkene isomerization process, we studied the influence of the diene substitution pattern on the rate of isomerization from **4-9** to **4-10** (Scheme 36). Addition of *in situ* prepared vinyl alkane to pivaloate **4-7** provided **4-18** in 80% yield. RCM of **4-18** using Grubbs 2nd generation catalyst in the presence of $\text{Ti}(\text{O}i\text{-Pr})_4$ gave **4-9** exclusively. No alkene isomerization was observed and homoallylic amide **4-10** was not detected in the reaction mixture.



Scheme 36. Preparation and RCM reaction in the presence of $\text{Ti}(\text{O}i\text{-Pr})_4$ of bis-terminal diene **4-18**.⁹⁸

Next, we performed the RCM in the absence of $\text{Ti}(\text{O}i\text{-Pr})_4$ (Scheme 37). Crude **4-9** was obtained in 77% yield. Product **4-9** was difficult to purify due to its chemical instability.

Therefore, the RCM reaction of **4-9** was conducted on larger scale in the absence of $\text{Ti}(\text{O}i\text{-Pr})_4$, and the crude intermediate was subjected to *m*-CPBA oxidation. Epoxide **4-17** was isolated in 11% overall yield and LCMS and NMR analysis suggested a 5:1 ratio of epimers at the hemiacetal carbon. The spectral data of epoxide **4-17** matched the spectra isolated from the route in Scheme 35. This result provides further support for the exclusive formation of alkene **4-9** from the RCM of bis-terminal alkene **4-18**. Unlike **4-8**, the presence or absence of $\text{Ti}(\text{O}i\text{-Pr})_4$ does not appear to have an effect on alkene isomerization for the RCM reaction of **4-18**.

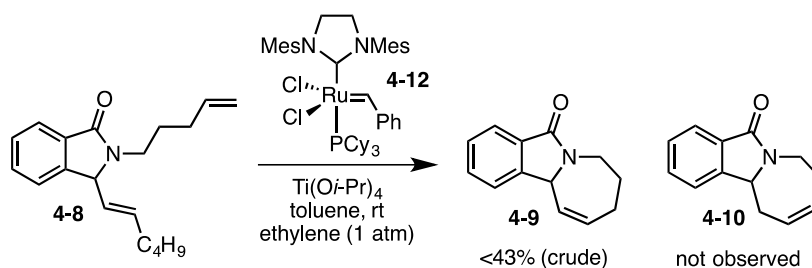


Scheme 37. RCM reaction in the absence of $\text{Ti}(\text{O}i\text{-Pr})_4$ of bis-terminal diene **4-18** and epoxide formation.⁹⁸

Our initial results suggested that the isomerization of **4-8** was primarily due to the chelating additive $\text{Ti}(\text{O}i\text{-Pr})_4$; however, the results of the RCM of **4-18** indicate that additional factors may be operational. While several reports have indicated that the decomposition products of the ruthenium catalysts are responsible for alkene isomerization, the isomerized alkene is only a minor byproduct and much less than in the case of **4-8** (Scheme 34).¹⁰⁴

Therefore, we proposed that the alkene isomerization process could also be attributed to the stability of the intermediate alkylidene complexes for each substrate. In the case of **4-8**, the resulting alkylidene complex could form a ruthenium hydride species, which would mediate alkene isomerization. In contrast, the metathesis of **4-18** results in a more reactive methylidene complex that is likely to react more quickly and is therefore unable to facilitate isomerization of product **4-9**.

To test this hypothesis, diene **4-8** was subjected to RCM in the presence of $\text{Ti}(\text{O}i\text{-Pr})_4$ under an atmosphere of ethylene. We envisioned that ethylene would react with the intermediate alkylidene complex to regenerate a catalytically active alkylidene, and thus mitigate alkene isomerization. Although a significant amount of starting material was recovered from this reaction, **4-9** was the only product observed (Scheme 38). This result supports our hypothesis that the alkene isomerization process is dependent on both the presence of $\text{Ti}(\text{O}i\text{-Pr})_4$ and the identity of the intermediate alkylidene species.



Scheme 38. RCM reaction of **4-8** in the presence of $\text{Ti}(\text{O}i\text{-Pr})_4$ under an atmosphere of ethylene.

4.3 CONCLUSION

The Wipf group has successfully developed a synthetic method to prepare libraries of functionalized isoindolinones. While preparing these novel tricyclic isoindolinones, an interesting alkene isomerization was observed during the RCM reaction. Further investigation of this isomerization process suggested that the alkene isomerization from allylic to homoallylic amides under RCM conditions is dependent on the presence of the Lewis acidic additive $\text{Ti}(\text{O}i\text{-Pr})_4$ as well as the substitution pattern of the α,ω -diene precursor.

5.0 PROGRESS TOWARD THE SYNTHESIS OF SESSILIFOLIAMIDE C

5.1 INTRODUCTION

5.1.1 Introduction to *Stemona* Alkaloids

The *Stemona* alkaloids represent a structurally diverse set of natural products with relatively complex structures. The extracts from several plants of the *Stemonaceae* family have been used in both China and Japan as insecticides and as a traditional medicine for the treatment of respiratory diseases.¹⁰⁵ To date, more than 139 *Stemona* alkaloids have been reported and most are characterized by either an exposed or hidden pyrrolo[1,2-*a*]azepine core (**5-1**).^{105b,106} Pilli and co-workers^{106b} have recently classified the *Stemona* alkaloids into eight groups based on their structural features: stenine (**I**), stemoamide (**II**), tuberostemospironine (**III**), stemonamine (**IV**), parvistemoline (**V**), stemofoline (**VI**), stemocurtisine (**VII**), and a miscellaneous group (**VIII**) (Figure 18). The miscellaneous group contains alkaloids that do not display the structural motifs contained in the other seven groups, or are the lone representative of a novel group.

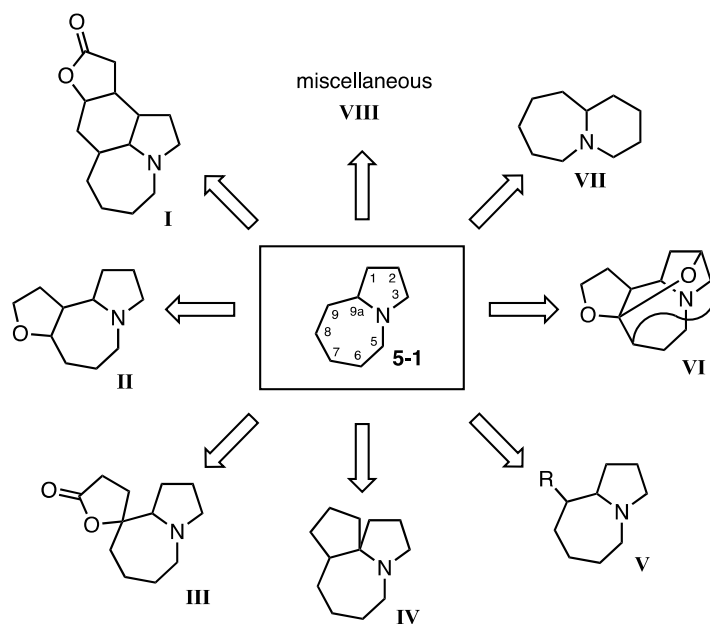
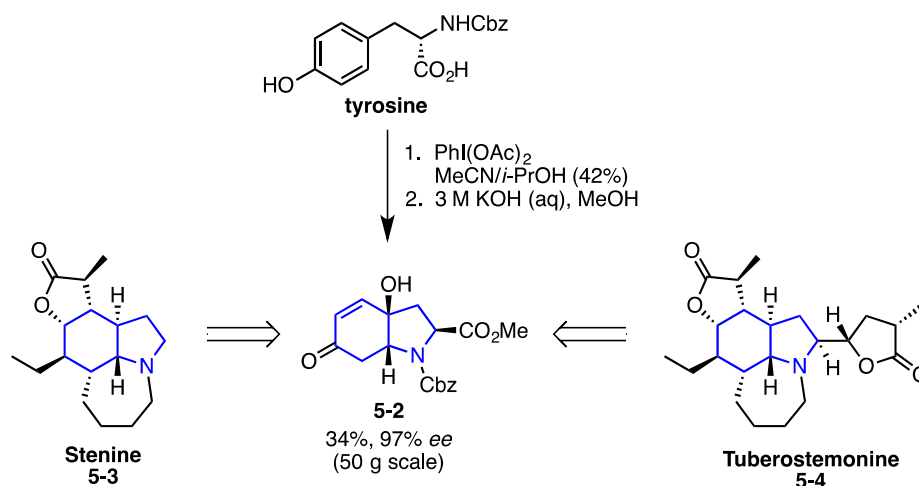


Figure 18. Classification of *Stemona* alkaloids into eight groups.^{106b}

The first total synthesis of a member of this class of natural products was that of croomine reported in 1989 by Williams and co-workers.¹⁰⁷ Since this seminal synthesis, a number of synthetic strategies and methodologies have been developed in an effort to synthesize *Stemona* alkaloids.^{106a,b,108} The Wipf group has remained active participants in the total synthesis of *Stemona* alkaloids since the 1990's.¹⁰⁹ In particular, Wipf and co-workers accomplished the total synthesis of stenine (**5-3**) and tuberostemonine (**5-4**) using an elegant scaffold-driven approach (Scheme 39).^{109a,b,109f,110} This strategy was based on the stereoselective oxidative cyclization of tyrosine to access hydroindolines (**5-2**) discovered and developed in their group.^{109a} More recently, Wipf and Hoye reported the first total synthesis of sessilifoliamide C using a convergent route featuring a [3,3]-sigmatropic rearrangement (See 5.1.2, Scheme 41).

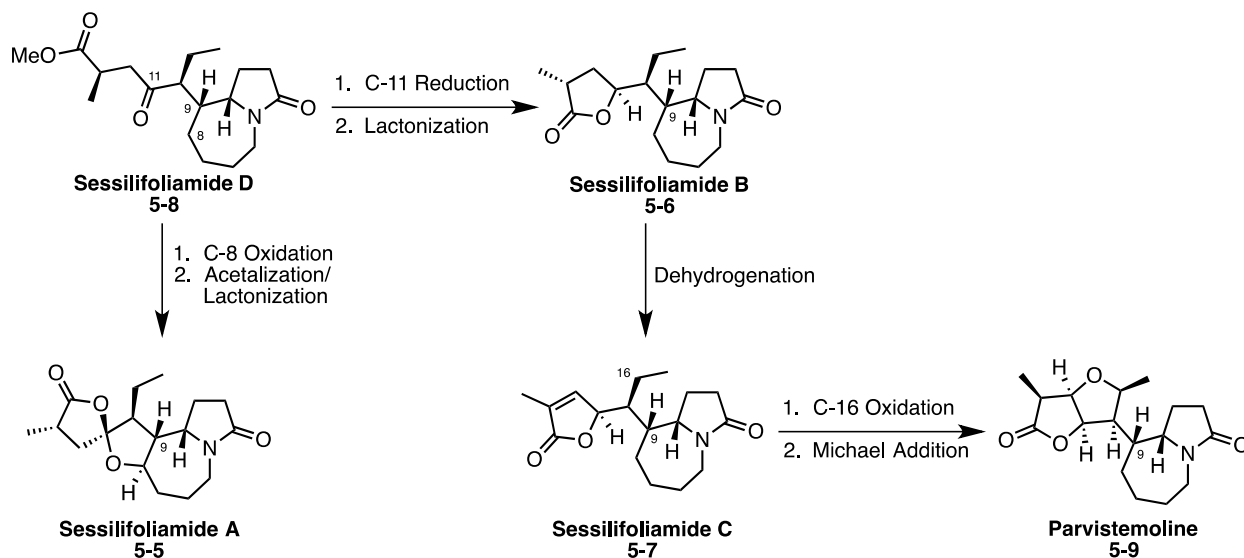


Scheme 39. Oxidative cyclization of Cbz-L-tyrosine and the conserved hydroindole core found in stenine and tuberoestemonine.^{109a}

5.1.2 Total Synthesis of (–)-Sessilifoliamide C in the Wipf Group

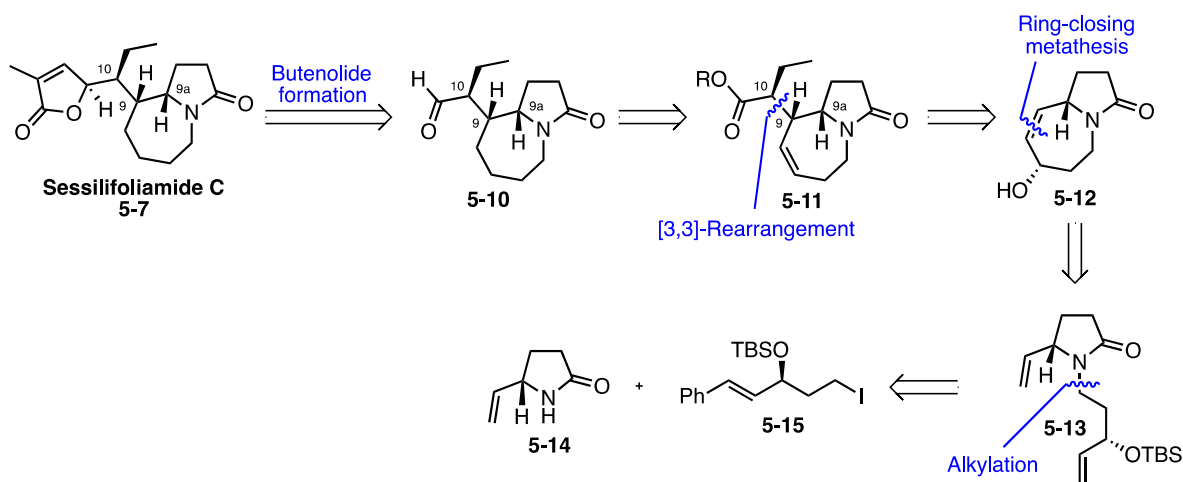
Sessilifoliamides A–D were isolated from the roots of *Stemona sessilifolia* in 2003 by Takeya and co-workers (Scheme 40).¹¹¹ Since 2003, the isolation of sessilifoliamides E–J has been reported by the same group.¹¹² Each of the sessilifoliamides A–D possess the characteristic pyrrolo[1,2-*a*]azepine core bearing a butenolide substituent at C-9. The structure and absolute configuration of sessilifoliamide C (**5-7**) was determined by chemical derivitization and comparison to a known analog of **5-5**, whose absolute confirmation was determined by X-ray analysis.¹¹¹ The structures of sessilifoliamides A–D bear striking resemblance to the previously identified alkaloid parvistemoline (**5-9**).¹¹³ A possible biosynthetic relationship between parvistemoline and sessilifoliamides A–D through oxidation and cyclization events was proposed by Wipf and Hoye (Scheme 40).^{109g} Accordingly, Wipf and Hoye investigated a unified and possibly biomimetic strategy toward sessilifoliamide A–D. They chose to synthesize (–)-

sessilifoliamide C first, due to its structural similarity to the more complex ring system present in parvistemoline.



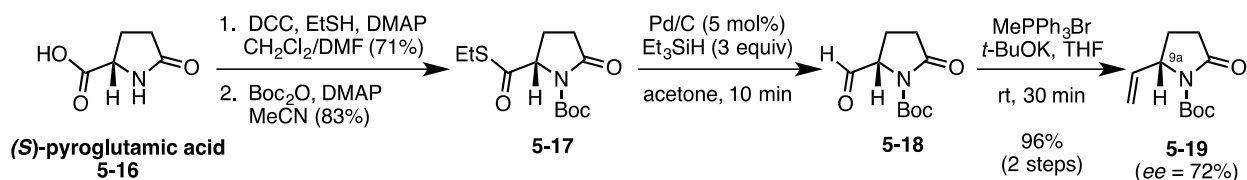
Scheme 40. Biosynthetic hypothesis based on the structural similarities between parvistemoline and sessilifoliamides.^{109g}

The Wipf group retrosynthetic strategy for the preparation of **5-7** relied upon the installation of the requisite stereocenters at C-9 and C-10 prior to construction of the butenolide (Scheme 41). Wipf and Hoye envisioned that these stereocenters would be constructed in a single step via a [3,3]-sigmatropic Claisen rearrangement.¹¹⁴ The key rearrangement precursor would be accessed by RCM of **5-12**, which would arise from the alkylation of known vinylpyrrolidinone **5-14**¹¹⁵ with iodide **5-15**¹¹⁶ (Scheme 41).

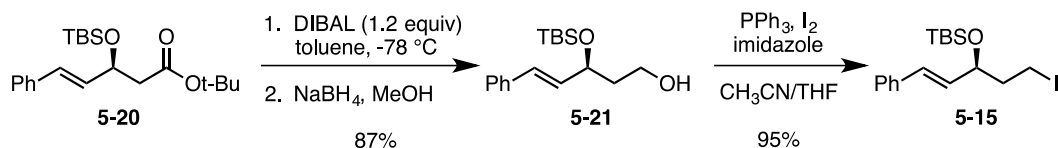


Scheme 41. Retrosynthetic approach for sessilifoliamide C.^{109g}

Methods for constructing the vinylpyrrolidine fragment **5-14** have been reported, but were found to suffer from laborious purifications, redox processes, or low-yielding eliminations.¹¹⁵ Therefore, Wipf and Hoye pursued an alternative strategy beginning with conversion of (*S*)-pyroglutamic acid **5-16** to the corresponding thioester followed by *N*-Boc protection to obtain **5-17** (Scheme 42). Fukuyama reduction¹¹⁷ of the thioester and Wittig olefination of the resulting aldehyde provided the desired vinylpyrrolidine **5-19** with 72% *ee* (Scheme 42). Next, Wipf and Hoye prepared the requisite iodide fragment by a two-step reduction and iodination of known *t*-butyl ester **5-20**.¹¹⁶ Ester **5-20** was synthesized on large scale using a previously reported enzymatic resolution strategy (Scheme 43).¹¹⁶

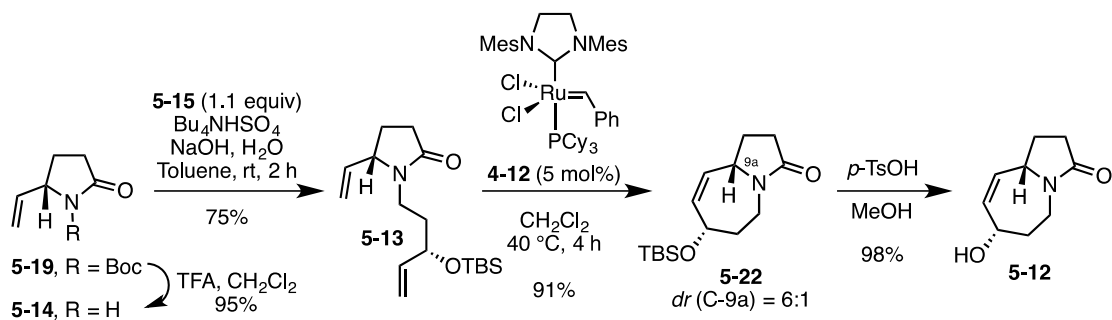


Scheme 42. Preparation of vinylpyrrolidinone **5-19**.



Scheme 43. Preparation of iodide fragment **5-15**.

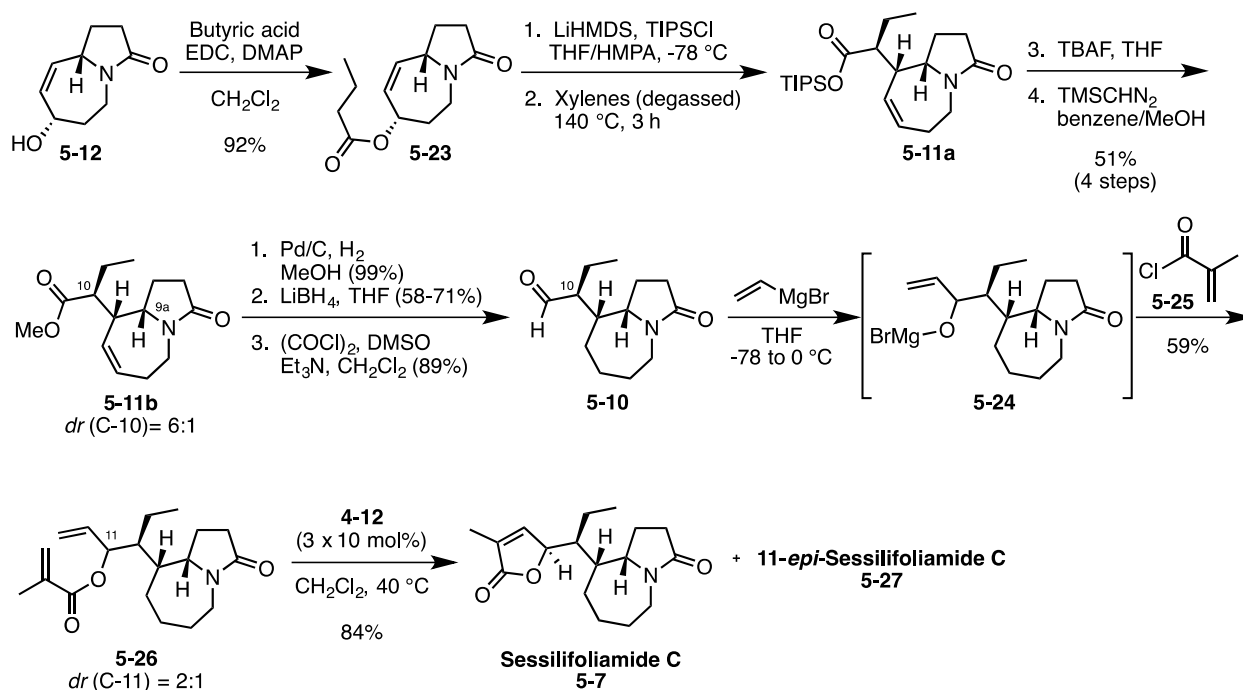
With the coupling partners in hand, the *N*-alkylation was explored after cleavage of the *N*-Boc group with TFA. Alkylation of amide **5-14** required optimization due to reproducibility and scalability issues. Phase-transfer conditions were found to be superior to other methods explored and provided RCM precursor **5-13** in good yield. RCM of diene **5-13** using Grubbs II generated the characteristic pyrrolo[1,2-*a*]azepine core in 91% yield as a 6:1 mixture of diastereomers at C-9a. Removal of the TBS protecting group under acidic conditions furnished alcohol **5-12**.



Scheme 44. Synthesis of key intermediate **5-12**.

At this stage, esterification of **5-23** using butyric acid produced the key [3,3]-sigmatropic Claisen rearrangement precursor (Scheme 45). Enolization of **5-23** with LiHMDS in the presence of TIPSCl generated TIPS-silyl ketene acetal, which was subjected to thermal rearrangement conditions to provided the desired silyl ester **5-11a**. Conversion of **5-11a** to the methylester **5-11b** to simplify analysis proceeded smoothly and provided the desired product in

51% yield over 4 steps as a 6:1 mixture of diastereomers at C-10 (Scheme 45). Hydrogenation of the double bond and conversion of the methyl ester to the aldehyde by a reduction/oxidation sequence allowed for chromatographic separation of the minor diastereomer to afford pure **5-10**. Construction of the butenolide by employing a known RCM strategy¹¹⁸ and subsequent MPLC separation of the reaction mixture revealed (–)-sessilifoliamide C (**5-7**) as the major isomer (Scheme 45). This represents the first synthesis of (–)-sessilifoliamide C, which was achieved in 18 steps from (S)-pyroglutamic acid in a 5.6% overall yield.

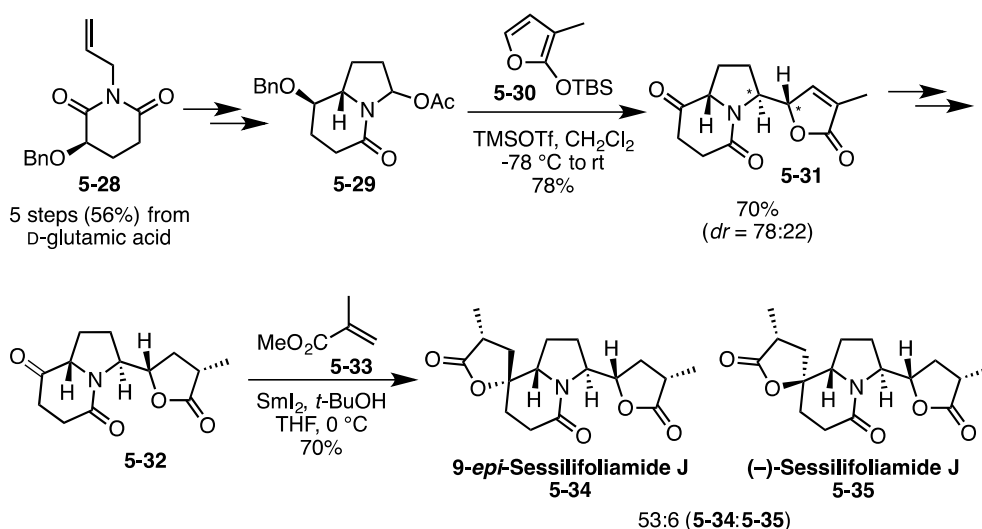


Scheme 45. Synthesis of sessilifoliamide C via a novel [3,3]-sigmatropic Claisen rearrangement strategy.

5.1.3 Total Synthesis of *epi*-Sessilifoliamide J and Sessilifoliamide J

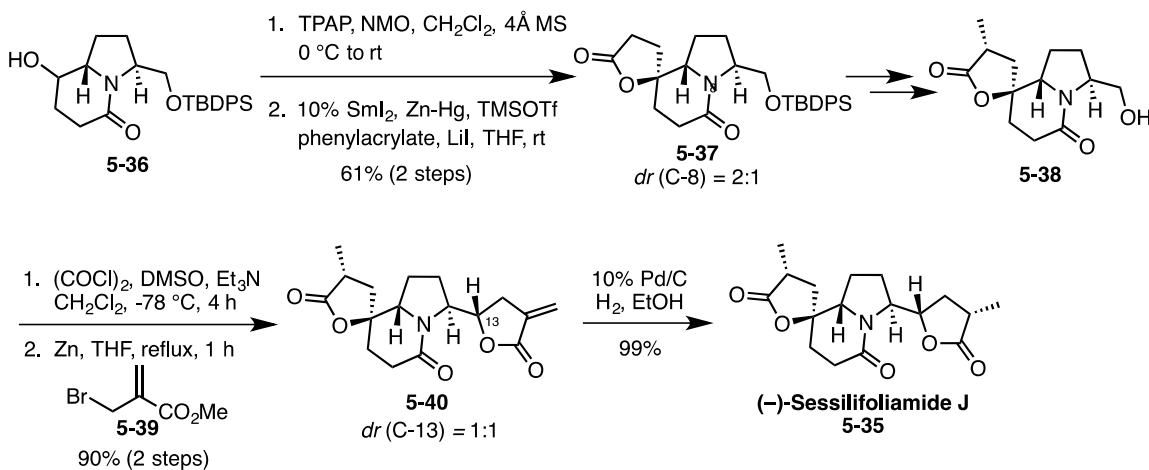
The synthesis of (–)-sessilifoliamide C by Wipf and Hoye represented the first total synthesis of a member of the sessilifoliamide family.^{109g} Since this report, the total synthesis of 9-*epi*-

sessilifoliamide J (**5-34**) and (–)-sessilifoliamide J (**5-35**) have been disclosed by Huang and co-workers.¹¹⁹ Sessilifoliamide J was isolated in 2008 and its structure and relative configuration was established by single crystal X-ray analysis (Scheme 46).^{112b} The first approach to sessilifoliamide J featured chiral building block **5-28** as a platform for the assembly of the tetracyclic scaffold (Scheme 46). This strategy was an extension of the continuing efforts in the Huang group to develop 3-hydroxyglutarimide-based synthetic methodologies.¹²⁰ The key glutarimide intermediate **5-28** was obtained in 5 steps and 56% overall yield from D-glutamic acid (Scheme 46).^{119a} Installation of the requisite butenolide fragment was accomplished by a vinylogous Mannich reaction¹²¹ of bicyclic *N,O*-acetal **5-29** and siloxyfuran **5-30**. The final spiro lactone moiety was constructed via the SmI₂-mediated coupling of methacrylate (**5-33**) with ketone **5-32** to provide a mixture of 4 isomers. The major component was assigned as 9-*epi*-sessilifoliamide J (**5-34**) and one of the minor component was (–)-sessilifoliamide J (**5-35**), allowing for the absolute configuration of **5-35** to be established (Scheme 46).^{119a}



Scheme 46. Asymmetric total synthesis of 9-*epi*-sessilifoliamide J and (–)-sessilifoliamide J.

Two years after they reported on the synthesis of 9-*epi*-sessilifoliamide J, Huang and co-workers published an alternative approach to (–)-sessilifoliamide J starting from known indolizindinone **5-36** (Scheme 47).^{119b,122} In light of their previous results, they sought to install the correct stereochemistry at C-8 using the lactonization conditions reported by Corey and Zheng.¹²³ This method provided a separable 2:1 diastereomeric mixture of lactones and the major isomer was the desired spiro lactone **5-37** (Scheme 47). Functional group interconversions of **5-37** generated the desired alcohol **5-38**. Construction of the final butenolide moiety via oxidation of **5-38** and subsequent addition of the organozinc reagent of **5-39** afforded a separable 1:1 mixture of diastereomers at C-13. Hydrogenation of the desired isomer **5-40** furnished (–)-sessilifoliamide J (**5-35**, Scheme 47).^{119b}

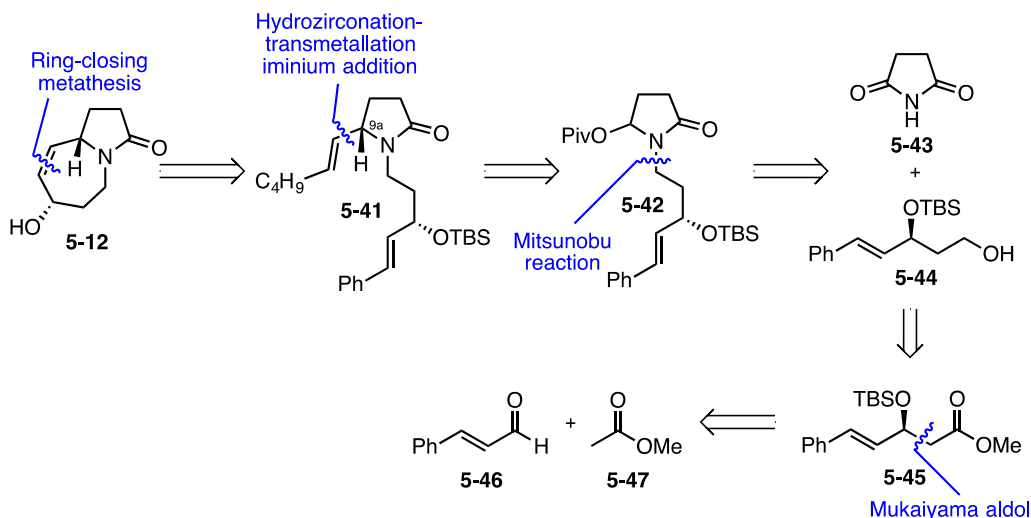


Scheme 47. Total synthesis of (–)-sessilifoliamide J.

5.2 RESULTS AND DISCUSSION

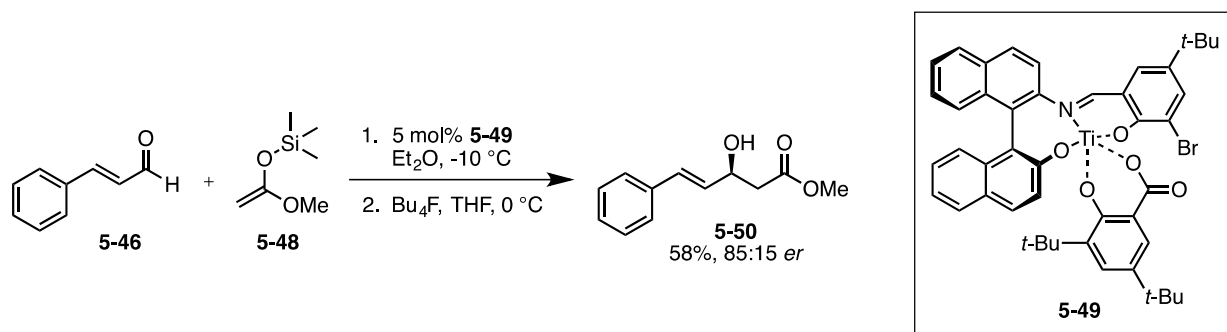
5.2.1 Second Generation Approach: Mitsunobu Reaction and Addition of *in situ* Generated Organoalanes to Acyliminium Ions

Our initial goal for the 2nd generation synthesis of sessilifoliamide C was to improve and streamline the synthesis of intermediate **5-12**. The 1st generation synthesis suffered from low stereoisomeric ratio at C-9a, low material throughput due to the use of a chiral resolution to generate fragment **5-15**, and the general difficulties in the scale up of the vinylpyrrolidinone **5-14**. To circumvent these issues, we envisioned installation of the vinyl group to proceed via addition of *in situ* generated organoalanes to the corresponding *N*-acyliminium ion of pivaloate **5-42** as described in Section 4.1 of this document. Pivaloate **5-42** would be accessed by a Mitsunobu reaction¹²⁴ of **5-44** with succinimide (**5-43**). Asymmetric Mukaiyama aldol reaction¹²⁵ between cinnamaldehyde (**5-46**) and methylacetate (**5-47**) would generate the requisite fragment **5-45**.



Scheme 48. Second-generation retrosynthetic analysis to intermediate **5-12**.

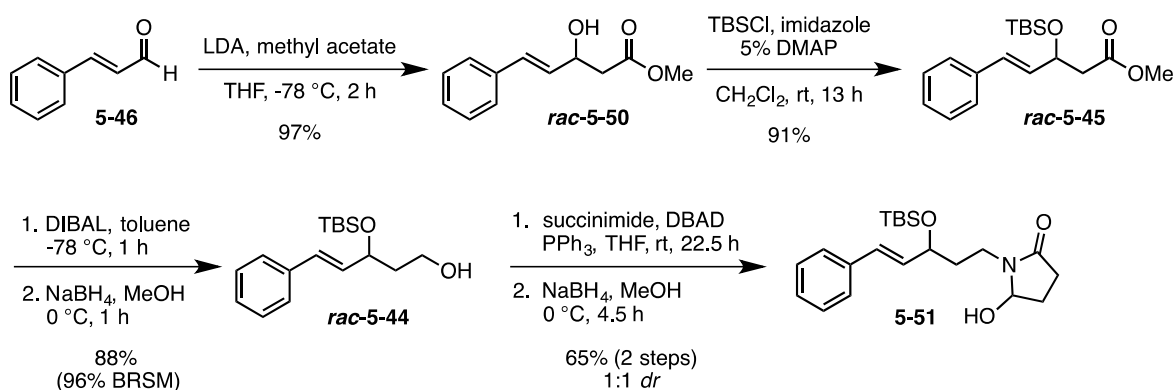
In the 1st generation approach, the synthesis of alcohol **5-21** was 6 steps and required a chiral resolution and a deprotection/reprotection sequence. To streamline this route and increase material throughput, we envisioned using an asymmetric aldol reaction to access alcohol **5-44** in 4 steps without chiral resolution and protection/deprotection sequences. The preparation of the enantiomer of **5-44** has been reported and was synthesized via catalytic asymmetric Mukaiyama aldol reaction in the presence of Carreira's chiral Ti(IV) complex **5-49** in 95% yield and with 98% *ee* (Scheme 49).¹²⁶ Using this approach, we prepared the requisite catalyst **5-49** and silyl ketene acetal **5-48** according to literature protocols.^{126c,127} Subjecting of cinnamaldehyde to the aforementioned conditions provided **5-50** in a modest yield and good enantiomeric ratio (Scheme 49). The enantiomeric ratio was determined by chiral HPLC analysis on a CHIRALCEL® OD column using a racemic standard (*rac*-**5-50**).



Scheme 49. Catalytic enantioselective Mukaiyama aldol additions using chiral Ti(IV) complex **5-49**.

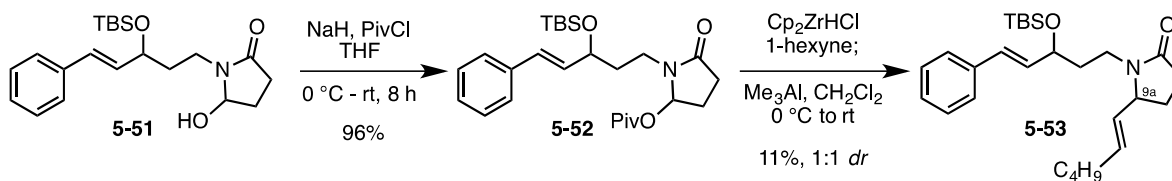
At this point we chose to proceed with the synthesis of intermediate **5-53** using racemic alcohol *rac*-**5-44** (Scheme 50). This would allow for racemic standards of each intermediate and rapid material throughput to evaluate the feasibility of the synthetic route. To this end, aldol reaction of methyl acetate and cinnamaldehyde followed by TBS protection of the resulting alcohol provided *rac*-**5-45** in 88% yield over two steps (Scheme 50).¹²⁸ Primary alcohol *rac*-**5-44** was readily accessed by a two-step reduction of ester *rac*-**5-45**. With desired alcohol

fragment **rac-5-44** in hand, the Mitsunobu alkylation of succinimide was explored. While both DEAD and DBAD provided the desired product **5-51** in good yields, separation of the corresponding hydrazide byproducts was difficult. Therefore, the crude material was subjected to NaBH₄. The presence of the hydrazide byproduct was inconsequential, and the desired alcohol **5-51** was isolated as a 1:1 mixture of diastereomers in good yield over the two steps (Scheme 50).



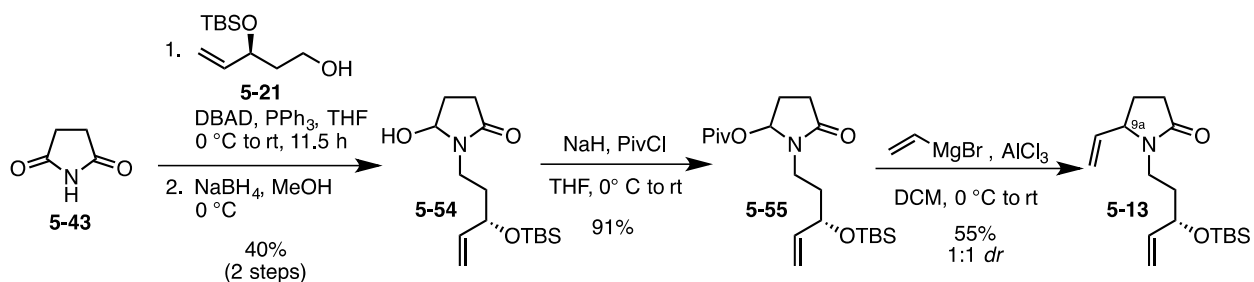
Scheme 50. Racemic synthesis of alcohol **5-51**.

The protection of alcohol **5-51** as the pivaloate required the use NaH as the base to ensure complete conversion of the starting material to key intermediate **5-52** (Scheme 51). Formation of hexenylalane and addition to the *in situ* generated iminium ion of **5-52** provided the desired RCM precursor **5-53** in 11% yield as a 1:1 mixture of diastereomers at C-9a (Scheme 51). Although the reaction did result in complete consumption of starting material, neither **5-51** nor **5-52** were isolated. This may be due to the acidic workup, which would result in cleavage of both the pivalyl and siloxy protecting groups. The polar nature of the resulting diol would render isolation from silica gel chromatography difficult.



Scheme 51. Addition of hexenylalane to the *in situ* generated iminium ion of **5-52**.

During the synthesis of **5-53**, we had been working on the addition of *in situ* generated vinyl alane to *N*-acyliminium ions (Section 4.2). In light of the success of this aforementioned method, we sought to utilize this strategy to circumvent the problems faced in the addition of hexenyl alane to **5-52**. At this point, we realized that the installation of a vinyl group would allow us generate intermediate **5-13** in the first generation synthesis. To achieve the second-generation synthesis of sessilifoliamide C (**5-7**), the previously synthesized alcohol **5-21**^{109g} was used as the Mitsunobu coupling partner. The Mitsunobu reaction of **5-21** with succinimide (**5-43**), followed by reduction and pivalate protection afforded **5-55** in good yields over three steps. Gratifyingly, *in situ* generation of the vinyl alane and addition to pivalate **5-55** provided **5-13** in modest yield as a 1:1 mixture of diastereomers.



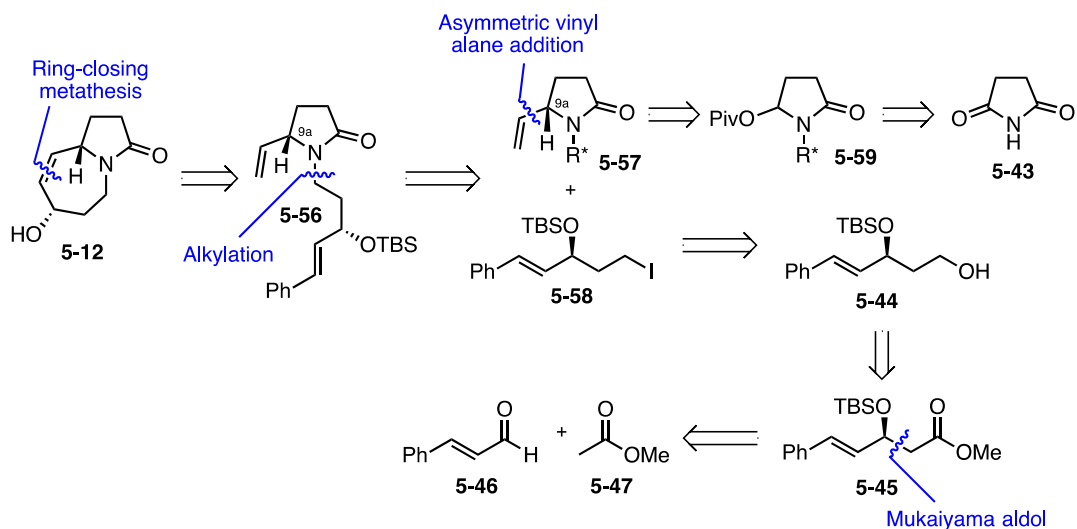
Scheme 52. Vinyl alane addition to **5-55**.

We successfully prepared **5-13**, a building block in our previous synthesis of sessilifoliamide C (Scheme 48). This second generation approach featured direct installation of

the requisite vinyl group via addition of *in situ* generated vinyl alane to an *N*-acyliminium ion. This method eliminates the synthesis of pyrrolidinone **5-19**, which was difficult to perform on scale in a reproducible manner. Although the synthesis of alcohol **5-21** is manageable on large scale (40 g), it is 7 linear steps, includes a chiral resolution, and a deprotection/reprotection sequence. The enantioselective Mukiyama aldol reaction in this second generation approach streamlines this sequence to 4 steps and eliminates the chiral resolution and deprotection/reprotection sequence, greatly enhancing material throughput. Additionally, the Mitsunobu reaction of commercially available succinimide (**5-43**) and **5-21** provides an attractive, more reproducible alternative to the phase transfer conditions used for the *N*-alkylation. Although we were able to make improvements upon the first generation synthesis, the diastereomeric ratio at C-9a will require further optimization to generate a synthetically tractable route.

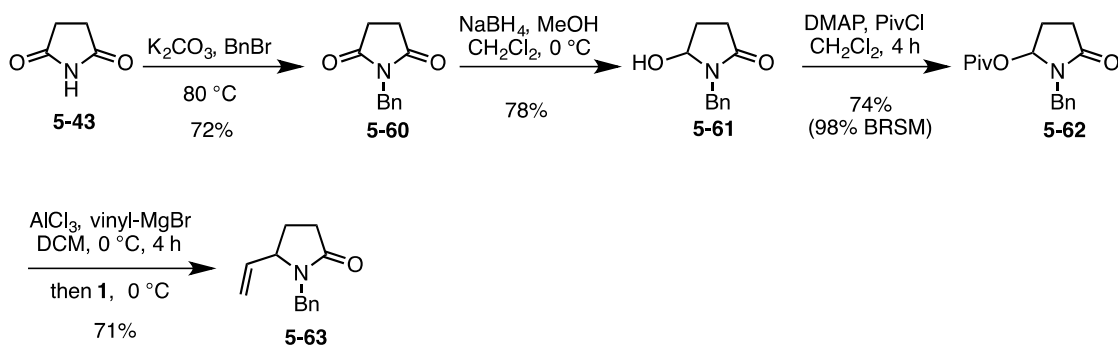
5.2.2 Third Generation Approach: Alkylation and Addition of *in situ* Generated Organoalanes to Acyliminium Ions Bearing a Chiral Auxiliary

To address the low diastereomeric ratio (*dr*) obtained from the vinyl alane addition reaction in Scheme 52, we designed a new synthetic strategy (Scheme 53). The key feature of this route would be the use of auxiliary R* to generate a chiral *N*-acyliminium ion equivalent. Cleavage of the chiral auxiliary (R*) and subsequent alkylation with iodide fragment **5-58** would provide the requisite RCM precursor **5-56**. Fragment **5-58** would arise from straightforward iodination of the previously synthesized alcohol **5-44**.



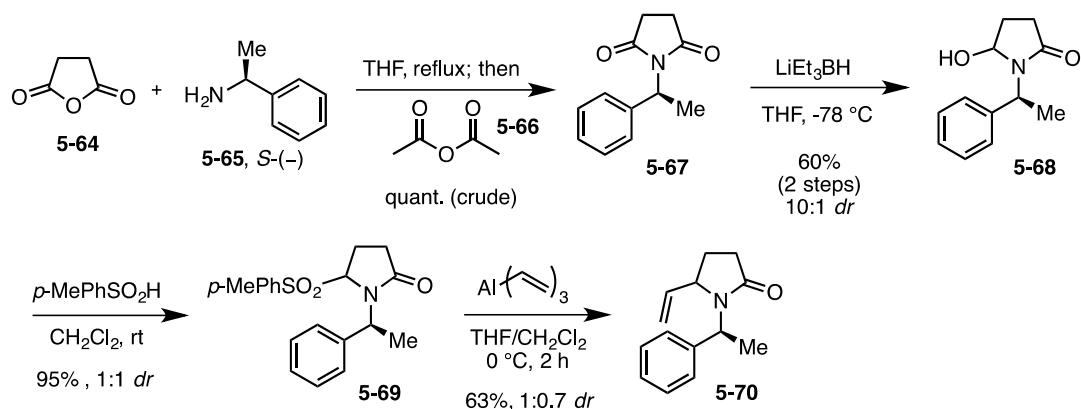
Scheme 53. Revised retrosynthesis of key intermediate **5-12** using a chiral auxiliary (R^*).

Prior to installation of a chiral auxiliary, a model system was prepared according to Scheme 54.¹²⁹ Beginning with commercially available succinimide (**5-43**), benzyl protection and mono-reduction worked well to provide pyrrolidinone **5-61**. Treatment of **5-61** with pivalyl chloride in the presence of DMAP afforded the desired *N*-acyliminium precursor **5-62**. Addition of the *in situ* generated vinyl alane to the pivaloate **5-62** proceeded smoothly to afford **5-63** in good yield.



Scheme 54. Model system for the asymmetric vinyl alane addition to pivaloate **5-62**.

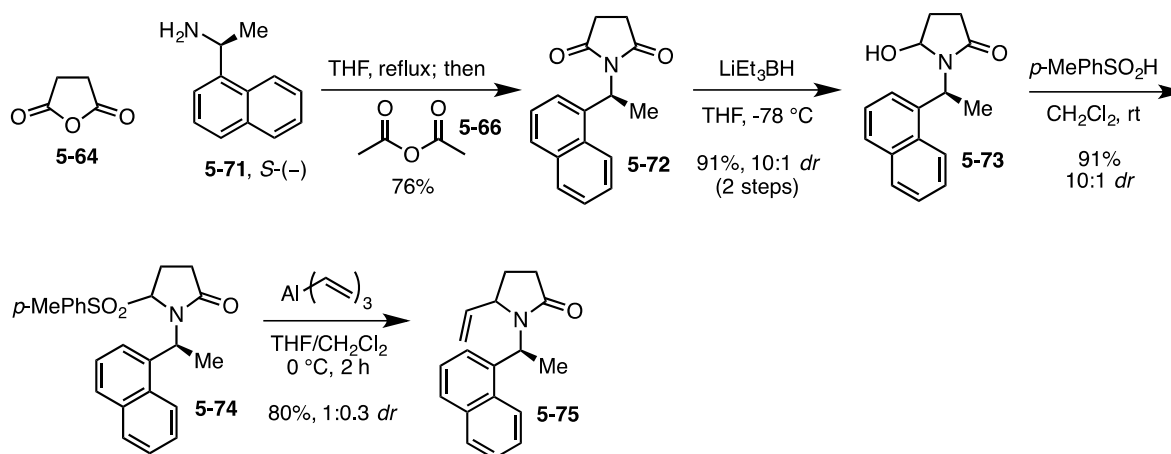
The first chiral auxiliary explored was *S*-(-)-phenylethyl (**5-65**). Synthesis of the requisite chiral *N*-acyliminium ion precursor **5-69** followed a literature protocol (Scheme 55).¹³⁰ Formation of succinimide **5-67** was achieved by treatment of succinic anhydride (**5-64**) with *S*-(-)-phenylethylamine and acetic anhydride in THF at reflux. Reduction of **5-67** afforded **5-68** as a *ca.* 10:1 mixture of diastereomers, as indicated by ¹H and ¹³C NMR. At this point, we chose to use the sulfinate protecting group, rather the pivalyl due to the greater stability and ease of preparation of the sulfinate. Treatment of this mixture with toluenesulfinic acid afforded the desired sulfinate protected substrate **5-69** as a 1:1 mixture of diastereomers. *In situ* generation of the chiral *N*-acyliminium ion of **5-69** and addition of vinyl alane proceeded smoothly; however, the *dr* was only 1:0.7.



Scheme 55. Synthesis of chiral *N*-acyliminium precursor **5-69** and vinyl alane addition.

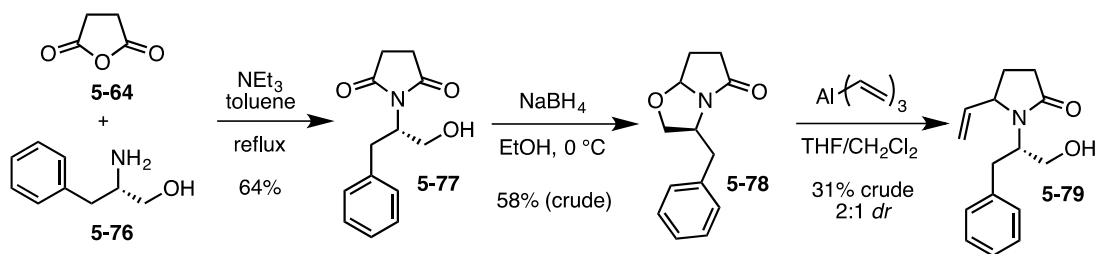
To increase the *dr* of the vinyl addition we synthesized the *S*-(-)-naphthylethyl derivative **5-72** in the same manner as Scheme 55 (Scheme 56). Condensation of *S*-(-)-naphthylethylamine with succinic anhydride and reduction of **5-72** with lithium triethylborohydride furnished **5-73** in good yield and *dr*. Protection of the alcohol as the sulfinate gave **5-74** in excellent yields with a 1:1 *dr*. Addition of *in situ* generated vinyl alane to chiral *N*-acyliminium ion of **5-74** provided **5-**

75 as a 1:0.3 mixture of diastereomers. Although the *dr* was improved compared with the corresponding *S*(-)-phenylethyl derivative **5-70**, optimization was still required to obtain a synthetically useful method.



Scheme 56. Synthesis of chiral *N*-acyliminium precursor **5-74** and vinyl alane addition.

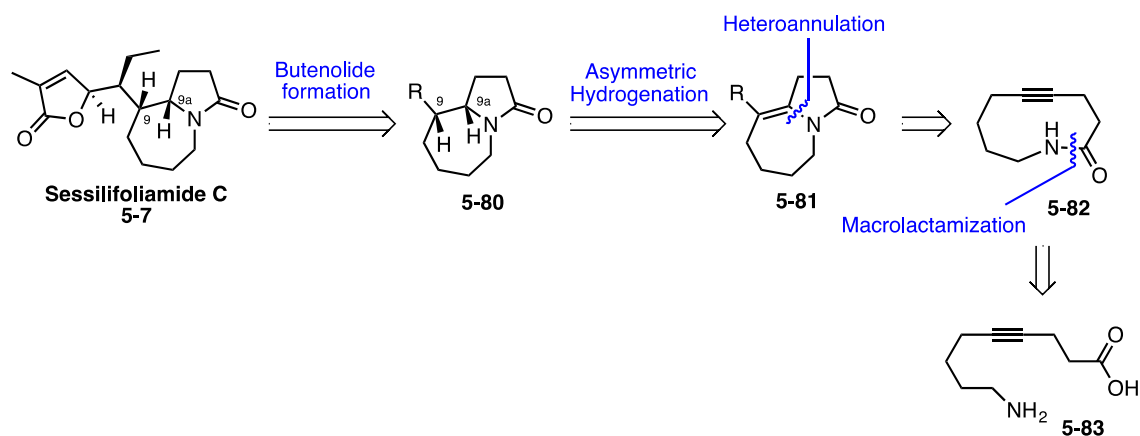
To further explore the effect of the chiral auxiliary on the *dr*, we synthesized **5-78** using L-phenylalaninol. We envisioned L-phenylalaninol would selectively delivery the organoalane via a chelated transition state and thus enhance the *dr*. This chiral induction strategy has been successfully applied to the addition of nucleophiles such as cuprates, silanes, and phosphites.¹³¹ We were pleased to find that treatment of **5-77** with NaBH₄ gave us the desired product **5-78**. The crude material was taken on to the vinyl alane addition, but gave low yields of the desired product and poor diastereoselectivity.



Scheme 57. Chiral induction via a chelated *N*-acyliminium ion of **5-78**.

5.2.3 Fourth Generation Approach: Transannular Ring Closure

It was evident that installation of the requisite vinyl functionality at C-X could not be achieved with optimal diastereoselectivity. Therefore, we redesigned our synthetic strategy to avoid the installation of this moiety and investigate a less traditional, more novel synthetic strategy. We envisioned the key feature of this route would be the constructing the pyrrolo[1,2-*a*]azepine core of sessilifoliamide C via a transannular ring closure of 10-membered lactam **5-82** (Scheme 58). Installation of the butenolide moiety would be dependent upon the method employed for the heteroannulation step. An asymmetric hydrogenation of the resulting double bond would allow for the simultaneous installation of C-9 and C-9a configurations in a stereocontrolled manner. The requisite intermediate **5-82** would be accessed via macrolactamization of amino acid **5-83**. This revised route represents a novel entry to the pyrrolo[1,2-*a*]azepine scaffold, and represents a potential unified approach to the synthesis of a number of *Stemona* alkaloids contain this characteristic feature.

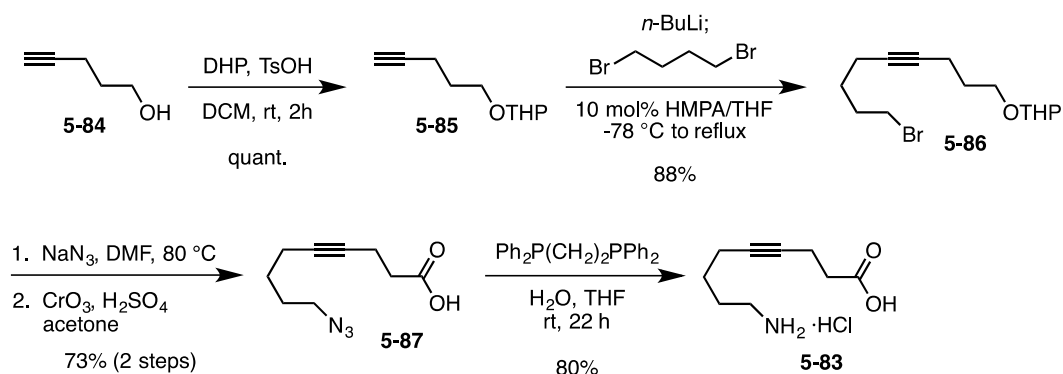


Scheme 58. Revised retrosynthetic strategy featuring a novel transannular ring closure to construct the pyrrolo[1,2-*a*]azepine core.

At the outset of this route, we recognized that the construction of the requisite 10-membered lactam **5-82** represented a synthetic challenge. The difficulty in forming medium-sized rings (8 to 11-membered) is attributed to the ring strain that develops during the transition state as a result of transannular interactions.¹³² These interactions result in substantial torsional and/or bond angle distortion. In lactam **5-69**, the ring strain will be further exacerbated by the inclusion of the alkyne moiety, which prefers to adopt bond angles of 180°. We reasoned that while construction of the 10-membered lactam would be challenging, the inherent ring strain would allow us to achieve the subsequent key heteroannulation reaction.

To this end, we chose to access the macrolactam by amide bond formation of the corresponding amino acid. Although closure of medium-sized ring lactams via amide C-N bond formation is demanding, successful approaches have been reported and reviewed.¹³³ To test the feasibility of this transformation we synthesized amino acid **5-83** according to Scheme 59. We began with protection of 5-pentyn-1-ol as the tetrahydropyranyl ether (**5-85**). Treatment of **5-85** with *n*-BuLi followed by dibromobutane provided the desired coupled product **5-86** in good

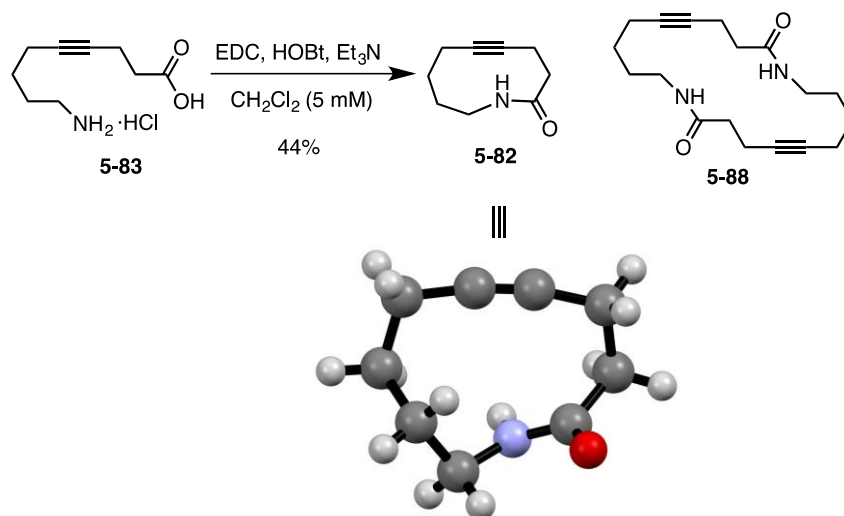
yield. Protection of the primary alcohol in **5-84** was necessary to obtain acceptable yields in the coupling reaction, in addition to mitigating the need for 2 equivalents of *n*-BuLi. Bromide **5-86** was converted to the azide using NaN₃ in DMF at 80 °C. Gratifyingly, THP removal and oxidation of the resulting alcohol was achieved in one step using Jones reagent. Staudinger reduction¹³⁴ of the azide went smoothly using PPh₃; however, purification of amino acid **5-83** was difficult due to contamination with triphenylphosphine oxide. Switching to 1,2-bis(diphenylphosphino)ethane provided the desired amino acid in good yields and allowed for isolation of pure **5-83** as the hydrochloride salt.



Scheme 59. Synthesis of requisite amino acid **5-83**.

With the requisite amino acid **5-83** in hand, we explored lactamization conditions to access **5-82**. We were pleased to find that treatment of **5-83** with EDC and HOBT under high dilution conditions provided the desired macrolactam in modest yield (Scheme 60). Formation of the undesired dimerized macrolactam **5-88** was also observed (<10%); however, product isolation was difficult due to the polarity of **5-88**. Elution of compound **5-88** from a silica gel column required an eluent mixture of >5% MeOH in CH₂Cl₂. As a result, it was isolated as an inseparable mixture with HOBT, and an isolated yield was not calculated.

The structure of **5-82** was confirmed by X-ray crystallographic analysis (Scheme 60). Notably, the crystal structure shows that angles of the alkyne deviates from the ideal angle of 180° , with values of 167.3° and 171.7° (Appendix A.3). Additionally, the amide adopts a trans configuration with a dihedral angle (ω) of -162.6° (Appendix A.3). A survey of the literature revealed crystal structures of 10-membered rings containing either the alkyne and amide moieties, but not both.¹³⁵ The bond angles associated with compounds containing a cyclodecyne core ranged from 167.7° to 169.4° and are in good agreement with those found for compound **5-82**.^{135b} The corresponding dihedral angles (ω) for known 10-membered lactams were between -167.1° and -168.3° , which are slightly larger than the dihedral angle in **5-82**.^{135a} The distortion of the amide bond in **5-82** is presumably due to the presence of the alkyne.

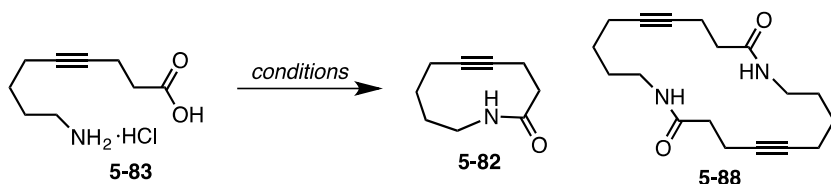


Scheme 60. Lactamization of **5-83** and the X-ray structure of **5-82**.

Next, we attempted to optimize the amide coupling conditions to favor the formation of desired lactam **5-82**. Dilution of the reaction mixture or heating to reflux gave comparable results (Table 12, entries 1 vs. 2 and 3), while the use of pentafluorophenyl diphenylphosphinate

(FDPP)¹³⁶ resulted in formation of the desired product **5-82** with good mass recovery. Unfortunately, the separation of **5-82** from the phosphine oxide byproducts could not be achieved. Similar purification issues were also encountered when HATU¹³⁷ and HOAt¹³⁷ were employed.

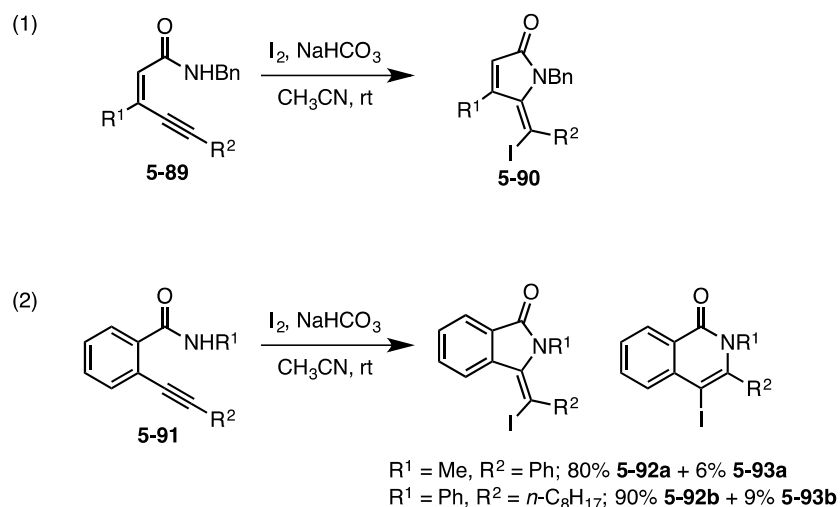
Table 12. Optimization of the macrolactamization of **5-83** to provide lactam **5-82**.



| entry | conditions | temp, time | results ^a |
|-------|--|-------------|---|
| 1 | EDC, HOBt, Et ₃ N, CH ₂ Cl ₂ (5 mM) | rt, 2.5 d | 5-82 (44%) |
| 2 | EDC, HOBt, Et ₃ N, CH ₂ Cl ₂ (1 mM) | rt, 2 d | 5-82 (28%) |
| 3 | EDC, HOBt, Et ₃ N, CH ₂ Cl ₂ (5 mM) | reflux, 2 d | 5-82 (26%) |
| 4 | FDPP, DIPEA, CH ₂ Cl ₂ (5 mM) | rt, 2 d | 5-82 (29%, 90% pure) |
| 5 | HATU, HOAt, CH ₂ Cl ₂ (5 mM) | rt, 2 d | 5-82 (inseparable sideproduct; 100% mass recovery) |

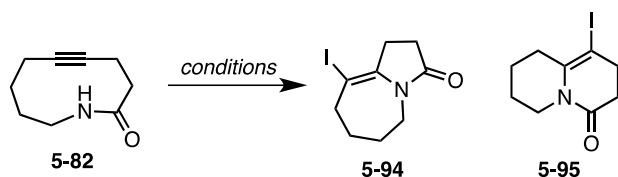
^a <10% of dimer **5-88** was observed in each of these reaction, but an isolated yield was not obtained.

At this stage, EDC and HOBt were the best conditions for the formation and isolation of the requisite macrolactam **5-82** and were therefore employed for the scale-up of intermediate **5-82**. With the key precursor in hand, we set out to explore the transannular ring closure. We began by investigating the electrophilic cyclization of **5-82** to access the halo-substituted pyrrolo[1,2-*a*]azepine. To our knowledge, halo-cyclization of cyclic alkynylamides to form γ -halo- γ -butyrolactams has not been investigated. Nonetheless, there are examples of intramolecular electrophilic cyclizations of acyclic *Z*-alkenylamides **5-89**¹³⁸ and alkynylanilines **5-91**¹³⁹ with ICl and I₂, respectively (Scheme 61).¹⁴⁰ In each case, the desired products are obtained in good yields and arise from 5-*exo* rather than 6-*endo* ring closure.



Scheme 61. Electrophilic cyclization of acyclic alkynylamides to access γ -iodo lactams.¹³⁸⁻¹³⁹

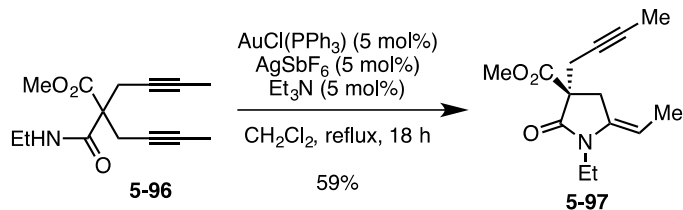
Based on these precedents, **5-82** was treated with I₂ and Na₂CO₃ in THF at room temperature. Unfortunately, the undesired quinolizinone **5-95** was formed exclusively in moderate yield (Table 13, entry 1). Compound **5-95** can be distinguished from compound **5-94** on the basis of the lactam carbonyl ¹³C shift. The five-membered ring products generally exhibit a ¹³C shift of *ca.* 174–180 ppm, while in the six-membered ring the carbonyl shift is at *ca.* 168–172 ppm. Performing the reaction in the presence of AgNO₃ did not change the selectivity of the cyclization. Using an alternative source of iodine, such as Barluenga's reagent,¹⁴¹ also provided modest yields of the undesired 6-*endo* cyclized product **5-95**.

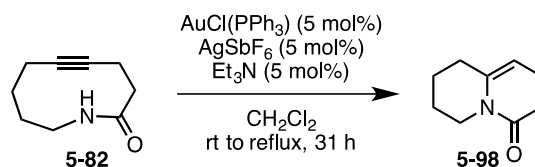
Table 13. Iodocyclization of lactam **5-82**.

| entry | conditions | results |
|-------|--|--------------------------------|
| 1 | I ₂ , Na ₂ CO ₃ , THF, rt, 1.5 h | 5-95 (55%) |
| 2 | I ₂ , AgNO ₃ , Na ₂ CO ₃ , THF, rt, o/n | 5-95 (54%) |
| 3 | IPy ₂ BF ₄ ·HBF ₄ , CH ₂ Cl ₂ , -60 °C, o/n | 5-95 (39%) ^a |

^a SM was recovered.

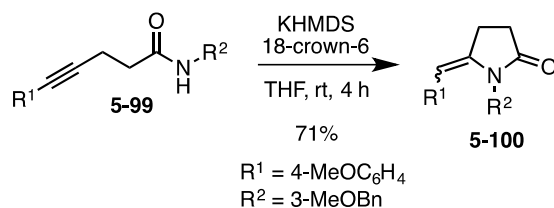
Iodocyclization was unsuccessful in generating the desired pyrrolo[1,2-*a*]azepine core; therefore, we explored alternative electrophilic cyclization conditions that would provide the corresponding enamide rather than the vinyl iodide. To this end, the gold-catalyzed cyclization of β -alkynylamide **5-96** has been reported to provide alkylidenelactam **5-97** (Scheme 62).¹⁴² The authors note that the use of catalytic Et₃N in addition to AuCl(PPh₃) strongly favored the formation of the 5-*exo* monocyclization to provide lactam **5-97**.¹⁴² Surprisingly, application of these reaction conditions to lactam **5-82** resulted in the exclusive formation of the 6-*endo* cyclized product **5-98** (Scheme 63).

**Scheme 62.** Gold-catalyzed cyclization reaction of bispropargylic amide **5-96**.¹⁴²



Scheme 63. Electrophilic cyclization of **5-82**.

At this stage it became evident that the inherent properties of our system favored 6-*endo* ring closure under electrophilic cyclization conditions. Therefore, we investigated methods for nucleophilic cyclization. To our knowledge, nucleophilic cyclization of cyclic β -alkynylamides to γ -alkylidene- γ -butyrolactams has not been investigated. A survey of the literature revealed that the most optimal conditions for the intramolecular nucleophilic cyclization of β -alkynylamides (**5-99**) are exposure to KHMDS and 18-crown-6 in THF at room temperature (Scheme 64).¹⁴³ The cyclization of β -alkynylamide **5-82** under these conditions furnished an inseparable 1.5:1.0 mixture of the desired pyrrolo[1,2-*a*]azepine **5-101** with the undesired quinolizinone **5-98** (Table 14, entry 1).

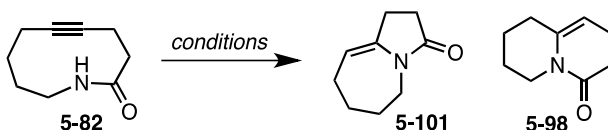


Scheme 64. Intramolecular cyclization of β -alkynylamides to γ -alkylidene- γ -butyrolactams.^{143a}

Pleased with these initial results, we set out to optimize the reaction conditions to obtain higher yields of **5-101** while suppressing the formation of **5-98**. We began by investigating the effect of the additives. The use of AgOTf in place of 18-crown-6 favored the formation of the 6-*endo* cyclization product **5-98**, while in the absence of any additive there was little preference for

either cyclization pathway (Table 14, entries 2 and 3). These results indicate that sequestration of the potassium cations to provide a “naked” anion enhances the selectivity for the desired 5-*endo* pathway. Based on this observation, we hypothesized that the use of a more polar solvent would also increase the preference for the desired product **5-101**. Gratifyingly, performing the cyclization reaction in DMF afforded the desired product **5-101** as a 2.5:1 ratio with the undesired product **5-98** (Table 14, entry 4). Further attempts to enhance the ratio in favor of the desired product **5-101** by lowering the reaction temperature or modifying the concentration were not successful (Table 14, entries 5-7). We also explored alternative bases such as NaH, KH, and KO*t*-Bu, but could not improve the ratio beyond 2.5:1 in favor of the desired product **5-101**.

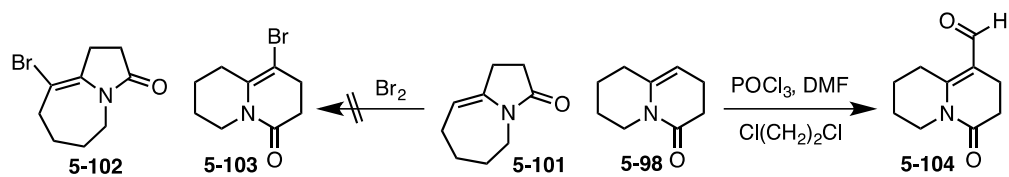
Table 14. Optimization of the intramolecular nucleophilic cyclization of β -alkynylamide **5-82**.



| entry | conditions ^a | yield (5-101 : 5-98) |
|-------|--|--------------------------------------|
| 1 | KHMDS, 18-crown-6, THF, rt, 1 h 15 min | 91% (1.5:1.0) |
| 2 | KHMDS, AgOTf, toluene, rt to 60 °C, 21 h | 90% (1.0:2.0) |
| 3 | KHMDS, THF, rt, 45 min | 79% (0.7:1.0) |
| 4 | KHMDS, 18-crown-6, DMF, rt, 40 min | 81% (2.5:1.0) |
| 5 | KHMDS, 18-crown-6, DMF, 0 °C, 20 min | 83% (2.5:1.0) |
| 6 | KHMDS, 18-crown-6, DMF (0.005 M), 0 °C, 30 min | 87% (2.5:1.0) |
| 7 | KHMDS, 18-crown-6, DMF (0.2 M), 0 °C, 20 min | 60% (2.5:1.0) |

^a All reactions were carried out at 0.03 M unless otherwise stated.

The mixture of products was taken on to investigate the functionalization of the enamide (Scheme 65). Initial attempts to generate vinyl bromide **5-102** resulted in over-bromination or decomposition. Formylation of the enamide using Vilsmeier reagent afforded a mixture of products, with the undesired formylated product **5-104** as the major constituent.



Scheme 65. Attempts to functionalize a mixture of enamides **5-101** and **5-98**.

5.3 CONCLUSION

We have developed a second-generation approach toward sessilifoliamide C utilizing a method previously developed by our group. This strategy allowed us to address and improve upon several issues in the first generation synthesis, namely the elimination of the chiral resolution and *N*-alkylation steps, as well as the installation of the vinyl moiety. Additionally, we achieved a novel entry to the pyrrolo[1,2-*a*]azepine core of the *Stemona* alkaloids by a transannular ring closure of a β -alkynyl lactam. Functionalization and elaboration of the pyrrolo[1,2-*a*]azepine enamide is currently underway.

6.0 EXPERIMENTAL PART

6.1 GENERAL EXPERIMENTAL

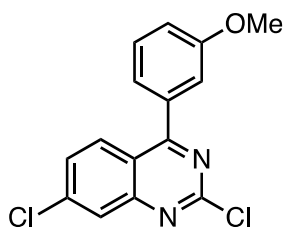
All glassware was dried in an oven at 140 °C for 2 h or flame dried and cooled under dry N₂ or Ar prior to use. All moisture sensitive reactions were performed using syringe-septum cap techniques under an atmosphere of dry N₂ or Ar. Reactions carried out below 0 °C employed an acetone/dry ice bath or a cyrocool and an isopropanol/ethanol bath. THF, Et₂O, and 1,4-dioxane were distilled from sodium/benzophenone ketyl; *i*-Pr₂NH, *i*-Pr₂NEt, and Et₃N were distilled from CaH₂ and stored over KOH; and CH₂Cl₂ and toluene were purified by passage through an activated alumina filtration system or by distillation from CaH₂. All other materials were obtained from commercial sources and used as received unless otherwise stated.

Reactions were monitored by thin-layer chromatography analysis using pre-coated silica gel 60 F₂₅₄ plates (EMD, 250 μm thickness) and visualization was accomplished with a 254 nm UV light and by staining with a KMnO₄ solution (1.5 g of KMnO₄ and 1.5 g of K₂CO₃ in 100 mL of a 0.1% NaOH solution) or Vaughn's reagent (4.8 g of (NH₄)₆Mo₇O₂₄•4 H₂O and 0.2 g of Ce(SO₄)₂ in 100 mL of a 3.5 N H₂SO₄ solution). Flash chromatography on SiO₂ (Silicycle, Silia-P Flash Silica Gel or SiliaFlash® P60, 40-63 μm) or Florisil® (100-200 mesh) was used to purify crude reaction mixtures. Concentrating under reduced pressure refers to the use of a rotary evaporator connected to a membrane vacuum pump or a PIAB Lab Vac H40 to remove

solvent. All desired products were placed under high vacuum (0.5-4 mmHg) to remove trace solvent.

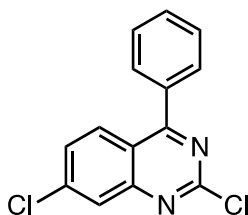
Melting points were determined using a Laboratory Devices Mel-Temp II in open capillary tubes and are uncorrected. Infrared spectra were determined as neat solids or oils on a Smiths Detection IdentifyIR FT-IR spectrometer. Mass spectra were obtained on a Micromass Autospec UK Limited double focusing instrument, a Q-TOF Ultima API, or a Thermo Scientific Exactive Orbitrap LC-MS. Microwave reactions were performed using a Biotage Initiator microwave reactor. ^1H and ^{13}C NMR spectra were recorded on a Bruker Avance 300 MHz, 400 MHz, 500 MHz, or 600 MHz instruments. Chemical shifts (δ) were reported in parts per million with the residual solvent peak used as an internal standard δ ^1H / ^{13}C (Solvent); 7.26 / 77.16 (CDCl_3); 2.50 / 39.52 (DMSO-d_6); and are tabulated as follows: chemical shift, multiplicity (s = singlet, d = doublet, t = triplet, q = quartet, quint = quintet, sext = sextet, sept = septet, m = multiplet), number of protons, and coupling constant(s). ^{13}C NMR spectra were obtained using a proton-decoupled pulse sequence and are tabulated by observed peak. CDCl_3 was filtered through dried basic alumina prior to sample preparation.

6.2 CHAPTER 1 EXPERIMENTAL PART



1-22a

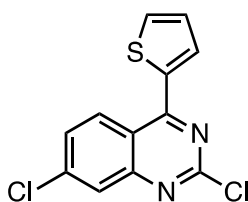
2,7-Dichloro-4-(3-methoxyphenyl)quinazoline (1-22a). To a reaction vial was added **1-21**²¹ (0.040 g, 0.17 mmol), Pd(OAc)₂ (0.0020 g, 0.009 mmol), and PPh₃ (0.007 g, 0.026 mmol). The reaction mixture was flushed with N₂. 3-Methoxyphenylboronic acid (0.029 g, 0.19 mmol) in freshly distilled and degassed DME (1.7 mL) and Na₂CO₃ (0.056 g, 0.53 mmol) in H₂O (0.30 mL) were added via syringe. The reaction mixture was sealed and heated at 80 °C for 16 h. The mixture was extracted with CH₂Cl₂ (4 x 5 mL). The combined organic layers were washed with brine (5 mL), dried (MgSO₄), and concentrated under reduced pressure. The crude residue was purified by chromatography on SiO₂ (1:20, EtOAc:hexanes) to provide **1-22a** (0.045 g, 86%) as a fluffy white solid: ¹H NMR (DMSO-*d*₆, 300 MHz,) δ 8.19 (d, 1 H, *J* = 0.9 Hz), 8.14 (d, 1 H, *J* = 5.4 Hz), 7.80 (dd, 1 H, *J* = 5.4, 1.2 Hz), 7.56 (app t, 1 H, *J* = 4.8 Hz), 7.36–7.31 (m, 2 H), 7.34 (dd, 1 H, *J* = 4.8, 1.2 Hz), 3.85 (s, 3 H).



1-22b

2,7-Dichloro-4-phenylquinazoline (1-22b). To a reaction vial was added **1-21**²¹ (0.041 g, 0.17 mmol), phenylboronic acid (0.023 g, 0.19 mmol), Pd(OAc)₂ (0.0020 g, 0.0087 mmol), and PPh₃ (0.0075 g, 0.028 mmol). Freshly distilled and degassed DME (1.5 mL) and Na₂CO₃ (0.057 g, 0.54 mmol) in H₂O (0.30 mL) were added via syringe, and the reaction mixture was sealed and heated at reflux for 18 h. The reaction mixture was cooled to room temperature, filtered through a pad of silica gel with EtOAc washings, and concentrated under reduced pressure. The crude residue was purified by chromatography on SiO₂ (1:50 EtOAc:hexanes to

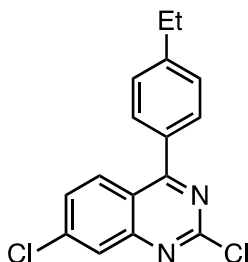
1:20 EtOAc:hexanes) to provide **1-22b** (0.033 g, 70%) as a pale green solid: ^1H NMR (DMSO- d_6 , 300 MHz) δ 8.18 (d, 1 H, $J = 2.1$ Hz), 8.12 (d, 1 H, $J = 9.0$ Hz), 7.80 (dd, 1 H, $J = 7.5, 1.8$ Hz), 7.83–7.78 (m, 2 H), 7.70–7.62 (m, 3 H); ^{13}C NMR (75 MHz, DMSO- d_6) δ 171.5, 157.0, 152.9, 140.4, 135.1, 131.0, 130.1, 129.6, 129.5, 128.8, 126.4, 120.0; MS (EI) m/z 274 ($[\text{M}]^+$, 58), 239 (100), 203 (43), 77 (51); HRMS (EI) m/z calcd for $\text{C}_{14}\text{H}_8\text{N}_2\text{Cl}_2$ (M^+) 274.0065, found 274.0060.



1-22c

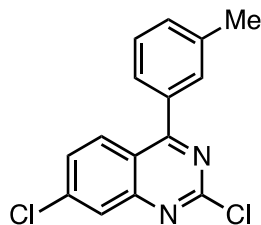
2,7-Dichloro-4-(thiophen-2-yl)quinazoline (1-22c). To a reaction vial was added **1-21**²¹ (0.040 g, 0.11 mmol), $\text{Pd}(\text{OAc})_2$ (0.0020 g, 0.0087 mmol), PPh_3 (0.0068 g, 0.026 mmol), and thiophene-2-boronic acid (0.024 g, 0.19 mmol). The reaction mixture was flushed with N_2 . Freshly distilled and degassed DME (1.5 mL) and Na_2CO_3 (0.056 g, 0.53 mmol) in H_2O (0.15 mL) were added via syringe. The reaction mixture was sealed and heated at reflux for 12 h. H_2O (5 mL) was added and the mixture was extracted with CH_2Cl_2 (4 x 10 mL). The combined organic layers were washed with H_2O (10 mL), dried (MgSO_4), and concentrated under reduced pressure. The crude residue was purified by chromatography on SiO_2 (1:20, EtOAc:hexanes) to provide **1-22c** (0.034 g, 71%) as a yellow-green solid: ^1H NMR (DMSO- d_6 , 300 MHz) δ 8.59 (d, 1 H, $J = 9.0$ Hz), 8.14 (dd, 1 H, $J = 3.9, 0.9$ Hz), 8.10 (dd, 1 H, $J = 5.1, 0.9$ Hz), 8.08 (d, 1 H, $J = 1.8$ Hz), 7.80 (dd, 1 H, $J = 9.0, 2.1$ Hz), 7.39 (dd, 1 H, $J = 5.1, 3.9$ Hz); ^{13}C NMR (DMSO- d_6 , 75 MHz) δ 162.9, 156.5, 153.3, 140.4, 138.7, 134.0, 133.9, 129.6, 129.4, 128.9, 126.5, 118.4;

MS (EI) m/z 280 ($[M]^+$, 95), 245 (68), 209 (43); HRMS (EI) m/z calcd for $C_{12}H_6Cl_2N_2S$ (M^+) 279.9629, found 279.9620.



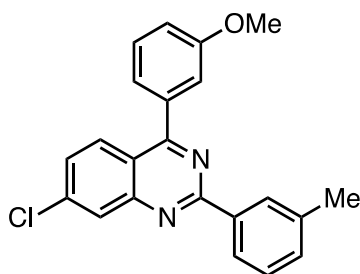
1-22d

2,7-Dichloro-4-(4-ethylphenyl)quinazoline (1-22d). To a reaction vial was added **1-21**²¹ (0.040 g, 0.17 mmol), Pd(OAc)₂ (0.0019 g, 0.0086 mmol), and PPh₃ (0.0068 g, 0.026 mmol). The reaction mixture was flushed with N₂. 4-Ethylphenylboronic acid (0.027 g, 0.18 mmol) in freshly distilled and degassed DME (1.7 mL) and Na₂CO₃ (0.056 g, 0.53 mmol) in H₂O (0.20 mL) were added via syringe. The reaction mixture was stirred at 80 °C under a N₂ atmosphere for 36 h. H₂O (1 mL) was added and the mixture was extracted with CH₂Cl₂ (4 x 5 mL). The combined organic layers were washed with brine (5 mL), dried (MgSO₄), and concentrated under reduced pressure. The crude residue was purified by chromatography on SiO₂ (1:20, EtOAc:hexanes) to provide **1-22d** (0.025 g, 49%) as a light green solid: ¹H NMR (DMSO-*d*₆, 300 MHz) δ 8.19–8.13 (m, 2 H), 7.80 (dd, 1 H, $J = 9.0, 2.1$ Hz), 7.75 (d, 2 H, $J = 8.1$ Hz), 7.50 (d, 2 H, $J = 7.8$ Hz), 2.75 (q, 2 H, $J = 7.5$ Hz), 1.26 (t, 3 H, $J = 7.5$ Hz).



1-22e

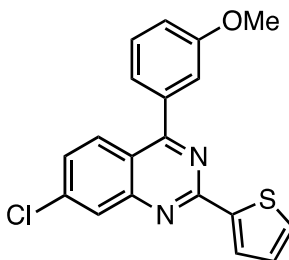
2,7-Dichloro-4-*m*-tolylquinazoline (1-22e). To a reaction vial was added **1-21**²¹ (0.061 g, 0.26 mmol), Pd(OAc)₂ (0.0030 g, 0.013 mmol), and PPh₃ (0.011 g, 0.041 mmol). The reaction mixture was flushed with N₂. 3-Methylphenylboronic acid (0.036 g, 0.26 mmol) in freshly distilled and degassed DME (1.0 mL) and Na₂CO₃ (0.085 g, 0.80 mmol) in H₂O (0.30 mL) were added via syringe. The reaction mixture was sealed and heated at reflux for 21 h. H₂O was added and the mixture was extracted with CH₂Cl₂ (4 x 15 mL). The combined organic layers were washed with H₂O, dried (MgSO₄), and concentrated under reduced pressure. The crude residue was purified by chromatography on SiO₂ (1:50, EtOAc:hexanes) to provide **1-22e** (0.025 g, 33%) as a light green solid: ¹H NMR (DMSO-*d*₆, 300 MHz) δ 8.15 (d, 1 H, *J* = 2.1 Hz), 8.11 (d, 1 H, *J* = 9.0 Hz), 7.78 (dd, 1 H, *J* = 9.0, 2.1 Hz), 7.61–7.48 (m, 4 H), 2.44 (s, 3 H); ¹³C NMR (DMSO-*d*₆, 75 MHz) δ 171.6, 157.0, 152.9, 140.4, 138.3, 135.0, 131.7, 130.4, 129.6, 129.4, 128.7, 127.4, 126.3, 120.0, 21.0; MS (EI) *m/z* 288 ([M]⁺, 79), 273 (76), 253 (86); HRMS (EI) *m/z* calcd for C₁₅H₁₀Cl₂N₂ (M⁺) 288.0221, found 288.0215.



1-23a

7-Chloro-4-(3-methoxyphenyl)-2-*m*-tolylquinazoline (1-23a). To a reaction vial was added **1-22a** (0.030 g, 0.098 mmol), Pd(OAc)₂ (0.0011 g, 0.0049 mmol), and PPh₃ (0.0039 g, 0.015 mmol). The reaction mixture was flushed with N₂. 3-Methylphenylboronic acid (0.014 g, 0.010 mmol) in freshly distilled and degassed DME (1.0 mL) and Na₂CO₃ (0.032 g, 0.30 mmol)

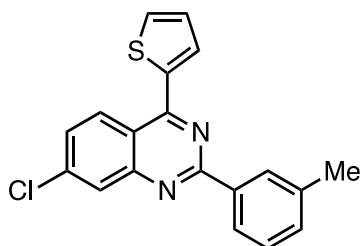
in H₂O (0.15 mL) were added via syringe. The reaction mixture was sealed and heated at reflux for 22 h. The mixture was extracted with CH₂Cl₂ (4 x 5 mL). The combined organic layers were washed with H₂O (5 mL), dried (MgSO₄), and concentrated under reduced pressure. The crude residue was purified by chromatography on SiO₂ (1:50, EtOAc:hexanes) to provide **1-23a** (0.030 g, 85%) as an off-white sticky solid: IR (ATR) 3047, 2999, 2918, 1560, 1539, 1331, 1288, 1243, 1049, 773 cm⁻¹; ¹H NMR (DMSO-*d*₆, 300 MHz) δ 8.36 (m, 2 H), 8.16 (d, 1 H, *J* = 2.1 Hz), 8.07 (d, 1 H, *J* = 9.0 Hz), 7.68 (dd, 1 H, *J* = 9.0, 2.1 Hz), 7.56 (app t, 1 H, *J* = 8.1 Hz), 7.48–7.34 (m, 4 H), 7.23 (dd, 1 H, *J* = 7.5, 1.8 Hz), 3.86 (s, 3 H), 2.43 (s, 3 H); ¹³C NMR (DMSO-*d*₆, 75 MHz) δ 168.0, 160.1, 159.3, 151.8, 139.1, 137.9, 137.0, 131.8, 129.9, 129.1, 128.72, 128.66, 128.4, 127.3, 125.6, 122.2, 119.8, 115.8, 115.4, 55.4, 21.1; MS (EI) *m/z* 360 ([M]⁺, 42), 345 (8), 325 (34); HRMS (EI) *m/z* calcd for C₂₂H₁₇ClN₂O (M⁺) 360.1029, found 360.1022.



1-23b

7-Chloro-4-(3-methoxyphenyl)-2-(thiophen-2-yl)quinazoline (1-23b). To a reaction vial was added **1-22a** (0.025 g, 0.082 mmol), Pd(OAc)₂ (0.0010 g, 0.0047 mmol), and PPh₃ (0.0033 g, 0.012 mmol). The reaction mixture was flushed with N₂. 2-Thiopheneboronic acid (0.011 g, 0.086 mmol) in freshly distilled and degassed DME (0.80 mL) and Na₂CO₃ (0.027 g, 0.24 mmol) in H₂O (0.15 mL) were added via syringe. The reaction mixture was sealed and

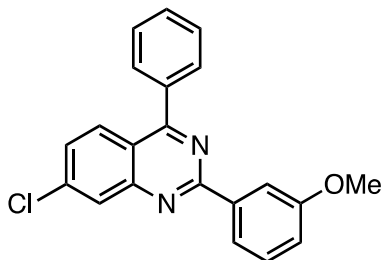
heated at reflux for 15 h. The mixture was extracted with CH₂Cl₂ (4 x 5 mL). The combined organic layers were washed with H₂O (5 mL), dried (MgSO₄), and concentrated under reduced pressure. The crude residue was purified by chromatography on SiO₂ (1:50, EtOAc:hexanes) to provide **1-23b** (0.018 g, 61%, 77% BRSM) as a pale green solid: ¹H NMR (DMSO-*d*₆, 300 MHz) δ 8.14–8.11 (m, 2 H), 8.06 (d, 1 H, *J* = 9.0 Hz), 7.85 (dd, 1 H, *J* = 5.1, 1.2 Hz), 7.68 (dd, 1 H, *J* = 9.0, 2.1 Hz), 7.57 (app t, 1 H, *J* 8.3 Hz), 7.40–7.36 (m, 2 H), 7.29–7.22 (m, 2 H), 3.87 (s, 3 H).



1-23c

2,7-Dichloro-4-(3-methoxyphenyl)quinazoline (1-23c). To a reaction vial was added **1-22c** (0.022 g, 0.080 mmol), Pd(OAc)₂ (0.0010 g, 0.0045 mmol), and PPh₃ (0.0030 g, 0.012 mmol). The reaction mixture was flushed with N₂. 3-Methylphenylboronic acid (0.012 g, 0.085 mmol) in freshly distilled and degassed DME (0.70 mL) and Na₂CO₃ (0.025 g, 0.24 mmol) in H₂O (0.15 mL) were added via syringe. The reaction mixture was sealed and heated at 75 °C for 24 h. The mixture was poured into H₂O (3.0 mL) and extracted with CH₂Cl₂ (4 x 10 mL). The combined organic layers were washed with H₂O (10 mL), dried (MgSO₄), and concentrated under reduced pressure. The crude residue was purified by chromatography on SiO₂ (1:50, EtOAc:hexanes) to provide **1-23c** (0.012 g, 45%) as a yellow-green solid: ¹H NMR (DMSO-*d*₆, 500 MHz) δ 8.61 (d, 1 H, *J* = 9.0 Hz), 8.39–8.35 (m, 2 H), 8.16 (d, 1 H, *J* = 2.5 Hz), 8.15 (dd, 1 H, *J* = 4.0, 1.0 Hz), 8.04 (dd, 1 H, *J* = 5.0, 0.5 Hz), 7.75 (dd, 1 H, *J* = 9.0, 2.0 Hz), 7.48 (app t,

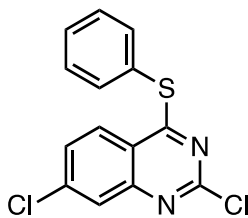
1 H), 7.42–7.38 (m, 2 H), 2.45 (s, 3 H); ^{13}C NMR (DMSO- d_6 , 75 MHz) δ 159.9, 159.7, 152.4, 140.7, 139.1, 137.9, 136.7, 132.4, 132.3, 131.9, 129.1, 128.7, 128.6, 128.5, 128.4, 127.4, 125.4, 118.3, 21.2; MS (EI) m/z 336 ($[\text{M}]^+$, 44), 280 (84), 245 (68), 209 (33), 149 (74), 57 (100); HRMS (EI) m/z calcd for $\text{C}_{19}\text{H}_{13}\text{ClN}_2\text{S}$ (M^+) 336.0488, found 336.0474.



1-23d

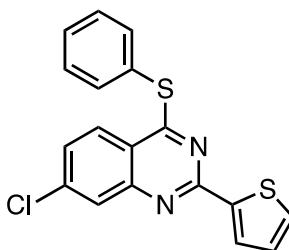
7-Chloro-2-(3-methoxyphenyl)-4-phenylquinazoline (1-23d). To a reaction vial was added **1-22b** (0.030 g, 0.098 mmol), $\text{Pd}(\text{OAc})_2$ (0.0011 g, 0.0049 mmol), and PPh_3 (0.0039 g, 0.015 mmol). The reaction mixture was flushed with N_2 . 3-Methoxyphenylboronic acid (0.014 g, 0.010 mmol) in freshly distilled and degassed DME (1.0 mL) and Na_2CO_3 (0.032 g, 0.30 mmol) in H_2O (0.15 mL) were added via syringe. The reaction mixture was sealed and heated under microwave irradiation at 120 °C for 40 min. The mixture was extracted with CH_2Cl_2 (4 x 5 mL). The combined organic layers were washed with H_2O (5 mL), dried (MgSO_4), and concentrated under reduced pressure. The crude residue was purified by chromatography on SiO_2 (1:50, EtOAc:hexanes) to provide **1-23d** (0.028 g, 75%) as a light yellow solid: IR (ATR) 3077, 3056, 1599, 1554, 1538, 1461, 1334, 1247, 1072, 1042, 932, 872, 833 cm^{-1} ; ^1H NMR (DMSO- d_6 , 300 MHz) δ 8.23 (d, 1 H, $J = 2.1$ Hz), 8.19 (d, 1 H, $J = 7.8$ Hz), 8.14–8.08 (m, 2 H), 7.90 (dd, 2 H, $J = 6.0, 2.1$ Hz), 7.73 (dd, 1 H, $J = 9.0, 2.1$ Hz), 7.70–7.64 (m, 3 H), 7.50 (app t, 1 H, $J = 8.1$ Hz), 7.16 (dd, 1 H, $J = 7.5, 1.8$ Hz), 3.87 (s, 3 H); HRMS (ESI)

m/z calcd for $C_{21}H_{16}ClN_2O$ ($[M+H]^+$) 347.0951, found 347.0932.



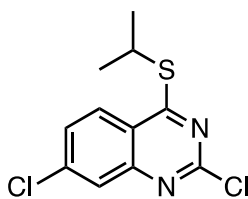
1-25

2,7-Dichloro-4-(phenylthio)quinazoline (1-25). To a solution of **1-21**²¹ (0.300 g, 1.28 mmol) in freshly distilled and degassed THF (21.0 mL) cooled to 0 °C was added a premixed solution of thiophenol (0.151 g, 1.33 mmol) and NaH (0.034 g, 1.42 mmol) in THF (2.0 mL) dropwise. The mixture was stirred for 15.5 h, warmed to room temperature, poured into ice cold H₂O, and extracted with EtOAc (5 x 50 mL). The combined organic layers were washed with H₂O, dried (MgSO₄), and concentrated under reduced pressure to give a light yellow residue. The crude residue was purified by chromatography on SiO₂ (1:10 EtOAc:hexanes) to provide **1-25** (0.294 g, 74%) as a light yellow-green solid: IR (ATR) 3047, 3062, 1549, 1461, 1329, 1137, 738 cm⁻¹; ¹H NMR (DMSO-*d*₆, 300 MHz,) δ 8.31 (d, 1 H, $J = 8.7$ Hz), 8.05 (d, 1 H, $J = 2.1$ Hz), 7.83 (dd, 1 H, $J = 9.0, 2.1$ Hz), 7.70–7.66 (m, 2 H), 7.59–7.55 (m, 3 H); ¹³C NMR (DMSO-*d*₆, 75 MHz) δ 174.4, 156.1, 150.1, 140.5, 135.5, 130.4, 129.8, 129.3, 126.6, 126.0, 125.4, 119.7; MS (EI) m/z 305 (M^+ , 100), 271 (21), 197 (18), 136 (53); HRMS (EI) m/z calcd for C₁₄H₈Cl₂N₂S (M^+) 305.9785, found 305.9782.



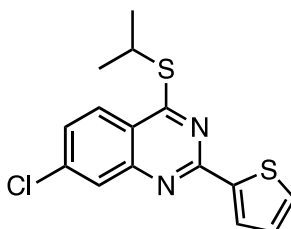
1-26a

7-Chloro-4-(phenylthio)-2-(thiophen-2-yl)quinazoline (1-26a). To a reaction vial was added **1-25** (0.039 g, 0.13 mmol), Pd(OAc)₂ (0.0015 g, 0.0060 mmol), PPh₃ (0.016 g, 0.060 mmol), and thiophene-2-boronic acid (0.017 g, 0.13 mmol). The reaction mixture was flushed with N₂. Freshly distilled and degassed DME (1.0 mL) and Na₂CO₃ (0.043 g, 0.40 mmol) in H₂O (0.15 mL) were added via syringe and the reaction mixture was sealed and heated at reflux for 23 h. The solution was extracted with CH₂Cl₂ (4 x 10 mL). The combined organic layers were washed with H₂O, dried (MgSO₄), and concentrated under reduced pressure. The crude residue was purified by chromatography on SiO₂ (1:20 EtOAc/hexanes) to provide **1-26a** (0.040 g, 87%) as a pale green solid: IR (ATR) 3060, 2920, 2851, 1601, 1536, 831, 740 cm⁻¹; ¹H NMR (DMSO-*d*₆, 300 MHz) δ 8.22 (d, 1H, *J* = 8.7 Hz), 8.01 (d, 1 H, *J* = 2.1 Hz), 7.76–7.70 (m, 4 H), 7.63–7.59 (m, 3 H), 7.55 (dd, 1 H, *J* = 3.6, 1.2 Hz), 7.13 (dd, 1 H, *J* = 5.1, 3.9 Hz); MS (EI) *m/z* 354 (M⁺, 72), 319 (12), 245 (100); HRMS (EI) *m/z* calcd for C₁₈H₁₁ClN₂S₂ (M⁺) 354.0052, found 354.0045.



1-28

2,7-Dichloro-4-(isopropylthio)quinazoline (1-28). To a solution of **1-21**²¹ (0.300 g, 1.28 mmol) in freshly distilled and degassed THF (13.0 mL) cooled to 0 °C was added a premixed solution of *i*-PrSH (0.12 mL, 1.28 mmol) and NaH (0.032 g, 1.35 mmol) in THF (2.0 mL) dropwise. The mixture was stirred for 16 h, warmed to room temperature, poured into ice cold H₂O, and extracted with EtOAc (5 x 25 mL). The combined organic layers were washed with H₂O, dried (MgSO₄), and concentrated under reduced pressure to give a light yellow residue. The residue was purified by chromatography on SiO₂ (1:50, EtOAc:hexanes) to provide **1-28** (0.291 g, 83%) as a light yellow crystalline solid: Mp 89.1–90.1 °C (EtOAc); IR (ATR) 3075, 2965, 2881, 1551, 1459, 1321, 1224, 1133, 852 cm⁻¹; ¹H NMR (DMSO-*d*₆, 300 MHz) δ 8.07 (d, 1 H, *J* = 9.0 Hz), 7.98 (d, 1 H, *J* = 2.1 Hz), 7.72 (dd, 1 H, *J* = 9.0, 2.1 Hz), 4.18 (sept, 1 H, *J* = 6.9 Hz), 1.46 (d, 6 H, *J* = 6.9 Hz); ¹³C NMR (DMSO-*d*₆, 75 MHz) δ 174.8, 156.0, 149.7, 140.1, 128.9, 126.6, 125.9, 120.2, 36.0, 22.2; MS (EI) *m/z* 272 ([M]⁺, 33), 230 (100), 195 (48), 161 (37); HRMS (EI) *m/z* calcd for C₁₁H₁₀Cl₂N₂S (M⁺) 271.9942, found 271.9946.

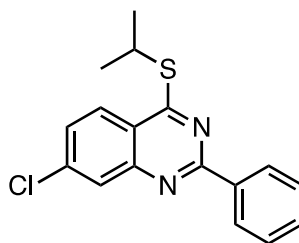


1-29a

7-Chloro-4-(isopropylthio)-2-(thiophen-2-yl)quinazoline (1-29a). General Protocol

A. To a reaction vial was added **1-28** (0.025 g, 0.092 mmol), Pd(OAc)₂ (0.0010 g, 0.0046 mmol), PPh₃ (0.0036 g, 0.014 mmol), Na₂CO₃ (0.030 g, 0.28 mmol), and thiophene-2-boronic acid (0.023 g, 0.18 mmol). The reaction mixture was flushed with N₂. Freshly distilled and degassed DME and H₂O (DME:H₂O, 10:1) were added via syringe to generate a 0.1 M solution

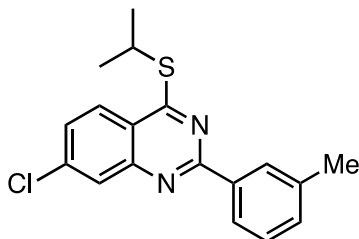
of **1-28**, and the reaction mixture was stirred at 75 °C under a N₂ atmosphere for 24 h. H₂O (1 mL) was added and the mixture was extracted with CH₂Cl₂ (4 x 5 mL). The combined organic layers were washed with brine (5 mL), dried (MgSO₄), and concentrated under reduced pressure. The crude residue was purified by chromatography on SiO₂ (1:50, EtOAc:hexanes) to give **1-29a** (0.029 g, 99%) as a light yellow solid: Mp 122.7–124.7 °C (DMSO); IR (ATR) 2973, 2917, 2855, 1524, 1437, 1327, 1236, 988, 837, 773, 714 cm⁻¹; ¹H NMR (DMSO-*d*₆, 300 MHz) δ 8.06 (dd, 1 H, *J* = 3.6, 1.2 Hz), 8.00 (d, 1 H, *J* = 8.7 Hz), 7.95 (d, 1 H, *J* = 2.1 Hz), 7.84 (dd, 1 H, *J* = 5.1, 1.5 Hz), 7.61 (dd, 1 H, *J* = 9.0, 2.1 Hz), 7.26 (dd, 1 H, *J* = 4.8, 3.6 Hz), 4.30 (sept, 1 H, *J* = 6.9 Hz), 1.53 (d, 6 H, *J* = 6.9 Hz); ¹³C NMR (DMSO-*d*₆, 75 MHz) δ 171.2, 156.0, 149.0, 142.8, 139.2, 131.7, 129.8, 128.8, 127.6, 127.0, 125.8, 120.0, 35.7, 22.4 ; MS (ESI) *m/z* 321 ([M+1]⁺, 100), 277 (65); HRMS (ESI) *m/z* calcd for C₁₅H₁₄ClN₂S₂ ([M+1]⁺) 321.0287, found 321.0271.



1-29b

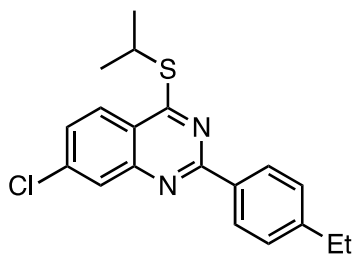
7-Chloro-4-(isopropylthio)-2-phenylquinazoline (1-29b). According to General Protocol A, **1-28** (0.040 g, 0.15 mmol), Pd(OAc)₂ (0.0016 g, 0.0073 mmol), PPh₃ (0.0058 g, 0.022 mmol), Na₂CO₃ (0.048 g, 0.45 mmol), and phenylboronic acid (0.027 g, 0.22 mmol) were heated at 75 °C for 33 h and provided a crude residue that was purified by chromatography on SiO₂ (1:50, EtOAc:hexanes) to afford **1-29b** (0.042 g, 92%) as a pale green fluffy solid: Mp 130.3–131.1 °C (DMSO); IR (ATR) 2956, 2924, 2863, 1552, 1530, 1329, 1301, 844, 773 cm⁻¹; ¹H NMR (DMSO-*d*₆, 300 MHz) δ 8.57–8.52 (m, 2 H), 8.08 (d, 1 H, *J* = 9.0 Hz), 8.06 (d, 1 H,

$J = 1.5$ Hz), 7.68 (dd, 1 H, $J = 8.7, 2.1$ Hz), 7.62–7.57 (m, 3 H), 4.42 (sept, 1 H, $J = 6.9$ Hz), 1.55 (d, 6 H, $J = 6.9$ Hz); ^{13}C NMR (DMSO- d_6 , 75 MHz) δ 171.2, 158.9, 149.2, 139.1, 137.0, 131.3, 128.8, 128.2, 128.1, 127.5, 125.7, 120.4, 35.4, 22.4; HRMS (ESI) m/z calcd for $\text{C}_{17}\text{H}_{16}\text{ClN}_2\text{S}$ ($[\text{M}+\text{H}]^+$) 315.0723, found 315.0726.



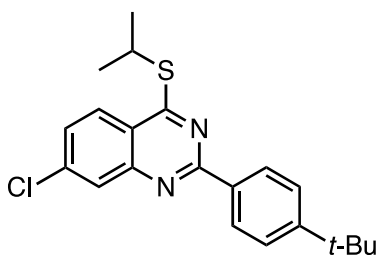
1-29c

7-Chloro-4-(isopropylthio)-2-*m*-tolylquinazoline (1-29c). According to General Protocol A, **1-28** (0.030 g, 0.11 mmol), $\text{Pd}(\text{OAc})_2$ (0.0012 g, 0.0055 mmol), PPh_3 (0.0044 g, 0.016 mmol), Na_2CO_3 (0.036 g, 0.34 mmol), and 3-methylphenylboronic acid (0.018 g, 0.13 mmol) were heated at 75 °C for 36 h and provided a crude residue that was purified by chromatography on SiO_2 (1:50, EtOAc:hexanes) to afford **1-29c** (0.032 g, 90%) as a white crystalline solid: Mp 114.4–115.1 °C (DMSO); IR (ATR) 2969, 2920, 2859, 1530, 1329, 768, 719 cm^{-1} ; ^1H NMR (DMSO- d_6 , 300 MHz) δ 8.37–8.30 (m, 2H), 8.07 (d, 1 H, $J = 6.5$ Hz), 8.05 (s, 1 H), 7.67 (dd, 1 H, $J = 8.9, 2.0$ Hz), 7.47 (app t, 1 H, $J = 7.6$ Hz), 7.40 (d, 1 H, $J = 7.6$ Hz), 4.40 (sept, 1 H, $J = 6.8$ Hz), 2.44 (s, 3 H), 1.55 (d, 6 H, $J = 6.8$ Hz); ^{13}C NMR (DMSO- d_6 , 75 MHz) δ 171.2, 159.0, 149.2, 139.0, 138.0, 137.0, 131.9, 128.8, 128.7, 128.0, 127.5, 125.7, 125.5, 120.3, 35.4, 22.4, 21.2; MS (EI) m/z 328 ($[\text{M}]^+$, 47), 286 (100), 253 (87), 91 (75); HRMS (EI) m/z calcd for $\text{C}_{18}\text{H}_{17}\text{ClN}_2\text{S}$ 328.0801 (M^+), found 328.0804.



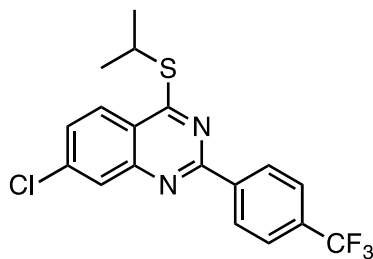
1-29d

7-Chloro-2-(4-ethylphenyl)-4-(isopropylthio)quinazoline (1-29d). According to General Protocol A, **1-28** (0.040 g, 0.15 mmol), Pd(OAc)₂ (0.0016 g, 0.0073 mmol), PPh₃ (0.0058 g, 0.022 mmol), Na₂CO₃ (0.048 g, 0.45 mmol), and 4-ethylphenylboronic acid (0.033 g, 0.22 mmol) were heated at 75 °C for 33 h and provided a crude residue that was purified by chromatography on SiO₂ (1:50, EtOAc:hexanes) to afford **1-29d** (0.048 g, 95%) as a pale green solid: Mp 124.1–125.9 °C (DMSO); IR (ATR) 3064, 2920, 1552, 1532, 1329, 1301, 990, 762, 699 cm⁻¹; ¹H NMR (DMSO-*d*₆, 300 MHz) δ 8.46 (d, 2 H, *J* = 8.4 Hz), 8.07 (d, 1 H, *J* = 9.0 Hz), 8.04 (d, 1 H, *J* = 2.1 Hz), 7.66 (dd, 1 H, *J* = 8.7, 2.1 Hz), 7.42 (d, 2 H, *J* = 8.1 Hz), 4.41 (sept, 1 H, *J* = 6.9 Hz), 2.71 (q, 2 H, *J* = 7.5 Hz), 1.55 (d, 6 H, *J* = 6.9 Hz), 1.24 (t, 3 H, *J* = 7.5 Hz); ¹³C NMR (DMSO-*d*₆, 150 MHz) δ 171.1, 159.0, 149.2, 147.4, 139.0, 134.6, 128.31, 128.27, 127.9, 127.4, 125.7, 120.3, 35.4, 28.2, 22.4, 15.4; HRMS (ESI) *m/z* calcd for C₁₉H₂₀ClN₂S ([M+H]⁺) 343.1036, found 343.1015.



1-29e

2-(4-*tert*-Butylphenyl)-7-chloro-4-(isopropylthio)quinazoline (1-29e). According to General Protocol A, **1-28** (0.040 g, 0.15 mmol), Pd(OAc)₂ (0.0016 g, 0.0073 mmol), PPh₃ (0.0058 g, 0.022 mmol), Na₂CO₃ (0.048 g, 0.45 mmol), and 4-*tert*-butylbenzeneboronic acid (0.039 g, 0.22 mmol) were heated at 75 °C for 25 h and provided a crude residue that was purified by chromatography on SiO₂ (1:50, EtOAc:hexanes) to afford **1-29e** (0.051 g, 93%) as a tan colored sticky solid: IR (ATR) 2959, 2864, 1551, 1528, 1465, 1327, 991, 848, 779 cm⁻¹; ¹H NMR (DMSO-*d*₆, 300 MHz) δ 8.46 (d, 2 H, *J* = 8.5 Hz), 8.06 (d, 1 H, *J* = 8.7 Hz), 8.04 (d, 1 H, *J* = 1.3 Hz), 7.66 (dd, 1 H, *J* = 8.7, 2.1 Hz), 7.60 (d, 2 H, *J* = 8.5 Hz), 4.40 (sept, 1 H, *J* = 6.8 Hz), 1.55 (d, 6 H, *J* = 6.8 Hz), 1.34 (s, 9 H) ; ¹³C NMR (DMSO-*d*₆, 150 MHz) δ 171.5, 159.4, 154.6, 149.7, 139.4, 134.8, 128.5, 128.3, 127.9, 126.2, 126.1, 120.7, 35.9, 35.2, 31.4, 22.9; MS (EI) *m/z* 370 ([M]⁺, 50), 328 (95), 313 (100), 240 (48); HRMS (EI) *m/z* calcd for C₂₁H₂₃ClN₂S (M⁺) 370.1270, found 370.1259.

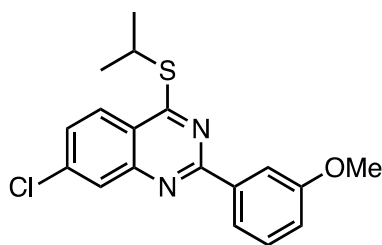


1-29f

7-Chloro-4-(isopropylthio)-2-(4-(trifluoromethyl)phenyl)quinazoline (1-29f).

According to General Protocol A, **1-28** (0.040 g, 0.15 mmol), Pd(OAc)₂ (0.0016 g, 0.0073 mmol), PPh₃ (0.0058 g, 0.022 mmol), Na₂CO₃ (0.048 g, 0.45 mmol), and 4-trifluoromethylphenylboronic acid (0.042 g, 0.22 mmol) were heated at 75 °C for 13 h and provided a crude residue that was purified by chromatography on SiO₂ (1:50, EtOAc:hexanes) to

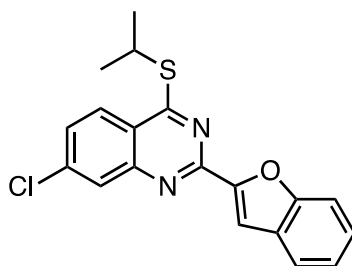
afford **1-29f** (0.049 g, 88%) as an off-white solid: Mp 142.1–144.0 °C (DMSO); IR (ATR) 2963, 2928, 2866, 1536, 1551, 1319, 1303, 1105, 1064, 852, 779 cm⁻¹; ¹H NMR (DMSO-*d*₆, 323 K, 300 MHz) δ 8.69 (d, 2 H, *J* = 8.0 Hz), 8.09 (d, 1 H, *J* = 8.9 Hz), 8.05 (d, 1 H, *J* = 2.0 Hz), 7.92 (d, 2 H, *J* = 8.3 Hz), 7.69 (dd, 1 H, *J* = 8.8, 2.1 Hz), 4.43 (sept, 1 H, *J* = 6.8 Hz), 1.57 (d, 6 H, *J* = 6.8 Hz); ¹³C NMR (DMSO-*d*₆, 323 K, 75 MHz) δ 171.5, 157.4, 148.7, 140.6, 139.0, 130.9, 130.5, 128.5, 128.3, 127.3, 125.7, 125.4, 125.34, 125.29, 125.2, 122.1, 120.3, 35.3, 22.2; MS (ESI) *m/z* 383 ([M+H]⁺, 100), 313 (10); HRMS (ESI) *m/z* calcd for C₁₈H₁₅ClF₃N₂S ([M+H]⁺) 383.0597, found 383.0563.



1-29g

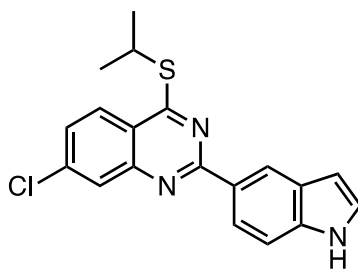
7-Chloro-4-(isopropylthio)-2-(3-methoxyphenyl)quinazoline (1-29g). According to General Protocol A, **1-28** (0.040 g, 0.15 mmol), Pd(OAc)₂ (0.0016 g, 0.0073 mmol), PPh₃ (0.0058 g, 0.022 mmol), Na₂CO₃ (0.048 g, 0.45 mmol), and 3-methoxyphenylboronic acid (0.034 g, 0.22 mmol) were heated at 75 °C for 17 h and provided a crude residue that was purified by chromatography on SiO₂ (1:50, EtOAc:hexanes) to afford **1-29g** (0.045 g, 89%) as an off-white solid: Mp 109.7–111.3 °C (EtOAc/hexanes); IR (ATR) 3068, 2920, 2859, 1599, 1552, 1534, 1452, 1329, 1047, 772 cm⁻¹; ¹H NMR (DMSO-*d*₆, 300 MHz) δ 8.10 (d, 1 H, *J* = 7.8 Hz), 8.07–7.99 (m, 3 H), 7.64 (dd, 1 H, *J* = 8.9, 2.0 Hz), 7.48 (app t, 1 H, *J* = 8.0 Hz), 7.14 (dd, 1 H, *J* = 8.2, 2.5 Hz), 4.35 (sept, 1 H, *J* = 6.8 Hz), 3.86 (s, 3 H), 1.54 (d, 6 H, *J* = 6.8 Hz);

^{13}C NMR (DMSO- d_6 , 75 MHz) δ 171.1, 159.6, 158.6, 149.0, 139.0, 138.4, 129.9, 128.1, 127.5, 125.7, 120.6, 120.3, 116.9, 113.2, 55.2, 35.5, 22.4; MS (ESI) m/z 345 ($[\text{M}+\text{H}]^+$, 100), 227 (27), 229 (21); HRMS (ESI) m/z calcd for $\text{C}_{18}\text{H}_{18}\text{ClN}_2\text{OS}$ ($[\text{M}+\text{H}]^+$) 345.0801, found 345.0828.



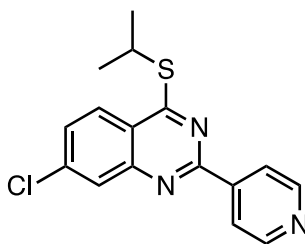
1-29h

2-(Benzofuran-2-yl)-7-chloro-4-(isopropylthio)quinazoline (1-29h). According to General Protocol A, **1-28** (0.040 g, 0.15 mmol), $\text{Pd}(\text{OAc})_2$ (0.0016 g, 0.0073 mmol), PPh_3 (0.0058 g, 0.022 mmol), Na_2CO_3 (0.048 g, 0.45 mmol), and benzo[*b*]furan-2-boronic acid (0.036 g, 0.22 mmol) were heated at 75 °C for 33 h and provided a crude residue that was purified by chromatography on SiO_2 (1:100, EtOAc:hexanes) to afford **1-29h** (0.041 g, 79%) as a pale green solid: Mp 168.7–169.9 °C (EtOAc/hexanes); IR (ATR) 3056, 2961, 2920, 2864, 1579, 1547, 1528, 1470, 1336, 954, 848, 754 cm^{-1} ; ^1H NMR (DMSO- d_6 , 300 MHz) δ 8.11 (d, 1 H, $J = 2.0$ Hz), 8.08 (d, 1 H, $J = 8.8$ Hz), 7.93 (s, 1 H), 7.84 (d, 1 H, $J = 7.7$ Hz), 7.78 (d, 1 H, $J = 8.1$ Hz), 7.70 (dd, 1 H, $J = 8.8, 1.9$ Hz), 7.48 (app t, 1 H, $J = 7.6$ Hz), 7.36 (app t, 1 H, $J = 7.7$ Hz), 4.41 (sept, 1 H, $J = 6.8$ Hz), 1.55 (d, 6 H, $J = 6.8$ Hz); ^{13}C NMR (DMSO- d_6 , 308 K, 75 MHz) δ 171.3, 155.4, 153.1, 152.5, 148.7, 139.2, 128.2, 127.7, 127.3, 126.5, 125.6, 123.5, 122.4, 120.4, 111.7, 110.8, 35.5, 22.3; MS (EI) m/z 354 ($[\text{M}]^+$, 43), 312 (100), 279 (50); HRMS (EI) m/z calcd for $\text{C}_{19}\text{H}_{15}\text{ClN}_2\text{OS}$ (M^+) 354.0594, found 354.0590.



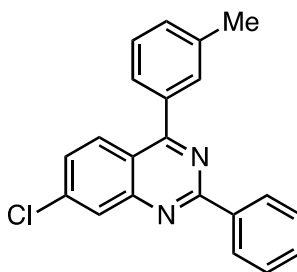
1-29i

7-Chloro-2-(1*H*-indol-5-yl)-4-(isopropylthio)quinazoline (1-29i). According to General Protocol A, **1-28** (0.040 g, 0.15 mmol), Pd(OAc)₂ (0.0047 g, 0.0029 mmol), PPh₃ (0.0058 g, 0.022 mmol), Na₂CO₃ (0.048 g, 0.45 mmol), and indole-5-boronic acid (0.027 g, 0.22 mmol) were heated at 75 °C for 48 h and provided a crude residue that was purified by chromatography on SiO₂ (1:100 to 1:10, EtOAc:hexanes) to afford **1-29i** (0.031 g, 60%) as a tan colored solid: Mp 191.7–193.2 °C (DMSO); IR (ATR) 3176, 2958, 2920, 2863, 1470, 1526, 1333, 1318, 1232, 850, 764, 731 cm⁻¹; ¹H NMR (DMSO-*d*₆, 300 MHz) δ 11.38 (s, 1 H), 8.82 (s, 1 H), 8.35 (dd, 1 H, *J* = 8.6, 1.6 Hz), 7.98 (d, 1 H, *J* = 8.9 Hz), 7.97 (d, 1 H, *J* = 2.0 Hz), 7.56 (dd, 1 H, *J* = 8.6, 2.2 Hz), 7.54 (d, 1 H, *J* = 8.6 Hz), 7.44 (app t, 1 H, *J* = 2.7 Hz), 6.62 (app t, 1 H, *J* = 2.0 Hz), 4.42 (sept, 1 H, *J* = 6.8 Hz), 1.55 (d, 6 H, *J* = 6.8 Hz); ¹³C NMR (DMSO-*d*₆, 75 MHz) δ 170.4, 160.4, 149.5, 138.7, 137.9, 128.0, 127.9, 127.1, 127.0, 126.7, 125.6, 121.6, 121.4, 121.3, 120.0, 111.6, 102.5, 35.2, 22.5; MS (EI) *m/z* 353 ([M]⁺, 10), 311 (12), 278 (18); HRMS (EI) *m/z* calcd for C₁₉H₁₆ClN₃S (M⁺) 353.0753, found 353.0756.



1-29k

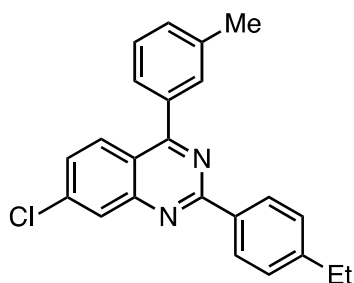
7-Chloro-4-(isopropylthio)-2-(pyridin-4-yl)quinazoline (1-29k). According to General Protocol A, **1-28** (0.040 g, 0.15 mmol), Pd(OAc)₂ (0.0016 g, 0.0073 mmol), PPh₃ (0.0058 g, 0.022 mmol), Na₂CO₃ (0.048 g, 0.45 mmol), and pyridine-4-boronic acid (0.027 g, 0.22 mmol) were heated at 75 °C for 48 h and provided a crude residue that was purified by chromatography on SiO₂ (1:100 to 1:5, EtOAc:hexanes) to afford **1-29k** (0.025 g, 53%) as a tan-colored solid: Mp 154.3–155.8 °C (DMSO); IR (ATR) 3023, 2969, 2920, 2864, 1599, 1547, 1526, 1464, 1331, 1310, 1239, 993, 824, 775 cm⁻¹; ¹H NMR (DMSO-*d*₆, 300 MHz) δ 8.85–8.81 (m, 2 H), 8.41–8.36 (m, 2 H), 8.15 (s, 1 H), 8.13 (d, 1 H, *J* = 5.8 Hz), 7.77 (dd, 1 H, *J* = 8.9, 2.1 Hz), 4.45 (sept, 1 H, *J* = 6.8 Hz), 1.56 (d, 6 H, *J* = 6.8 Hz); ¹³C NMR (DMSO-*d*₆, 75 MHz) δ 171.8, 157.0, 150.3, 148.6, 144.0, 139.1, 128.7, 127.5, 125.5, 121.6, 120.7, 35.4, 22.2; MS (EI) *m/z* 317 ([M+2]⁺, 22), 315 ([M]⁺, 38), 272 (18), 240 (40), 78 (61); HRMS (EI) *m/z* calcd for C₁₆H₁₄ClN₃S (M⁺) 315.0597, found 315.0602.



1-23f

7-Chloro-2-phenyl-4-*m*-tolylquinazoline (1-23f). General Protocol B. To a reaction vial was added **1-29b** (0.028 g, 0.090 mmol), CuTC (0.038 g, 0.20 mmol), Pd(PPh₃)₄ (0.0057 g, 0.0045 mmol), and 3-methylphenylboronic acid (0.027 g, 0.20 mmol). The reaction mixture was flushed with N₂ and freshly distilled and degassed THF was added via syringe to generate a 0.06 M solution of **1-29b**. The reaction mixture was stirred vigorously at 50 °C under a N₂

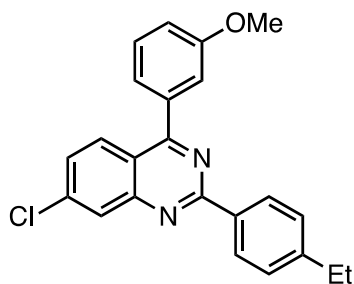
atmosphere for 26 h. A saturated solution of NaHCO₃ (1 mL) was added and the solution was extracted with CH₂Cl₂ (4 x 5 mL), dried (MgSO₄), and concentrated under reduced pressure. The crude residue was purified by chromatography on SiO₂ (1:100, EtOAc:hexanes) to afford **1-23f** (0.028 g, 89%) as a pale yellow sticky solid: IR (ATR) 3058, 3030, 2914, 2851, 1556, 1532, 1336, 913, 766, 695, 682 cm⁻¹; ¹H NMR (DMSO-*d*₆, 300 MHz) δ 8.63–8.56 (m, 2 H), 8.22 (d, 1 H, *J* = 2.1 Hz), 8.11 (d, 1 H, *J* = 9.0 Hz), 7.73 (dd, 1 H, 9.0, 2.1 Hz), 7.70 (s, 1 H), 7.67 (d, 1 H, *J* = 7.6 Hz), 7.62–7.57 (m, 3 H), 7.54 (d, 1 H, *J* = 7.5 Hz), 7.49 (d, 1 H, *J* = 7.4 Hz), 2.47 (s, 3 H); ¹³C NMR (DMSO-*d*₆, 75 MHz) δ 168.3, 160.0, 151.9, 139.1, 138.1, 137.1, 136.6, 131.2, 131.0, 130.4, 129.1, 128.8, 128.6, 128.4, 128.3, 127.3, 127.2, 119.8, 21.1; MS (EI) *m/z* 330 ([M]⁺, 17), 329 ([M-1]⁺, 43), 238 (43), 91 (100); HRMS (EI) *m/z* calcd for C₂₁H₁₅ClN₂ (M⁺) 330.0924, found 330.0930.



1-23g

7-Chloro-2-(4-ethylphenyl)-4-*m*-tolylquinazoline (1-23g). According to General Protocol B, **1-29d** (0.028 g, 0.083 mmol), CuTC (0.035 g, 0.18 mmol), Pd(PPh₃)₄ (0.0053 g, 0.0041 mmol), and 3-methylphenylboronic acid (0.025 g, 0.18 mmol) were heated at 50 °C for 19 h and provided a crude residue that was purified by chromatography on SiO₂ (1:100, EtOAc:hexanes) to afford **1-23g** (0.027 g, 89%) as a pale yellow sticky solid: IR (ATR) 2963, 2935, 2883, 1599, 1552, 1528, 1336, 846, 786, 701 cm⁻¹; ¹H NMR (DMSO-*d*₆, 300 MHz) δ 8.49

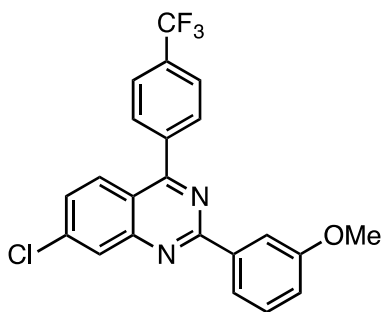
(d, 2 H, $J = 8.3$ Hz), 8.17 (d, 1 H, $J = 2.0$ Hz), 8.07 (d, 1 H, $J = 8.9$ Hz), 7.69 (dd, 1 H, $J = 9.0$, 2.1 Hz), 7.68 (s, 1 H), 7.64 (d, 1 H, $J = 7.5$ Hz), 7.54 (t, 1 H, $J = 7.5$ Hz), 7.48 (d, 1 H, $J = 7.6$ Hz), 7.41 (d, 2 H, $J = 8.4$ Hz), 2.71 (q, 2 H, $J = 7.6$ Hz), 2.47 (s, 3 H), 1.24 (t, 3 H, $J = 7.6$ Hz); ^{13}C NMR (DMSO- d_6 , 75 MHz) δ 168.3, 160.1, 151.9, 147.3, 139.0, 138.2, 136.6, 134.7, 131.0, 130.4, 129.2, 128.6, 128.4, 128.2, 127.23, 127.20, 119.7, 28.2, 21.1, 15.4; MS (EI) m/z 358 ($[\text{M}]^+$, 32), 357 ($[\text{M}-1]^+$, 81), 91 (100); HRMS (EI) m/z calcd for $\text{C}_{23}\text{H}_{19}\text{ClN}_2$ (M^+) 358.1237, found 358.1230.



1-23h

7-Chloro-2-(4-ethylphenyl)-4-(3-methoxyphenyl)quinazoline (1-23h). According to General Protocol B, **1-29d** (0.046 g, 0.13 mmol), CuTC (0.057 g, 0.30 mmol), Pd(PPh₃)₄ (0.0086 g, 0.0067 mmol), and 3-methoxyphenylboronic acid (0.045 g, 0.30 mmol) were heated at 50 °C for 22 h and provided a crude residue that was purified by chromatography on SiO₂ (1:200 to 1:20, EtOAc:hexanes) to afford **1-23h** (0.042 g, 83%) as a yellow solid: Mp 88.3–89.7 °C (EtOAc/hexanes); IR (ATR) 3064, 3002, 2959, 2930, 2827, 1597, 1554, 1528, 1334, 1247, 1236, 1042, 909, 783 cm⁻¹; ^1H NMR (DMSO- d_6 , 300 MHz) δ 8.51 (d, 2 H, $J = 8.3$ Hz), 8.19 (d, 1 H, $J = 2.1$ Hz), 8.11 (d, 1 H, $J = 9.0$ Hz), 7.71 (dd, 1 H, $J = 8.9$, 2.2 Hz), 7.58 (t, 1 H, $J = 8.3$ Hz), 7.45–7.38 (m, 4 H), 7.27–7.22 (m, 1 H), 3.87 (s, 3 H), 2.71 (q, 2 H, $J = 7.6$ Hz), 1.24 (t, 3 H, $J = 7.6$ Hz); ^{13}C NMR (DMSO- d_6 , 75 MHz) δ 168.0, 160.1, 159.3, 151.9, 147.3, 139.1, 138.0,

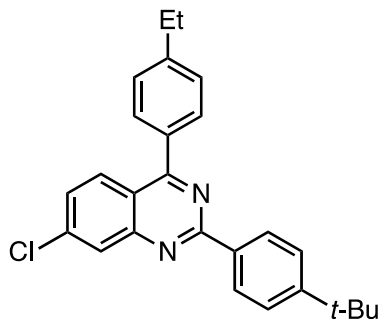
134.7, 129.92, 129.88, 129.2, 128.5, 128.3, 127.2, 122.2, 119.8, 115.9, 115.3, 55.4, 28.2, 15.4; MS (ESI) m/z 375 ($[M+1]^+$, 100), 227 (30); HRMS (ESI) m/z calcd for $C_{23}H_{20}ClN_2O$ ($[M+H]^+$) 375.1264, found 375.1259.



1-23i

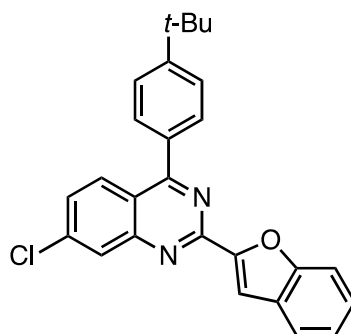
7-Chloro-2-(4-methoxyphenyl)-4-(4-(trifluoromethyl)phenyl)quinazoline (1-23i).

According to General Protocol B, **1-29g** (0.031 g, 0.091 mmol), CuTC (0.038 g, 0.20 mmol), Pd(PPh₃)₄ (0.0058 g, 0.0045 mmol), and 4-trifluoromethylphenylboronic acid (0.038 g, 0.20 mmol) were heated at 50 °C for 19 h and provided a crude residue that was purified by chromatography on SiO₂ (1:50, EtOAc:hexanes) to afford **1-23i** (0.033 g, 87%) as a white solid: Mp 159.0–159.9 °C (DMSO); IR (ATR) 2950, 2918, 2844, 1538, 1321, 1278, 1167, 1122, 1105, 1064, 1043, 777 cm⁻¹; ¹H NMR (DMSO-*d*₆, 600 MHz) δ 8.22 (d, 1 H, *J* = 2.0 Hz), 8.15 (d, 1 H, *J* = 7.7 Hz), 8.09 (d, 2 H, *J* = 8.1), 8.08 (s, 1 H), 8.05 (d, 1 H, *J* = 8.9 Hz), 8.02 (d, 2 H, *J* = 8.2 Hz), 7.71 (dd, 1 H, *J* = 8.9, 2.0 Hz), 7.48 (t, 1 H, *J* = 8.0 Hz), 7.15 (dd, 1 H, *J* = 8.0, 2.3 Hz), 3.86 (s, 3 H); ¹³C NMR (DMSO-*d*₆, 150 MHz) δ 166.9, 159.8, 159.7, 151.8, 140.5, 139.4, 138.3, 130.9, 130.7, 130.5, 130.3, 129.9, 128.82, 128.79, 127.4, 125.7, 125.64, 125.61, 125.0, 123.2, 120.8, 119.8, 119.1, 117.0, 113.4, 55.3; HRMS (ESI) m/z calcd for $C_{22}H_{15}ClF_3N_2O$ ($[M+H]^+$) 415.0825, found 415.0806.



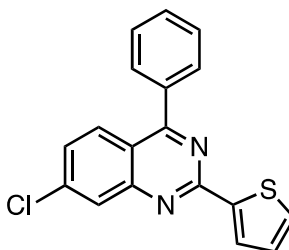
1-23k

2-(4-*tert*-Butylphenyl)-7-chloro-4-(4-ethylphenyl)quinazoline (1-23k). According to General Protocol B, **1-29e** (0.047 g, 0.13 mmol), CuTC (0.053 g, 0.28 mmol), Pd(PPh₃)₄ (0.0080 g, 0.0063 mmol), and 4-ethylphenylboronic acid (0.042 g, 0.28 mmol) were heated at 50 °C for 19 h and provided a crude residue that was purified by chromatography on SiO₂ (1:50, EtOAc:hexanes) to afford **1-23k** (0.043 g, 86%) as a white crystalline solid: IR (ATR) 2959, 2866, 1599, 1552, 1528, 1472, 1388, 1336, 850, 786, 703 cm⁻¹; ¹H NMR (DMSO-*d*₆, 600 MHz) δ 8.46 (d, 2 H, *J* = 8.5 Hz), 8.12 (d, 1 H, *J* = 2.1 Hz), 8.06 (d, 1 H, *J* = 8.9 Hz), 7.77 (d, 2 H, *J* = 8.0 Hz), 7.64 (dd, 1 H, *J* = 8.9, 2.1 Hz), 7.56 (d, 2 H, *J* = 8.6 Hz), 7.46 (d, 2 H, *J* = 8.1 Hz), 2.74 (q, 2 H, *J* = 7.6 Hz), 1.32 (s, 9 H), 1.26 (t, 3 H, *J* = 7.6 Hz); ¹³C NMR (DMSO-*d*₆, 150 MHz) δ 167.9, 160.1, 153.9, 152.0, 146.4, 138.9, 134.5, 134.1, 130.1, 129.1, 128.2, 128.12, 128.09, 127.2, 125.5, 119.6, 34.6, 31.0, 28.1, 15.5; HRMS (ESI) *m/z* calcd for C₂₆H₂₆ClN₂ ([M+H]⁺) 401.1785, found 401.1775.



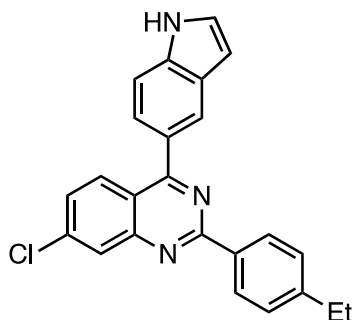
1-23m

2-(Benzofuran-2-yl)-4-(4-*tert*-butylphenyl)-7-chloroquinazoline (1-23m). According to General Protocol B, **1-29h** (0.036 g, 0.10 mmol), CuTC (0.043 g, 0.22 mmol), Pd(PPh₃)₄ (0.0064 g, 0.0051 mmol), and 4-*tert*-butylphenylboronic acid (0.040 g, 0.22 mmol) were heated at 50 °C for 27 h and provided a crude residue that was purified by chromatography on SiO₂ (1:100, EtOAc:hexanes) to afford **1-23m** (0.039 g, 91%) as a yellow crystalline solid: Mp 193.7–195.4 °C (DMSO); IR (ATR) 2961, 2920, 2864, 1552, 1523, 1474, 1334, 846, 783, 759 cm⁻¹; ¹H NMR (DMSO-*d*₆, 300 MHz) δ 8.26 (d, 1H, *J* = 1.8 Hz), 8.14 (d, 1 H, *J* = 8.9 Hz), 7.96 (s, 1 H), 7.84 (d, 2 H, *J* = 8.2 Hz), 7.83–7.72 (m, 3 H), 7.70 (d, 2 H, *J* = 8.2 Hz), 7.48 (t, 1 H, *J* = 7.6 Hz), 7.36 (t, 1 H, *J* = 7.5 Hz), 1.40 (s, 9 H); ¹³C NMR (DMSO-*d*₆, 323 K, 75 MHz) δ 168.1, 155.2, 153.6, 153.3, 153.1, 151.4, 139.1, 133.2, 129.5, 129.0, 128.4, 127.7, 126.9, 126.3, 125.2, 123.3, 122.1, 119.7, 111.5, 110.3, 34.4, 30.7; MS (EI) *m/z* 412 ([M]⁺, 100), 397 (59), 355 (33), 251 (74); HRMS (EI) *m/z* calcd for C₂₆H₂₁ClN₂O (M⁺) 412.1342, found 412.1338.



1-23n

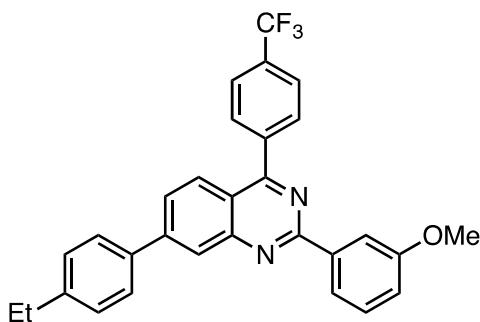
7-Chloro-4-phenyl-2-(thiophen-2-yl)quinazoline (1-23n). According to General Protocol B, **1-29a** (0.025 g, 0.078 mmol), CuTC (0.033 g, 0.17 mmol), Pd(PPh₃)₄ (0.0041 g, 0.0039 mmol), and phenylboronic acid (0.021 g, 0.17 mmol) were heated at 50 °C for 13 h and provided a crude residue that was purified by chromatography on SiO₂ (1:50, EtOAc:hexanes) to afford **1-23n** (0.024 g, 97%) as an off-white flaky solid: Mp 172.9–174.0 °C (DMSO); IR (ATR) 3066, 2917, 1526, 1426, 770, 701 cm⁻¹; ¹H NMR (DMSO-*d*₆, 300 MHz) δ 8.16–8.10 (m, 2 H), 8.05 (d, 1 H, *J* = 9.0 Hz), 7.88–7.81 (m, 3 H), 7.72–7.63 (m, 4 H), 7.27 (dd, 1 H *J* = 5.1, 3.6 Hz); ¹³C NMR (DMSO-*d*₆, 75 MHz) δ 168.4, 157.2, 151.8, 142.9, 139.4, 136.2, 131.7, 130.5, 130.0, 129.3, 128.8, 128.1, 126.8, 119.6; MS (EI) *m/z* 322 ([M]⁺, 100), 321 ([M-1]⁺, 74), 287 (75), 245 (30); HRMS (EI) *m/z* calcd for C₁₈H₁₁ClN₂S₂ (M⁺) 322.0331, found 322.0327.



1-23o

7-Chloro-2-(4-ethylphenyl)-4-(1H-indol-5-yl)quinazoline (1-23o). According to General Protocol B, **1-29d** (0.015 g, 0.044 mmol), CuTC (0.018 g, 0.096 mmol), Pd(PPh₃)₄ (0.0028 g, 0.0022 mmol), and indole-5-boronic acid (0.016 g, 0.096 mmol) were heated at 50 °C for 48 h and provided a crude residue that was purified by chromatography on SiO₂ (1:20, THF:toluene) to afford **1-23o** (0.012 g, 66%, 90% pure) as a yellow solid: Mp 172.8–174.2 °C (THF/Toluene); IR (ATR) 3213, 3205, 2956, 2915, 2848, 1599, 1551, 1530, 1461, 1336, 852,

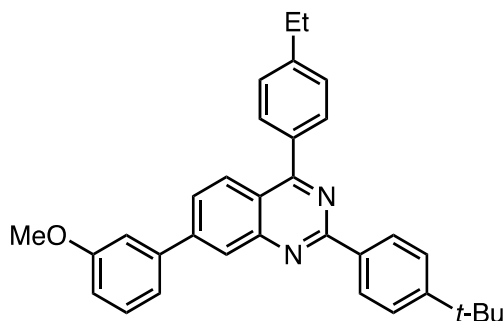
772, 729 cm^{-1} ; ^1H NMR (DMSO- d_6 , 300 MHz) δ 11.48 (s, 1 H), 8.53 (d, 2 H, $J = 8.3$ Hz), 8.23 (d, 1 H, $J = 9.0$ Hz), 8.15 (d, 1 H, $J = 2.1$ Hz), 8.13 (s, 1 H), 7.70 (dd, 1 H, $J = 8.9, 2.2$ Hz), 7.66 (s, 2 H), 7.53 (t, 1 H, $J = 2.8$ Hz), 7.42 (d, 2 H, $J = 8.4$ Hz), 6.65 (dd, 1 H, $J = 2.8, 2.0$ Hz), 2.71 (q, 2 H, $J = 7.6$ Hz), 1.24 (t, 3 H, $J = 7.6$ Hz); ^{13}C NMR (DMSO- d_6 , 75 MHz) δ 169.2, 160.0, 152.2, 147.1, 138.6, 137.1, 135.0, 129.8, 128.4, 128.2, 127.9, 127.6, 127.5, 127.1, 127.0, 123.3, 122.9, 119.9, 111.7, 102.3, 28.2, 15.4; MS (ESI) m/z 384 ($[\text{M}+1]^+$, 100), 343 (80); HRMS (ESI) m/z calcd for $\text{C}_{24}\text{H}_{19}\text{ClN}_3$ ($[\text{M}+\text{H}]^+$) 384.1268, found 384.1273.



1-24b

7-(4-Ethylphenyl)-2-(3-methoxyphenyl)-4-(4-(trifluoromethyl)phenyl)quinazoline (1-24b). According to General Protocol A, **1-23i** (0.028 g, 0.067 mmol), $\text{Pd}(\text{OAc})_2$ (0.0015 g, 0.0067 mmol), PPh_3 (0.0053 g, 0.020 mmol), Na_2CO_3 (0.044 g, 0.42 mmol), and 4-ethylphenylboronic acid (0.040 g, 0.27 mmol) were heated at reflux for 34 h and provided a crude residue that was purified by chromatography on SiO_2 (1:100, EtOAc:hexanes) to afford **1-24b** (0.026 g, 81%) as an off-white solid: Mp 173.0–174.1 $^\circ\text{C}$ (EtOAc/hexanes); IR (ATR) 2963, 2922, 2850, 1618, 1538, 1333, 1105, 1068, 788 cm^{-1} ; ^1H NMR (DMSO- d_6 , 600 MHz) δ 8.40 (d, 1 H, $J = 1.7$ Hz), 8.22 (d, 1 H, $J = 7.8$ Hz), 8.16 (d, 1 H, $J = 2.5$ Hz), 8.15 (d, 2 H, $J = 8.2$ Hz), 8.12 (d, 1 H, $J = 8.7$ Hz), 8.07 (dd, 1 H, $J = 8.1, 1.7$ Hz), 8.05 (d, 2 H, $J = 8.0$ Hz), 7.88

(d, 2 H, $J = 8.2$ Hz), 7.51 (t, 1 H, $J = 7.9$ Hz), 7.42 (d, 2 H, $J = 8.2$ Hz), 7.16 (dd, 1 H, $J = 8.0$, 2.5 Hz), 3.88 (s, 3 H), 2.7 (q, 2 H, $J = 7.6$ Hz), 1.25 (t, 3 H, $J = 7.6$ Hz); ^{13}C NMR (DMSO- d_6 , 150 MHz) δ 166.4, 159.7, 159.2, 151.8, 145.9, 144.9, 140.9, 138.8, 135.6, 130.9, 130.4, 130.1, 129.9, 128.8, 127.4, 127.28, 127.25, 125.7, 125.6, 125.08, 125.05, 123.3, 120.7, 120.0, 116.7, 113.2, 55.3, 27.9, 15.5; HRMS (ESI) m/z calcd for $\text{C}_{30}\text{H}_{24}\text{F}_3\text{N}_2\text{O}$ ($[\text{M}+\text{H}]^+$) 485.1841, found 485.1835. This structure was confirmed by X-ray analysis (Appendix A.1).

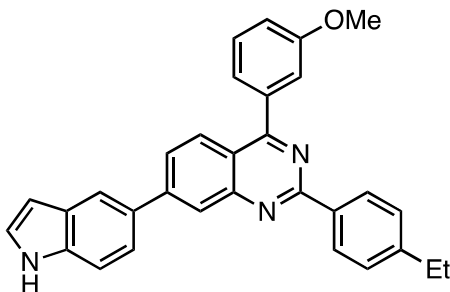


1-24c

2-(4-*tert*-Butylphenyl)-4-(4-ethylphenyl)-7-(3-methoxyphenyl)quinazoline (1-24c).

According to General Protocol A, **1-23k** (0.038 g, 0.094 mmol), $\text{Pd}(\text{OAc})_2$ (0.0021 g, 0.0094 mmol), PPh_3 (0.0075 g, 0.028 mmol), Na_2CO_3 (0.062 g, 0.58 mmol), and 3-methoxyphenylboronic acid (0.057 g, 0.38 mmol) were heated at reflux for 22 h and provided a crude residue that was purified by chromatography on SiO_2 (1:200 to 1:50, EtOAc:hexanes) to afford **1-24c** (0.038 g, 86%) as a pale green solid: Mp 89.2–91.0 °C (EtOAc); IR (ATR) 3063, 2959, 2866, 1552, 1528, 1338, 852, 773 cm^{-1} ; ^1H NMR (DMSO- d_6 , 300 MHz) δ 8.55 (d, 2 H, $J = 8.6$ Hz), 8.37 (d, 1 H, $J = 1.7$ Hz), 8.18 (d, 1 H, $J = 8.7$ Hz), 8.03 (dd, 1 H, $J = 8.8$, 1.8 Hz), 7.86 (d, 2 H, $J = 8.1$ Hz), 7.61 (d, 2 H, $J = 8.6$ Hz), 7.52 (d, 2 H, $J = 8.2$ Hz), 7.51–7.49 (m, 1 H), 7.47 (dd, 2 H, $J = 7.1$, 1.7 Hz), 7.11–7.03 (m, 1 H), 3.89 (s, 3 H), 2.78 (q, 2 H, $J = 7.5$ Hz), 1.35 (s,

9 H), 1.30 (t, 3 H, $J = 7.6$ Hz); ^{13}C NMR (DMSO- d_6 , 75 MHz) δ 167.6, 159.9, 159.6, 153.6, 151.8, 146.3, 145.4, 140.0, 134.9, 134.5, 130.4, 130.1, 128.2, 128.1, 127.6, 126.9, 125.6, 125.5, 120.2, 119.7, 114.7, 112.7, 55.3, 34.7, 31.1, 28.1, 15.5; MS (EI) m/z 472 ($[\text{M}]^+$, 100), 457 (79); HRMS (EI) m/z calcd for $\text{C}_{33}\text{H}_{32}\text{N}_2\text{O}$ (M^+) 472.2515, found 472.2510.

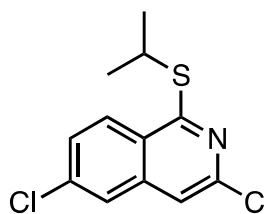


1-24d

2-(4-ethylphenyl)-7-(1H-indol-5-yl)-4-(3-methoxyphenyl)quinazoline (1-24d). According to General Protocol A, **1-23h** (0.025 g, 0.067 mmol), $\text{Pd}(\text{OAc})_2$ (0.0015 g, 0.0067 mmol), PPh_3 (0.0053 g, 0.020 mmol), Na_2CO_3 (0.044 g, 0.41 mmol), and indole-5-boronic acid (0.043 g, 0.27 mmol) were heated at reflux for 48 h and provided a crude residue that was purified by chromatography on SiO_2 (toluene to 1:20 THF/toluene) to afford **1-24d** (0.020 g, 66%) as a yellow solid: Mp 81.7–82.2 °C (EtOAc); IR (ATR) 3418, 2958, 2926, 2851, 1716, 1606, 1532, 1340, 1236, 1044, 794 cm^{-1} ; ^1H NMR (DMSO- d_6 , 300 MHz) δ 11.31 (s, 1H), 8.55 (d, 2 H, $J = 8.3$ Hz), 8.34 (d, 1 H, $J = 1.3$ Hz), 8.16–8.12 (m, 2 H), 8.09 (dd, 1 H, $J = 8.8, 1.6$ Hz), 7.69 (dd, 1 H, $J = 8.6, 1.7$ Hz), 7.63–7.55 (m, 2 H), 7.48–7.40 (m, 5 H), 7.25 (ddd, 1 H, $J = 8.3, 2.5, 0.9$ Hz), 6.59–6.55 (m, 1 H), 3.89 (s, 3 H), 2.72 (q, 2 H, $J = 7.6$ Hz), 1.26 (t, 3 H, $J = 7.6$ Hz); ^{13}C NMR (DMSO- d_6 , 75 MHz) δ 167.4, 159.5, 159.4, 151.9, 147.4, 146.8, 138.5, 136.3, 135.3, 129.8, 129.3, 128.4, 128.3, 128.2, 127.3, 127.2, 126.6, 124.5, 122.2, 120.7, 119.5, 119.4, 115.6,

115.3, 112.3, 102.0, 55.4, 28.2, 15.4; HRMS (ESI) m/z calcd for $C_{31}H_{25}N_3O$ ($[M+H]^+$) 456.2076, found 456.2091.

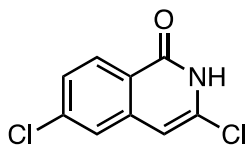
6.3 CHAPTER 2 EXPERIMENTAL PART



2-20

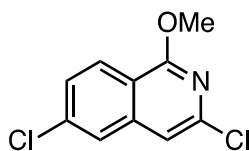
3,6-Dichloro-1-(isopropylthio)isoquinoline (2-20). To a solution of **2-19** (0.20 g, 0.83 mmol) in freshly distilled THF (7.0 mL) cooled to 0 °C under an atmosphere of N_2 was added a premixed solution of NaH (0.022 g, 0.92 mmol) and *i*-PrSH (0.087 mL, 0.92 mmol) in THF (2.0 mL) dropwise. The mixture was stirred for 24 h at 0 °C. After 16 h an additional amount of NaH (0.011 g, 0.046 mmol) and *i*-PrSH (0.04 mL) premixed in THF (1 mL) was added dropwise. The mixture continued to stir at 0 °C until the starting material was completely consumed as indicated by TLC. The reaction mixture was warmed to room temperature, poured into ice cold H_2O , and extracted with EtOAc (4 x 15 mL). The combined organic layers were washed with H_2O (10 mL), dried ($MgSO_4$), and concentrated under reduced pressure to provide **2-20** (0.23 g, 100%) as an off-white solid: Mp 94.1–95.4 °C (EtOAc); IR (ATR) 3064, 2967, 2924, 1605, 1539, 1472, 1347, 1331, 1277, 1077, 986 cm^{-1} ; 1H NMR ($DMSO-d_6$, 300 MHz) δ 8.13–8.06 (m, 2 H), 7.71 (d, 1 H, $J = 0.3$ Hz), 7.68 (dd, 1 H, $J = 8.9, 2.2$ Hz), 4.12 (sept, 1 H, $J = 6.8$ Hz), 1.45 (d, 6 H, $J = 6.8$ Hz); ^{13}C NMR ($DMSO-d_6$, 75 MHz) δ 160.8, 144.4, 138.0,

136.7, 128.5, 126.4, 125.7, 123.3, 114.9, 35.4, 22.6; MS (ESI) m/z 272 ($[M+1]^+$, 80), 227 (100); HRMS (ESI) m/z calcd for $C_{12}H_{12}Cl_2NS$ ($[M+H]^+$) 272.0068, found 272.0044.



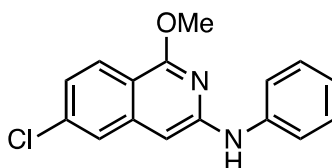
2-23

3,6-Dichloroisoquinolin-1-ol (2-23). To a solution of **2-19** (0.030 g, 0.13 mmol) in THF (1.2 mL) was added $KOSiMe_3$ (0.17 g, 1.2 mmol). The vial was sealed and the mixture was stirred at 80 °C for 3 h. The white slurry was cooled to room temperature, diluted with CH_2Cl_2 (2 mL) and EtOAc (2 mL). Sat. aq. NH_4Cl (2 mL) was added and the mixture was extracted with EtOAc (4 x 15 mL). The combined organic layers were washed with H_2O (10 mL), dried ($MgSO_4$), and concentrated under reduced pressure to provide **2-23** (0.029 g, 100%) as a white solid: Mp 243.1–244.6 °C (EtOAc); IR (ATR) 2857, 1655, 1616, 1595, 1543, 1452, 1422, 1321, 1245, 1150, 1073 cm^{-1} ; 1H NMR ($DMSO-d_6$, 300 MHz) δ 12.43 (s, 1 H), 8.12 (d, 1 H, $J = 8.6$ Hz), 7.76 (s, 1 H), 7.51 (dd, 1 H, $J = 8.5, 1.5$ Hz), 6.75 (s, 1 H); ^{13}C NMR ($DMSO-d_6$, 75 MHz) δ 161.7, 139.0, 138.0, 129.1, 126.9, 125.0; MS (EI) m/z 213 ($[M]^+$, 89), 178 (63), 123 (100); HRMS (EI) m/z calcd for $C_9H_5Cl_2NO$ (M^+) 212.9748, found 212.9740.



2-24

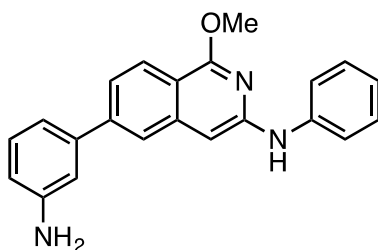
3,6-Dichloro-1-methoxyisoquinoline (2-24). To a solution of 1,3,6-trichloroisoquinoline (**2-19**) 17 (1.00 g, 4.3 mmol) in anhyd. MeOH (43 mL) was added NaOMe (1.39 g, 25.7 mmol). The solution was stirred at reflux under an atmosphere of N₂ for 4 h. The mixture was cooled to room temperature, diluted with EtOAc, quenched with 1 M HCl, and stirred for 5 min. The reaction mixture was poured into H₂O and extracted with EtOAc. The combined organic layers were washed with brine, dried (MgSO₄), and concentrated under reduced pressure to provide **2-24** (0.950 g, 97%) as a white solid: Mp 106.2–107.1 °C; IR (ATR, neat) 3077, 3085, 3027, 2152, 1616, 1564, 1448, 1376, 1357, 1322, 1195, 1089, 902, 874, 822, 662 cm⁻¹; ¹H NMR (DMSO-*d*₆, 400 MHz) δ 8.10 (d, 1 H, *J* = 8.9 Hz), 7.98 (d, 1 H, *J* = 2.0 Hz), 7.60 (dd, 1 H, *J* = 8.9, 2.1 Hz), 7.50 (s, 1 H), 4.06 (s, 3 H); ¹³C NMR (DMSO-*d*₆, 100 MHz) δ 160.1, 142.5, 140.0, 136.8, 127.8, 126.0, 124.7, 115.8, 112.4, 54.6; HRMS (ESI) *m/z* calcd for C₁₀H₈NOCl₂ ([M+H]⁺) 227.9983, found 227.9985.



2-25

6-Chloro-1-methoxy-N-phenylisoquinolin-3-amine (2-25). To a reaction vial containing **2-24** (0.500 g, 2.19 mmol), Pd(OAc)₂ (0.098 g, 0.438 mmol), Xantphos (0.317 g, 0.548 mmol), and Cs₂CO₃ (1.44 g, 4.38 mmol) under an atmosphere of Ar was added toluene (73 mL) and aniline (0.22 mL, 2.41 mmol). The reaction was heated to 80 °C under an atmosphere of Ar for 2.5 h. The reaction mixture was cooled to room temperature, filtered through Celite® with EtOAc washings, and concentrated under reduced pressure to give a

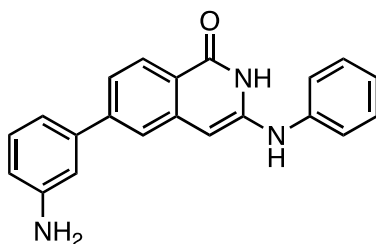
brown-orange residue. The residue was adsorbed onto SiO₂ and purified by chromatography on SiO₂ (100% hexanes, 2:98 to 10:90, EtOAc:hexanes) to provide **2-25** (0.303 g, 49%, 57% BRSM) as a yellow solid: Mp 98.3–100.1°C; IR (ATR, neat) 3353, 3049, 3031, 2952, 1622, 1596, 1558, 1374, 1316, 1303, 1169 cm⁻¹; ¹H NMR (DMSO-*d*₆, 400 MHz) δ 9.02 (s, 1 H), 7.95 (d, 1 H, *J* = 8.8 Hz), 7.73 (d, 1 H, *J* = 1.9 Hz), 7.55 (d, 2 H, *J* = 7.7 Hz), 7.29 (t, 2 H, *J* = 7.5 Hz), 7.18 (dd, 1 H, *J* = 8.8, 2.0 Hz), 6.91 (t, 1 H, *J* = 7.3 Hz), 6.65 (s, 1 H), 4.07 (s, 3 H); ¹³C NMR (DMSO-*d*₆, 100 MHz) δ 159.8, 150.7, 141.5, 141.4, 135.8, 128.8, 126.0, 123.3, 122.7, 120.7, 118.5, 111.6, 92.5, 53.9; HRMS (ESI) *m/z* calcd for C₁₆H₁₄N₂OCl ([M+H]⁺) 285.0795, found 285.0782.



2-27

6-(3-Aminophenyl)-1-methoxy-N-phenylisoquinolin-3-amine (2-27). To a reaction vial containing **2-25** (0.419 g, 1.47 mmol), KF (0.256 g, 4.41 mmol), Pd₂(dba)₃ (0.273 g, 0.294 mmol), and 3-aminophenylboronic acid (0.470 g, 2.94 mmol) under an atmosphere of Ar was added P(*t*-Bu)₃ (0.124 g, 0.588 mmol) dissolved in freshly distilled and degassed 1,4-dioxane (2.0 mL) followed by an additional amount of 1,4-dioxane (7.5 mL). The reaction vial was sealed and heated to 120 °C for 3 h. The reaction mixture was cooled to room temperature and filtered through Celite® with EtOAc washings. The combined organic layers were concentrated under reduced pressure to give an orange-yellow residue. The polarity of the

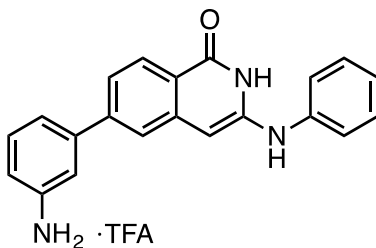
impurities required two chromatographic separations for optimal purification. The residue was adsorbed onto SiO₂ and purified by chromatography on SiO₂ (100% CH₂Cl₂, 2:98, MeOH:CH₂Cl₂) to provide the desired product as a mixture with a more apolar impurity. In order to separate the mixture further, the material was absorbed onto SiO₂ and purified by chromatography on SiO₂ (100% hexanes, 5% EtOAc/hexanes, 20% EtOAc/hexanes, 100% EtOAc) to provide **2-27** (0.359 g, 72%) as a red-brown solid: Mp 165.7–167.5 °C (CHCl₃); IR (ATR, neat) 3375, 3029, 2393, 1623, 1594, 1573, 1493, 1446, 1422, 1374, 1336, 1299, 1158, 1105, 688 cm⁻¹; ¹H NMR (DMSO-*d*₆, 400 MHz) δ 8.89 (s, 1 H), 8.01 (d, 1 H, *J* = 8.6 Hz), 7.75 (s, 1 H), 7.57 (d, 2 H, *J* = 8.1 Hz), 7.43 (d, 1 H, *J* = 8.4 Hz), 7.28 (t, 2 H, *J* = 7.7 Hz), 7.13 (t, 1 H, *J* = 7.7 Hz), 6.99–6.85 (m, 3 H), 6.75 (s, 1 H), 6.61 (d, 1 H, *J* = 7.9 Hz), 5.20 (s, 2 H), 4.09 (s, 3 H); ¹³C NMR (DMSO-*d*₆, 125 MHz) δ 159.6, 149.9, 149.2, 143.1, 142.0, 140.7, 140.3, 129.4, 128.7, 124.2, 121.70, 121.65, 120.2, 118.1, 114.7, 113.7, 112.42, 112.39, 93.8, 53.8; HRMS (ESI) *m/z* calcd for C₂₂H₂₀N₃O ([M+H]⁺) 342.1606, found 342.1623.



2-15

6-(3-Aminophenyl)-3-(phenylamino)isoquinolin-1(2H)-one (2-15). To a flask containing **2-27** (0.241 g, 0.705 mmol) under an atmosphere of Ar was added 4 M HCl in 1,4-dioxane (24.1 mL). The reaction vial was sealed and heated to 80 °C for 28 h. (Note: The reaction progress was monitored by ¹H NMR of an aliquot from the crude reaction mixture.) The

reaction mixture was cooled to room temperature and concentrated under reduced pressure to provide a yellow-brown solid. The solid was suspended in H₂O and neutralized (pH 7) with sat. aq. NaHCO₃. The suspension was filtered and washed with H₂O and ether to provide **2-15** (0.190 g, 82%) as a light yellow-brown solid: Mp 184.7 °C (dec); IR (ATR, neat) 3316, 1635, 1594, 1551, 1495, 1484, 1437, 1340, 1288 cm⁻¹; ¹H NMR (DMSO-*d*₆, 400 MHz) δ 10.72 (s, 1 H), 8.04 (d, 1 H, *J* = 8.3 Hz), 7.99 (s, 1 H), 7.58 (d, 1 H, *J* = 1.5 Hz), 7.40–7.31 (m, 3 H), 7.20 (d, 2 H, *J* = 7.6 Hz), 7.12 (t, 1 H, *J* = 7.8 Hz), 7.00 (t, 1 H, *J* = 7.4 Hz), 6.94 (t, 1 H, *J* = 1.8 Hz), 6.87 (d, 1 H, *J* = 7.6 Hz), 6.61 (dd, 1 H, *J* = 8.0, 1.4 Hz), 6.13 (s, 1 H), 5.39 (bs, 2 H); ¹³C NMR (DMSO-*d*₆, 125 MHz) δ 162.0, 148.7, 144.7, 141.7, 140.7, 140.4, 140.2, 129.44, 129.35, 127.2, 122.3, 121.9, 121.5, 120.0, 119.2, 114.9, 114.0, 112.6, 85.0; HRMS (ESI) *m/z* calcd for C₂₁H₁₈N₃O ([M+H]⁺) 328.1450, found 328.1478.



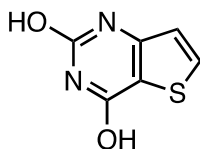
2-16

6-(3-Aminophenyl)-3-(phenylamino)isoquinolin-1(2H)-one TFA salt (2-16). To a flask containing **2-15** (0.220 g, 0.673 mmol) suspended in CH₂Cl₂ under an atmosphere of N₂ was added trifluoroacetic acid (60.6 μL, 0.808 mmol). The suspension was stirred at room temperature for 10 min, filtered, and washed with H₂O and a minimal amount of CH₂Cl₂ and Et₂O. Product **2-16** was isolated as a yellow-brown solid (0.222 g, 75%): Mp 197.1 °C (dec); IR (ATR, neat) 3001, 1687, 1638, 1597, 1555, 1497, 1476, 1437, 1343, 1200, 1120 cm⁻¹; ¹H NMR

(DMSO-*d*₆, 400 MHz) δ 10.75 (bs, 1 H), 8.06 (d, 1 H, $J = 8.3$ Hz), 7.99 (bs, 1 H), 7.62 (d, 1 H, $J = 1.4$ Hz), 7.39 (dd, 1 H, $J = 8.4, 1.7$ Hz), 7.33 (d, 2 H, $J = 7.5$ Hz), 7.30–7.24 (m, 1 H), 7.21 (d, 2 H, $J = 7.6$ Hz), 7.17–7.11 (m, 2 H), 7.01 (t, 1 H, $J = 7.3$ Hz), 6.87–6.81 (m, 1 H), 6.13 (s, 1 H); ¹³C NMR (DMSO-*d*₆, 100 MHz) δ 162.0, 143.7, 142.0, 141.9, 140.6, 140.5, 129.9, 129.4, 127.4, 122.5, 122.0, 121.3, 120.2, 119.9, 119.4, 117.7, 116.4, 84.7; HRMS (ESI) m/z calcd for C₂₁H₁₈N₃O ([M+H]⁺) 328.1450, found 328.1479. ICP (Pd) = 18 ppm.

6.4 CHAPTER 3 EXPERIMENTAL PART

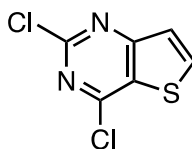
6.4.1 Thieno[3,2-*d*]pyrimidine-Based Inhibitors



3-10

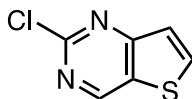
Thieno[3,2-*d*]pyrimidine-2,4-diol (3-10).⁷⁵ To a solution of methyl 3-aminothiophene-2-carboxylate **3-9** (5.00 g, 31.8 mmol) in glacial AcOH (35.0 mL) and H₂O (31 mL) was added KOCN (8.06 g, 95.4 mmol) in H₂O (18.0 mL) dropwise. The resulting slurry was stirred at room temperature for 20 h, and filtered. The solid was placed in a flask, flushed with N₂, treated with 2 N aq. NaOH (85 mL), and stirred at room temperature for 3 h. The slurry was filtered to remove any undissolved material. The solution was acidified with conc. aq. HCl until a pH of 5-6 was obtained. The precipitate was filtered and the solid was dried at 50 °C to provide **3-10**

(3.49 g, 65%) as a white solid: ^1H NMR (DMSO- d_6 , 300 MHz) δ 11.56 (s, 1 H), 11.21 (s, 1 H), 8.05 (d, 1 H, $J = 5.3$ Hz), 6.90 (d, 1 H, $J = 5.3$ Hz).



3-11

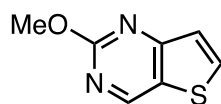
2,4-Dichlorothieno[3,2-*d*]pyrimidine (3-11).⁷⁵ To a solution of **3-10** (0.500 g, 2.97 mmol) and *N,N*-dimethylaniline (0.29 mL, 2.23 mmol) in MeCN (2.5 mL) cooled to 0 °C was slowly added POCl₃ (1.4 mL, 14.9 mmol). The purple slurry was heated to 80–85 °C and stirred for 48 h. A second portion of POCl₃ (1.0 mL) was added after 24 h. The resulting clear purple solution was poured into ice and water and stirred for 5 min. The slurry was filtered, and the solid was dried at 45 °C. The solid was dissolved in EtOAc, washed with sat. aq. NaHCO₃, and stirred with activated charcoal. The solution was filtered through Celite® and concentrated to provide **3-11** (0.482 g, 79%) as a yellow solid: Mp 138.8–139.3 °C (H₂O); IR (ATR, neat) 3066, 3088, 1545, 1508, 1307, 1204, 798 cm⁻¹; ^1H NMR (DMSO- d_6 , 300 MHz) δ 8.70 (d, 1 H, $J = 5.4$ Hz), 7.74 (d, 1 H, $J = 5.4$ Hz); ^{13}C NMR (DMSO- d_6 , 75 MHz) δ 163.6, 154.8, 154.7, 142.4, 129.3, 124.1; HRMS (EI) m/z calcd for C₆H₂N₂SCl₂ (M⁺) 203.9316, found 203.9312.



3-12

2-Chlorothieno[3,2-*d*]pyrimidine (3-12).⁷⁶ To a solution of **3-11** (0.044 g, 0.022 mmol) and NaHCO₃ (0.027 g, 0.32 mmol) in EtOH (2.0 mL) was added 10% Pd/C (0.0089 g, 20% by

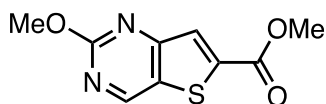
wt). The suspension was stirred at room temperature under an atmosphere of H₂ for 23 h. A second portion of 10% Pd/C (0.0089 g, 20% by wt) was added after 12 h. The reaction mixture was filtered through Celite® with EtOAc washings. The filtrate was washed with H₂O/brine (4:1), dried (MgSO₄), and concentrated under reduced pressure to provide **3-12** (0.033 g, 90%) as white solid: Mp 164.9–165.5 °C (EtOAc); IR (ATR, neat) 3105, 3051, 2924, 1543, 1515, 1456, 1420, 1334, 1349, 1301, 1159, 794 cm⁻¹; ¹H NMR (DMSO-*d*₆, 300 MHz) δ 9.50 (s, 1 H), 8.64 (d, 1 H, *J* = 5.4 Hz), 7.64 (d, 1 H, *J* = 5.4 Hz); ¹³C NMR (DMSO-*d*₆, 75 MHz) δ 162.7, 156.3, 155.3, 142.2, 130.1, 122.9; MS (EI) *m/z* 170 (M⁺, 100), 135 (72); HRMS (EI) *m/z* calcd for C₆H₃N₂SCl (M⁺) 169.9705, found 169.9700.



3-13

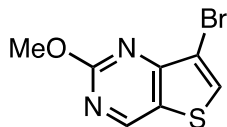
2-Methoxythieno[3,2-*d*]pyrimidine (3-13). To a solution of **3-12** (0.146 g, 0.86 mmol) in MeOH (20 mL) was added NaOMe (0.130 g, 2.41 mmol). The solution was heated at reflux for 37 h. An additional 1.4 equiv of NaOMe (0.065 g) was added after 24 h (Note: The reaction was complete in 7 h with comparable yields when 4.2 equiv of NaOMe were added at the start of the reaction). The reaction mixture was cooled to room temperature, quenched with 1 N aq. HCl (2.0 mL), and extracted with CH₂Cl₂ (4 x 10 mL). The combined organic layers were washed with H₂O (10 mL), dried (MgSO₄), and concentrated under reduced pressure to provide **3-13** (0.125 g, 88%) as an off-white solid: Mp 167.0–168.5 °C (CH₂Cl₂); IR (ATR, neat) 3071, 3025, 2917, 1558, 1528, 1478, 1379, 1295, 1249, 1031, 796, 677 cm⁻¹; ¹H NMR (DMSO-*d*₆, 300 MHz) δ 9.30 (d, 1 H, *J* = 0.6 Hz), 8.45 (d, 1 H, *J* = 5.4 Hz), 7.47 (dd, 1 H, *J* = 5.4, 0.7 Hz), 3.96 (s,

3 H); ^{13}C NMR (DMSO- d_6 , 75 MHz) δ 163.4, 162.4, 154.8, 139.9, 124.8, 122.9, 54.6; MS (EI) m/z 166 (M^+ , 29), 84 (100); HRMS (EI) m/z calcd for $\text{C}_7\text{H}_6\text{N}_2\text{OS}$ (M^+) 166.0201, found 166.0201.



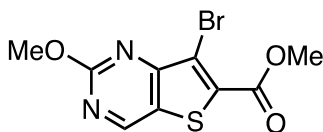
3-16

Methyl 2-methoxythieno[3,2-*d*]pyrimidine-6-carboxylate (3-16). To a reaction vial charged with $\text{TMPMgCl}\cdot\text{LiCl}$ (0.13 mL, 0.16 mmol) cooled to $-50\text{ }^\circ\text{C}$ was added a solution of **3-13** (0.020 g, 0.12 mmol) in THF (0.25 mL) dropwise. The solution was stirred at $-50\text{ }^\circ\text{C}$ for 2 h. Methyl cyanoformate (11 μL , 0.14 mmol) in THF (0.12 mL) was added dropwise at $-50\text{ }^\circ\text{C}$ and the solution was warmed to $0\text{ }^\circ\text{C}$ over 1 h. The reaction was quenched at $0\text{ }^\circ\text{C}$ with sat. aq. NH_4Cl (0.5 mL). The reaction mixture was diluted with EtOAc and the organic layer was washed with sat. aq. NH_4Cl (2 x 2 mL). The aqueous layers were then extracted with EtOAc (4 x 5 mL). The combined organics were washed with brine (5 mL), dried (MgSO_4), and concentrated under reduced pressure to give an orange residue. The residue was adsorbed onto SiO_2 and purified by chromatography on SiO_2 (1:20 EtOAc:hexanes, 1:10 EtOAc:hexanes, 1:4 EtOAc:hexanes) to provide **3-16** (0.015 g, 53%, 93% pure) as a pale green solid: Mp $176.6\text{--}177.7\text{ }^\circ\text{C}$ (EtOAc); IR (ATR) 2959, 1713, 1569, 1478, 1431, 1385, 1174 cm^{-1} ; ^1H NMR (DMSO- d_6 , 300 MHz) δ 9.45 (s, 1 H), 8.03 (s, 1 H), 3.98 (s, 3 H), 3.93 (s, 3 H); ^{13}C NMR (DMSO- d_6 , 75 MHz) δ 163.7, 161.8, 160.5, 156.8, 143.0, 128.2, 127.0, 54.9, 53.3; MS (ESI) m/z 247 ($[\text{M}+\text{Na}]^+$, 95), 227 (100), 223 (65); HRMS (ESI) m/z calcd for $\text{C}_9\text{H}_8\text{N}_2\text{O}_3\text{S}$ ($[\text{M}+\text{Na}]^+$) 247.0153, found 247.0134.



3-20

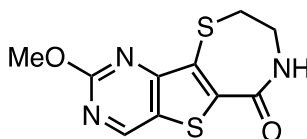
7-Bromo-2-methoxythieno[3,2-*d*]pyrimidine (3-20). To a reaction vial containing **3-13** (0.100 g, 0.602 mmol) and AcOH (1.5 mL) under an atmosphere of N₂ was added Br₂ (93.0 μL, 1.81 mmol). The reaction vial was sealed and heated to 70 °C for 24 h. The mixture was cooled to room temperature, quenched with sat. aq. NaHCO₃, and extracted with EtOAc. The combined organic layers were washed with sat. aq. Na₂S₂O₃, sat. aq. NaHCO₃, and brine, dried (MgSO₄) and concentrated under reduced pressure to give a white solid. The solid was adsorbed onto SiO₂ and purified by chromatography on SiO₂ (1:20 EtOAc:hexanes, 1:10 EtOAc:hexanes, 3:20 EtOAc:hexanes, 100% EtOAc) to provide **3-20** (0.0583 g, 40%) as a white solid: Mp 115.3–115.9 °C (EtOAc); IR (ATR, neat) 3090, 3019, 2956, 1567, 1524, 1474, 1463, 1370, 1312, 1271 cm⁻¹; ¹H NMR (DMSO-*d*₆, 300 MHz) δ 9.34 (s, 1 H), 8.61 (s, 1 H), 4.01 (s, 3 H); ¹³C NMR (DMSO-*d*₆, 75 MHz) δ 163.9, 158.4, 155.8, 136.7, 124.0, 106.8, 54.8; HRMS (EI) *m/z* calcd for C₇H₅N₂OSBr (M⁺) 243.9306, found 243.9304.



3-21

Methyl 7-bromo-2-methoxythieno[3,2-*d*]pyrimidine-6-carboxylate (3-21). To a reaction vial containing **3-20** (0.040 g, 0.16 mmol) and THF (0.6 mL) cooled to –55 to –60 °C under an atmosphere of argon was added TMPMgCl·LiCl (0.17 mL, 0.22 mmol) dropwise. The white slurry became a clear yellow solution after the addition of TMPMgCl·LiCl and was stirred

for 2 h at -55 to -60 °C, turning into a pale yellow slurry at the end of this time. Methyl cyanofornate (0.016 mL, 0.20 mmol) in THF (0.10 mL) was added dropwise at -50 °C and the solution was stirred for 2 h while warming to 0 °C. The pale yellow slurry turned pale yellow-orange as it warmed to 0 °C. The reaction was quenched at 0 °C with sat. aq. NH_4Cl (0.5 mL). The mixture was diluted with EtOAc and the organic layer was washed with sat. aq. NH_4Cl (2 x 5 mL). The combined aqueous layers were extracted with EtOAc (2 x 5 mL). The combined organic layers were washed with brine (5 mL), dried (MgSO_4), and concentrated under reduced pressure to provide **3-21** (0.048 g, 97%) as a yellow solid: Mp 180.9 – 181.4 °C (EtOAc); IR (ATR, neat) 2956 , 2915 , 2848 , 1735 , 1569 , 1472 , 1382 , 1213 , 1031 , 788 cm^{-1} ; ^1H NMR (DMSO- d_6 , 300 MHz) δ 9.49 (s, 1 H), 4.04 (s, 3 H), 3.95 (s, 3 H); ^{13}C NMR (DMSO- d_6 , 75 MHz) δ 164.1, 160.6, 158.3, 157.4, 136.3, 124.8, 113.9, 55.0, 53.3; MS (EI) m/z 302 (M^+ , 100), 274 (45); HRMS (ESI) m/z calcd for $\text{C}_9\text{H}_8\text{BrN}_2\text{O}_3\text{S}$ ($[\text{M}+\text{H}]^+$) 302.9439, found 302.9418.



kmg-NB4-23

2-Methoxy-7*H*,8*H*,9*H*-1,4-thiazepino[7',6'-5,4]thiopheno[3,2-*d*]pyrimidin-6-one

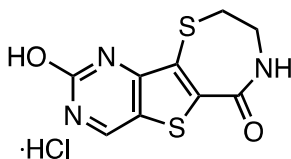
(kmg-NB4-23). To a solution of **3-21** (0.041 g, 0.14 mmol) in DMF (1.3 mL) under an atmosphere of N_2 was added cysteamine·HCl (0.063 g, 0.54 mmol) in one portion and DBU (0.17 mL, 1.1 mmol) dropwise. The reaction mixture turned dark blue upon addition of DBU and after stirring for 20 min, the mixture was a pale purple colored slurry. The reaction mixture was stirred at room temperature for 1.5 h, and then heated to 70 °C for 9 h 50 min. The resulting yellow slurry was diluted with EtOAc, washed with 2 M aq. HCl, and filtered (H_2O and EtOAc

washings). Residual DMF was removed by azeotropic distillation with heptane to provide **kmg-NB4-23** (0.025 g, 68%) as a pale yellow solid: Mp 308 °C (dec); IR (ATR, neat) 3260, 3153, 3015, 1636, 1554, 1495, 1467, 1374, 1269, 1353, 1323 cm⁻¹; ¹H NMR (DMSO-*d*₆, 300 MHz) δ 9.36 (s, 1 H), 8.70 (t, 1 H, *J* = 5.4 Hz), 3.98 (s, 1 H), 3.68 (app dd, 2 H, *J* = 6.0 Hz), 3.40–3.36 (m, 2 H); ¹³C NMR (DMSO-*d*₆, 75 MHz) δ 164.2, 163.1, 159.6, 155.9, 138.5, 129.7, 124.1, 54.8, 42.7, 31.9; HRMS (ESI) *m/z* calcd for C₁₀H₁₀N₃O₂S₂ ([M+H]⁺) 268.0214, found 268.0237. This structure was confirmed by X-ray analysis (Appendix A.2) and the structure has been deposited at the Cambridge Crystallographic Data Centre (CCDC 822403).

General Procedure for Solubility Determination of **kmg-NB4-23** Formulations.

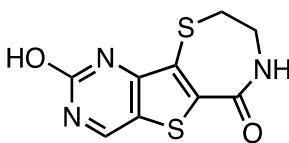
Preparation of DMSO/H₂O solutions. Solutions of DMSO and HPLC-grade H₂O were prepared in volumetric flasks by dissolving the appropriate amount of DMSO in HPLC-grade H₂O to generate a 20% (w/v) solution.

Solubility measurements. To a 1-dram vial containing **kmg-NB4-23** was added the appropriate formulation solution. The solution was stirred overnight at 60-90 °C and cooled to room temperature. An aliquot of the solution was filtered through 0.45 μm syringe filters and diluted with the appropriate volume of DMSO/H₂O (20%, w/v). The solution was analyzed by UV/VIS (366.5 nm) and the concentration was determined using a previously generated calibration curve ($y = 8200.2x + 0.0233$).



kmg-NB4-69A

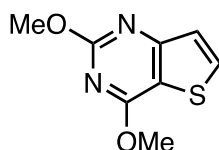
2-Hydroxy-7H,8H,9H-1,4-thiazepino[7',6'-5,4]thiopheno[3,2-d]pyrimidin-6-one (**hydrochloride salt**) (**kmg-NB4-69A**). To a reaction vial containing **kmg-NB4-23** (0.050 g, 0.19 mmol) was added HCl in dioxane (5 mL). The reaction vial was sealed and heated to 80 °C for 32 h. The reaction mixture was cooled to room temperature and concentrated under reduced pressure to give an orange solid. Starting material still remained by crude ¹H NMR and the solid was resubjected to the above reaction condition for an additional 48 h. The reaction mixture was cooled to room temperature and concentrated under reduced pressure to give an orange solid. Starting material still remained by crude ¹H NMR and the solid was resubjected to HCl in dioxane (11 mL) and stirred at 80 °C for 3 d. The solvent was evaporated in vacuo and the resulting orange solid was washed with THF and dried to provide **kmg-NB4-69A** (0.046 g, 85%) as an orange solid: Mp 335.9 °C (dec); IR (ATR) 3452, 3267, 3176, 2591, 2032, 1912, 1700, 1623, 1463, 1240 cm⁻¹; ¹H NMR (DMSO-*d*₆, 400 MHz) δ 9.20 (s, 1 H), 8.74 (t, 1 H, *J* = 6.2 Hz), 7.79 (bs, 1 H), 3.68–3.60 (m, 2 H), 3.39–3.32 (m, 2 H); ¹³C NMR (DMSO-*d*₆, 100 MHz) δ 164.0, 161.0, 159.7, 153.6, 140.9, 128.4, 119.6, 42.6, 32.2; HRMS (ESI) *m/z* calcd for C₉H₈N₃O₂S₂ ([M+H]⁺) 254.0058, found 254.0041.



kmg-NB4-77A3

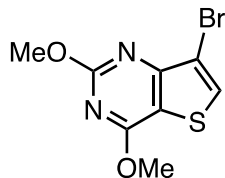
2-Hydroxy-7H,8H,9H-1,4-thiazepino[7',6'-4,5]thiopheno[3,2-d]pyrimidin-6-one (**kmg-NB4-77A3**). To a flask containing **kmg-NB4-69A** (0.015 g, 0.052 mmol) dissolved in MeOH (30 mL) was added poly(4-vinylpyridine) (0.015 g, 0.14 mmol). The solution was stirred at room temperature for 10 min. The solution was filtered and the filtrate was concentrated under

reduced pressure to provide **kmg-NB4-77A3** (0.012 g, 90%) as a yellow-orange solid: Mp 280.1 °C (dec); IR (ATR, neat) 3264, 3008, 2917, 1618, 1566, 1491, 1452, 1387, 1338 cm⁻¹; ¹H NMR (DMSO-*d*₆, 600 MHz) δ 8.86 (s, 1 H), 8.53 (t, 1 H, *J* = 5.3 Hz), 3.65–3.60 (m, 2 H), 3.51 (bs, 1 H), 3.30–3.26 (m, 2 H); ¹³C NMR (DMSO-*d*₆, 100 MHz) δ 164.9, 164.7, 162.1, 153.5, 135.5, 129.4, 115.4, 42.8, 31.9; HRMS (ESI) *m/z* calcd for C₉H₈N₃O₂S₂ ([M+Na]⁺) 275.9877, found 275.9899.



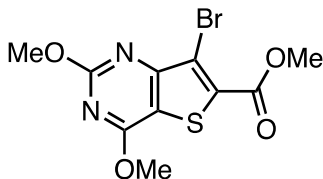
3-23

2,4-Dimethoxythiopheno[3,2-*d*]pyrimidine (3-23). To a solution of **3-11** (0.082 g, 0.40 mmol) in MeOH (8.0 mL) was added NaOMe (0.091 g, 1.69 mmol). The solution was heated at reflux for 2 d. After the first 24 h, an additional portion of NaOMe (2.1 equiv) was added. The reaction mixture was cooled to room temperature and quenched with 1 M aq. HCl (2.0 mL) and extracted with CH₂Cl₂ (4 x 10 mL). The combined organic layers were washed with H₂O (10 mL), dried (MgSO₄), and concentrated under reduced pressure to provide **3-23** (0.073 g, 92%) as a light yellow solid: Mp 271.3 °C (dec); IR (ATR, neat) 3079, 3016, 2988, 2947, 2917, 2848, 1575, 1547, 1484, 1465, 1333, 1307, 1197 cm⁻¹; ¹H NMR (DMSO-*d*₆, 400 MHz) δ 8.25 (d, 1 H, *J* = 5.3 Hz), 7.40 (d, 1 H, *J* = 5.4 Hz), 4.05 (s, 3 H), 3.93 (s, 3 H); ¹³C NMR (DMSO-*d*₆, 100 MHz) δ 165.2, 163.6, 163.0, 136.4, 123.4, 110.9, 54.6, 54.2; HRMS (ESI) *m/z* calcd for C₈H₉N₂O₂S ([M+H]⁺) 197.0385, found 197.0396.



3-24

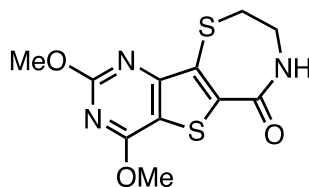
7-Bromo-2,4-dimethoxythiopheno[3,2-*d*]pyrimidine (3-24). To a vial containing **3-23** (0.10 g, 0.51 mmol) dissolved in AcOH (3.3 mL, 0.15 M) was added Br₂ (0.08 mL). The reaction vial was sealed and stirred at room temperature for 32 h. The reaction mixture was quenched with sat. aq. NaHCO₃ and extracted with EtOAc (3 x 10 mL). The combined organic layers were washed with sat. aq. Na₂S₂O₃ (3 x 5 mL) and NaHCO₃ (5 mL), dried (MgSO₄), and concentrated under reduced pressure to give a white solid. The solid was adsorbed onto SiO₂ and purified by chromatography on SiO₂ (100% hexanes, 1:100 EtOAc:hexanes, 1:50 EtOAc:hexanes, 1:20 EtOAc:hexanes) to provide **3-24** (0.083 g, 59%, 69% BRSM) as a white solid: Mp 189.3–191.2 °C (EtOAc); IR (ATR, neat) 3079, 2947, 2848, 1569, 1547, 1467, 1329, 1199 cm⁻¹; ¹H NMR (DMSO-*d*₆, 400 MHz) δ 8.47 (s, 1 H), 4.10 (s, 3 H), 4.00 (s, 3 H); ¹³C NMR (DMSO-*d*₆, 100 MHz) δ 165.5, 164.2, 159.1, 133.1, 110.5, 107.3, 54.8, 54.7; MS (EI) *m/z* 274 ([M]⁺, 100), 244 (50). HRMS (ESI) *m/z* calcd for C₈H₈N₂O₂SBr ([M+H]⁺) 274.9490, found 274.9495.



3-25

Methyl 7-bromo-2,4-dimethoxythiopheno[4,5-*d*]pyrimidine-6-carboxylate (3-25). To a reaction vial containing **3-24** (0.050 g, 0.18 mmol) and THF (0.4 mL) cooled to –50 °C under

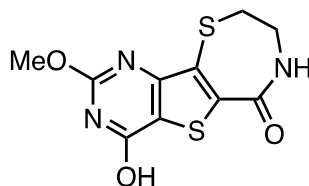
an atmosphere of Ar was added TMPMgCl·LiCl (0.3 mL, 0.29 mmol) dropwise. The white slurry became a clear yellow solution after the addition of TMPMgCl·LiCl and was stirred for 2 h at -45 to -50 °C. Methyl cyanoformate (0.02 mL, 0.24 mmol) in THF (0.2 mL) was added dropwise via syringe at -50 °C, and the solution was stirred for 1 h while warming to 0 °C. The yellow solution became a white slurry upon addition of methyl cyanoformate. The reaction was quenched at 0 °C with sat. aq. NH_4Cl (2 mL). The reaction mixture was diluted with EtOAc and the organic layer was washed with sat. aq. NH_4Cl (4 x 5 mL). The combined aqueous layers were extracted with EtOAc (3 x 5 mL). The combined organic extracts were washed with sat. aq. NH_4Cl (5 mL) and brine (5 mL), dried (MgSO_4), and concentrated under reduced pressure to give a white solid. The solid was adsorbed onto SiO_2 and purified by chromatography on SiO_2 (1:100 EtOAc:hexanes, 1:50 EtOAc:hexanes, 1:20 EtOAc:hexanes, 100% EtOAc) to provide **3-25** (0.050 g, 82%) as a white solid: Mp 197.8 – 198.5 °C (EtOAc); IR (ATR, neat) 3014, 2958, 2867, 1728, 1575, 1541, 1502, 1474, 1452, 1329, 1225 cm^{-1} ; ^1H NMR ($\text{DMSO-}d_6$, 400 MHz) δ 4.12 (s, 3 H), 4.02 (s, 3 H), 3.93 (s, 3 H); ^{13}C NMR ($\text{DMSO-}d_6$, 100 MHz) δ 165.9, 164.3, 160.5, 159.1, 133.5, 114.6, 112.6, 55.2, 55.0, 53.3; MS (EI) m/z 332 (M^+ , 100). HRMS (ESI) m/z calcd for $\text{C}_{10}\text{H}_{10}\text{N}_2\text{O}_4\text{SBr}$ ($[\text{M}+\text{H}]^+$) 332.9545, found 332.9563.



kmg-NB5-13C

2,4-Dimethoxy-7H,8H,9H-1,4-thiazepino[7',6'-5,4]thiopheno[3,2-d]pyrimidin-6-one (kmg-NB5-13C). To a solution of **3-25** (0.100 g, 0.300 mmol) in DMF (3.0 mL) under an

atmosphere of Ar was added cysteamine hydrochloride (0.139 g, 1.20 mmol) in one portion and DBU (0.38 mL, 2.49 mmol) dropwise. The white slurry became a clear yellow solution after the addition of DBU, and after stirring for 5 min a white precipitate formed. The pale yellow slurry was stirred at room temperature for 3 h. The slurry was diluted with EtOAc (10 mL) and H₂O (2 mL), and poured into an Erlenmeyer flask. 2 M aq. HCl (0.65 mL) was added, and the mixture was stirred for 5 minutes. The solid was collected by suction filtration and washed with H₂O and EtOAc to provide **kmg-NB5-13C** (0.069 g, 77%) as a white solid: Mp 288.0 °C (dec); IR (ATR, neat) 3321, 1642, 1579, 1545, 1491, 1476, 1458, 1346, 1331, 1206 cm⁻¹; ¹H NMR (DMSO-*d*₆, 500 MHz) δ 8.65 (t, 1 H, *J* = 5.7 Hz), 4.09 (s, 3 H), 3.96 (s, 3 H), 3.69–3.64 (m, 2 H), 3.38–3.34 (m, 2 H); ¹³C NMR (DMSO-*d*₆, 125 MHz) δ 165.5, 164.1, 163.5, 159.9, 135.9, 130.3, 111.5, 54.74, 54.72, 42.8, 31.8.

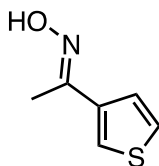


kmg-NB5-15A

4-Hydroxy-2-methoxy-7*H*,8*H*,9*H*-1,4-thiazepino[7',6'-5,4]thiopheno[3,2-*d*]pyrimidin-6-one (kmg-NB5-15A). To a reaction vial containing **kmg-NB5-13C** (0.015 g, 0.050 mmol) in THF (0.5 mL) was added KOSiMe₃ (0.029 g, 0.202 mmol). The white slurry turned to a clear yellow solution after the addition of KOSiMe₃, and after 2 min a white precipitate formed. The slurry was stirred at 80 °C for 22 h. After 18 h, an additional amount of KOSiMe₃ (0.014 g, 0.101 mmol) was added. The reaction mixture was diluted with EtOAc and quenched with sat. aq. NH₄Cl (2 mL). The solid was collected by suction filtration and washed

with H₂O to provide **kmg-NB5-15** (0.0069 g, 48%) as a white solid. An additional amount of **kmg-NB5-15** (0.0041 g, 29%) was isolated from extraction of the filtrate. In total, 0.011 g (77%) of **kmg-NB5-15A** was isolated as a white solid: Mp 295.0 °C (dec); IR (ATR, neat) 3266, 3170, 2740, 1674, 1646, 1603, 1465, 1407, 1316 cm⁻¹; ¹H NMR (DMSO-*d*₆, 400 MHz) δ 12.72 (s, 1 H), 8.56 (t, 1 H, *J* = 5.2 Hz), 3.94 (s, 3 H), 3.66–3.60 (m, 2 H), 3.32–3.28 (m, 2 H); ¹³C NMR (DMSO-*d*₆, 125 MHz) δ 164.0, 158.4, 156.8, 153.8, 135.7, 130.6, 118.6, 54.9, 42.7, 31.9; MS (EI) *m/z* 283 (M⁺, 100). HRMS (ESI) *m/z* calcd for C₁₀H₉N₃O₃S₂Na ([M+Na]⁺) 305.9983, found 305.9995.

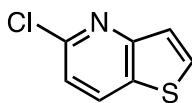
6.4.2 Thieno[3,2-*b*]-Based Inhibitors



3-30

1-(Hydroxyimino)-1-(3-thienyl)ethane (3-30).⁸² To a solution of NH₂OH·HCl (3.27 g, 46.6 mmol) in EtOH (116 mL) was added 3-acetylthiophene (**3-29**) (3.00 g, 23.3 mmol) in EtOH (23.3 mL). A solution of Na₂CO₃ (2.47 g, 23.3 mmol) in H₂O (23.3 mL) was added dropwise over 20 min, and the resulting slurry was heated at 60–65 °C for 12 h. The reaction mixture was cooled to room temperature and concentrated under reduced pressure until most of the EtOH was removed. The reaction mixture was diluted with H₂O (50 mL) and extracted with ether (3 x 50 mL). The combined organic layers were dried (MgSO₄) and concentrated under reduced pressure. The white solid was adsorbed onto SiO₂ and purified by chromatography on SiO₂ (1:50 to 1:10, EtOAc:hexanes) to provide **3-30** (2.80 g, 85%) as a white crystalline solid: Mp

118.8 – 119.6 °C (EtOAc); IR (ATR, neat) 3282, 3210, 3102, 3088, 2915, 1644, 1467, 1420, 1364, 1281, 1199, 1096, 1003, 947, 887, 865, 781, 759, 721 cm⁻¹; ¹H NMR (CDCl₃, 300 MHz) δ 8.37 (bs, 1 H), 7.47 (dd, 1 H, *J* = 2.9, 1.3 Hz), 7.42 (dd, 1 H, *J* = 5.1, 1.3 Hz), 7.31 (dd, 1 H, *J* = 5.1, 2.9 Hz), 2.28 (s, 3 H); ¹³C NMR (CDCl₃, 125 MHz) δ 152.5, 138.7, 126.4, 125.1, 124.0, 12.7; HRMS (ESI) *m/z* calcd for C₆H₇NOS (M⁺) 141.0248, found 141.0238.

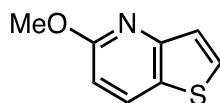


3-32

5-Chlorothiopheno[3,2-*b*]pyridine (3-32).⁸¹ *N*-(3-thienyl)acetamide (**3-31**).^{81a} A solution of **3-30** (1.71 g, 12.1 mmol) in PPA (10 mL) was stirred at 100 °C for 30 min. The viscous suspension became a clear, bright orange viscous semi-liquid after 10 min. The solution was poured into sat. aq. Na₂CO₃ and extracted twice with EtOAc. The combined organic layers were washed with sat. aq. NaHCO₃, H₂O, and brine, and concentrated under reduced pressure to give a tan colored crystalline solid that turned green upon standing. The material was absorbed onto SiO₂ and purified by chromatography on SiO₂ (1:4 EtOAc:hexanes, 1:1 EtOAc:hexanes, 100% EtOAc) to provide **3-31** (1.46 g, 85% crude) as a tan colored crystalline solid. The mixture was taken on without further purification. Diagnostic peaks: ¹H NMR (CDCl₃, 300 MHz) δ 7.55 (dd, 1 H, *J* = 3.2, 1.3 Hz), 7.22 (dd, 1 H, *J* = 5.2, 3.2 Hz), 6.98 (dd, 1 H, *J* = 5.2, 1.4 Hz), 2.16 (s, 3 H).

5-Chlorothiopheno[3,2-*b*]pyridine (**3-32**).^{81b} To a reaction vial containing DMF (0.80 mL, 10.3 mmol) cooled to 0 °C under an atmosphere of Ar was added POCl₃ (2.73 mL, 29.0 mmol) dropwise. Freshly distilled 1,2-dichloroethane (6.9 mL) was added followed by a

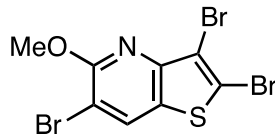
solution of **3-31** (1.46 g, 10.3 mmol) in 1,2-dichloroethane (20.5 mL). The clear orange solution was stirred at room temperature for 15 minutes, and a solid white precipitate formed. The mixture was heated at reflux for 21 h, and the precipitate dissolved upon heating. After 21 h, the clear orange solution was cooled to room temperature and poured into water containing NaOAc (4.28 g, 51.7 mmol) and stirred at reflux for 30 minutes. The mixture was extracted with EtOAc. The combined organic layers were washed with sat. aq. NaHCO₃ and brine, dried (MgSO₄), and concentrated under reduced pressure to give a dark red residue that solidified upon standing. The crude material was adsorbed onto SiO₂ and purified by chromatography on SiO₂ (100% hexanes, 1:100 EtOAc:hexanes, 1:20 EtOAc:hexanes, 100% EtOAc) to provide **3-32** (0.94 g, 46% from **3-31**) was isolated as a white crystalline solid: Mp 75.7–76.9°C (EtOAc); IR (ATR, neat) 3102, 3090, 3075, 3062, 1558, 1536, 1482, 1385, 1148, 1118, 1077, 1036, 904, 889, 816, 771, 703, 677 cm⁻¹; ¹H NMR (CDCl₃, 400 MHz) δ 8.10 (dd, 1 H, *J* = 8.5, 0.6 Hz), 7.78 (d, 1 H, *J* = 5.5 Hz), 7.48 (dd, 1 H, *J* = 5.6, 0.6 Hz), 7.25 (d, 1 H, *J* = 8.4 Hz); ¹³C NMR (CDCl₃, 100 MHz) δ 155.9, 149.1, 132.8, 132.4, 131.7, 124.6, 119.4; HRMS (ESI) *m/z* calcd for C₇H₄CINS (M⁺) 168.9753, found 168.9768.



3-33

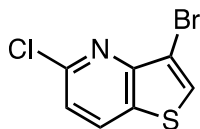
5-Methoxythiopheno[3,2-*b*]pyridine (3-33). To a vial containing **3-32** (0.296 g, 1.75 mmol) was added 25% wt. NaOMe in MeOH (8.9 mL). The reaction vial was sealed and heated at 80 °C for 21 h. The reaction mixture was cooled to room temperature, quenched with 2 M aq. HCl, and extracted with EtOAc (3 x 15 mL). The combined organic layers were washed

with brine (15 mL), dried (MgSO₄), and concentrated under reduced pressure to give a yellow liquid. The crude liquid was purified by chromatography on SiO₂ (1:50, EtOAc:hexanes) to provide **3-33** (0.213 g, 80%) as a pale yellow liquid: IR (ATR, neat) 3102, 3074, 3003, 2975, 2943, 1577, 1553, 1497, 1446, 1387, 1327, 1256, 1199, 1143, 1018 cm⁻¹; ¹H NMR (CDCl₃, 400 MHz) δ 7.95 (d, 1 H, *J* = 8.6 Hz), 7.63 (d, 1 H, *J* = 5.3 Hz), 7.39 (d, 1 H, *J* = 5.4 Hz), 6.74 (d, 1 H, *J* = 8.7 Hz), 4.01 (s, 3 H); ¹³C NMR (CDCl₃, 100 MHz) δ 162.8, 153.6, 132.5, 130.0, 126.2, 124.3, 108.6, 53.4; HRMS (ESI) *m/z* calcd for C₈H₈NOS (M⁺) 312.0299, found 312.0266.



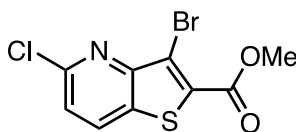
3-34

2,3,6-Tribromo-5-methoxythiopheno[3,2-*b*]pyridine (3-34). To a vial containing **3-33** (0.032 g, 0.192 mmol) dissolved in AcOH (1.3 mL, 0.15 M) was added Br₂ (0.03 mL) dropwise. The reaction vial was sealed and stirred at room temperature for 1 h. The reaction mixture was quenched with sat. aq. NaHCO₃, stirred for 5 minutes, and extracted with EtOAc (3 x 10 mL). The combined organics were washed with sat. aq. Na₂S₂O₃ (3 x 5 mL) and sat. aq. NaHCO₃ (5 mL), dried (MgSO₄), and concentrated under reduced pressure to provide **3-34** (0.057 g, 73%) as a fluffy white solid: Mp 192.7–193.3 °C (EtOAc); IR (ATR, neat) 3102, 3055, 2992, 2945, 2917, 2891, 2850, 1562, 1480, 1459, 1372, 1232, 1048, 1003, 762, 747 cm⁻¹; ¹H NMR (DMSO-*d*₆, 400 MHz) δ 8.79 (s, 1 H), 4.04 (s, 3 H); ¹³C NMR (DMSO-*d*₆, 100 MHz) δ 158.4, 147.5, 136.3, 126.8, 119.8, 112.1, 104.7, 54.6. GC-MS *m/z* 400 (M⁺, 100).



3-36

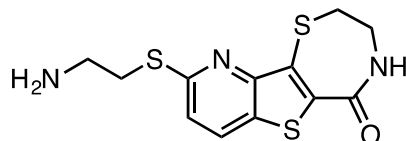
3-Bromo-5-chlorothieno[3,2-*b*]pyridine (3-36). To a reaction vial containing **3-32** (0.401 g, 2.36 mmol) dissolved in AcOH (16.0 mL) was added Br₂ (0.37 mL, 7.09 mmol). The reaction vial was sealed and stirred at 80 °C for 9 h. The reaction mixture was cooled to room temperature, diluted with EtOAc, and poured into sat. aq. NaHCO₃. The reaction mixture was then extracted with EtOAc (3x), and the combined organic layers were washed with sat. aq. Na₂S₂O₃, sat. aq. NaHCO₃, and brine. The organic layers were dried (MgSO₄) and concentrated under reduced pressure to provide a light pink solid. The material was adsorbed onto SiO₂ and purified by chromatography on SiO₂ (100% hexanes, 1:99 EtOAc:hexanes) to provide **3-36** as a white solid (0.409 g, 63%, 90% pure). The material was taken on to the next step without further purification: Mp 112.8–114.0 °C (Et₂O); IR (ATR, neat) 3109, 3044, 1553, 1527, 1486, 1381, 1297, 1146, 1118, 964, 772 cm⁻¹; ¹H NMR (CDCl₃, 400 MHz) δ 8.13 (d, 1 H, *J* = 8.5 Hz), 7.81 (s, 1 H), 7.36 (d, 1 H, *J* = 8.4 Hz); ¹³C NMR (CDCl₃, 125 MHz) δ 152.0, 150.4, 133.3, 130.9, 129.0, 120.8, 109.4; HRMS (ESI) *m/z* calcd for C₇H₃BrClNS (M⁺) 246.8858, found 246.8835.



3-37

Methyl 3-bromo-5-chlorothieno[3,2-*b*]pyridine-2-carboxylate (3-37). To a solution of **3-36** (0.300 g, 1.09 mmol) in THF (3.3 mL) cooled to -50 °C under an atmosphere of Ar was

added $\text{TMPMgCl}\cdot\text{LiCl}$ (1.85 mL, 1.74 mmol). The solution was stirred at $-40\text{ }^\circ\text{C}$ to $-50\text{ }^\circ\text{C}$ for 2 h. Methyl cyanofomate (0.11 mL, 1.43 mmol) was added and the solution was allowed to warm to $0\text{ }^\circ\text{C}$ over 1 h 45 min. The solution was quenched at $0\text{ }^\circ\text{C}$ with sat. aq. NH_4Cl and stirred for 5 min at $0\text{ }^\circ\text{C}$. The reaction mixture was then diluted with EtOAc and the organic layer was washed with sat. aq. NH_4Cl (3x). The combined aqueous layers were then extracted with EtOAc (3x). The combined organic layers were washed with sat. aq. NH_4Cl (3x) and brine, dried (MgSO_4), and concentrated under reduced pressure to give a yellow residue. The crude residue was purified by chromatography on SiO_2 (100% hexanes, 1:99 to 5:95 EtOAc:hexanes) to provide **3-37** (0.254 g, 76%, 95% pure) as a white solid: Mp $195.3\text{--}197.0\text{ }^\circ\text{C}$ (Et_2O); IR (ATR, neat) $3103, 2949, 1719, 1508, 1236, 1118, 1092, 936, 831\text{ cm}^{-1}$; ^1H NMR (CDCl_3 , 500 MHz) δ 8.14 (d, 1 H, $J = 8.5\text{ Hz}$), 7.46 (d, 1 H, $J = 8.5\text{ Hz}$), 4.01 (s, 3 H); ^{13}C NMR (CDCl_3 , 125 MHz) δ 161.3, 152.3, 151.3, 133.5, 132.43, 132.39, 123.5, 116.2, 53.1; HRMS (ESI) m/z calcd for $\text{C}_9\text{H}_5\text{BrClNO}_2\text{S}$ (M^+) 304.8913, found 304.8938.

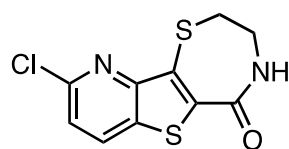


kmg-NB6-19B

9-(2-Aminoethylthio)-2H,3H,4H-1,4-thiazepino[7',6'-4,5]thiopheno[3,2-*b*]pyridin-5-one

(kmg-NB6-19B). To a solution of **3-37** (0.0500 g, 0.155 mmol) in DMF (1.5 mL) under a atmosphere of Ar was added cysteamine hydrochloride (0.0720 g, 0.620 mmol) in one portion and DBU (189 μL , 1.24 mmol) dropwise. The reaction mixture was stirred at room temperature for 1.5 h, and then sealed and heated to $70\text{ }^\circ\text{C}$ for 12 h. The solution was cooled to room temperature, diluted with EtOAc, and 1 M aq. HCl was added. The mixture was extracted with

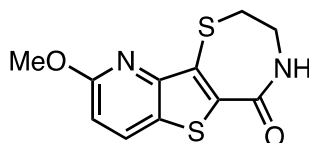
EtOAc (3x). A precipitate formed in the aqueous extracts and was collected by suction filtration to provide **kmg-NB6-19B** (0.031 g, 58%) as a yellow-green solid: Mp 263.7 °C (dec, H₂O); IR (ATR, neat) 3262, 3157, 3016, 2917, 2587, 1635, 1558, 1489, 1463, 1387, 1342, 1234, 1133 cm⁻¹; ¹H NMR (DMSO-*d*₆, 500 MHz) δ 8.57 (t, 1 H, *J* = 6.0 Hz), 8.36 (d, 1 H, *J* = 8.6 Hz), 8.09 (bs, 2 H), 7.49 (d, 1 H, *J* = 8.6 Hz), 3.72-3.66 (m, 2 H), 3.45 (t, 2 H, *J* = 6.5 Hz), 3.39–3.35 (m, 2 H), 3.30 – 3.25 (m, 2 H); ¹³C NMR (DMSO-*d*₆, 100 MHz) δ 164.4, 155.3, 152.5, 133.0, 131.7, 130.8, 129.4, 120.6, 42.9, 38.0, 31.7, 27.4; HRMS (ESI) *m/z* calcd for C₁₂H₁₄N₃OS₃ ([M+H]⁺) 312.0299, found 312.0266.



kmg-NB6-22A

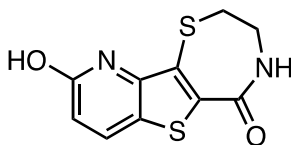
9-Chloro-2*H*,3*H*,4*H*-1,4-thiazepino[7',6'-4,5]thiopheno[3,2-*b*]pyridin-5-one (kmg-NB6-22A). To a colorless solution of **3-37** (0.020 g, 0.062 mmol) in DMF (0.62 mL) under an atmosphere of Ar was added cysteamine hydrochloride (0.011 g, 0.093 mmol) in one portion and DBU (28 μL, 0.19 mmol) dropwise. The reaction mixture was stirred at room temperature under an atmosphere of Ar for 1 h. the reaction mixture was diluted with EtOAc, and H₂O was added and the solution was extracted with EtOAc (3 x 5 mL). The combined organic layers were washed with H₂O (4 x 5 mL) and brine (5 mL), dried (MgSO₄), and concentrated under reduced pressure to give the desired product as a light green solid. The material was adsorbed onto SiO₂ and purified by chromatography on SiO₂ (100% CH₂Cl₂, 2:98 MeOH:CH₂Cl₂) to provide **kmg-NB6-22A** (0.015 g, 91%) as a light yellow-green solid: Mp 273.3 °C (dec, MeOH/CH₂Cl₂); IR (ATR, neat) 3256, 3156, 3025, 2919, 1637, 1553, 1532, 1495, 1456, 1389, 1344, 1158, 1131,

971, 813 cm^{-1} ; ^1H NMR (CDCl_3 , 300 MHz) δ 8.61 (t, 1 H, $J = 4.9$ Hz), 8.57 (d, 1 H, $J = 8.6$ Hz), 7.63 (d, 1 H, $J = 8.5$ Hz), 3.74–3.64 (m, 2 H), 3.42–3.35 (m, 2 H); ^{13}C NMR (CDCl_3 , 125 MHz) δ 164.2, 152.4, 148.0, 134.7, 134.5, 132.0, 130.7, 122.2, 42.8, 31.8; HRMS (ESI) m/z calcd for $\text{C}_{10}\text{H}_8\text{ClN}_2\text{OS}_2$ ($[\text{M}+\text{H}]^+$) 270.9767, found 270.9798.



kmg-NB6-38

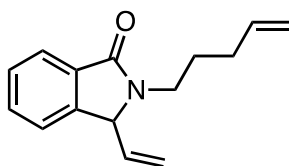
9-Methoxy-2H,3H,4H-1,4-thiazepino[7',6'-4,5]thiopheno[3,2-*b*]pyridin-5-one (kmg-NB6-38). To a reaction vial containing **kmg-NB6-22A** (0.050 g, 0.19 mmol) was added 25% wt. NaOMe in MeOH (1.7 mL). The solution was heated to 80 °C for 14 h. The reaction mixture was cooled to room temperature and extracted with EtOAc (3x), washed with brine, dried (MgSO_4), and concentrated under reduced pressure to provide **kmg-NB6-38** (0.024 g, 49%) as a white solid: Mp 289.1–291.1 °C (EtOAc); IR (ATR, neat) 3262, 3148, 3018, 2917, 1629, 1575, 1493, 1458, 1389, 1346, 1267, 1232, 1143, 1087 cm^{-1} ; ^1H NMR (CDCl_3 , 400 MHz) δ 8.48 (t, 1 H, $J = 4.3$ Hz), 8.34 (d, 1 H, $J = 7.0$ Hz), 7.01 (d, 1 H, $J = 7.0$ Hz), 3.93 (s, 3 H), 3.69–3.65 (m, 2 H), 3.36 – 3.33 (m, 2 H); ^{13}C NMR (CDCl_3 , 100 MHz) δ 164.6, 162.0, 149.9, 133.9, 132.5, 130.7, 126.3, 111.4, 53.2, 42.9, 31.7; HRMS (ESI) m/z calcd for $\text{C}_{11}\text{H}_{11}\text{N}_2\text{O}_2\text{S}_2$ ($[\text{M}+\text{H}]^+$) 267.0262, found 267.0291.



kmg-NB6-41

9-Hydroxy-2*H*,3*H*,4*H*-1,4-thiazepino[7',6'-4,5]thiopheno[3,2-*b*]pyridin-5-one (kmg-NB6-41). To a reaction vial containing **kmg-NB6-38** (0.012 g, 0.046 mmol) was added 4 M aq. HCl in 1,4-dioxane (1.0 mL). The reaction vial was sealed and heated to 80 °C for 24 h. The reaction mixture was cooled to room temperature and concentrated under reduced pressure to provide a bright yellow solid. The solid was suspended in H₂O and the pH was adjusted to 7 with sat. aq. Na₂CO₃. The solid was collected by suction filtration to provide **kmg-NB6-41** (0.014 g, 63%) as a tan-colored solid: Mp 263.7 °C (dec, Et₂O); IR (ATR, neat) 3262, 3143, 3010, 2910, 1625, 1560, 1472, 1418 cm⁻¹; ¹H NMR (DMSO-*d*₆, 500 MHz) δ 11.29 (bs, 1 H), 8.47 (t, 1 H, *J* = 5.7 Hz), 8.23 (d, 1 H, *J* = 8.6 Hz), 6.79 (d, 1 H, *J* = 5.9 Hz), 3.69–3.62 (m, 2 H), 3.34–3.30 (m, 2 H); HRMS (ESI) *m/z* calcd for C₁₀H₉N₂O₂S₂ ([M+H]⁺) 253.0105, found 253.0130.

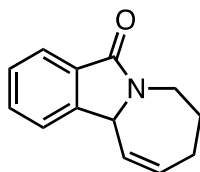
6.5 CHAPTER 4 EXPERIMENTAL PART



4-18

2-(Pent-4-enyl)-3-vinylisindolin-1-one (4-18). To a flask containing AlCl₃ (3.73 g, 27.9 mmol) in CH₂Cl₂ (16 mL) cooled to 0 °C under an atmosphere of Ar was added vinylmagnesium bromide (1.0 M in THF, 83.6 mL, 83.9 mmol) dropwise over 20 minutes. The solution was stirred at 0 °C for 4 h. Compound **4-7**⁹⁷ (3.00 g, 9.95 mmol) in CH₂Cl₂ (9.0 mL) was added in one portion and the reaction was allowed to stirred at 0 °C for 1 h and then warmed to room temperature and stirred for 3 h. The reaction mixture was cooled to 0 °C and carefully

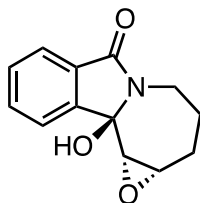
quenched with 1 M aq. HCl, warmed to room temperature, and extracted with CH₂Cl₂. The combined organic extracts were washed with brine, dried (MgSO₄), and concentrated under reduced pressure to provide a brown residue. The residue was purified by chromatography on SiO₂ (100% hexanes, 5:95 to 10:90 EtOAc:hexanes) to provide **4-18** (1.80 g, 80%) as an orange oil: IR (ATR, neat) 3074, 2923, 1685, 1639, 1614, 1596, 1467, 1437, 1400, 1312, 1275, 1094 cm⁻¹; ¹H NMR (CDCl₃, 500 MHz) δ 7.83 (d, 1 H, *J* = 7.5 Hz), 7.52 (t, 1 H, *J* = 7.5 Hz), 7.46 (t, 1 H, *J* = 7.5 Hz), 7.34 (d, 1 H, *J* = 7.4 Hz) 5.82 (dddd, 1 H, *J* = 16.9, 13.2, 10.2, 6.6 Hz), 5.65–5.56 (m, 1 H), 5.52–5.42 (m, 2 H), 5.04 (d, 1 H, *J* = 17.2 Hz), 4.97 (d, 1 H, *J* = 10.2 Hz), 4.87 (d, 1 H, *J* = 8.2 Hz), 3.87 (ddd, 1 H, *J* = 14.5, 7.6, 7.6 Hz), 3.22 (ddd, 1 H, *J* = 14.0, 8.6, 5.5 Hz), 2.14–2.05 (m, 2 H), 1.80–1.65 (m, 2 H); ¹³C NMR (CDCl₃, 125 MHz) δ 168.2, 144.2, 137.8, 135.3, 132.2, 131.6, 128.6, 123.6, 123.1, 120.9, 115.2, 64.3, 40.1, 31.2, 27.7; HRMS (ESI) *m/z* calcd for C₁₅H₁₈NO ([M+H]⁺) 228.1383, found 228.1380.



4-9

7H, 8H, 9H, 11aH-Azepino[7,1-a]isoindolin-5-one (4-9). To a solution of **4-18** (0.060 g, 0.26 mmol) in toluene (50 mL) at room temperature under an atmosphere of N₂ was added Grubbs 2nd generation catalyst (0.011 g, 0.013 mmol). The solution was stirred at room temperature for 15.5 h. The entire reaction mixture was directly applied to a column of Florisil® and eluted with 100% hexanes and then 30:70 EtOAc:hexanes to afford **4-9** (0.041 g, 77%) as a crude yellow oil; ¹H NMR (CDCl₃, 500 MHz) δ 7.79 (d, 1 H, *J* = 7.6 Hz), 7.53 (t, 1 H, *J* =

7.5 Hz), 7.47–7.40 (m, 2 H), 5.85–5.75 (m, 2 H), 5.20 (s, 1 H), 4.32 (ddd, 1 H, $J = 13.6, 9.1, 4.2$ Hz), 3.35 (ddd, 1 H, $J = 10.6, 6.7, 3.9$ Hz), 2.36–2.30 (m, 2 H), 2.10–2.01 (m, 1 H), 1.95–1.88 (m, 1 H); ^{13}C NMR (CDCl_3 , 125 MHz) δ 168.3, 145.2, 132.2, 131.9, 131.7, 128.2, 127.3, 123.6, 122.0, 60.7, 43.5, 28.4, 26.0; HRMS (ESI) m/z calcd for $\text{C}_{13}\text{H}_{14}\text{NO}$ ($[\text{M}+\text{H}]^+$) 200.1070, found 200.1067.



4-17

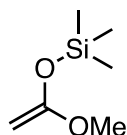
10b-Hydroxy-2H, 3H, 4H, 10cH, 1aH-isoindolino[2,1-a]oxirano[2,3-c]azaperhydro-pin-6-one (4-17). To a solution of **4-18** (0.050 g, 0.220 mmol) in toluene (40 mL) at room temperature under an atmosphere of N_2 was added Grubbs 2nd generation catalyst (0.009 g, 0.011 mmol). The solution was stirred at room temperature for 14 h. The reaction mixture was concentrated under reduced pressure to provide **4-9** as a crude residue. The residue was taken onto the next step without further purification.

To a flask containing crude **4-9** in CH_2Cl_2 (4.0 mL) at room temperature open to air was added NaHCO_3 (0.185 g, 2.20 mmol) and *m*-CPBA (0.542 g, 2.20 mmol). The reaction mixture was stirred at room temperature open to air for 33 h. The reaction mixture was diluted with CH_2Cl_2 and washed with sat. aq. NaHCO_3 and sat. aq. Na_2CO_3 . The aqueous layers were then extracted with CH_2Cl_2 . The combined organic layers were washed with brine, dried (MgSO_4), and concentrated under reduced pressure to provide **4-17** (0.057 g, 11% from **4-18**) as a colorless residue: *ca.* 5:1 *dr* by LCMS and NMR analysis; major diastereomer: ^1H NMR (CDCl_3 ,

500 MHz) δ 7.68–7.64 (m, 2 H), 7.60 (t, 1 H, $J = 7.5$ Hz), 7.49–7.45 (m, 1 H), 3.86 (d, 1 H, $J = 14.5$ Hz), 3.54 (d, 1 H, $J = 4.2$ Hz), 3.46–3.41 (m, 1 H), 3.37–3.31 (m, 2 H), 2.84–2.77 (m, 1 H), 2.49–2.41 (m, 1 H), 2.18–2.09 (m, 1 H), 1.69–1.61 (m, 1 H); ^{13}C NMR (CDCl_3 , 125 MHz) δ 166.9, 145.9, 132.7, 131.0, 130.3, 123.7, 121.8, 89.6, 59.2, 57.8, 37.9, 28.0, 24.2; HRMS (ESI) m/z calcd for $\text{C}_{13}\text{H}_{14}\text{NO}$ ($[\text{M}+\text{H}]^+$) 232.0968, found 232.0966.

6.6 CHAPTER 5 EXPERIMENTAL PART

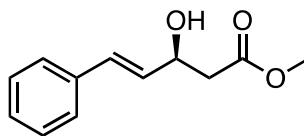
6.6.1 Second Generation Approach



5-48

(1-Methoxyvinyl)oxytrimethylsilane (**5-48**).^{127a} To a solution of *i*-Pr₂NH (2.3 mL, 16.2 mmol) in THF (16 mL) at 0 °C under an atmosphere of N₂ was added *n*-BuLi (1.6 M solution in hexanes, mL, 9.2 mL) dropwise. The solution was stirred for 30 min at 0 °C and cooled to -78 °C. A mixture of MeOAc (**5-47**) (1.1 mL, 13.5 mmol) and TMSCl (2.05 mL, 16.2 mmol) in THF (7.5 mL) was added. Once addition was complete, the resulting solution was warmed to room temperature and stirred for 3 h. The THF was evaporated and hexanes was added. The resulting precipitate was removed by filtration through a pad of Celite® with hexanes washings. The combined filtrate was concentrated under reduced pressure and purified by distillation. The solvent was removed at 50 mmHg at room temperature and the product was collected at 30 mmHg and 55 °C to provide **5-48** (0.385 g, 19%) as a clear, colorless liquid. The

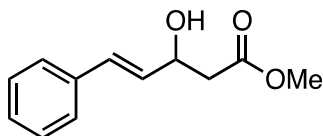
product was used in the next reaction without further purification: ^1H NMR (CDCl_3 , 300 MHz) δ 3.55 (s, 3 H), 3.22 (d, 1 H, $J = 2.8$ Hz), 3.11 (d, 1 H, $J = 2.8$ Hz), 0.23 (s, 9 H).



5-50

(3*S*,4*E*)-Methyl 3-hydroxy-5-phenylpent-4-enoate (5-50).^{126a,b} To a solution of **5-49**^{126c,127b} (0.086 g, 0.17 mmol) in toluene (65 mL) at room temperature under an atmosphere of N_2 was added $\text{Ti}(i\text{-PrO})_4$ (0.022 mL, 0.075 mmol). The solution was stirred at room temperature for 1 h. At this time, 3,5-di-*tert*-butylsalicylic acid (0.023 g, 0.090 mmol) in toluene (5 mL) was added and the solution was stirred at room temperature for an additional 1 h. The solvent was removed under reduced pressure, and the residue was taken up in Et_2O (30 mL) and cooled to -78 °C. Cinnamaldehyde (**5-46**) (0.19 mL, 1.5 mmol) and **5-48** (0.263 g, 1.80 mmol) were added sequentially and the solution was kept at -10 °C for 20 h. The solution was warmed to 0 °C for 4 h. The reaction mixture was quenched by addition of sat. aq. NaHCO_3 and was extracted with Et_2O . The combined organic layers were washed with brine, dried (MgSO_4), and concentrated under reduced pressure to yield a yellow residue. The residue was taken up in THF and cooled to 0 °C. TBAF (0.90 mL, 1.6 mmol, 1 M in THF) was added and the solution was stirred at 0 °C for 30 min. The reaction was quenched with sat. aq. NaHCO_3 was added and extracted with Et_2O . The organic layers were washed with brine, dried (MgSO_4), and concentrated under reduced pressure to provide a yellow residue. The residue was adsorbed onto SiO_2 and purified by chromatography on SiO_2 (100% hexanes to 30:70 EtOAc :hexanes) to afford **5-50** (0.18 g, 58%) as a yellow oil: 85:15 *er* (determined by chiral HPLC analysis on a

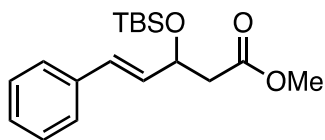
CHIRALCEL® OD column; 90:10, hexanes:*i*-PrOH; 1.0 mL/min; *R*: 13.74 min, *S*: 18.21 min); ¹H NMR (DMSO-*d*₆, 500 MHz) δ 7.38 (d, 2 H, *J* = 7.3 Hz), 7.32 (t, 2 H, *J* = 7.3 Hz), 7.25 (t, 1 H, *J* = 5.2 Hz), 6.66 (d, 1 H, *J* = 15.9 Hz), 6.22 (dd, 1 H, *J* = 15.9, 6.2 Hz), 4.73 (dddd, 1 H, *J* = 7.7, 6.0, 4.6, 1.3 Hz), 3.73 (s, 3 H), 2.70–2.60 (m, 2 H).



rac-5-50

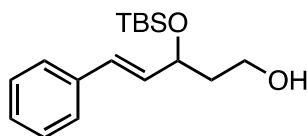
(*E*)-Methyl 3-hydroxy-5-phenylpent-4-enoate (*rac*-5-50).¹²⁸ To a solution of diisopropylamine (0.59 mL, 4.1 mmol) in anhyd. THF (10 mL) at -78 °C under an atmosphere of N₂ was slowly added *n*-BuLi (1.6 M in hexanes, 2.6 mL, 4.1 mmol). The resulting solution was warmed to 0 °C and stirred for 15 min. The solution was cooled to -78 °C and MeOAc (**5-47**) (0.3 mL, 3.8 mmol) was added. The solution was stirred at -78 °C for 5 min and *trans*-cinnamaldehyde (**5-46**) (0.48 mL, 3.75 mmol) in anhyd. THF (2.5 mL) was added over 5 min. The resulting solution was stirred at -78 °C for 2 h. The reaction was quenched by the addition of H₂O (5 mL) at -78 °C and slowly warmed to room temperature. The mixture was extracted with EtOAc, washed with brine, dried (MgSO₄), and concentrated under reduced pressure to provide a colorless residue. The residue was adsorbed onto SiO₂ and purified by chromatography on SiO₂ (100% hexanes, 10:90 EtOAc:hexanes, 15:85 EtOAc:hexanes) to provide *rac*-5-50 (0.749 g, 97%) as a clear, yellow oil: ¹H NMR (CDCl₃, 400 MHz) δ 7.38 (d, 2 H, *J* = 7.2 Hz), 7.32 (t, 2 H, *J* = 7.2 Hz), 7.24 (t, 1 H, *J* = 7.2 Hz), 6.66 (d, 1 H, *J* = 15.9 Hz), 6.22 (dd, 1 H, *J* = 15.9, 6.2 Hz), 4.68–4.60 (m, 1 H), 3.73 (s, 3 H), 2.73–2.60 (m, 2 H); retention time of

enantiomers determined by chiral HPLC analysis on a CHIRALCEL® OD column; 90:10, hexanes:*i*-PrOH; 1.0 mL/min; *R*: 13.36 min, *S*: 17.62 min.



rac-5-45

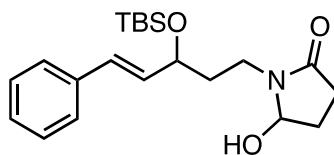
(*E*)-Methyl 3-(*tert*-butyldimethylsilyloxy)-5-phenylpent-4-enoate (*rac*-5-45).¹²⁸ To a solution of *rac*-5-50 (0.546 g, 2.65 mmol), DMAP (0.0160 g, 0.132 mmol), and imidazole (0.727 g, 10.6 mmol) in CH₂Cl₂ (13 mL) at room temperature under an atmosphere of N₂ was added TBSCl (0.598 g, 3.97 mmol). Upon addition of the TBSCl, a precipitate formed. The solution was stirred at room temperature for 13 h. The reaction mixture was quenched by addition of H₂O and was extracted with Et₂O. The organic layers were washed with brine, dried (MgSO₄), and concentrated under reduced pressure to provide a clear, colorless oil. The oil was purified by chromatography on SiO₂ (100% hexanes, 5% Et₂O/hexanes) to afford *rac*-5-45 (0.772 g, 91%) as a clear, light yellow oil: IR (ATR, neat) 2951, 2926, 2885, 2854, 1735, 1435, 1361, 1249, 1163, 1109, 1072, 1048, 966 cm⁻¹; ¹H NMR (CDCl₃, 400 MHz) δ 7.39–7.28 (m, 4 H), 7.27–7.21 (m, 1 H), 6.57 (d, 1 H, *J* = 15.9 Hz), 6.18 (dd, 1 H, *J* = 15.9, 6.7 Hz), 4.80–4.73 (m, 1 H), 3.68 (s, 3 H), 2.63 (dd, 1 H, *J* = 14.5, 8.2 Hz), 2.53 (dd, 1 H, *J* = 14.5, 5.1 Hz), 0.89 (s, 9 H), 0.08 (s, 3 H), 0.06 (s, 3 H); ¹³C NMR (CDCl₃, 125 MHz) δ 171.6, 136.8, 131.8, 130.1, 128.7, 127.8, 126.6, 70.9, 51.7, 44.0, 25.9, 18.3, -4.1, -4.9; HRMS (ESI) *m/z* calcd for C₁₈H₂₈O₃SiNa ([M+Na]⁺) 343.1705, found 343.1736.



rac-5-44

(*E*)-3-(*tert*-butyldimethylsilyloxy)-5-phenylpent-4-en-1-ol (*rac-5-44*). To a solution of DIBAL-H (0.501 g, 3.52 mmol) in toluene (2.4 mL, 1.5 M solution) cooled to $-78\text{ }^{\circ}\text{C}$ under an atmosphere of N_2 was added ***rac-5-45*** (0.751 g, 2.34 mmol) in toluene (23 mL) dropwise over 10 min. The reaction mixture was stirred at $-78\text{ }^{\circ}\text{C}$ for 1 h. The reaction mixture was quenched with sat. aq. NH_4Cl (2 mL) at $-78\text{ }^{\circ}\text{C}$ and allowed to warm to room temperature. Sat. aq. Rochelle's salt was added, and the solution was poured into a separatory funnel containing brine. The mixture was extracted with EtOAc. The combined organic layers were washed with sat. aq. Rochelle's salt and brine, dried (MgSO_4), and concentrated under reduced pressure to provide a clear residue. The residue was taken up in MeOH (11.5 mL) and cooled to $0\text{ }^{\circ}\text{C}$ under an atmosphere of N_2 . NaBH_4 (0.136 g, 3.52 mmol) was added in one portion and the solution was stirred for 1 h. The reaction was quenched with sat. aq. NH_4Cl , warmed to room temperature, and extracted with EtOAc. The combined organic layers were washed with brine, dried (MgSO_4), and concentrated under reduced pressure to provide a clear, yellow oil. The oil was adsorbed onto SiO_2 and purified by chromatography on SiO_2 (100% hexanes, 10:90 to 20:80 Et_2O :hexanes) to provide ***rac-5-44*** (0.606 g, 88%, 96% BRSM) as a clear, yellow oil: IR (ATR, neat) 3405, 2951, 2926, 2883, 2854, 1471, 1359, 1251, 1117, 1051, 964, 833, 774, 746, 692 cm^{-1} ; ^1H NMR (CDCl_3 , 500 MHz) δ 7.40–7.30 (m, 4 H), 7.27–7.23 (m, 1 H), 6.55 (d, 1 H, $J = 16.0$ Hz), 6.21 (dd, 1 H, $J = 15.9, 6.4$ Hz) 4.60 (ddt, 1 H, $J = 6.4, 4.6, 1.2$ Hz), 3.91–3.83 (m, 1 H), 3.80–3.72 (m, 1 H), 2.51 (bs, 1 H), 1.92 (dddd, 1 H, $J = 12.9, 10.4, 6.4, 3.9$ Hz), 1.82 (dddd, 1 H, $J = 12.4, 8.7, 8.1, 4.4$ Hz), 0.93 (s, 9 H), 0.13 (s, 3 H), 0.08 (s, 3 H); ^{13}C NMR

(CDCl₃, 125 MHz) δ 136.9, 132.3, 129.8, 128.7, 127.7, 126.6, 73.3, 60.4, 39.8, 26.0, 18.3, -4.1, -4.8.

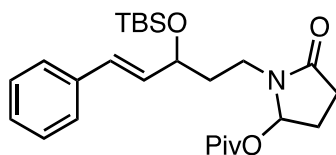


5-51

(*E*)-1-(3-((*tert*-Butyldimethylsilyloxy)-5-phenylpent-4-en-1-yl)-5-hydroxypyrrolidin-2-one (5-51). To a solution of *rac*-5-44 (0.0500 g, 0.171 mmol), succinimide (5-43) (0.0190 g, 0.188 mmol), and PPh₃ (0.0500 g, 0.188 mmol) in THF (1.0 mL) cooled to 0 °C under an atmosphere of Ar was added DBAD (0.0440 g, 0.188 mmol) in THF (0.2 mL) dropwise. The solution was warmed to room temperature and stirred for 22.5 h. After 18 h, the reaction was not complete by TLC; therefore, an additional 0.5 equiv of succinimide (5-43), PPh₃, and DBAD was added. The reaction was quenched with sat. aq. NH₄Cl and extracted with EtOAc. The combined organic layers were washed with brine, dried (MgSO₄), and concentrated under reduced pressure. The crude residue was adsorbed onto SiO₂ and purified by chromatography on SiO₂ (100% hexanes, 5:95 to 20:80 EtOAc:hexanes) to provide ((*E*)-1-(3-((*tert*-butyldimethylsilyloxy)-5-phenylpent-4-en-1-yl)pyrrolidine-2,5-dione, 0.0621 g, 78%, 80% pure) as a yellow oil. The product was contaminated with di-*tert*-butyl hydrazodiformate and was taken onto the next step without further purification. Diagnostic peaks for the desired product: IR (ATR, neat) 2949, 2926, 2854, 1696, 1493, 1446, 1400, 1366, 1338, 1249, 1068, 1081, 1003, 967, 910, 835, 775, 731, 693 cm⁻¹; ¹H NMR (CDCl₃, 400 MHz) δ 7.36 (d, 2 H, *J* = 7.4 Hz), 7.31 (t, 2 H, *J* = 7.3 Hz), 7.22 (t, 1 H, *J* = 7.1 Hz), 6.52 (d, 1 H, *J* = 15.9 Hz), 6.15 (dd, 1 H, *J* = 15.9, 6.4 Hz), 4.37 (q, 1 H, *J* = 5.8 Hz), 3.71–3.62 (m, 1 H), 3.62–3.52 (m, 1 H), 2.61 (s, 4 H),

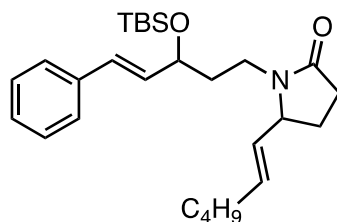
1.93–1.80 (m, 2 H), 0.92 (s, 9 H), 0.09 (s, 3 H), 0.05 (s, 3 H); ^{13}C NMR (CDCl_3 , 125 MHz) δ 177.3, 136.9, 132.1, 129.9, 128.7, 127.7, 126.5, 71.7, 35.6, 28.3, 28.2, 26.0, 18.3, –4.1, –4.8; HRMS (ESI) m/z calcd for $\text{C}_{21}\text{H}_{30}\text{NO}_3\text{Si}$ ($[\text{M}]^+$) 372.1995, found 372.1993.

To a solution of ((*E*)-1-(3-(*tert*-butyldimethylsilyloxy)-5-phenylpent-4-enyl)pyrrolidine-2,5-dione (0.060 g, 0.16 mmol) in MeOH (1.6 mL) at 0 °C under an atmosphere of N_2 was added NaBH_4 (0.018 g, 0.48 mmol). The reaction mixture was stirred at 0 °C for 1 h. An additional amount of NaBH_4 (0.018 g, 0.48 mmol) was added every hour until the reaction was complete. The reaction was monitored by the disappearance of starting material by TLC. The reaction was complete after 4.5 h. The reaction was diluted with CH_2Cl_2 , quenched with sat. aq. NaHCO_3 , and extracted with EtOAc. The combined organic layers were washed with H_2O , dried (MgSO_4), and concentrated under reduced pressure to provide a crude residue. The residue was adsorbed onto SiO_2 and purified by chromatography on SiO_2 (100% hexanes, 10:90 to 40:60 EtOAc:hexanes) to provide **5-51** (0.042 g, 65% from *rac*-**5-44**, 1:1 *dr*) as a clear, light yellow oil: IR (ATR, neat) 3300, 2949, 2926, 2854, 1735, 1663, 1461, 1448, 1420, 1247, 1163, 1068, 1046, 966, 910, 833, 775, 731, 667, 692cm^{-1} ; ^1H NMR (CDCl_3 , 400 MHz) δ 7.39 – 7.27 (m, 4 H), 7.25 – 7.20 (m, 1 H), 6.51 (d, 1 H, $J = 15.9$ Hz), 6.17 (dd, 0.5 H, $J = 15.9, 2.8$ Hz), 6.16 (dd, 0.5 H, $J = 15.9, 2.6$ Hz), 5.28–5.16 (m, 1 H), 4.45–4.33 (m, 1 H), 3.57–3.46 (m, 1 H), 3.43–3.30 (m, 2 H), 2.59–2.45 (m, 1 H), 2.33–2.16 (m, 2 H), 1.93–1.75 (m, 4 H), 0.92 (s, 9 H), 0.09 (s, 3 H), 0.07 (s, 3 H); ^{13}C NMR (CDCl_3 , 125 MHz) δ 174.8, 174.7, 136.91, 136.90, 132.33, 132.30, 130.0, 129.8, 128.74, 128.72, 127.71, 121.69, 126.6, 126.5, 84.0, 83.8, 72.3, 72.2, 37.2, 36.4, 35.9, 29.0, 28.52, 28.46, 26.1, 18.4, –4.00, –4.03, –4.56, –4.58; HRMS (ESI) m/z calcd for $\text{C}_{21}\text{H}_{33}\text{NO}_3\text{SiNa}$ ($[\text{M}+\text{Na}]^+$) 398.2127, found 398.2156.



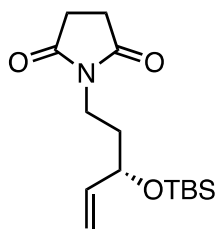
5-52

(E)-1-(3-(*tert*-Butyldimethylsilyloxy)-5-phenylpent-4-enyl)-5-oxopyrrolidin-2-yl 2,2-dimethylpropanoate (5-52). To a solution of **5-51** (0.050 g, 0.13 mmol) in THF (1.0 mL) at 0 °C under an atmosphere of N₂ was added NaH (0.0030 g, 0.14 mmol). The solution was stirred at 0 °C for 20 min and then at room temperature for 10 min. Upon warming to room temperature, vigorous gas evolution was observed. After 10 min the gas evolution ceased and the reaction mixture was cooled to 0 °C. Trimethylacetyl chloride (0.018 mL, 0.15 mmol) in THF (0.3 mL) was added dropwise and the solution was slowly warmed to room temperature and stirred for 7.5 h. The reaction mixture was quenched with sat. aq. NH₄Cl and extracted with EtOAc. The combined organic layers were washed with brine, dried (MgSO₄), and concentrated under reduced pressure to provide **5-52** (0.059 g, 96%, 1:1 *dr*) as a light yellow viscous oil: ¹H NMR (CDCl₃, 400 MHz) δ 7.38–7.18 (m, 4 H), 6.50 (dd, 1 H, *J* = 15.9, 4.0 Hz), 6.20 (t, 1 H, *J* = 5.1), 6.13 (dd, 1 H, *J* = 15.8, 6.4 Hz), 4.39–4.28 (m, 1 H), 3.66–3.53 (m, 1 H), 3.17–3.05 (m, 1 H), 2.59–2.44 (m, 1 H), 2.37–2.20 (m, 2 H), 1.98–1.86 (m, 2 H), 1.84–1.70 (m, 1 H), 2.96 (d, 9 H, *J* = 3.0 Hz), 0.90 (s, 9 H), 0.07 (s, 3 H), 0.04 (s, 3 H); ¹³C NMR (CDCl₃, 100 MHz) δ 178.2, 175.8, 175.7, 136.92, 136.91, 132.5, 132.2, 129.9, 129.6, 128.68, 128.65, 127.61, 127.60, 126.55, 126.5, 85.4, 85.0, 71.83, 71.77, 39.03, 39.01, 37.9, 37.7, 36.3, 35.9, 28.6, 28.5, 27.2, 27.1, 26.2, 26.1, 26.0, 18.3, –4.1, –4.7, –4.8.



5-53

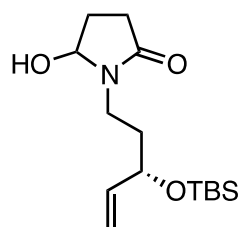
1-((E)-3-((*tert*-Butyldimethylsilyl)oxy)-5-phenylpent-4-en-1-yl)-5-((E)-hex-1-en-1-yl)pyrrolidin-2-one (5-53). To a solution of 1-hexyne (0.030 mL, 0.25 mmol) in CH₂Cl₂ (2.5 mL) at room temperature under an atmosphere of N₂ was added zirconocene hydrogen chloride (0.065 g, 0.25 mmol) and the resulting suspension was stirred at room temperature for 10 min. The resulting yellow solution was cooled to 0 °C and Me₃Al (1.0 M in CH₂Cl₂, 0.23 mL, 0.25 mmol) was added and the solution was stirred at 0 °C for 10 min. **5-52** (0.580 g, 0.126 mmol) was added and the mixture was warmed to room temperature and stirred for 6 h. The reaction mixture was quenched with sat. aq. NH₄Cl and extracted with CH₂Cl₂. The combined organic layers were dried (MgSO₄) and concentrated under reduced pressure to provide a yellow residue. The residue was purified by chromatography on SiO₂ (100% hexanes, 10:90 to 25:75 EtOAc:hexanes) to provide **5-53** (0.0060 g, 11%) as a clear, colorless oil: ¹H NMR (CDCl₃, 300 MHz) δ 7.34–7.18 (m, 5 H), 6.50 (dd, 1 H, *J* = 16.1, 4.9 Hz), 6.14 (dd, 1 H, *J* = 16.0, 6.4 Hz), 5.72–5.59 (m, 1 H), 5.28–5.17 (m, 1 H), 4.40–4.26 (m, 1 H), 4.03–3.93 (m, 1 H), 3.67–3.46 (m, 1 H), 3.10–2.93 (m, 1 H), 2.44–2.24 (m, 2 H), 2.19–1.96 (m, 2 H), 1.80–1.65 (m, 4 H), 1.38–1.25 (m, 4 H), 1.25–1.20 (m, 3 H), 0.91 (s, 9 H), 0.07 (s, 3 H), 0.04 (s, 3 H).



5-54a

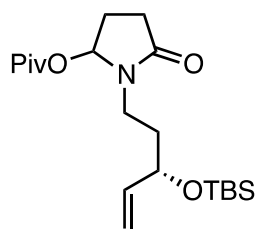
(S)-1-(3-((*tert*-Butyldimethylsilyl)oxy)pent-4-en-1-yl)pyrrolidine-2,5-dione (5-54a).

To a solution of **5-21**^{109g} (0.214 mL, 0.989 mmol), succinimide (**5-43**) (0.100 g, 0.989 mmol), and PPh₃ (0.262 g, 0.989 mmol) in THF (5.7 mL) cooled to 0 °C under an atmosphere of N₂ was added DBAD (0.232 g, 0.989 mmol) in THF (1.0 mL) dropwise. The reaction mixture was stirred at 0 °C for 30 min and was then warmed to room temperature and stirred for 11.5 h. The reaction was quenched with sat. aq. NH₄Cl and extracted with EtOAc. The combined organic layers were washed with brine, dried (MgSO₄), and concentrated under reduced pressure to provide a yellow residue. The residue was adsorbed onto SiO₂ and purified by chromatography on SiO₂ (5:95 to 20:80 EtOAc:hexanes) to provide **5-54a** (0.138 g, 45%) as a yellow oil: IR (ATR, neat) 2951, 2928, 2883, 2853, 1773, 1696, 1461, 1443, 1402, 1361, 1338, 1249, 1171, 1087, 1029, 923, 833, 774, 660 cm⁻¹; ¹H NMR (CDCl₃, 500 MHz) δ 5.81 (ddd, 1 H, *J* = 17.1, 10.4, 5.9 Hz), 5.20 (dt, 1 H, *J* = 17.2, 1.5 Hz), 5.07 (dt, 1 H, *J* = 10.4, 1.4 Hz), 4.20 (app q, 1 H, *J* = 5.9 Hz), 3.64–3.49 (m, 2 H), 2.67 (s, 4 H), 1.80–1.73 (m, 2 H), 0.91 (s, 9 H), 0.07 (s, 3 H), 0.03 (s, 3 H); ¹³C NMR (CDCl₃, 125 MHz) δ 177.2, 140.6, 114.7, 71.9, 35.5, 35.4, 28.3, 26.0, 18.4, -4.3, -4.8; HRMS (ESI) *m/z* calcd for C₁₅H₂₈NO₃Si ([M+H]⁺) 298.1838, found 298.1833.



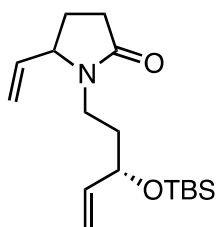
5-54

1-((S)-3-((tert-butyldimethylsilyl)oxy)pent-4-en-1-yl)-5-hydroxypyrrolidin-2-one (5-54). To a solution of **5-54a** (0.121 g, 0.406 mmol) in MeOH (2.0 mL) at 0 °C under an atmosphere of N₂ was added NaBH₄ (0.0157 g, 0.406 mmol). The reaction mixture was stirred at 0 °C for 24 h. An additional amount of NaBH₄ (6 equiv) was added until the reaction was complete. The reaction was monitored by the disappearance of starting material by TLC. The reaction was quenched with sat. aq. NH₄Cl and extracted with EtOAc. The combined organic layers were washed with brine, dried (MgSO₄), and concentrated under reduced pressure to provide **5-54** (0.103 g, 85%, 40% from **5-43**) as a pale, yellow oil. The oil was taken on to the next step without further purification: ¹H NMR (CDCl₃, 400 MHz) δ 5.82 (ddd, 1 H, *J* = 16.5, 10.4, 5.9 Hz), 5.28–5.13 (m, 2 H), 5.08 (d, 1 H, *J* = 10.4 Hz), 4.29–4.17 (m, 1 H), 3.50–3.40 (m, 1 H), 3.38–3.28 (m, 1 H), 3.03–2.90 (m, 1 H), 2.61–2.47 (m, 1 H), 2.35–2.25 (m, 2 H), 1.90–1.76 (m, 3 H), 0.90 (s, 9 H), 0.07 (s, 3 H), 0.05 (s, 3 H).



5-55

1-((S)-3-((*tert*-Butyldimethylsilyl)oxy)pent-4-en-1-yl)-5-oxopyrrolidin-2-yl pivalate (5-55). To a solution of **5-54** (0.030 g, 0.10 mmol) in THF (0.8 mL) at 0 °C under an atmosphere of N₂ was added NaH (0.021 g, 0.88 mmol). The solution was stirred at 0 °C for 10 min and then at room temperature for 30 min. The reaction was cooled to 0 °C and trimethylacetyl chloride (14 μL, 0.11 mmol) in THF (0.2 mL) was added dropwise. The solution was slowly warmed to room temperature and stirred for 6 h. The reaction mixture was quenched with sat. aq. NH₄Cl and extracted with EtOAc. The combined organic layers were washed with brine, dried (MgSO₄), and concentrated under reduced pressure to provide **5-55** (0.0349 g, 91%) as a yellow oil: ¹H NMR (CDCl₃, 300 MHz) δ 6.18 (dd, 1 H, *J* = 5.3, 1.9 Hz), 5.77 (dddd, 1 H, *J* = 17.1, 10.4, 5.9, 0.8 Hz), 5.16 (dt, 1 H, *J* = 17.1, 3.8, 1.5 Hz), 5.04 (dt, 1 H, *J* = 10.4, 5.6, 1.3 Hz), 4.20–4.10 (m, 1 H), 3.59–3.43 (m, 1 H), 3.17–3.03 (m, 1 H), 2.60–2.45 (m, 1 H), 2.39–2.22 (m, 2 H), 1.93 (td, 1 H, *J* = 10.2, 1.3 Hz), 1.86–1.76 (m, 1 H), 1.74–1.60 (m, 1 H), 1.18 (s, 9 H), 0.04 (s, 3 H), 0.02 (s, 3 H).

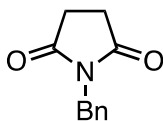


5-13

1-((S)-3-((*tert*-Butyldimethylsilyl)oxy)pent-4-en-1-yl)-5-vinylpyrrolidin-2-one (5-13).^{109g} To a flask containing AlCl₃ (0.0466 g, 0.350 mmol) in CH₂Cl₂ (0.2 mL) cooled to 0 °C under an atmosphere of Ar was added vinylmagnesiumbromide (1.0 M in THF, 1.0 mL, 1.0 mmol) dropwise. Upon addition of the vinylmagnesiumbromide, the white slurry turned clear yellow and then cloudy yellow. The cloudy orange-yellow mixture was stirred at 0 °C for 4 h.

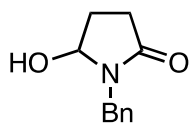
5-55 (0.0349 g, 0.117 mmol) in CH₂Cl₂ (0.11 mL) was added in one portion and the reaction was stirred at 0 °C for 1 h. The reaction mixture was carefully quenched with 1.0 M HCl at 0 °C. The solution was extracted with CH₂Cl₂ and 1.0 M HCl was added to the extraction until the organic layer became clear. The combined organic extracts were washed with brine, dried (MgSO₄), and concentrated under reduced pressure to provide a yellow oil. The oil was adsorbed onto SiO₂ and purified by chromatography on SiO₂ (100% hexanes, 10:90 to 30:70 EtOAc:hexanes) to provide **5-13** (0.0155 g, 55%, 1:1 *dr*) as a pale yellow oil: IR (ATR, neat) 2951, 2928, 2855, 1737, 1685, 1417, 1249, 1174, 1158, 1081, 1027, 923, 833, 775, 731 cm⁻¹; ¹H NMR (CDCl₃, 400 MHz) δ 5.78 (ddd, 1 H, *J* = 16.8, 10.4, 5.8 Hz), 5.65 (dddd, 1 H, *J* = 17.1, 10.0, 8.6, 3.3 Hz), 5.27–5.12 (m, 3 H), 5.04 (tt, 1 H, *J* = 10.3, 1.3 Hz), 4.19–4.10 (m, 1 H), 4.06–3.98 (m, 1 H), 3.59–3.47 (m, 1 H), 3.05–2.90 (m, 1 H), 2.45–2.26 (m, 2 H), 2.26–2.16 (m, 1 H), 1.79–1.63 (m, 3 H), 0.88 (d, 9 H, *J* = 2.2 Hz), 0.04 (d, 3 H, *J* = 1.2 Hz), 0.02 (d, 3 H, *J* = 2.5 Hz); ¹³C NMR (CDCl₃, 100 MHz) δ 174.94, 179.90, 141.2, 140.7, 138.1, 137.9, 118.1, 118.0, 114.6, 114.2, 72.1, 72.0, 61.8, 61.5, 37.7, 37.4, 35.4, 35.3, 30.3, 26.0, 25.7, 25.6, 18.33, 18.29, -4.2, -4.3, -4.7, -4.8; HRMS (ESI) *m/z* calcd for C₁₇H₃₂NO₂Si ([M+H]⁺) 310.2202, found 310.2191; retention time of diastereomers determined by chiral SFC analysis on a CHIRALPAK® IA column; 3% MeOH/CO₂; 2.5 mL/min; 220 nm; 6.46 min and 7.92 min.

6.6.2 Third Generation Approach



5-60

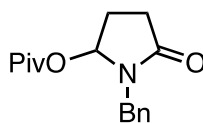
1-Benzylpyrrolidine-2,5-dione (5-60).^{129a} To a flask containing succinimide (**5-43**) (1.06 g, 10.5 mmol) and K₂CO₃ (1.45 g, 10.5 mmol) under an atmosphere of Ar was added BnBr (1.51 mL, 12.9 mmol). The reaction mixture was heated at 80 °C for 5 h. The reaction mixture was diluted with EtOAc and filtered to remove solids. The filtrate was concentrated under reduced pressure to provide a white crystalline solid. The material was adsorbed onto SiO₂ and purified by chromatography on SiO₂ (100% hexanes, 20:80 to 40:60 EtOAc:hexanes) to afford **5-60** (1.42 g, 72%) as a white crystalline solid: Mp 102.5–103.7 °C (EtOAc); IR (ATR, neat) 3072, 3034, 2971, 1765, 1689, 1586, 1495, 1456, 1426, 1398, 1342, 1308, 1297, 1163, 1148 cm⁻¹; ¹H NMR (CDCl₃, 500 MHz) δ 7.41–7.37 (m, 2 H), 7.31–7.27 (m, 3 H), 4.66 (s, 2 H), 2.71 (s, 4 H); ¹³C NMR (CDCl₃, 125 MHz) δ 177.0, 135.9, 129.1, 128.8, 128.1, 42.6, 28.3; HRMS (ESI) *m/z* calcd for C₁₁H₁₂NO₂ ([M+H]⁺) 190.0868, found 190.0840.



5-61

1-Benzyl-5-hydroxypyrrolidin-2-one (5-61).^{129b} To a solution of **5-60** (2.00 g, 10.6 mmol) in MeOH (35 mL) and CH₂Cl₂ (13 mL) at 0 °C under an atmosphere of Ar was added NaBH₄ (0.480 g, 12.7 mmol). The reaction mixture was stirred at 0 °C for 13 h. An additional amount of NaBH₄ (0.480 g, 12.7 mmol) was added at 0 °C and stirring was continued for 12 h. After the first 24 h, an additional amount of NaBH₄ (0.480 g, 12.7 mmol) was added every 12 h until the starting material was consumed as indicated by a ¹H NMR of an aliquot of the reaction mixture. The reaction mixture was concentrated under reduced pressure to provide a white solid. The solid was diluted with CH₂Cl₂ and quenched with sat. aq. NH₄Cl and extracted

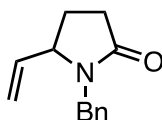
with CH₂Cl₂. The combined organic layers were dried (MgSO₄) and concentrated under reduced pressure to provide a white solid. The solid was adsorbed onto SiO₂ and purified by chromatography on SiO₂ (100% CH₂Cl₂, 2:98 to 6:94 CH₂Cl₂:MeOH) to afford **5-61** (1.58 g, 78%) as a white solid: Mp 109.9–111.6 °C (CH₂Cl₂); IR (ATR, neat) 3156, 2928, 1635, 1480, 1441, 1426, 1331, 1282, 1260, 1176, 1157, 1074, 997, 947, 753, 697 cm⁻¹; ¹H NMR (CDCl₃, 400 MHz) δ 7.38–7.23 (m, 5 H), 5.12–5.05 (m, 1 H), 4.83 (d, 1 H, *J* = 14.8 Hz), 4.22 (d, 1 H, *J* = 14.8 Hz), 2.70–2.58 (m, 2 H), 2.43–2.23 (m, 2 H), 1.95–1.84 (m, 1 H); ¹³C NMR (CDCl₃, 125 MHz) δ 174.9, 136.6, 128.9, 128.5, 127.8, 82.7, 43.6, 29.0, 28.3; HRMS (ESI) *m/z* calcd for C₁₁H₁₄NO₂ ([M+H]⁺) 192.1025, found 192.1043.



5-62

1-Benzyl-5-oxopyrrolidin-2-yl 2,2-dimethylpropanoate (5-62). To a solution of **5-61** (0.30 g, 1.6 mmol) in CH₂Cl₂ (15 mL) at room temperature under an atmosphere of N₂ was added Et₃N (0.67 mL, 4.7 mmol), DMAP (0.039 g, 0.31 mmol), and pivaloyl chloride (0.39 mL, 3.14 mmol). The mixture was stirred at room temperature for 4 h. The reaction was quenched with sat. aq. NH₄Cl and extracted with CH₂Cl₂. The combined organic layers were washed with sat. aq. NaHCO₃ and H₂O, dried (MgSO₄), and concentrated under reduced pressure to provide a yellow residue. The residue was adsorbed onto SiO₂ and purified by chromatography on SiO₂ (100% hexanes, 10:90 to 15:85 EtOAc:hexanes) to afford **5-62** (0.318 g, 74%, 98% BRSM): Mp 58.6–60.3 °C (EtOAc); IR (ATR, neat) 2973, 2958, 2934, 2872, 1689, 1497, 1480, 1443, 1417, 1366, 1277, 1251, 1131, 1027, 951, 887, 744, 701 cm⁻¹; ¹H NMR (CDCl₃, 400 MHz) δ 7.35–

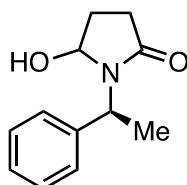
7.23 (m, 5 H), 5.07 (d, 1 H, $J = 5.5$ Hz), 4.80 (d, 1 H, $J = 14.8$ Hz), 4.10 (d, 1 H, $J = 14.8$ Hz), 2.64 (ddd, 1 H, $J = 17.8, 9.2, 9.2$ Hz), 2.42 (ddd, 1 H, $J = 17.2, 9.8, 2.3$ Hz), 2.36–2.24 (m, 1 H), 1.95 (ddd, 1 H, $J = 14.1, 9.2, 1.3$ Hz), 1.12 (s, 9 H); ^{13}C NMR (CDCl_3 , 125 MHz) δ 178.1, 175.8, 136.4, 128.8, 128.4, 127.9, 84.5, 44.7, 39.0, 28.5, 27.0, 26.2; HRMS (ESI) m/z calcd for $\text{C}_{16}\text{H}_{21}\text{NO}_3$ ($[\text{M}+\text{Na}]^+$) 298.1419, found 298.1424.



5-63

1-Benzyl-5-vinylpyrrolidin-2-one (5-63). To a flask containing AlCl_3 (0.291 g, 2.18 mmol) in CH_2Cl_2 (1.3 mL) cooled to 0 °C under an atmosphere of Ar was added vinylmagnesiumbromide (1.0 M in THF, 6.5 mL, 6.5 mmol) dropwise. Upon addition of the vinylmagnesiumbromide, the white slurry became a clear yellow solution and then a cloudy orange-yellow solution. The cloudy orange-yellow mixture was stirred at 0 °C for 4 h. **5-62** (0.200 g, 0.726 mmol) in CH_2Cl_2 (0.65 mL) was added in one portion and the reaction was allowed to stir at 0 °C for 1 h. Upon addition of **5-62**, the mixture became a clear yellow solution. The reaction mixture was carefully quenched with 1 M HCl at 0 °C. The solution was extracted with CH_2Cl_2 and 1.0 M HCl was added to the extraction until the organic layer became clear. The combined organic layers were washed with brine, dried (MgSO_4), and concentrated under reduced pressure to provide an orange oil. The oil was taken up in Et_2O and washed with sat. aq. NaHCO_3 to remove the remaining pivalic acid. The combined aqueous layers were then extracted with Et_2O . The combined organic layers were dried (MgSO_4) and concentrated under reduced pressure to provide **5-63** (0.519 mmol, 71%) as an orange oil: ^1H NMR (CDCl_3 ,

400 MHz) δ 7.36–7.17 (m, 5 H), 5.64 (app dt, 1 H, $J = 18.1, 9.7$ Hz), 5.22 (d, 1 H, $J = 10.0$ Hz), 5.14 (d, 1 H, $J = 17.0$ Hz), 4.99 (d, 1 H, $J = 14.7$ Hz), 3.92–3.80 (m, 2 H), 2.54–2.34 (m, 2 H), 2.23–2.11 (m, 1 H), 1.81–1.74 (m, 1 H).

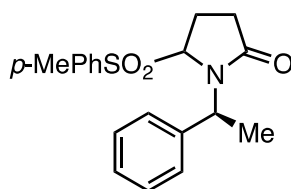


5-68

5-Hydroxy-1-((S)-1-phenylethyl)pyrrolidin-2-one (5-68).^{130a} To a solution of succinic anhydride (1.00 g, 8.17 mmol) in THF (8.2 mL) at room temperature was added (*S*)-(-)-1-phenylethylamine (**5-65**) (1.05 mL, 8.17 mmol) dropwise. The mixture was heated at reflux for 2 h. The solution was cooled to room temperature and the solvent removed under reduced pressure. Acetic anhydride (**5-64**) (8.2 mL) was added and the mixture was heated at reflux for 2 h. The reaction mixture turned from a clear yellow solution to a clear orange solution after 15 min. The mixture was cooled to room temperature and poured onto ice. The mixture was extracted with CH_2Cl_2 . The combined organic extracts were washed with sat. aq. NaHCO_3 and brine, dried (MgSO_4), and concentrated under reduced pressure to provide (*S*)-1-(1-phenylethyl)pyrrolidine-2,5-dione (**5-67**) as an orange residue. The product was taken on to the next step without purification.

To a solution of **5-67** (0.399 g, 1.96 mmol) in THF (65 mL) at -78 °C under an atmosphere of N_2 was added LiEt_3BH (2.9 mL, 2.9 mmol, 1.0 M in THF) dropwise. The solution was stirred at -78 °C for 2.5 h. The reaction was quenched with sat. aq. NaHCO_3 , warmed to 0 °C, and H_2O_2 (10 drops) was added. The solution was kept at 0 °C for 20 min. The reaction

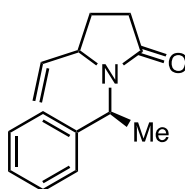
mixture was concentrated under reduced pressure and the aqueous residue was extracted with CH₂Cl₂. The combined organic layers were washed with brine, dried (MgSO₄), and concentrated under reduced pressure to provide a white solid. The material was purified by chromatography on SiO₂ (100% CH₂Cl₂, 1:99 to 5:95 MeOH:CH₂Cl₂) to provide **5-68** (0.240 g, 60%, >10:1 *dr*) as a white crystalline solid. The minor diastereomer could not be detected by ¹H NMR but was observed in the ¹³C NMR. Mp 101.2–102.5 °C (EtOAc); IR (ATR, neat) 3193, 3033, 2984, 2939, 1638, 1603, 1493, 1450, 1443, 1417, 1383, 1359, 1323, 1281, 1247, 1208, 1176, 1158, 1074, 1059, 984, 913, 788, 699, 669 cm⁻¹; ¹H NMR (CDCl₃, 500 MHz) major diastereomer: δ 7.38–7.34 (m, 4 H), 7.33–7.27 (m, 1 H), 5.39 (q, 1 H, *J* = 7.2 Hz), 4.93 (app td, 1 H, *J* = 7.2, 1.6 Hz), 2.66 (app dt, 1 H, *J* = 17.6, 9.0 Hz), 2.34 (dddd, 1 H, *J* = 17.3, 9.9, 3.0, 1.0 Hz), 2.19–2.08 (m, 1 H), 1.83 (dddd, 1 H, *J* = 13.9, 9.3, 3.1, 1.7 Hz), 1.63 (d, 3 H, *J* = 7.2 Hz); ¹³C NMR (CDCl₃, 125 MHz) major diastereomer: δ 174.7, 140.0, 128.8, 127.9, 127.7, 82.4, 50.4, 29.1, 29.0, 18.9; minor diastereomer: δ 175.0, 129.1, 128.1, 127.5, 81.7, 49.8, 29.2, 28.6, 17.2; HRMS (ESI) *m/z* calcd for C₁₂H₁₆NO₂ ([M+H]⁺) 206.1181, found 206.1193.



5-69

5-Oxo-1-((S)-1-phenylethyl)pyrrolidin-2-yl-4-methylbenzenesulfinate (5-69).^{130b} To a solution of **5-68** (0.0500 g, 0.243 mmol) in CH₂Cl₂ (2.4 mL) was added toluenesulfinic acid¹⁴⁴ (0.0761 g, 0.487 mmol). The solution was stirred at room temperature for 4.5 h. The solution was quenched with 5% aq. Na₂CO₃ and extracted with CH₂Cl₂. The combined organic layers were

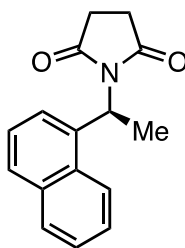
washed with brine, dried (MgSO₄), and concentrated under reduced pressure to provide **5-69** (0.0797 g, 95% crude, 1:1 *dr*) as a white solid. The material was taken on without further purification. Characteristic signals for the diastereomeric mixture (reported as observed): ¹H NMR (CDCl₃, 400 MHz) δ 7.68 (d, 2 H, *J* = 8.3 Hz), 7.58 (d, 2 H, *J* = 8.3 Hz), 7.38–7.20 (m, 14 H), 5.32 (q, 1 H, *J* = 7.1 Hz), 4.87 (q, 1 H, *J* = 7.2 Hz), 4.55 (dd, 1 H, *J* = 8.5, 1.0 Hz), 4.12 (d, 1 H, *J* = 8.1 Hz), 2.38 (s, 3 H), 2.35 (s, 3 H), 2.35–1.90 (d, 3 H, *J* = 7.2 Hz), 1.90 (d, 3 H, *J* = 7.2 Hz), 1.80 (d, 3 H, *J* = 7.2 Hz).



5-70

1-((S)-1-Phenylethyl)-5-vinylpyrrolidin-2-one (5-70). Vinyl alane generation: To a flask containing AlCl₃ (0.260 g, 1.95 mmol) in CH₂Cl₂ (0.7 mL) cooled to 0 °C under an atmosphere of Ar was added vinylmagnesium bromide (1.0 M in THF, 5.8 mL, 3.4 mmol) dropwise. The solution was stirred at 0 °C for 4 h. To a separate flame-dried flask under an atmosphere of N₂ was added the vinyl alane solution (0.3 M in CH₂Cl₂, 3.1 mL, 0.928 mmol). The flask was cooled to 0 °C and **5-69** (0.0797 g, 0.232 mmol) was added in one portion. The reaction mixture was kept at 0 °C for 2 h. The reaction mixture was quenched with sat. aq. NH₄Cl, warmed to room temperature, and extracted with CH₂Cl₂. 1 M aq. HCl was added to separate the emulsion. The combined organic layers were washed with brine, dried (MgSO₄), and concentrated under reduced pressure to provide a viscous, yellow oil. The oil was purified by chromatography on SiO₂ (100% CH₂Cl₂, 1:99 MeOH:CH₂Cl₂) to provide **5-70** (0.0316 g, 63%,

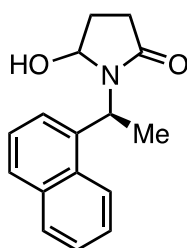
0.7:1 *dr*) as a yellow oil: IR (ATR, neat) 3079, 3062, 3057, 3047, 2975, 2926, 2919, 2870, 2854, 2848, 1678, 1493, 1450, 1402, 1254, 992, 919, 699 cm^{-1} ; ^1H NMR (CDCl_3 , 300 MHz) major diastereomer: δ 7.36–7.20 (m, 5 H), 5.80 (ddd, 1 H, $J = 17.0, 10.0, 8.0$ Hz), 5.45 (q, 1 H, $J = 7.3$ Hz), 5.09–4.95 (m, 1 H), 4.95 (d, 1 H, $J = 17.1$ Hz), 3.71 (td, 1 H, $J = 8.4, 4.2$ Hz), 2.56–2.25 (m, 4 H), 1.55 (d, 3 H, $J = 7.3$ Hz); minor diastereomer: δ 7.36–7.20 (m, 3.5 H), 5.29 (ddd, 0.7 H, $J = 17.0, 9.8, 8.7$ Hz), 5.18 (q, 0.7 H, $J = 7.2$ Hz), 5.09–4.95 (m, 0.7 H), 4.86 (dd, 0.7 H, $J = 10.0, 1.0$ Hz), 4.13 (td, 0.7 H, $J = 8.0, 6.3$ Hz), 2.22–2.18 (m, 2.8 H), 1.66 (d, 2.1 H, $J = 7.3$ Hz); ^{13}C NMR (CDCl_3 , 100 MHz) major diastereomer: δ 175.1, 140.2, 140.0, 128.5, 127.8, 127.5, 116.3, 60.0, 50.7, 30.2, 26.6, 18.1; minor diastereomer: δ 175.3, 142.0, 139.1, 128.2, 127.6, 127.2, 116.4, 61.2, 50.6, 30.7, 26.5, 16.7. HRMS (ESI) m/z calcd for $\text{C}_{14}\text{H}_{18}\text{NO}$ ($[\text{M}+\text{H}]^+$) 216.1388, found 216.1367.



5-72

(S)-1-(1-(Naphthalen-1-yl)ethyl)pyrrolidine-2,5-dione (5-72).¹⁴⁵ To a solution of succinic anhydride (**5-51**) (0.145 g, 1.45 mmol) in THF (1.5 mL) at room temperature was added (*S*)-(-)-1-(1-naphthyl)ethylamine (**5-71**) (0.234 mL, 1.45 mmol) dropwise. The mixture was heated at reflux for 2 h. The solution was cooled to room temperature and concentrated under reduced pressure. Acetic anhydride (**5-64**) (1.45 mL) was added and the mixture was heated at reflux for 2 h. The mixture was cooled to room temperature and poured onto ice. The mixture

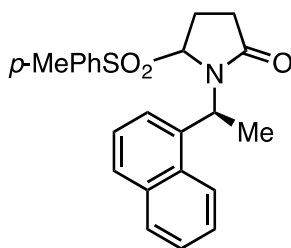
was extracted with CH₂Cl₂. The combined organic extracts were washed with sat. aq. NaHCO₃ and brine, dried (MgSO₄), and concentrated under reduced pressure to provide a brown solid. The brown solid was purified by chromatography on SiO₂ (100% hexanes, 10:90 to 80:20 EtOAc:hexanes) to provide **5-72** (0.280 g, 76%) as a brown crystalline solid: ¹H NMR (CDCl₃, 300 MHz) δ 8.08 (d, 1 H, *J* = 8.3 Hz), 7.94 (d, 1 H, *J* = 7.8 Hz), 7.90–7.79 (m, 2 H), 7.57–7.44 (m, 3 H), 6.17 (q, 1 H, *J* = 7.1 Hz), 2.60 (s, 4 H), 1.92 (d, 3 H, *J* = 7.2 Hz).



5-73

5-Hydroxy-1-((S)-1-(naphthalen-1-yl)ethyl)pyrrolidin-2-one (5-73). To a solution of **5-72** (0.228 g, 0.899 mmol) in THF (30 mL) at –78 °C under an atmosphere of N₂ was added LiEt₃BH (1.3 mL, 1.3 mmol, 1.0 M in THF) dropwise. The solution was stirred at –78 °C for 40 min. The reaction was quenched with sat. aq. NaHCO₃, warmed to 0 °C, and H₂O₂ (10 drops) was added. The solution was kept at 0 °C for 20 min. The reaction mixture was concentrated under reduced pressure and the aqueous residue was extracted with CH₂Cl₂. The combined organic layers were washed with brine, dried (MgSO₄), and concentrated under reduced pressure to provide a white solid. The material was purified by chromatography on SiO₂ (100% CH₂Cl₂, 1:99 to 5:95 MeOH:CH₂Cl₂) to provide **5-73** in two batches. The first batch was isolated as a 1:1 mixture of diastereomers (0.041 g, 18%), and the second batch, was isolated as a single diastereomer (0.167 g, 73%). In total, 0.208 g (0.816 mmol, 91%, 10:1 *dr*) of the desired product was obtained. Major diastereomer: Mp 196.8–198.6 °C (EtOAc); IR (ATR, neat) 3228, 2978,

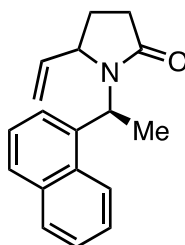
2967, 2947, 2934, 1646, 1596, 1508, 1443, 1415, 1398, 1322, 1249, 1238, 1185, 1165, 1107, 1072, 1053, 913, 803, 779, 721, 684 cm⁻¹; ¹H NMR (CDCl₃, 500 MHz) δ 7.90–7.81 (m, 3 H), 7.71 (d, 1 H, *J* = 7.1 Hz), 7.54–7.48 (m, 3 H), 6.06 (q, 1 H, *J* = 7.0 Hz), 4.45 (td, 1 H, *J* = 6.6, 2.2 Hz), 2.67 (ddd, 1 H, *J* = 17.3, 9.4, 7.9 Hz), 2.34 (ddd, 1 H, *J* = 17.3, 10.0, 4.0 Hz), 1.95 (dddd, 1 H, *J* = 14.0, 9.9, 7.8, 6.3 Hz), 1.80 (d, 3 H, *J* = 7.0 Hz), 1.71 (dddd, 1 H, *J* = 13.6, 9.5, 4.0, 2.2 Hz); ¹³C NMR (CDCl₃, 125 MHz) δ 174.2, 134.5, 134.0, 131.8, 129.1, 129.0, 127.2, 126.2, 125.2, 124.8, 123.2, 82.5, 46.6, 29.1, 28.6, 19.2; HRMS (ESI) *m/z* calcd for C₁₆H₁₈NO₂ ([M+H]⁺) 256.1338, found 256.1356. Characteristic signals for the minor diastereomer: ¹H NMR (CDCl₃, 500 MHz) δ 8.19 (d, 1 H, *J* = 8.5 Hz), 7.89–7.83 (m, 2 H), 7.69 (d, 1 H, *J* = 7.2 Hz), 7.60–7.56 (m, 1 H), 7.53–7.47 (m, 2 H), 6.18 (q, 1 H, *J* = 6.9 Hz), 5.37 (d, 1 H, *J* = 5.9 Hz), 2.70–2.60 (m, 1 H), 2.35–2.28 (m, 1 H), 2.14–2.05 (m, 1 H), 1.97–1.88 (m, 1 H), 1.82–1.76 (m, 1 H), 1.71 (d, 3 H, *J* = 7.0 Hz).



5-74

1-((S)-1-(Naphthalen-1-yl)ethyl)-5-oxopyrrolidin-2-yl 4-methylbenzenesulfinate (5-74). To a solution of **5-73** (0.0500 g, 0.196 mmol) in CH₂Cl₂ (2.0 mL) was added toluenesulfonic acid¹⁴⁴ (0.0612 g, 0.392 mmol). The solution was stirred at room temperature for 4.5 h. The solution was quenched with 5% aq. Na₂CO₃ and extracted with CH₂Cl₂. The combined organic layers were washed with brine, dried (MgSO₄), and concentrated under reduced pressure to

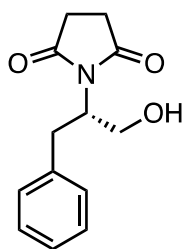
provide **5-74** (0.0698 g, 91%, 10:1 *dr*) as a white solid. The material was taken on without further purification. Major diastereomer: $^1\text{H NMR}$ (CDCl_3 , 400 MHz) δ 7.93–7.87 (m, 3 H), 7.62 (d, 2 H, $J = 8.3$ Hz), 7.60–7.54 (m, 2 H), 7.50–7.41 (m, 2 H), 7.32 (d, 2 H, $J = 8.0$ Hz), 6.07 (q, 1 H, $J = 7.0$ Hz), 3.71 (d, 1 H, $J = 8.5$ Hz), 2.42 (s, 3 H), 2.17–2.11 (m, 1 H), 2.09 (d, 3 H, $J = 7.0$ Hz), 2.06–1.88 (m, 2 H), 1.80–1.68 (m, 1 H). Characteristic signals for the minor diastereomer: $^1\text{H NMR}$ (CDCl_3 , 400 MHz) δ 5.85 (q, 0.1 H, $J = 7.3$ Hz), 4.53 (d, 0.1 H, $J = 8.4$ Hz), 2.50 (s, 0.3 H).



5-75

1-((S)-1-(Naphthalen-1-yl)ethyl)-5-vinylpyrrolidin-2-one (5-75). Vinyl alane generation: To an oven-dried 2-5 mL microwave vial containing AlCl_3 (0.0428 g, 0.321 mmol) in CH_2Cl_2 (0.20 mL) at 0 °C under an atmosphere of N_2 was added vinylmagnesium bromide (1.0 mL, 1.0 M in THF, 1.0 mmol). The solution was stirred at 0 °C for 4 h and then cooled to –30 °C. To the vial containing the vinyl alane solution at –30 °C was added **5-74** (0.0316 g, 0.0803 mmol). The reaction mixture was stirred at –30 °C for 2.5 h. The reaction mixture was warmed to –20 °C and stirred overnight. The reaction mixture was quenched with 1 M aq. HCl and extracted with CH_2Cl_2 . The combined organic layers were washed with brine, dried (MgSO_4), and concentrated under reduced pressure to provide a viscous, yellow oil. The oil was purified by chromatography on SiO_2 (100% CH_2Cl_2 , 1:99 MeOH: CH_2Cl_2) to provide **5-75** (0.012 g, 57%, *dr* 0.3:1) as a yellow oil: IR (ATR, neat) 3074, 3049, 2973, 2887, 1670, 1597,

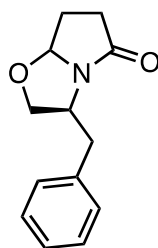
1508, 1396, 1238, 1193, 990, 921, 803, 772, 729. Major diastereomer: ^1H NMR (CDCl_3 , 300 MHz) δ 7.93–7.79 (m, 3 H), 7.58–7.42 (m, 4 H), 6.09 (q, 1 H, $J = 6.9$ Hz), 5.79 (dt, 1 H, $J = 17.1, 9.4$ Hz), 4.99 (d, 1 H, $J = 9.9$ Hz), 4.71 (d, 1 H, $J = 17.1$ Hz), 3.20 (td, 1 H, $J = 8.6, 3.7$ Hz), 2.60–2.24 (m, 2 H), 1.93–1.77 (m, 1 H), 1.71 (d, 3 H, $J = 7.2$ Hz), 1.63–1.50 (m, 1 H); ^{13}C NMR (CDCl_3 , 100 MHz) δ 174.6, 139.9, 134.5, 133.8, 132.0, 128.9, 128.8, 127.0, 126.0, 125.6, 124.8, 123.4, 116.4, 60.1, 47.2, 30.1, 26.2, 18.6. HRMS (ESI) m/z calcd for $\text{C}_{18}\text{H}_{20}\text{NO}$ ($[\text{M}+\text{H}]^+$) 266.1545, found 166.1537. Characteristic signals for the minor diastereomer: ^1H NMR (CDCl_3 , 300 MHz) δ 4.55 (d, 0.3 H, $J = 17.0$ Hz), 4.28 (d, 0.3 H, $J = 9.9$ Hz), 4.06 (td, 0.3 H, $J = 8.1, 4.7$ Hz); ^{13}C NMR (CDCl_3 , 100 MHz) δ 174.9, 138.2, 136.2, 133.6, 132.4, 128.7, 128.6, 126.6, 125.7, 125.3, 124.8, 123.9, 114.5, 59.8, 46.6, 30.3, 27.2, 17.0.



5-77

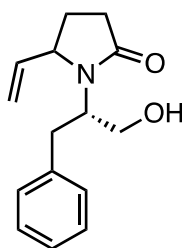
(S)-1-(1-Hydroxy-3-phenylpropan-2-yl)pyrrolidine-2,5-dione (5-77).¹⁴⁶ To a flask containing 3,4-dihydrofuran-2,5-dione (**5-64**) (1.30 g, 13.0 mmol) and L-phenylalaninol (**5-76**) (2.00 g, 13.0 mmol) in freshly distilled toluene (125 mL) at room temperature under an atmosphere of N_2 was added Et_3N (3.6 mL, 26 mmol). The solution was heated at reflux for 20 h. The reaction mixture was concentrated under reduced pressure to give a yellow solid. The solid was purified by chromatography on SiO_2 (5:95 to 10:90 $\text{MeOH}:\text{CH}_2\text{Cl}_2$) to provide **5-77** (1.94 g, 64%) as a pale yellow solid: Mp 113.0–116.2 $^\circ\text{C}$ (CH_2Cl_2); IR (ATR, neat) 3409, 3061, 3029,

2971, 2880, 1761, 1733, 1679, 1416, 1402, 1372, 1301, 1187, 1165, 1048, 1020, 951, 822, 762, 703 cm^{-1} ; ^1H NMR (CDCl_3 , 400 MHz) δ 7.30–7.15 (m, 5 H), 4.51 (td, 1 H, $J = 7.2, 3.2$ Hz), 4.00 (dd, 1 H, $J = 12.0, 7.2$ Hz), 3.83 (dd, 1 H, $J = 12.0, 3.2$ Hz), 3.15–3.07 (m, 2 H), 2.62–2.51 (m, 4 H); ^{13}C NMR (CDCl_3 , 100 MHz) δ 178.2, 137.3, 129.1, 128.6, 126.9, 62.3, 55.8, 33.8, 28.0; HRMS (ESI) m/z calcd for $\text{C}_{13}\text{H}_{16}\text{NO}_3$ ($[\text{M}+\text{H}]^+$) 234.1130, found 234.1113.



5-78

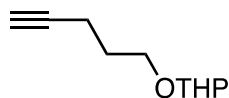
(3S)-3-Benzyltetrahydropyrrolo[2,1-*b*]oxazol-5(6H)-one (5-78).¹⁴⁶ To a flask containing **5-77** (0.200 g, 0.857 mmol) in EtOH (8.5 mL) at 0 °C under an atmosphere of N_2 was added NaBH_4 (0.331 g, 8.57 mmol). The reaction mixture was stirred at 0 °C for 2 h. The reaction mixture was diluted with EtOAc and quenched with sat. aq. NH_4Cl at 0 °C. The mixture was warmed to room temperature and extracted with EtOAc. The combined organic layers were washed with brine, dried (MgSO_4), and concentrated under reduced pressure to give a colorless residue. Compound **5-78** was the major product by LC/HRMS and attempts to purify this compound by chromatography on SiO_2 (100% CH_2Cl_2 , 5:95 to 10:90 MeOH: CH_2Cl_2) were unsuccessful. The mixture was taken on to the next step without further purification. LC-HRMS (ESI) m/z calcd for peak at 2.14 min $\text{C}_{13}\text{H}_{16}\text{NO}_2$ ($[\text{M}+\text{H}]^+$) 218.1176, found 218.1169.



5-79

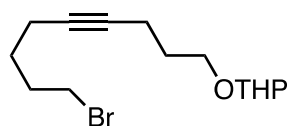
1-((S)-1-Hydroxy-3-phenylpropan-2-yl)-5-vinylpyrrolidin-2-one (5-79). Vinyl alane generation: To a flask containing AlCl_3 (0.265 g, 1.99 mmol) in CH_2Cl_2 (0.20 mL) at $0\text{ }^\circ\text{C}$ under an atmosphere of N_2 was added vinylmagnesium bromide (6.2 mL, 1.0 M in THF, 1.0 mmol). The solution was stirred at $0\text{ }^\circ\text{C}$ for 4 h. To the vial containing the vinyl alane solution at $0\text{ }^\circ\text{C}$ was added **5-78** (0.108 g, 0.497 mmol) in CH_2Cl_2 (0.5 mL). The reaction mixture was stirred at $0\text{ }^\circ\text{C}$ for 3.5 h. The reaction was quenched with sat. aq. NH_4Cl and 1 M aq. HCl was added. The aqueous layer was extracted with CH_2Cl_2 . The combined organic layers were washed with brine, dried (MgSO_4), and concentrated under reduced pressure to provide a yellow residue. The material was purified by chromatography on SiO_2 (100% CH_2Cl_2 , 1:99 $\text{MeOH}:\text{CH}_2\text{Cl}_2$) to give **5-79** (0.0378 g, 31% crude, 2:1 *dr*) as a crude yellow oil. Characteristic signals for the major diastereomer: ^1H NMR (CDCl_3 , 400 MHz) δ 7.34–7.15 (m, 5 H), 5.02 (dd, 1 H, $J = 6.1$, 2.4 Hz), 4.42–4.32 (m, 1 H), 4.06 (t, 1 H, $J = 8.6$ Hz), 3.68–3.60 (m, 1 H), 3.03 (dd, 1 H, $J = 13.9$, 5.8 Hz), 2.77 (dd, 1 H, $J = 13.8$, 8.3 Hz), 2.62 (dd, 1 H, $J = 10.4$, 7.2 Hz), 2.51 (dd, 1 H, $J = 10.5$, 4.5 Hz), 2.43–3.28 (m, 1 H), 2.17 (dd, 1 H, $J = 17.2$, 9.1 Hz), 2.07–1.91 (m, 1 H), 1.86 (dd, 1 H, $J = 13.5$, 8.8 Hz). Characteristic signals for the minor diastereomer: ^1H NMR (CDCl_3 , 400 MHz) δ 7.34–7.15 (m, 2.5 H), 5.10 (d, 0.5 H, $J = 6.0$ Hz), 4.56–4.47 (m, 0.5 H), 3.68–3.60 (m, 0.5 H), 3.38 (t, 0.5 H, $J = 8.5$ Hz), 2.88 (dd, 0.5 H, $J = 13.2$, 9.0 Hz), 2.70 (dd, 0.5 H, $J = 13.3$, 6.1 Hz), 2.67 (dd, 0.5 H, $J = 3.1$ Hz), 2.46 (dd, 0.5 H, $J = 10.7$, 4.7 Hz), 2.43–2.28 (m, 0.5 H), 2.07–1.91 (m, 1.5 H).

6.6.3 Fourth Generation Approach



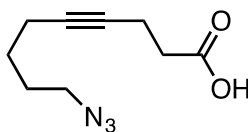
5-85

2-(Pent-4-yn-1-yloxy)tetrahydro-2H-pyran (5-85). To a solution of 4-pentyn-1-ol (**5-84**) (15.0 mL, 158 mmol), 3,4-dihydro-2H-pyran (17.5 mL, 190 mmol) in CH₂Cl₂ (200 mL) was added *p*-toluenesulfonic acid monohydrate (0.0601 g, 0.316 mmol). The mixture was stirred at room temperature for 1 h. During the course of the reaction, the solution turned a deep blue color. The reaction mixture was quenched with sat. aq. NaHCO₃ (at which time the teal color dissipated to give a yellow-orange colored solution) and extracted with CH₂Cl₂. The combined organic layers were washed with brine, dried (MgSO₄), and concentrated under reduced pressure to give an orange oil. The material was purified by chromatography on SiO₂ (100% hexanes, 5:95 to 15:85 Et₂O:hexanes) to provide **5-85** (27.4 g, quant.) as a light yellow oil: IR (ATR, neat) 3290, 2937, 2869, 1465, 1439, 1351, 1322, 1199, 1180, 1156, 1135, 1118, 1074, 1061, 1033, 1020, 992, 969, 867, 815 cm⁻¹; ¹H NMR (CDCl₃, 400 MHz) δ 4.62–4.57 (m, 1 H), 3.90–3.79 (m, 2 H), 3.54–3.44 (m, 2 H), 2.34–2.28 (m, 2 H), 1.94 (t, 1 H, *J* = 2.6 Hz), 1.87–1.77 (m, 3 H), 1.75–1.67 (m, 1 H), 1.60–1.47 (m, 4 H); ¹³C NMR (CDCl₃, 100 MHz) δ 99.0, 84.1, 68.6, 65.9, 62.4, 30.8, 28.8, 25.6, 19.7, 15.5; HRMS (ESI) *m/z* calcd for C₁₀H₁₇O₂ ([M+H]⁺) 169.1229, found 169.1232.



5-86

2-((9-Bromonon-4-yn-1-yl)oxy)tetrahydro-2H-pyran (5-86). To a solution of **5-85** (26.6 g, 158 mmol) in THF (390 mL) and HMPA (2.8 mL, 15.8 mmol) cooled to -78 °C under an atmosphere of Ar was added n-BuLi (1.6 M in THF, 118 mL, 190 mmol) dropwise. The reaction mixture was warmed to -40 °C, stirred for 30 min, and 1,4-dibromobutane (95.3 mL, 790 mmol) was added dropwise. The solution was warmed to room temperature over 1 h and then heated to reflux. The mixture was stirred at reflux for 29 h. The reaction mixture was diluted with Et₂O and brine was added. The aqueous layer was extracted with Et₂O. The combined organic layers were washed with brine, dried (MgSO₄), and concentrated under reduced pressure to provide a crude yellow oil. The oil was purified in two separate batches by chromatography on SiO₂ (100% hexanes, 2:98 to 10:90 EtOAc:hexanes) to afford the **5-86** (41.9 g, 88%) as a pale yellow oil: ¹H NMR (CDCl₃, 400 MHz) δ 4.62–4.57 (m, 1 H), 3.91–3.77 (m, 2 H), 3.54–3.45 (m, 2 H), 3.43 (t, 2 H, *J* = 6.8 Hz), 2.29–2.23 (m, 2 H), 2.22–2.16 (m, 2 H), 2.01–1.92 (m, 2 H), 1.85–1.70 (m, 4 H), 1.65–1.47 (m, 6 H).

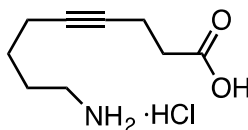


5-87

9-Azidonon-4-ynoic acid (5-87). To a solution of **5-86** (18.15 g, 59.9 mmol) in DMF (300 mL) at room temperature under an atmosphere of N₂ was added NaN₃ (4.67 g, 71.8 mmol). The solution was heated to 80 °C and stirred for 25 h. The reaction mixture was cooled to room temperature, poured into H₂O, and extracted with Et₂O. The combined organic layers were washed with H₂O (5x) and brine, dried (MgSO₄), and concentrated under reduced pressure to provide crude 2-((9-azidonon-4-yn-1-yl)oxy)tetrahydro-2H-pyran as a yellow oil. The crude

material was taken on without further purification due to the potentially explosive nature of the azide.

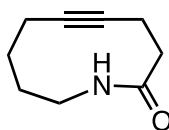
To a solution of crude 2-((9-azidonon-4-yn-1-yl)oxy)tetrahydro-2*H*-pyran (15.9 g, 59.9 mmol) in acetone (120 mL) at 0 °C was added freshly prepared Jones reagent (2.5 M, 71.8 mL, 180 mmol). The reaction mixture was stirred at 0 °C for 7 h. After 3 h, the reaction was not complete by TLC and an additional amount of Jones reagent (2.5 M, 10 mL) was added. After complete consumption of starting material, the reaction mixture was quenched with *i*-PrOH and concentrated under reduced pressure to give a crude residue. The residue was extracted with Et₂O. The combined organic layers were washed with brine, dried (MgSO₄), and concentrated under reduced pressure to give a yellow oil. The material was adsorbed onto SiO₂ and purified by chromatography on SiO₂ (100% hexanes, 5:95 to 1:1 EtOAc:hexanes) to provide **5-87** (8.51 g, 73%) as a pale yellow solid: IR 3072, 2923, 2093, 1702, 1627, 1603, 1502, 1416 cm⁻¹; ¹H NMR (CDCl₃, 400 MHz) δ 11.46 (bs, 1 H), 3.30 (t, 2 H, *J* = 6.6 Hz), 2.60–2.54 (m, 2 H), 2.51–2.45 (m, 2 H), 2.25–2.16 (m, 2 H), 1.71 (quint, 2 H, *J* = 7.0 Hz), 1.56 (quint, 2 H, *J* = 7.2 Hz); ¹³C NMR (CDCl₃, 400 MHz) δ 178.7, 80.5, 78.6, 51.1, 33.9, 27.9, 26.0, 18.3, 14.5.



5-83

9-Aminonon-4-ynoic acid hydrochloride (5-83). To a flask containing **5-87** (0.100 g, 0.495 mmol) in THF (2.5 mL) and H₂O (3 drops) was added PPh₂(CH₂)₂PPh₂ (0.122 g, 0.307 mmol). The reaction was stirred at room temperature for 21 h. The reaction was monitored by IR, and the disappearance of the azide stretch at 2091 cm⁻¹ was used to indicate completion of

the reaction. The reaction mixture was concentrated under reduced pressure to give a yellow solid. The solid was suspended in 10% aq. HCl and stirred for 5 min. The suspension was filtered and the filtrate was concentrated under reduced pressure to provide **5-83** as the HCl salt (0.084 g, 80%): IR 3072, 2902, 2613, 1696, 1623, 1609, 1502 cm^{-1} ; ^1H NMR (D_2O , 400 MHz) δ 3.03 (t, 2 H, $J = 7.5$ Hz), 2.61–2.56 (m, 2 H), 2.50–2.45 (m, 2 H), 2.24 (tt, 2 H, $J = 6.8, 2.3$ Hz), 1.81–1.72 (m, 2 H), 1.61–1.52 (m, 2 H); ^{13}C NMR (CDCl_3 , 100 MHz) δ 177.7, 81.8, 80.4, 39.7, 34.0, 26.5, 25.5, 18.0, 14.6; HRMS (ESI) m/z calcd for $\text{C}_9\text{H}_{16}\text{NO}_2$ ($[\text{M}+\text{H}]^+$) 170.1181, found 170.1187.

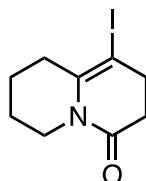


5-82

3,4,7,8,9,10-Hexahydro-azecin-2-one (5-82). To a flask containing **5-83** (1.23 g, 5.98 mmol) in CH_2Cl_2 (1250 mL) was added Et_3N (1.68 mL, 12.0 mmol) and 1-hydroxybenzotriazole (10.2 g, 1.37 mmol). The solution was stirred for 15 min and 1-(3-dimethylaminopropyl)-3-ethylcarbodiimide hydrochloride (1.49 g, 7.77 mmol) was added. The solution was stirred at room temperature for 65.5 h. The starting material did not completely dissolve and remained a fine suspension throughout the reaction. The reaction mixture was quenched with H_2O and extracted with CH_2Cl_2 . The combined organic layers were dried (MgSO_4) and concentrated under reduced pressure to provide a yellow residue. The residue was adsorbed onto SiO_2 and purified by chromatography on SiO_2 (100% CH_2Cl_2 , 1:99 to 5:95 $\text{MeOH}:\text{CH}_2\text{Cl}_2$) to provide **5-82** (0.401 g, 2.65 mmol, 44%) as a light yellow residue that crystallized upon standing: IR (ATR, neat) 3312, 3081, 2933, 2858, 1645, 1541, 1435, 1310, 1277 cm^{-1} ; ^1H NMR (CDCl_3 ,

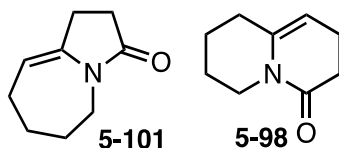
500 MHz) δ 5.96 (bs, 1 H), 3.30–3.20 (m, 2 H), 2.50–2.42 (m, 2 H), 2.30–2.24 (m, 2 H), 2.16–2.06 (m, 2 H), 1.74 (m, 4 H); ^{13}C NMR (CDCl_3 , 125 MHz) δ 173.6, 87.3, 80.5, 40.8, 37.3, 26.4, 26.2, 20.2, 17.2; HRMS (ESI) m/z calcd for $\text{C}_9\text{H}_{14}\text{NO}$ ($[\text{M}+\text{H}]^+$) 152.1070, found 152.1067.

This structure was confirmed by X-ray analysis (Appendix A.3).



5-95

1-Iodo-2,3,6,7,8,9-hexahydro-4H-quinolizin-4-one (5-95). To a solution of **5-82** (0.0300 g, 0.198 mmol) in THF (6 mL) was added I_2 (0.0757 g, 0.298 mmol), Na_2CO_3 (0.0637 g, 0.595 mmol), and AgNO_3 (0.0340 g, 0.198 mmol). The reaction mixture was stirred at room temperature for 20 h. The solvent was removed under reduced pressure and the residue was dissolved in EtOAc, washed with sat. aq. $\text{Na}_2\text{S}_2\text{O}_3$, brine, and dried (MgSO_4). The solution was concentrated under reduced pressure to give a dark yellow residue. The material was purified by chromatography on SiO_2 (100% hexanes, 10:90 to 25:75 EtOAc:hexanes) to provide **5-95** as a sticky yellow residue (0.0297 g, 54%): ^1H NMR (CDCl_3 , 400 MHz) δ 3.67–3.58 (m, 2 H), 2.76–2.69 (m, 2 H), 2.58–2.48 (m, 4 H), 1.72–1.60 (m, 4 H); ^{13}C NMR (CDCl_3 , 125 MHz) δ 169.8, 138.5, 72.7, 41.4, 34.5, 33.4, 33.0, 23.1, 21.5.; HRMS (ESI) m/z calcd for $\text{C}_9\text{H}_{14}\text{NOI}$ ($[\text{M}+\text{H}]^+$) 278.0036, found 278.0033.



1.5:1.0 mixture (5-101:5-98)

2,3,6,7,8,9-Hexahydro-4H-quinolizin-4-one (5-101) and 1,2,5,6,7,8-Hexahydro-3H-pyrrolo[1,2-a]azepin-3-one (5-98). To a solution of **5-82** (0.0200 g, 0.132 mmol) in THF (4.0 mL) at room temperature under an atmosphere of N₂ was added KHMDS (0.0132 g, 0.0661 mmol) and 18-crown-6 (0.0141 g, 0.0529 mmol). The solution was stirred at room temperature for 1 h 15 min. The solution was poured slowly into an ice/water mixture and extracted with EtOAc. The combined organic layers were washed with brine, dried (MgSO₄), and concentrated under reduced pressure to give a crude residue. The residue is an inseparable mixture of the desired product **5-101** and the undesired product **5-98** (0.0181, 91%):

Characteristic peaks for **5-101**: ¹H NMR (CDCl₃, 400 MHz) δ 4.95 (t, 0.7 H, *J* = 4.4 Hz), 3.68–3.58 (m, 1.4 H), 2.48–2.41 (m, 1.4 H), 2.29 (t, 1.4 H, *J* = 5.7 Hz), 2.22–2.14 (m, 1.4 H), 1.72–1.65 (m, 1.4 H), 1.63–1.56 (m, 1.4 H); ¹³C NMR (CDCl₃, 125 MHz) δ 170.7, 138.0, 103.8, 40.6, 32.0, 29.6, 23.8, 22.0, 19.4.

Characteristic peaks for **5-98**: ¹H NMR (CDCl₃, 400 MHz) δ 4.68 (t, 1 H, *J* = 5.0 Hz), 3.68–3.58 (m, 2 H), 2.60–2.53 (m, 2 H), 2.48–2.41 (m, 2 H), 2.22–2.14 (m, 2 H), 1.77–1.72 (m, 4 H); ¹³C NMR (CDCl₃, 125 MHz) δ 176.6, 139.8, 102.3, 44.1, 30.0, 28.2, 27.34, 27.29, 25.9.

APPENDIX A

X-RAY DATA

A.1 X-RAY STRUCTURE AND DATA FOR 1-24B

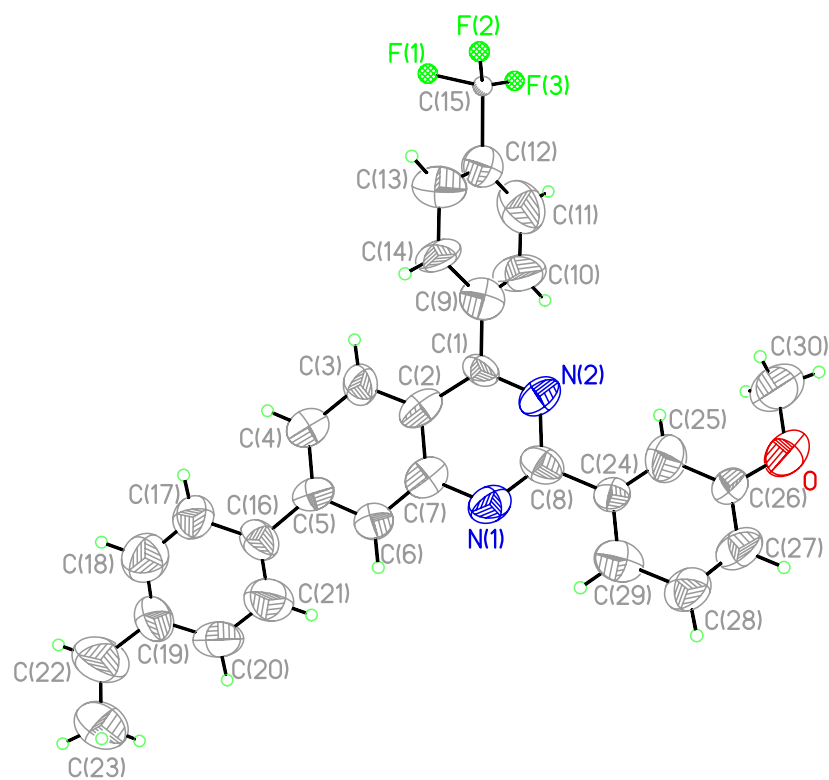


Figure 19. X-Ray crystal structure of 1-24b.

Table 15. Crystal data and structure refinement for **1-24b**.

| | | |
|---|---|-----------------|
| Identification code | kg927s | |
| Empirical formula | C ₃₀ H ₂₃ F ₃ N ₂ O | |
| Formula weight | 484.50 | |
| Temperature | 203(2) K | |
| Wavelength | 0.71073 Å | |
| Crystal system | Monoclinic | |
| Space group | C2/c | |
| Unit cell dimensions | a = 52.85(3) Å | α = 90° |
| | b = 4.431(3) Å | β = 99.786(12)° |
| | c = 20.755(12) Å | γ = 90° |
| Volume | 856.96(6) Å ³ | |
| Z | 4 | |
| Density (calculated) | 1.172 g/cm ³ | |
| Absorption coefficient | 0.604 mm ⁻¹ | |
| F(000) | 328 | |
| Crystal size | 0.03 x 0.05 x 0.21 mm ³ | |
| Theta range for data collection | 2.26 to 25.09°. | |
| Index ranges | -63<=h<=62, -5<=k<=5, -24<=l<=24 | |
| Reflections collected | 17398 | |
| Independent reflections | 4253 [R(int) = 0.2705] | |
| Completeness to theta = 25.09° | 99.4 % | |
| Absorption correction | multi-scan (Sadabs) | |
| Refinement method | Full-matrix least-squares on F ² | |
| Data / restraints / parameters | 4253 / 6 / 301 | |
| Goodness-of-fit on F² | 1.667 | |
| Final R indices [I>2σ(I)] | R1 = 0.1804, wR2 = 0.3834 | |
| R indices (all data) | R1 = 0.3980, wR2 = 0.4424 | |
| Largest diff. peak and hole | 1.611 and -0.674 e.Å ⁻³ | |

Table 16. Atomic coordinates (x 10⁴) and equivalent isotropic displacement parameters (Å² x 10³) for **1-24b**.

| | x | y | z | U(eq) |
|------|----------|-----------|----------|--------------|
| O | 906(2) | 2750(30) | 2458(5) | 113(4) |
| N(1) | 1474(2) | 7440(20) | 363(6) | 70(3) |
| C(1) | 1000(2) | 9430(30) | -202(7) | 54(4) |
| F(1) | -45(3) | 14670(30) | -1766(8) | 249(7) |
| N(2) | 1019(2) | 7680(30) | 311(5) | 69(3) |
| C(2) | 1217(3) | 10530(30) | -469(7) | 62(4) |
| F(2) | -151(3) | 10920(40) | -1712(8) | 251(7) |
| C(3) | 1210(3) | 12480(30) | -980(7) | 71(4) |
| F(3) | -147(3) | 13810(30) | -971(7) | 233(6) |
| C(4) | 1438(3) | 13450(30) | -1169(7) | 63(4) |
| C(5) | 1674(3) | 12470(30) | -860(6) | 57(4) |
| C(6) | 1689(3) | 10260(30) | -360(7) | 77(5) |

| | | | | |
|-------|---------|-----------|-----------|---------|
| C(7) | 1460(3) | 9390(30) | -173(7) | 62(4) |
| C(8) | 1265(3) | 6800(30) | 592(8) | 67(4) |
| C(9) | 736(3) | 10170(30) | -487(8) | 76(4) |
| C(10) | 580(3) | 11430(40) | -132(8) | 106(6) |
| C(11) | 328(3) | 12190(40) | -391(9) | 112(6) |
| C(12) | 243(3) | 11770(30) | -1019(8) | 75(4) |
| C(13) | 393(3) | 10510(30) | -1433(8) | 93(5) |
| C(14) | 643(3) | 9890(30) | -1152(6) | 76(5) |
| C(15) | -60(6) | 12660(50) | -1353(11) | 330(20) |
| C(16) | 1917(3) | 13580(30) | -1036(8) | 71(4) |
| C(17) | 1916(3) | 14500(40) | -1691(8) | 85(5) |
| C(18) | 2134(4) | 15680(40) | -1836(9) | 103(6) |
| C(19) | 2361(3) | 16010(40) | -1409(10) | 93(5) |
| C(20) | 2357(3) | 15040(40) | -772(10) | 109(6) |
| C(21) | 2136(3) | 13870(40) | -600(9) | 100(6) |
| C(22) | 2596(3) | 17530(40) | -1579(10) | 152(9) |
| C(23) | 2832(3) | 16460(50) | -1318(9) | 156(9) |
| C(24) | 1280(3) | 4780(30) | 1188(6) | 50(3) |
| C(25) | 1082(3) | 4660(30) | 1519(8) | 89(5) |
| C(26) | 1099(3) | 2970(30) | 2082(8) | 68(4) |
| C(27) | 1311(3) | 1490(30) | 2298(7) | 81(5) |
| C(28) | 1518(3) | 1460(40) | 1990(8) | 85(5) |
| C(29) | 1506(3) | 3250(30) | 1404(8) | 77(5) |
| C(30) | 673(3) | 4560(40) | 2260(8) | 139(7) |

U(eq) is defined as one third of the trace of the orthogonalized U^{ij} tensor.

Table 17. Bond lengths (Å) and angles (°) for **1-24b**.

| | |
|------------|-----------|
| O-C(26) | 1.390(15) |
| O-C(30) | 1.468(16) |
| N(1)-C(7) | 1.400(15) |
| N(1)-C(8) | 1.307(15) |
| C(1)-N(2) | 1.309(15) |
| C(1)-C(9) | 1.456(16) |
| C(1)-C(2) | 1.440(16) |
| F(1)-C(15) | 1.25(2) |
| F(1)-F(2) | 1.76(2) |
| F(1)-F(3) | 1.86(2) |
| N(2)-C(8) | 1.385(15) |
| C(2)-C(7) | 1.422(16) |
| C(2)-C(3) | 1.365(16) |
| F(2)-C(15) | 1.12(2) |
| C(3)-C(4) | 1.398(15) |
| C(3)-H(3A) | 0.9400 |
| F(3)-C(15) | 1.11(2) |
| C(4)-C(5) | 1.372(14) |
| C(4)-H(4A) | 0.9400 |
| C(5)-C(6) | 1.418(16) |
| C(5)-C(16) | 1.476(17) |
| C(6)-C(7) | 1.388(16) |
| C(6)-H(6A) | 0.9400 |

| | |
|-----------------|-----------|
| C(8)-C(24) | 1.517(17) |
| C(9)-C(10) | 1.320(18) |
| C(9)-C(14) | 1.389(16) |
| C(10)-C(11) | 1.391(19) |
| C(10)-H(10A) | 0.9400 |
| C(11)-C(12) | 1.319(18) |
| C(11)-H(11A) | 0.9400 |
| C(12)-C(13) | 1.380(17) |
| C(12)-C(15) | 1.68(3) |
| C(13)-C(14) | 1.378(15) |
| C(13)-H(13A) | 0.9400 |
| C(14)-H(14A) | 0.9400 |
| C(16)-C(21) | 1.349(17) |
| C(16)-C(17) | 1.419(17) |
| C(17)-C(18) | 1.347(18) |
| C(17)-H(17A) | 0.9400 |
| C(18)-C(19) | 1.37(2) |
| C(18)-H(18A) | 0.9400 |
| C(19)-C(20) | 1.39(2) |
| C(19)-C(22) | 1.509(19) |
| C(20)-C(21) | 1.377(19) |
| C(20)-H(20A) | 0.9400 |
| C(21)-H(21A) | 0.9400 |
| C(22)-C(23) | 1.355(18) |
| C(22)-H(22A) | 0.9800 |
| C(22)-H(22B) | 0.9800 |
| C(23)-H(23A) | 0.9700 |
| C(23)-H(23B) | 0.9700 |
| C(23)-H(23C) | 0.9700 |
| C(24)-C(29) | 1.379(15) |
| C(24)-C(25) | 1.352(16) |
| C(25)-C(26) | 1.378(17) |
| C(25)-H(25A) | 0.9400 |
| C(26)-C(27) | 1.308(16) |
| C(27)-C(28) | 1.358(17) |
| C(27)-H(27A) | 0.9400 |
| C(28)-C(29) | 1.444(18) |
| C(28)-H(28A) | 0.9400 |
| C(29)-H(29A) | 0.9400 |
| C(30)-H(30A) | 0.9700 |
| C(30)-H(30B) | 0.9700 |
| C(30)-H(30C) | 0.9700 |
| C(26)-O-C(30) | 117.7(12) |
| C(7)-N(1)-C(8) | 119.4(13) |
| N(2)-C(1)-C(9) | 113.6(13) |
| N(2)-C(1)-C(2) | 123.9(12) |
| C(9)-C(1)-C(2) | 122.5(14) |
| C(15)-F(1)-F(2) | 39.3(10) |
| C(15)-F(1)-F(3) | 35.3(11) |
| F(2)-F(1)-F(3) | 67.0(7) |
| C(8)-N(2)-C(1) | 116.6(13) |

| | |
|--------------------|-----------|
| C(1)-C(2)-C(7) | 115.8(13) |
| C(1)-C(2)-C(3) | 126.5(14) |
| C(7)-C(2)-C(3) | 117.7(15) |
| C(15)-F(2)-F(1) | 44.7(12) |
| C(4)-C(3)-C(2) | 120.0(14) |
| C(4)-C(3)-H(3A) | 119.9 |
| C(2)-C(3)-H(3A) | 120.1 |
| C(15)-F(3)-F(1) | 40.5(13) |
| C(5)-C(4)-C(3) | 122.2(13) |
| C(5)-C(4)-H(4A) | 118.9 |
| C(3)-C(4)-H(4A) | 118.9 |
| C(4)-C(5)-C(6) | 119.6(13) |
| C(4)-C(5)-C(16) | 122.6(14) |
| C(6)-C(5)-C(16) | 117.8(13) |
| C(7)-C(6)-C(5) | 117.0(13) |
| C(7)-C(6)-H(6A) | 121.7 |
| C(5)-C(6)-H(6A) | 121.3 |
| C(6)-C(7)-N(1) | 117.7(14) |
| C(6)-C(7)-C(2) | 123.2(14) |
| N(1)-C(7)-C(2) | 118.9(14) |
| N(2)-C(8)-N(1) | 125.2(15) |
| N(2)-C(8)-C(24) | 115.2(13) |
| N(1)-C(8)-C(24) | 119.5(14) |
| C(1)-C(9)-C(10) | 120.9(15) |
| C(1)-C(9)-C(14) | 122.4(14) |
| C(10)-C(9)-C(14) | 116.4(14) |
| C(9)-C(10)-C(11) | 122.3(16) |
| C(9)-C(10)-H(10A) | 118.4 |
| C(11)-C(10)-H(10A) | 119.3 |
| C(12)-C(11)-C(10) | 119.4(17) |
| C(12)-C(11)-H(11A) | 120.7 |
| C(10)-C(11)-H(11A) | 119.9 |
| C(11)-C(12)-C(13) | 122.5(16) |
| C(11)-C(12)-C(15) | 121.0(17) |
| C(13)-C(12)-C(15) | 116.5(15) |
| C(12)-C(13)-C(14) | 115.4(14) |
| C(12)-C(13)-H(13A) | 122.3 |
| C(14)-C(13)-H(13A) | 122.3 |
| C(9)-C(14)-C(13) | 123.6(14) |
| C(9)-C(14)-H(14A) | 118.1 |
| C(13)-C(14)-H(14A) | 118.3 |
| F(2)-C(15)-F(3) | 127(3) |
| F(2)-C(15)-F(1) | 96.0(18) |
| F(3)-C(15)-F(1) | 104(2) |
| F(2)-C(15)-C(12) | 113(2) |
| F(3)-C(15)-C(12) | 107(2) |
| F(1)-C(15)-C(12) | 107(2) |
| C(21)-C(16)-C(17) | 118.4(15) |
| C(21)-C(16)-C(5) | 123.4(16) |
| C(17)-C(16)-C(5) | 118.1(15) |
| C(18)-C(17)-C(16) | 117.6(16) |

| | |
|---------------------|-----------|
| C(18)-C(17)-H(17A) | 121.1 |
| C(16)-C(17)-H(17A) | 121.2 |
| C(17)-C(18)-C(19) | 125.6(18) |
| C(17)-C(18)-H(18A) | 117.1 |
| C(19)-C(18)-H(18A) | 117.3 |
| C(20)-C(19)-C(18) | 115.4(16) |
| C(20)-C(19)-C(22) | 120.4(19) |
| C(18)-C(19)-C(22) | 124.1(19) |
| C(19)-C(20)-C(21) | 120.7(16) |
| C(19)-C(20)-H(20A) | 119.7 |
| C(21)-C(20)-H(20A) | 119.6 |
| C(16)-C(21)-C(20) | 122.1(17) |
| C(16)-C(21)-H(21A) | 118.8 |
| C(20)-C(21)-H(21A) | 119.0 |
| C(19)-C(22)-C(23) | 119.3(17) |
| C(19)-C(22)-H(22A) | 108.3 |
| C(23)-C(22)-H(22A) | 106.9 |
| C(19)-C(22)-H(22B) | 107.3 |
| C(23)-C(22)-H(22B) | 107.5 |
| H(22A)-C(22)-H(22B) | 107.0 |
| C(22)-C(23)-H(23A) | 110.0 |
| C(22)-C(23)-H(23B) | 108.8 |
| H(23A)-C(23)-H(23B) | 109.5 |
| C(22)-C(23)-H(23C) | 109.6 |
| H(23A)-C(23)-H(23C) | 109.5 |
| H(23B)-C(23)-H(23C) | 109.5 |
| C(29)-C(24)-C(25) | 121.4(14) |
| C(29)-C(24)-C(8) | 118.7(14) |
| C(25)-C(24)-C(8) | 119.8(14) |
| C(24)-C(25)-C(26) | 120.4(15) |
| C(24)-C(25)-H(25A) | 119.7 |
| C(26)-C(25)-H(25A) | 119.8 |
| C(27)-C(26)-C(25) | 119.4(16) |
| C(27)-C(26)-O | 116.1(15) |
| C(25)-C(26)-O | 124.4(15) |
| C(26)-C(27)-C(28) | 123.8(16) |
| C(26)-C(27)-H(27A) | 118.1 |
| C(28)-C(27)-H(27A) | 118.1 |
| C(27)-C(28)-C(29) | 117.9(15) |
| C(27)-C(28)-H(28A) | 121.0 |
| C(29)-C(28)-H(28A) | 121.2 |
| C(24)-C(29)-C(28) | 117.0(14) |
| C(24)-C(29)-H(29A) | 121.5 |
| C(28)-C(29)-H(29A) | 121.5 |
| O-C(30)-H(30A) | 109.4 |
| O-C(30)-H(30B) | 109.5 |
| H(30A)-C(30)-H(30B) | 109.5 |
| O-C(30)-H(30C) | 109.5 |
| H(30A)-C(30)-H(30C) | 109.5 |
| H(30B)-C(30)-H(30C) | 109.5 |

Symmetry transformations used to generate equivalent atoms.

Table 18. Anisotropic displacement parameters ($\text{\AA}^2 \times 10^3$) for **1-24b**.

| | U^{11} | U^{22} | U^{33} | U^{23} | U^{13} | U^{12} |
|-------|----------|----------|----------|----------|----------|----------|
| O | 107(9) | 142(11) | 89(9) | 45(8) | 12(8) | 24(8) |
| N(1) | 70(8) | 58(7) | 76(9) | 12(7) | -5(7) | -1(7) |
| C(1) | 37(8) | 77(10) | 49(9) | -13(8) | 13(7) | 1(8) |
| N(2) | 80(9) | 80(9) | 41(7) | -5(7) | -6(6) | 2(7) |
| C(2) | 84(11) | 42(9) | 51(10) | -4(8) | -12(9) | 3(8) |
| C(3) | 72(11) | 84(11) | 63(11) | 13(9) | 31(9) | 23(9) |
| C(4) | 75(10) | 45(9) | 64(10) | -6(7) | -3(9) | -1(8) |
| C(5) | 60(9) | 62(9) | 45(9) | -17(8) | -1(7) | 20(8) |
| C(6) | 60(10) | 90(12) | 82(12) | 27(10) | 13(9) | 15(9) |
| C(7) | 81(11) | 38(9) | 63(10) | -7(8) | 0(9) | 0(8) |
| C(8) | 55(10) | 72(11) | 74(12) | -15(9) | 8(10) | -9(9) |
| C(9) | 76(11) | 66(10) | 85(13) | -9(9) | 11(10) | -2(8) |
| C(10) | 73(11) | 173(18) | 67(12) | -18(12) | -4(10) | 28(11) |
| C(11) | 114(15) | 127(15) | 103(15) | -25(12) | 39(12) | -18(13) |
| C(13) | 75(11) | 97(12) | 103(13) | -20(11) | 1(10) | 4(10) |
| C(14) | 66(10) | 113(12) | 40(9) | -8(9) | -18(7) | 5(9) |
| C(16) | 60(10) | 88(11) | 66(12) | -17(9) | 16(9) | -14(9) |
| C(17) | 89(13) | 105(13) | 62(12) | -1(10) | 15(10) | 17(11) |
| C(18) | 109(15) | 98(13) | 101(14) | 11(11) | 15(14) | -2(13) |
| C(19) | 78(14) | 103(13) | 104(15) | 24(12) | 32(12) | -9(11) |
| C(20) | 64(11) | 133(16) | 124(17) | 34(13) | -4(11) | 10(11) |
| C(21) | 80(13) | 98(13) | 124(16) | 10(12) | 17(14) | 10(11) |
| C(22) | 83(14) | 160(18) | 210(20) | 75(17) | 30(16) | -1(13) |
| C(23) | 80(13) | 220(20) | 170(20) | 52(17) | 20(14) | -20(15) |
| C(24) | 50(9) | 53(9) | 43(9) | -6(7) | -4(7) | -12(8) |
| C(25) | 97(13) | 70(11) | 102(14) | 24(10) | 20(11) | -1(9) |
| C(26) | 61(10) | 83(11) | 56(10) | 18(9) | -1(9) | -4(9) |
| C(27) | 91(12) | 96(13) | 51(11) | 2(9) | -2(11) | 19(11) |
| C(28) | 87(13) | 113(14) | 52(11) | -1(10) | 3(9) | 12(10) |
| C(29) | 66(11) | 53(10) | 112(14) | -8(9) | 10(10) | -4(8) |
| C(30) | 115(15) | 200(20) | 99(14) | 38(14) | 16(12) | 49(16) |

The anisotropic atomic displacement factor exponent takes the form: $-2\pi^2 [h^2 a^{*2} U_{11} + \dots + 2 h k a^* b^* U_{12}]$.

Table 19. Hydrogen coordinates ($\times 10^4$) and isotropic displacement parameters ($\text{\AA}^2 \times 10^3$) for **1-24b**.

| | x | y | z | U(eq) |
|--------|----------|----------|----------|--------------|
| H(3A) | 1051 | 13182 | -1206 | 85 |
| H(4A) | 1430 | 14812 | -1518 | 75 |
| H(6A) | 1848 | 9432 | -164 | 93 |
| H(10A) | 642 | 11824 | 312 | 127 |
| H(11A) | 219 | 13008 | -121 | 135 |
| H(13A) | 329 | 10105 | -1875 | 112 |
| H(14A) | 757 | 9253 | -1426 | 91 |
| H(17A) | 1769 | 14287 | -2012 | 102 |
| H(18A) | 2131 | 16342 | -2268 | 123 |
| H(20A) | 2506 | 15187 | -455 | 131 |
| H(21A) | 2138 | 13260 | -166 | 121 |
| H(22A) | 2590 | 19656 | -1455 | 182 |
| H(22B) | 2583 | 17464 | -2056 | 182 |

| | | | | |
|--------|------|-------|-------|-----|
| H(23A) | 2962 | 17581 | -1495 | 235 |
| H(23B) | 2843 | 14341 | -1425 | 235 |
| H(23C) | 2859 | 16703 | -847 | 235 |
| H(25A) | 931 | 5748 | 1365 | 107 |
| H(27A) | 1320 | 391 | 2688 | 97 |
| H(28A) | 1664 | 314 | 2154 | 102 |
| H(29A) | 1646 | 3367 | 1180 | 93 |
| H(30A) | 557 | 4257 | 2569 | 208 |
| H(30B) | 589 | 3940 | 1827 | 208 |
| H(30C) | 719 | 6678 | 2251 | 208 |

A.2 X-RAY STRUCTURE AND DATA FOR KMG-NB4-23

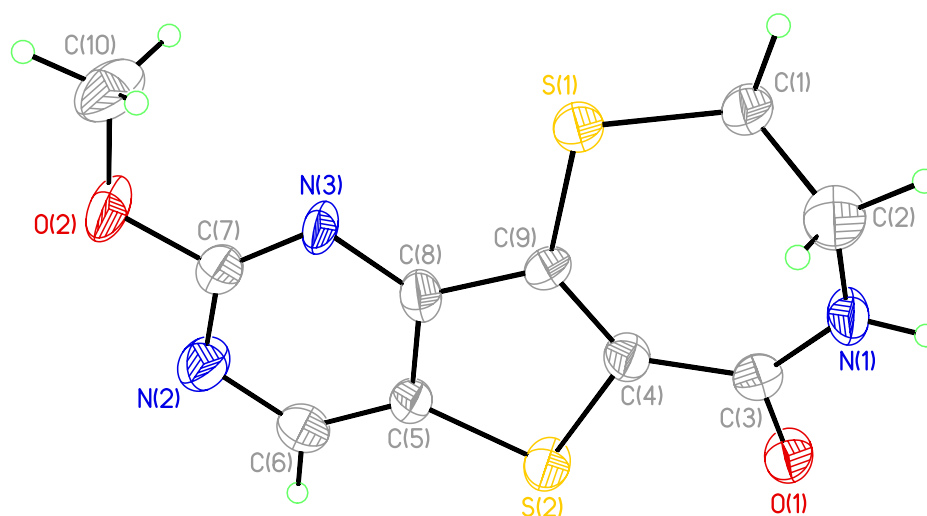


Figure 20. X-Ray crystal structure of **kmg-NB4-23**.

Table 20. Crystal data and structure refinement for **kmg-NB4-23**.

| | | |
|-----------------------------|------------------|---------------------------|
| Identification code | kg57a2 | |
| Empirical formula | C10 H9 N3 O2 S2 | |
| Formula weight | 267.32 | |
| Temperature | 203(2) K | |
| Wavelength | 0.71073 Å | |
| Crystal system | Triclinic | |
| Space group | P-1 | |
| Unit cell dimensions | a = 5.117(8) Å | $\alpha = 86.01(3)^\circ$ |
| | b = 9.387(14) Å | $\beta = 84.90(3)^\circ$ |
| | c = 11.362(17) Å | $\gamma = 89.39(3)^\circ$ |

| | |
|---|---|
| Volume | 542.3(14) Å ³ |
| Z | 2 |
| Density (calculated) | 1.637 Mg/m ³ |
| Absorption coefficient | 0.483 mm ⁻¹ |
| F(000) | 276 |
| Crystal size | 0.12 x 0.04 x 0.04 mm ³ |
| Theta range for data collection | 1.80 to 25.00°. |
| Index ranges | -6<=h<=6, -11<=k<=11, -13<=l<=13 |
| Reflections collected | 3927 |
| Independent reflections | 1886 [R(int) = 0.1134] |
| Completeness to theta = 25.00° | 98.8 % |
| Absorption correction | Multi-scan (Sadabs) |
| Max. and min. transmission | 0.9810 and 0.9444 |
| Refinement method | Full-matrix least-squares on F ² |
| Data / restraints / parameters | 1886 / 0 / 155 |
| Goodness-of-fit on F² | 1.625 |
| Final R indices [I>2sigma(I)] | R1 = 0.1430, wR2 = 0.3333 |
| R indices (all data) | R1 = 0.1958, wR2 = 0.3435 |
| Extinction coefficient | 0.002(7) |
| Largest diff. peak and hole | 1.884 and -0.643 e.Å ⁻³ |
| Largest diff. peak and hole | 1.884 and -0.643 e.Å ⁻³ |

Table 21. Atomic coordinates (x 10⁴) and equivalent isotropic displacement parameters (Å² x 10³) for **kmg-NB4-**

23.

| | x | y | z | U(eq) |
|-------|-----------|-----------|----------|--------------|
| S(1) | 3845(6) | 9715(4) | 6478(3) | 37(1) |
| S(2) | 4548(6) | 6602(3) | 9408(3) | 37(1) |
| O(1) | 8301(15) | 8413(9) | 9949(7) | 40(2) |
| O(2) | -2411(15) | 5532(9) | 5947(7) | 42(2) |
| N(1) | 7763(18) | 10403(11) | 8781(8) | 37(3) |
| N(2) | -620(20) | 4696(12) | 7552(9) | 44(3) |
| N(3) | 561(17) | 7016(10) | 6665(8) | 28(2) |
| C(1) | 6650(20) | 10723(14) | 6710(11) | 40(3) |
| C(2) | 6620(30) | 11326(15) | 7905(12) | 51(4) |
| C(3) | 7200(20) | 9026(14) | 9113(10) | 32(3) |
| C(4) | 5200(20) | 8249(13) | 8598(10) | 29(3) |
| C(5) | 2360(20) | 6112(13) | 8448(10) | 30(3) |
| C(6) | 950(20) | 4912(14) | 8421(11) | 39(3) |
| C(7) | -720(20) | 5827(14) | 6758(10) | 34(3) |
| C(8) | 2160(20) | 7171(13) | 7516(10) | 32(3) |
| C(9) | 3810(20) | 8392(13) | 7597(9) | 26(3) |
| C(10) | -2590(30) | 6601(16) | 4988(12) | 51(4) |

U(eq) is defined as one third of the trace of the orthogonalized U^{ij} tensor.

Table 22. Bond lengths (Å) and angles (°) for **kmg-NB4-23.**

| | |
|-----------|-----------|
| S(1)-C(9) | 1.714(11) |
|-----------|-----------|

| | |
|------------------|-----------|
| S(1)-C(1) | 1.778(12) |
| S(2)-C(5) | 1.718(12) |
| S(2)-C(4) | 1.762(11) |
| O(1)-C(3) | 1.252(12) |
| O(2)-C(7) | 1.363(14) |
| O(2)-C(10) | 1.437(14) |
| N(1)-C(3) | 1.348(15) |
| N(1)-C(2) | 1.435(13) |
| N(1)-H(1C) | 0.8700 |
| N(2)-C(7) | 1.348(14) |
| N(2)-C(6) | 1.355(15) |
| N(3)-C(7) | 1.294(15) |
| N(3)-C(8) | 1.337(14) |
| C(1)-C(2) | 1.505(19) |
| C(1)-H(1A) | 0.9800 |
| C(1)-H(1B) | 0.9800 |
| C(2)-H(2A) | 0.9800 |
| C(2)-H(2B) | 0.9800 |
| C(3)-C(4) | 1.449(16) |
| C(4)-C(9) | 1.391(15) |
| C(5)-C(6) | 1.348(17) |
| C(5)-C(8) | 1.411(15) |
| C(6)-H(6A) | 0.9400 |
| C(8)-C(9) | 1.445(16) |
| C(10)-H(10A) | 0.9700 |
| C(10)-H(10B) | 0.9700 |
| C(10)-H(10C) | 0.9700 |
| C(9)-S(1)-C(1) | 102.5(5) |
| C(5)-S(2)-C(4) | 92.5(5) |
| C(7)-O(2)-C(10) | 115.5(10) |
| C(3)-N(1)-C(2) | 128.4(11) |
| C(3)-N(1)-H(1C) | 115.8 |
| C(2)-N(1)-H(1C) | 115.8 |
| C(7)-N(2)-C(6) | 113.0(11) |
| C(7)-N(3)-C(8) | 114.9(10) |
| C(2)-C(1)-S(1) | 115.4(9) |
| C(2)-C(1)-H(1A) | 108.4 |
| S(1)-C(1)-H(1A) | 108.4 |
| C(2)-C(1)-H(1B) | 108.4 |
| S(1)-C(1)-H(1B) | 108.4 |
| H(1A)-C(1)-H(1B) | 107.5 |
| N(1)-C(2)-C(1) | 114.0(12) |
| N(1)-C(2)-H(2A) | 108.7 |
| C(1)-C(2)-H(2A) | 108.7 |
| N(1)-C(2)-H(2B) | 108.7 |
| C(1)-C(2)-H(2B) | 108.7 |
| H(2A)-C(2)-H(2B) | 107.6 |
| O(1)-C(3)-N(1) | 119.3(11) |
| O(1)-C(3)-C(4) | 118.0(10) |
| N(1)-C(3)-C(4) | 122.5(10) |
| C(9)-C(4)-C(3) | 137.6(10) |

| | |
|---------------------|-----------|
| C(9)-C(4)-S(2) | 111.5(9) |
| C(3)-C(4)-S(2) | 110.6(8) |
| C(6)-C(5)-C(8) | 117.2(10) |
| C(6)-C(5)-S(2) | 131.6(9) |
| C(8)-C(5)-S(2) | 111.1(9) |
| C(5)-C(6)-N(2) | 123.0(11) |
| C(5)-C(6)-H(6A) | 118.5 |
| N(2)-C(6)-H(6A) | 118.5 |
| N(3)-C(7)-N(2) | 130.2(11) |
| N(3)-C(7)-O(2) | 120.9(10) |
| N(2)-C(7)-O(2) | 108.8(10) |
| N(3)-C(8)-C(5) | 121.5(11) |
| N(3)-C(8)-C(9) | 125.3(10) |
| C(5)-C(8)-C(9) | 113.3(10) |
| C(4)-C(9)-C(8) | 111.6(10) |
| C(4)-C(9)-S(1) | 130.9(9) |
| C(8)-C(9)-S(1) | 117.5(8) |
| O(2)-C(10)-H(10A) | 109.5 |
| O(2)-C(10)-H(10B) | 109.5 |
| H(10A)-C(10)-H(10B) | 109.5 |
| O(2)-C(10)-H(10C) | 109.5 |
| H(10A)-C(10)-H(10C) | 109.5 |
| H(10B)-C(10)-H(10C) | 109.5 |

Symmetry transformations used to generate equivalent atoms.

Table 23. Anisotropic displacement parameters ($\text{\AA}^2 \times 10^3$) for **kmg-NB4-23**.

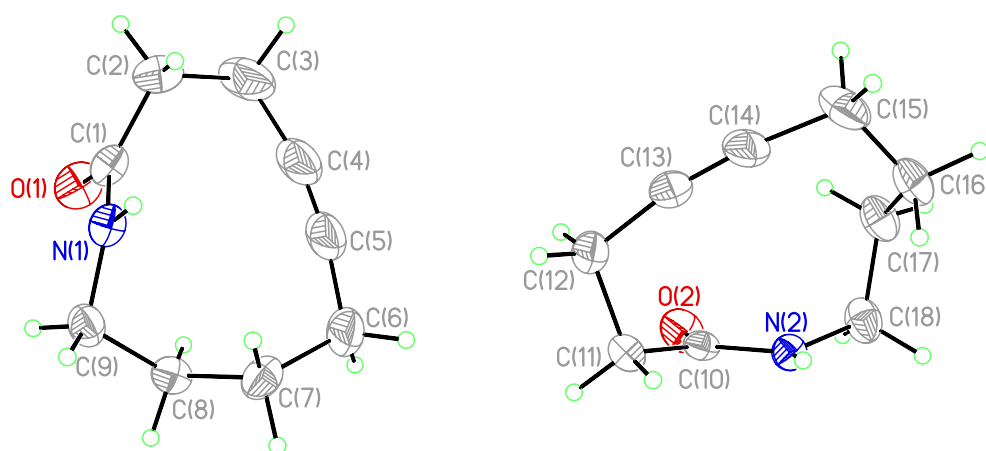
| | U^{11} | U^{22} | U^{33} | U^{23} | U^{13} | U^{12} |
|-------|----------|----------|----------|----------|----------|----------|
| S(1) | 41(2) | 38(2) | 32(2) | 11(2) | -16(1) | -12(1) |
| S(2) | 52(2) | 26(2) | 35(2) | 8(2) | -19(2) | -9(1) |
| O(1) | 46(5) | 38(6) | 37(5) | 11(4) | -22(4) | -9(4) |
| O(2) | 48(5) | 36(6) | 46(5) | -9(5) | -25(4) | -7(4) |
| N(1) | 43(6) | 32(7) | 39(6) | 8(5) | -21(5) | -15(5) |
| N(2) | 58(7) | 38(7) | 38(6) | 5(6) | -17(5) | -12(5) |
| N(3) | 33(5) | 22(6) | 31(5) | -3(5) | -15(4) | -8(4) |
| C(1) | 52(8) | 38(9) | 32(7) | 8(6) | -18(6) | -13(6) |
| C(2) | 67(9) | 40(9) | 48(9) | 21(7) | -34(7) | -10(7) |
| C(3) | 34(7) | 34(8) | 27(7) | 0(6) | -5(5) | -3(5) |
| C(4) | 32(6) | 24(7) | 30(6) | 2(6) | -7(5) | -2(5) |
| C(5) | 32(6) | 32(8) | 26(6) | 2(6) | -7(5) | -7(5) |
| C(6) | 47(7) | 34(8) | 35(7) | 8(6) | -5(6) | -8(6) |
| C(7) | 38(7) | 35(8) | 29(7) | -1(6) | -8(5) | -7(6) |
| C(8) | 32(6) | 30(8) | 35(7) | 0(6) | -7(5) | -10(5) |
| C(9) | 28(6) | 30(7) | 22(6) | 1(5) | -8(5) | 0(5) |
| C(10) | 71(10) | 43(9) | 42(8) | 2(7) | -24(7) | 4(7) |

The anisotropic atomic displacement factor exponent takes the form: $-2\pi^2 [h^2 a^{*2} U_{11} + \dots + 2 h k a^* b^* U_{12}]$.

Table 24. Hydrogen coordinates ($\times 10^4$) and isotropic displacement parameters ($\text{\AA}^2 \times 10^3$) for **kmg-NB4-23**.

| | x | y | z | U(eq) |
|--------|----------|----------|----------|--------------|
| H(1C) | 8983 | 10780 | 9144 | 45 |
| H(1A) | 8208 | 10111 | 6601 | 48 |
| H(1B) | 6839 | 11515 | 6100 | 48 |
| H(2A) | 7562 | 12234 | 7816 | 61 |
| H(2B) | 4793 | 11526 | 8188 | 61 |
| H(6A) | 1058 | 4193 | 9033 | 46 |
| H(10A) | -3839 | 6300 | 4463 | 77 |
| H(10B) | -881 | 6728 | 4552 | 77 |
| H(10C) | -3168 | 7497 | 5303 | 77 |

A.3 X-RAY STRUCTURE AND DATA FOR 5-82

**Figure 21.** X-Ray structure of **5-82**.**Table 25.** Sample and crystal data for **5-82**.

| | |
|----------------------------|------------------------------------|
| Identification code | kgw313 |
| Chemical formula | $\text{C}_9\text{H}_{13}\text{NO}$ |
| Formula weight | 151.21 |
| Temperature | 150(2) K |
| Wavelength | 1.54178 \AA |
| Crystal size | 0.050 x 0.200 x 0.220 mm |
| Crystal habit | clear colourless plate |
| Crystal system | triclinic |
| Space group | P -1 |

| | | |
|-----------------------------|------------------|----------------------------|
| Unit cell dimensions | a = 5.0049(2) Å | $\alpha = 61.976(2)^\circ$ |
| | b = 13.9446(5) Å | $\beta = 86.991(2)^\circ$ |
| | c = 14.1160(5) Å | $\gamma = 80.346(2)^\circ$ |

Table 26. Data collection and structure refinement for **5-82**.

| | | | |
|--|---|--------------|--------------|
| Diffractometer | Bruker Apex II CCD | | |
| Radiation source | IMuS micro-focus, Cu | | |
| Theta range for data collection | 3.55 to 68.20° | | |
| Index ranges | -5<=h<=6, -16<=k<=16, -16<=l<=16 | | |
| Reflections collected | 6549 | | |
| Independent reflections | 2944 [R(int) = 0.0116] | | |
| Coverage of independent reflections | 94.5% | | |
| Absorption correction | multi-scan | | |
| Max. and min. transmission | 0.9704 and 0.0518 | | |
| Structure solution technique | direct methods | | |
| Structure solution program | SHELXS-97 (Sheldrick, 2008) | | |
| Refinement method | Full-matrix least-squares on F ² | | |
| Refinement program | SHELXL-97 (Sheldrick, 2008) | | |
| Function minimized | $\Sigma w(F_o^2 - F_c^2)^2$ | | |
| Data / restraints / parameters | 2944 / 0 / 303 | | |
| Goodness-of-fit on F² | 1.687 | | |
| Final R indices | 2716 data; I>2 σ (I) | R1 = 0.0368, | wR2 = 0.1288 |
| | all data | R1 = 0.0392, | wR2 = 0.1312 |
| Weighting scheme | $w=1/[\sigma^2(F_o^2)+(0.0680P)^2+0.0000P]$ where $P=(F_o^2+2F_c^2)/3$ | | |
| Largest diff. peak and hole | 0.258 and -0.153 eÅ ⁻³ | | |
| R.M.S. deviation from mean | 0.032 eÅ ⁻³ | | |

Table 27. Atomic coordinates and equivalent isotropic atomic displacement parameters (Å²) for **5-82**.

| | x/a | y/b | z/c | U(eq) |
|----|-------------|-------------|-------------|--------------|
| O1 | 0.00406(17) | 0.69089(8) | 0.16071(8) | 0.0420(3) |
| N1 | 0.44114(19) | 0.71443(8) | 0.13998(8) | 0.0282(2) |
| C1 | 0.2445(2) | 0.65632(9) | 0.18969(9) | 0.0295(3) |
| C2 | 0.3299(3) | 0.54820(10) | 0.28819(12) | 0.0420(3) |
| C3 | 0.2251(4) | 0.56095(14) | 0.38646(13) | 0.0624(5) |
| C4 | 0.3092(4) | 0.65934(13) | 0.38185(11) | 0.0599(5) |
| C5 | 0.3783(4) | 0.74595(13) | 0.35722(11) | 0.0602(5) |
| C6 | 0.4603(5) | 0.85500(13) | 0.31095(12) | 0.0616(5) |
| C7 | 0.5388(3) | 0.89312(11) | 0.19378(11) | 0.0383(3) |

| | x/a | y/b | z/c | U(eq) |
|-----|-------------|-------------|-------------|-----------|
| C8 | 0.3100(2) | 0.90224(9) | 0.12018(9) | 0.0312(3) |
| C9 | 0.3812(3) | 0.83097(10) | 0.06401(9) | 0.0349(3) |
| O2 | 0.52466(16) | 0.88098(8) | 0.66978(7) | 0.0403(3) |
| N2 | 0.9572(2) | 0.87788(7) | 0.70979(7) | 0.0266(2) |
| C10 | 0.7654(2) | 0.87879(8) | 0.64672(8) | 0.0252(3) |
| C11 | 0.8635(3) | 0.87068(9) | 0.54739(9) | 0.0319(3) |
| C12 | 0.8696(3) | 0.75114(11) | 0.56838(11) | 0.0434(3) |
| C13 | 0.0224(3) | 0.67468(10) | 0.66891(11) | 0.0413(3) |
| C14 | 0.1347(3) | 0.62617(10) | 0.75519(11) | 0.0422(3) |
| C15 | 0.2557(3) | 0.57986(12) | 0.86342(11) | 0.0484(4) |
| C16 | 0.2399(3) | 0.66848(11) | 0.89891(10) | 0.0397(3) |
| C17 | 0.9516(3) | 0.72801(11) | 0.89685(9) | 0.0375(3) |
| C18 | 0.9111(3) | 0.85202(11) | 0.82130(10) | 0.0382(3) |

U(eq) is defined as one third of the trace of the orthogonized U_{ii} tensor.

Table 28. Bond lengths (Å) for **5-82**.

| | | | |
|----------|------------|----------|------------|
| O1-C1 | 1.2329(15) | N1-C1 | 1.3334(15) |
| N1-C9 | 1.4539(16) | N1-H1N | 0.918(17) |
| C1-C2 | 1.5051(17) | C2-C3 | 1.535(2) |
| C2-H2A | 1.008(18) | C2-H2B | 0.966(18) |
| C3-C4 | 1.473(3) | C3-H3A | 1.00(2) |
| C3-H3B | 1.05(2) | C4-C5 | 1.197(3) |
| C5-C6 | 1.468(3) | C6-C7 | 1.532(2) |
| C6-H6A | 0.99(2) | C6-H6B | 1.02(3) |
| C7-C8 | 1.5358(16) | C7-H7A | 0.993(17) |
| C7-H7B | 0.994(17) | C8-C9 | 1.5283(18) |
| C8-H8A | 0.974(15) | C8-H8B | 0.977(16) |
| C9-H9A | 0.977(19) | C9-H9B | 0.986(19) |
| O2-C10 | 1.2308(15) | N2-C10 | 1.3377(14) |
| N2-C18 | 1.4551(15) | N2-H2N | 0.858(17) |
| C10-C11 | 1.5092(16) | C11-C12 | 1.5451(17) |
| C11-H11A | 0.973(16) | C11-H11B | 1.011(16) |
| C12-C13 | 1.4678(18) | C12-H12B | 1.02(2) |
| C12-H12A | 0.99(2) | C13-C14 | 1.194(2) |
| C14-C15 | 1.4687(19) | C15-C16 | 1.526(2) |
| C15-H15B | 1.00(2) | C15-H15A | 1.00(2) |
| C16-C17 | 1.5333(18) | C16-H16B | 1.015(17) |
| C16-H16A | 1.014(19) | C17-C18 | 1.5299(18) |
| C17-H17A | 0.968(17) | C17-H17B | 0.974(18) |
| C18-H18A | 1.022(18) | C18-H18B | 1.011(18) |

Table 29. Bond angles (°) for **5-82**.

| | | | |
|--------------|------------|---------------|------------|
| C1-N1-C9 | 121.51(10) | C1-N1-H1N | 117.8(9) |
| C9-N1-H1N | 119.4(9) | O1-C1-N1 | 122.45(11) |
| O1-C1-C2 | 121.28(11) | N1-C1-C2 | 116.16(10) |
| C1-C2-C3 | 107.86(11) | C1-C2-H2A | 111.6(9) |
| C3-C2-H2A | 108.6(9) | C1-C2-H2B | 111.0(10) |
| C3-C2-H2B | 108.1(11) | H2A-C2-H2B | 109.6(14) |
| C4-C3-C2 | 109.26(12) | C4-C3-H3A | 109.1(14) |
| C2-C3-H3A | 110.7(14) | C4-C3-H3B | 113.8(13) |
| C2-C3-H3B | 107.4(13) | H3A-C3-H3B | 106.5(18) |
| C5-C4-C3 | 167.32(15) | C4-C5-C6 | 171.72(15) |
| C5-C6-C7 | 110.63(12) | C5-C6-H6A | 109.1(13) |
| C7-C6-H6A | 108.9(12) | C5-C6-H6B | 112.3(13) |
| C7-C6-H6B | 110.7(14) | H6A-C6-H6B | 105.0(18) |
| C6-C7-C8 | 114.13(13) | C6-C7-H7A | 105.4(9) |
| C8-C7-H7A | 109.3(10) | C6-C7-H7B | 109.0(10) |
| C8-C7-H7B | 108.0(9) | H7A-C7-H7B | 111.0(13) |
| C9-C8-C7 | 113.97(10) | C9-C8-H8A | 107.4(9) |
| C7-C8-H8A | 111.2(8) | C9-C8-H8B | 107.1(10) |
| C7-C8-H8B | 110.7(10) | H8A-C8-H8B | 106.0(12) |
| N1-C9-C8 | 112.13(9) | N1-C9-H9A | 107.8(10) |
| C8-C9-H9A | 109.5(10) | N1-C9-H9B | 107.9(10) |
| C8-C9-H9B | 109.3(10) | H9A-C9-H9B | 110.1(14) |
| C10-N2-C18 | 122.12(10) | C10-N2-H2N | 119.1(10) |
| C18-N2-H2N | 116.1(10) | O2-C10-N2 | 122.68(11) |
| O2-C10-C11 | 121.35(10) | N2-C10-C11 | 115.89(10) |
| C10-C11-C12 | 108.45(10) | C10-C11-H11A | 109.6(9) |
| C12-C11-H11A | 107.7(9) | C10-C11-H11B | 110.7(9) |
| C12-C11-H11B | 109.7(9) | H11A-C11-H11B | 110.6(12) |
| C13-C12-C11 | 109.47(10) | C13-C12-H12B | 113.8(11) |
| C11-C12-H12B | 107.6(11) | C13-C12-H12A | 109.5(10) |
| C11-C12-H12A | 106.8(11) | H12B-C12-H12A | 109.3(16) |
| C14-C13-C12 | 169.13(13) | C13-C14-C15 | 171.96(14) |
| C14-C15-C16 | 110.86(10) | C14-C15-H15B | 107.8(11) |
| C16-C15-H15B | 111.9(12) | C14-C15-H15A | 112.1(12) |
| C16-C15-H15A | 108.5(12) | H15B-C15-H15A | 105.7(15) |
| C15-C16-C17 | 114.12(12) | C15-C16-H16B | 106.9(9) |
| C17-C16-H16B | 109.5(9) | C15-C16-H16A | 107.6(10) |
| C17-C16-H16A | 111.0(11) | H16B-C16-H16A | 107.5(13) |
| C18-C17-C16 | 114.00(11) | C18-C17-H17A | 109.4(9) |
| C16-C17-H17A | 109.0(9) | C18-C17-H17B | 106.6(10) |
| C16-C17-H17B | 110.6(10) | H17A-C17-H17B | 107.0(13) |
| N2-C18-C17 | 112.57(10) | N2-C18-H18A | 107.1(10) |

| | | | |
|--------------|-----------|---------------|-----------|
| C17-C18-H18A | 109.9(10) | N2-C18-H18B | 105.3(10) |
| C17-C18-H18B | 110.2(9) | H18A-C18-H18B | 111.6(14) |

Table 30. Torsion angles (°) for **5-82**.

| | | | |
|-----------------|------------|-----------------|-------------|
| C9-N1-C1-O1 | 13.74(17) | C9-N1-C1-C2 | -162.56(10) |
| O1-C1-C2-C3 | -68.01(16) | N1-C1-C2-C3 | 108.34(14) |
| C1-C2-C3-C4 | -51.52(18) | C2-C3-C4-C5 | 25.5(10) |
| C3-C4-C5-C6 | 2.(2) | C4-C5-C6-C7 | -15.2(15) |
| C5-C6-C7-C8 | 59.76(18) | C6-C7-C8-C9 | -121.75(12) |
| C1-N1-C9-C8 | 77.12(13) | C7-C8-C9-N1 | 61.17(14) |
| C18-N2-C10-O2 | 15.63(16) | C18-N2-C10-C11 | -161.14(10) |
| O2-C10-C11-C12 | -75.32(14) | N2-C10-C11-C12 | 101.50(11) |
| C10-C11-C12-C13 | -51.91(15) | C11-C12-C13-C14 | 25.5(9) |
| C12-C13-C14-C15 | 4.5(19) | C13-C14-C15-C16 | -15.2(12) |
| C14-C15-C16-C17 | 56.73(17) | C15-C16-C17-C18 | -119.29(13) |
| C10-N2-C18-C17 | 82.94(13) | C16-C17-C18-N2 | 61.73(14) |

Table 31. Anisotropic atomic displacement parameters (\AA^2) for **5-82**.

| | U ₁₁ | U ₂₂ | U ₃₃ | U ₂₃ | U ₁₃ | U ₁₂ |
|-----|-----------------|-----------------|-----------------|-----------------|-----------------|-----------------|
| O1 | 0.0186(4) | 0.0511(5) | 0.0599(6) | -0.0280(5) | -0.0005(4) | -0.0076(4) |
| N1 | 0.0192(5) | 0.0375(5) | 0.0335(5) | -0.0204(4) | 0.0028(4) | -0.0074(4) |
| C1 | 0.0205(5) | 0.0359(6) | 0.0399(6) | -0.0238(5) | 0.0035(4) | -0.0068(4) |
| C2 | 0.0398(8) | 0.0307(6) | 0.0526(8) | -0.0168(6) | 0.0037(6) | -0.0079(5) |
| C3 | 0.0802(13) | 0.0449(8) | 0.0426(8) | -0.0052(6) | 0.0172(8) | -0.0130(8) |
| C4 | 0.0936(13) | 0.0484(9) | 0.0275(6) | -0.0139(6) | 0.0077(7) | 0.0008(8) |
| C5 | 0.1016(14) | 0.0479(9) | 0.0284(6) | -0.0203(6) | -0.0018(7) | 0.0039(8) |
| C6 | 0.1020(14) | 0.0458(8) | 0.0433(8) | -0.0292(7) | -0.0169(8) | 0.0037(8) |
| C7 | 0.0354(7) | 0.0363(6) | 0.0494(7) | -0.0254(6) | -0.0076(5) | -0.0024(5) |
| C8 | 0.0251(6) | 0.0310(6) | 0.0331(6) | -0.0114(5) | -0.0008(5) | -0.0043(4) |
| C9 | 0.0369(7) | 0.0414(7) | 0.0269(5) | -0.0142(5) | 0.0028(5) | -0.0133(5) |
| O2 | 0.0194(4) | 0.0486(5) | 0.0427(5) | -0.0129(4) | 0.0006(3) | -0.0054(3) |
| N2 | 0.0217(5) | 0.0283(5) | 0.0294(5) | -0.0136(4) | -0.0001(4) | -0.0023(3) |
| C10 | 0.0218(5) | 0.0202(5) | 0.0274(5) | -0.0058(4) | -0.0012(4) | -0.0031(4) |
| C11 | 0.0356(7) | 0.0297(6) | 0.0252(5) | -0.0087(4) | -0.0025(5) | -0.0037(5) |
| C12 | 0.0603(9) | 0.0359(7) | 0.0368(7) | -0.0198(5) | -0.0112(6) | -0.0023(6) |
| C13 | 0.0569(8) | 0.0261(6) | 0.0419(7) | -0.0179(5) | -0.0061(6) | -0.0007(5) |
| C14 | 0.0522(8) | 0.0260(6) | 0.0422(7) | -0.0139(5) | -0.0055(6) | 0.0054(5) |
| C15 | 0.0544(9) | 0.0358(7) | 0.0373(7) | -0.0075(5) | -0.0065(6) | 0.0103(6) |
| C16 | 0.0307(6) | 0.0455(7) | 0.0317(6) | -0.0106(5) | -0.0069(5) | 0.0016(5) |
| C17 | 0.0319(7) | 0.0475(7) | 0.0268(6) | -0.0137(5) | 0.0019(5) | -0.0017(5) |
| C18 | 0.0406(7) | 0.0436(7) | 0.0325(6) | -0.0226(5) | -0.0032(5) | 0.0041(5) |

| U_{11} | U_{22} | U_{33} | U_{23} | U_{13} | U_{12} |
|--|----------|----------|----------|----------|----------|
| The anisotropic atomic displacement factor exponent takes the form: $-2\pi^2 [h^2 a^{*2} U_{11} + \dots + 2 h k a^* b^* U_{12}]$. | | | | | |

Table 32. Hydrogen atomic coordinates and isotropic atomic displacement parameters (\AA^2) for **5-82**.

| | x/a | y/b | z/c | $U(\text{eq})$ |
|------|----------|------------|------------|----------------|
| H1N | 0.616(3) | 0.6833(12) | 0.1653(12) | 0.036(4) |
| H2A | 0.533(4) | 0.5270(13) | 0.2958(13) | 0.044(4) |
| H2B | 0.251(3) | 0.4902(14) | 0.2868(14) | 0.050(4) |
| H3A | 0.300(5) | 0.4949(19) | 0.4543(19) | 0.079(6) |
| H3B | 0.014(5) | 0.5638(18) | 0.3868(18) | 0.081(7) |
| H6A | 0.306(4) | 0.9087(18) | 0.3137(17) | 0.070(6) |
| H6B | 0.613(5) | 0.8568(19) | 0.354(2) | 0.085(7) |
| H7A | 0.692(3) | 0.8368(13) | 0.1959(13) | 0.042(4) |
| H7B | 0.595(3) | 0.9666(14) | 0.1646(13) | 0.045(4) |
| H8A | 0.146(3) | 0.8817(11) | 0.1600(11) | 0.032(3) |
| H8B | 0.260(3) | 0.9782(13) | 0.0642(13) | 0.042(4) |
| H9A | 0.541(4) | 0.8514(14) | 0.0211(14) | 0.048(4) |
| H9B | 0.226(4) | 0.8419(14) | 0.0177(14) | 0.052(4) |
| H2N | 1.124(3) | 0.8722(12) | 0.6921(12) | 0.033(4) |
| H11A | 1.048(3) | 0.8864(12) | 0.5337(12) | 0.036(4) |
| H11B | 0.739(3) | 0.9229(13) | 0.4835(12) | 0.037(4) |
| H12B | 0.949(4) | 0.7454(16) | 0.5028(16) | 0.061(5) |
| H12A | 0.680(4) | 0.7385(14) | 0.5755(14) | 0.056(5) |
| H15B | 1.158(4) | 0.5184(16) | 0.9131(16) | 0.062(5) |
| H15A | 1.450(4) | 0.5455(16) | 0.8675(16) | 0.062(5) |
| H16B | 1.356(3) | 0.7238(13) | 0.8486(13) | 0.045(4) |
| H16A | 1.327(4) | 0.6325(14) | 0.9735(15) | 0.053(5) |
| H17A | 0.825(3) | 0.6951(13) | 0.8766(12) | 0.040(4) |
| H17B | 0.904(3) | 0.7189(14) | 0.9681(14) | 0.046(4) |
| H18A | 1.045(4) | 0.8874(14) | 0.8421(14) | 0.048(4) |
| H18B | 0.717(4) | 0.8862(14) | 0.8225(13) | 0.048(4) |

BIBLIOGRAPHY

1. (a) Kalinin, V. N. *Synthesis* **1992**, 413-432. (b) Schröter, S.; Stock, C.; Bach, T. *Tetrahedron* **2005**, *61*, 2245-2267. (c) Rossi, R.; Bellina, F.; Lessi, M. *Adv. Synth. Catal.* **2012**, *354*, 1181-1255.
2. (a) Fry, D. W.; Kraker, A. J.; McMichael, A.; Ambroso, L. A.; Nelson, J. M.; Leopold, W. R.; Connors, R. W.; Bridges, A. J. *Science* **1994**, *265*, 1093-1095. (b) Strawn, L. M.; Shawver, L. K. *Expert Opin. Invest. Drugs* **1998**, *7*, 553-573. (c) Uckun, F. M.; Sudbeck, E. A.; Mao, C.; Ghosh, S.; Liu, X. P.; Vassilev, A. O.; Navara, C. S.; Narla, R. K. *Curr. Cancer Drug Targets* **2001**, *1*, 59-71.
3. Bedi, P. M. S.; Kumar, V.; Mahajan, M. P. *Bioorg. Med. Chem. Lett.* **2004**, *14*, 5211-5213.
4. Foster, B. A.; Coffey, H. A.; Morin, M. J.; Rastinejad, F. *Science* **1999**, *286*, 2507-2510.
5. Bernotas, R. C.; Ullrich, J. W.; Travins, J. M.; Wrobel, J. E.; Unwalla, R. J. WO2009010683 A2, Feb 12, 2009.
6. Selvam, T. P.; Kumar, P. V. *Res. Pharm.* **2011**, *1*, 1-21.
7. Gundla, R.; Kazemi, R.; Sanam, R.; Muttineni, R.; Sarma, J. A. R. P.; Dayam, R.; Neamati, N. *J. Med. Chem.* **2008**, *51*, 3367-3377.
8. (a) Baselga, J.; Rischin, D.; Ranson, M.; Calvert, H.; Raymond, E.; Kieback, D. G.; Kaye, S. B.; Gianni, L.; Harris, A.; Bjork, T.; Averbuch, S. D.; Feyereislova, A.;

- Swaisland, H.; Rojo, F.; Albanell, J. *J. Clin. Oncol.* **2002**, *20*, 4292-4302. (b) Wakeling, A. E.; Guy, S. P.; Woodburn, J. R.; Ashton, S. E.; Curry, B. J.; Barker, A. J.; Gibson, K. *H. Cancer Res.* **2002**, *62*, 5749-5754.
9. da Silva, J. F. M.; Walters, M.; Al-Damluji, S.; Ganellin, C. R. *Bioorg. Med. Chem.* **2008**, *16*, 7254-7263.
10. (a) Lu, Q.; Mangalagiu, I.; Benneche, T.; Undheim, K. *Acta Chem. Scand.* **1997**, *51*, 302-306. (b) Mangalagiu, I.; Benneche, T.; Undheim, K. *Tetrahedron Lett.* **1996**, *37*, 1309-1312.
11. Mangalagiu, I.; Benneche, T.; Undheim, K. *Acta Chem. Scand.* **1996**, *50*, 914-917.
12. Charpiot, B.; Brun, J.; Donze, I.; Naef, R.; Stefani, M.; Mueller, T. *Bioorg. Med. Chem. Lett.* **1998**, *8*, 2891-2896.
13. Kosugi, M.; Sasazawa, K.; Shimizu, Y.; Migita, T. *Chem. Lett.* **1977**, *6*, 301-302.
14. (a) Miyaura, N.; Suzuki, A. *J. Chem. Soc., Chem. Commun.* **1979**, 866-867. (b) Miyaura, N.; Yamada, K.; Suzuki, A. *Tetrahedron Lett.* **1979**, *20*, 3437-3440.
15. Wipf, P.; George, K. M. *Synlett* **2010**, 644-648.
16. Kabri, Y.; Verhaeghe, P.; Gellis, A.; Vanelle, P. *Molecules* **2010**, *15*, 2949-2961.
17. Garcia, Y.; Schoenebeck, F.; Legault, C. Y.; Merlic, C. A.; Houk, K. N. *J. Am. Chem. Soc.* **2009**, *131*, 6632-6639.
18. Legault, C. Y.; Garcia, Y.; Merlic, C. A.; Houk, K. N. *J. Am. Chem. Soc.* **2007**, *129*, 12664-12665.
19. Mayer, P. M.; Parkinson, C. J.; Smith, D. M.; Radom, L. *J. Chem. Phys.* **1998**, *108*, 604-615.

20. Baboul, A. G.; Curtiss, L. A.; Redfern, P. C.; Raghavachari, K. *J. Chem. Phys.* **1999**, *110*, 7650-7657.
21. Curd, F. H. S.; Landquist, J. K.; Rose, F. L. *J. Chem. Soc.* **1948**, 1759-1766.
22. Liebeskind, L. S.; Srogl, J. *Org. Lett.* **2002**, *4*, 979-981.
23. (a) Tikad, A.; Routier, S.; Akssira, M.; Leger, J.-M.; Jarry, C.; Guillaumet, G. *Org. Lett.* **2007**, *9*, 4673-4676. (b) Riadi, Y.; Massip, S.; Leger, J.-M.; Jarry, C.; Lazar, S.; Guillaumet, G. *Tetrahedron* **2012**, *68*, 5018.
24. (a) Barder, T. E.; Walker, S. D.; Martinelli, J. R.; Buchwald, S. L. *J. Am. Chem. Soc.* **2005**, *127*, 4685-4696. (b) Billingsley, K.; Buchwald, S. L. *J. Am. Chem. Soc.* **2007**, *129*, 3358-3366.
25. Lefterov, I. *University of Pittsburgh, Department of Environmental and Occupational Health. Unpublished results.*
26. (a) Decornez, H.; Gulyás-Forró, A.; Papp, Á.; Szabó, M.; Sármay, G.; Hajdú, I.; Cseh, S.; Dormán, G.; Kitchen, Douglas B. *ChemMedChem* **2009**, *4*, 1273-1278. (b) Peng, J.; Lin, W.; Jiang, D.; Yuan, S.; Chen, Y. *J. Comb. Chem.* **2007**, *9*, 431-436. (c) Wipf, P.; Minion, D. J.; Halter, R. J.; Berggren, M. I.; Ho, C. B.; Chiang, G. G.; Kirkpatrick, L.; Abraham, R.; Powis, G. *Org. Biomol. Chem.* **2004**, *2*, 1911-1920.
27. (a) Boutros, R.; Lobjois, V.; Ducommun, B. *Nat. Rev. Cancer* **2007**, *7*, 495-507. (b) Lyon, M. A.; Ducruet, A. P.; Wipf, P.; Lazo, J. S. *Nat. Rev. Drug Discovery* **2002**, *1*, 961-976.
28. Kristjánisdóttir, K.; Rudolph, J. *Chemistry & Biology* **2004**, *11*, 1043-1051.
29. (a) Contour-Galcera, M.-O.; Sidhu, A.; Prévost, G.; Bigg, D.; Ducommun, B. *Pharmacol. Ther.* **2007**, *115*, 1-12. (b) Lazo, J. S.; Wipf, P. *Anti-Cancer Agents Med. Chem.* **2008**, *8*,

- 837-842. (c) Vintonyak, V. V.; Antonchick, A. P.; Rauh, D.; Waldmann, H. *Curr. Opin. Chem. Biol.* **2009**, *13*, 272-283. (d) Lavecchia, A.; Di Giovanni, C.; Novellino, E. *Mini-Rev. Med. Chem.* **2012**, *12*, 62-73.
30. Adapted from: Boutros, R.; Lobjois, V.; Ducommun, B. *Nat. Rev. Cancer* **2007**, *7*, 495-507.
31. (a) Reynolds, R. A.; Yem, A. W.; Wolfe, C. L.; Deibel Jr, M. R.; Chidester, C. G.; Watenpaugh, K. D. *J. Mol. Biol.* **1999**, *293*, 559-568. (b) Fauman, E. B.; Cogswell, J. P.; Lovejoy, B.; Rocque, W. J.; Holmes, W.; Montana, V. G.; Piwnica-Worms, H.; Rink, M. J.; Saper, M. A. *Cell* **1998**, *93*, 617-625.
32. Rudolph, J. *Biochemistry* **2007**, *46*, 3595-3604.
33. Chen, W.; Wilborn, M.; Rudolph, J. *Biochemistry* **2000**, *39*, 10781-10789.
34. (a) Savitsky, P. A.; Finkel, T. *J. Biol. Chem.* **2002**, *277*, 20535-20540. (b) Sohn, J.; Rudolph, J. *Biochemistry* **2003**, *42*, 10060-10070. (c) Buhrman, G.; Parker, B.; Sohn, J.; Rudolph, J.; Mattos, C. *Biochemistry* **2005**, *44*, 5307-5316.
35. Johnston, P. A.; Foster, C. A.; Tierno, M. B.; Shun, T. Y.; Shinde, S. N.; Paquette, W. D.; Brummond, K. M.; Wipf, P.; Lazo, J. S. *Assay Drug Dev. Technol.* **2009**, *7*, 250-265.
36. Kucherenko, T. T.; Gutsul, R.; Kisel, V. M.; Kovtunencko, V. A. *Tetrahedron* **2004**, *60*, 211-217.
37. Price, C. C.; Rogers, R. G.; Bachmann, W.; Morin, R. D. E. *Org. Synth. Coll. Vol. 3* **1955**, 174.
38. George Rosenker, K. M.; Paquette, W. D.; Johnston, P. A.; Sharlow, E. R.; Lazo, J. S.; Wipf, P. *Unpublished results*.

39. Brisson, M.; Nguyen, T.; Wipf, P.; Joo, B.; Day, B. W.; Skoko, J. S.; Schreiber, E. M.; Foster, C.; Bansal, P.; Lazo, J. S. *Mol. Pharmacol.* **2005**, *68*, 1810-1820.
40. Ling, K.-Q.; Chen, X.-Y.; Fun, H.-K.; Huang, X.-Y.; Xu, J.-H. *J. Chem. Soc., Perkin Trans. 1* **1998**, 4147-4158.
41. Potikha, L. M.; Shkilna, N. V.; Kisil, V. M.; Kovtunencko, V. A. *Chem. Heterocycl. Comp.* **2004**, *40*, 1052-1062.
42. Soares, K. M.; Blackmon, N.; Shun, T. Y.; Shinde, S. N.; Takyi, H. K.; Wipf, P.; Lazo, J. S.; Johnston, P. A. *Assay Drug Dev. Technol.* **2010**, *8*, 152-174.
43. Eiseman, J. L. *Unpublished results*.
44. (a) LaValle, C. R.; George, K. M.; Sharlow, E. R.; Lazo, J. S.; Wipf, P.; Wang, Q. J. *BBA - Rev. Cancer* **2010**, *1806*, 183-192. (b) Fu, Y.; Rubin, C. S. *EMBO Rep.* **2011**, *12*, 785-796.
45. (a) Johannes, F. J.; Prestle, J.; Eis, S.; Oberhagemann, P.; Pfizenmaier, K. *J. Biol. Chem.* **1994**, *269*, 6140-6148. (b) Valverde, A. M.; Sinnott-Smith, J.; Van Lint, J.; Rozengurt, E. *Proc. Natl. Acad. Sci. U. S. A.* **1994**, *91*, 8572-8576.
46. Sturany, S.; Van Lint, J.; Muller, F.; Wilda, M.; Hameister, H.; Hocker, M.; Brey, A.; Gern, U.; Vandenhede, J.; Gress, T.; Adler, G.; Seufferlein, T. *J. Biol. Chem.* **2001**, *276*, 3310-3318.
47. Hayashi, A.; Seki, N.; Hattori, A.; Kozuma, S.; Saito, T. *Biochim. Biophys. Acta* **1999**, *1450*, 99-106.
48. (a) Rozengurt, E.; Rey, O.; Waldron, R. T. *J. Biol. Chem.* **2005**, *280*, 13205-13208. (b) Wang, Q. J. *Trends Pharmacol. Sci.* **2006**, *27*, 317-323. (c) Rozengurt, E. *Physiology* **2011**, *26*, 23-33.

49. (a) Waldron, R. T.; Iglesias, T.; Rozengurt, E. *Electrophoresis* **1999**, *20*, 382-390. (b) Waldron, R. T.; Rozengurt, E. *J. Biol. Chem.* **2003**, *278*, 154-163. (c) Zugaza, J. L.; Sinnett-Smith, J.; Van Lint, J.; Rozengurt, E. *EMBO J.* **1996**, *15*, 6220-6230.
50. (a) Jacamo, R.; Sinnett-Smith, J.; Rey, O.; Waldron, R. T.; Rozengurt, E. *J. Biol. Chem.* **2008**, *283*, 12877-12887. (b) Matthews, S. A.; Rozengurt, E.; Cantrell, D. *J. Biol. Chem.* **1999**, *274*, 26543-26549.
51. Sinnett-Smith, J.; Jacamo, R.; Kui, R.; Wang, Y. M.; Young, S. H.; Rey, O.; Waldron, R. T.; Rozengurt, E. *J. Biol. Chem.* **2009**, *284*, 13434-13445.
52. (a) Storz, P.; Doppler, H.; Johannes, F. J.; Toker, A. *J. Biol. Chem.* **2003**, *278*, 17969-17976. (b) Storz, P.; Doppler, H.; Toker, A. *Mol. Cell. Biol.* **2005**, *25*, 8520-8530. (c) Waldron, R. T.; Rozengurt, E. *J. Biol. Chem.* **2000**, *275*, 17114-17121.
53. (a) Ha, C. H.; Jhun, B. S.; Kao, H. Y.; Jin, Z. G. *Arterioscler. Thromb. Vasc. Biol.* **2008**, *28*, 1782-1788. (b) Ha, C. H.; Wang, W.; Jhun, B. S.; Wong, C.; Hausser, A.; Pfizenmaier, K.; McKinsey, T. A.; Olson, E. N.; Jin, Z. G. *J. Biol. Chem.* **2008**, *283*, 14590-14599. (c) Wang, S.; Li, X.; Parra, M.; Verdin, E.; Bassel-Duby, R.; Olson, E. N. *Proc. Natl. Acad. Sci. U. S. A.* **2008**, *105*, 7738-7743.
54. (a) Bankaitis, V. A. *Science* **2002**, *295*, 290-291. (b) Cuenda, A.; Nebreda, A. R. *Cell* **2009**, *136*, 209-210. (c) Ghanekar, Y.; Lowe, M. *Trends Cell Biol.* **2005**, *15*, 511-514.
55. (a) Prigozhina, N. L.; Waterman-Storer, C. M. *Curr. Biol.* **2004**, *14*, 88-98. (b) Woods, A. J.; White, D. P.; Caswell, P. T.; Norman, J. C. *EMBO J.* **2004**, *23*, 2531-2543.
56. (a) Matthews, S. A.; Liu, P.; Spitaler, M.; Olson, E. N.; McKinsey, T. A.; Cantrell, D. A.; Scharenberg, A. M. *Mol. Cell. Biol.* **2006**, *26*, 1569-1577. (b) Marklund, U.; Lightfoot, K.; Cantrell, D. *Immunity* **2003**, *19*, 491-501. (c) Medeiros, R. B.; Dickey, D. M.; Chung,

- H.; Quale, A. C.; Nagarajan, L. R.; Billadeau, D. D.; Shimizu, Y. *Immunity* **2005**, *23*, 213-226.
57. (a) Jaggi, M.; Rao, P. S.; Smith, D. J.; Hemstreet, G. P.; Balaji, K. C. *Biochem. Biophys. Res. Commun.* **2003**, *307*, 254-260. (b) Chen, J.; Deng, F.; Singh, S. V.; Wang, Q. J. *Cancer Res.* **2008**, *68*, 3844-3853. (c) Eiseler, T.; Doppler, H.; Yan, I. K.; Goodison, S.; Storz, P. *Breast Cancer Res.* **2009**, *11*, R13. (d) Kim, M.; Jang, H. R.; Kim, J. H.; Noh, S. M.; Song, K. S.; Cho, J. S.; Jeong, H. Y.; Norman, J. C.; Caswell, P. T.; Kang, G. H.; Kim, S. Y.; Yoo, H. S.; Kim, Y. S. *Carcinogenesis* **2008**, *29*, 629-637.
58. (a) Fielitz, J.; Kim, M. S.; Shelton, J. M.; Qi, X.; Hill, J. A.; Richardson, J. A.; Bassel-Duby, R.; Olson, E. N. *Proc. Natl. Acad. Sci. U. S. A.* **2008**, *105*, 3059-3063. (b) Monovich, L.; Vega, R. B.; Meredith, E.; Miranda, K.; Rao, C.; Capparelli, M.; Lemon, D. D.; Phan, D.; Koch, K. A.; Chapo, J. A.; Hood, D. B.; McKinsey, T. A. *FEBS Lett.* **2010**, *584*, 631-637.
59. (a) Altschmied, J.; Haendeler, J. *Arterioscler. Thromb. Vasc. Biol.* **2008**, *28*, 1689-1690. (b) Ha, C. H.; Jin, Z. G. *Mol. Cells* **2009**, *28*, 1-5.
60. (a) Jaggi, M.; Rao, P. S.; Smith, D. J.; Wheelock, M. J.; Johnson, K. R.; Hemstreet, G. P.; Balaji, K. C. *Cancer Res.* **2005**, *65*, 483-492. (b) Sinnott-Smith, J.; Zhukova, E.; Hsieh, N.; Jiang, X.; Rozengurt, E. *J. Biol. Chem.* **2004**, *279*, 16883-16893. (c) Wong, C.; Jin, Z. *G. J. Biol. Chem.* **2005**, *280*, 33262-33269.
61. Adapted from: Wang, Q. J. *Trends Pharmacol. Sci.* **2006**, *27*, 317-323.
62. Gschwendt, M.; Dieterich, S.; Rennecke, J.; Kittstein, W.; Mueller, H. J.; Johannes, F. J. *FEBS Lett.* **1996**, *392*, 77-80.

63. Martiny-Baron, G.; Kazanietz, M. G.; Mischak, H.; Blumberg, P. M.; Kochs, G.; Hug, H.; Marme, D.; Schachtele, C. *J. Biol. Chem.* **1993**, *268*, 9194-9197.
64. (a) Stewart, J. R.; Christman, K. L.; O'Brian, C. A. *Biochem. Pharmacol.* **2000**, *60*, 1355-1359. (b) Haworth, R. S.; Avkiran, M. *Biochem. Pharmacol.* **2001**, *62*, 1647-1651. (c) Aggarwal, B. B.; Bhardwaj, A.; Aggarwal, R. S.; Seeram, N. P.; Shishodia, S.; Takada, Y. *Anticancer Res.* **2004**, *24*, 2783-2840.
65. Gschwendt, M.; Kittstein, W.; Johannes, F. J. *FEBS Lett.* **1998**, *421*, 165-168.
66. Sharlow, E. R.; Giridhar, K. V.; LaValle, C. R.; Chen, J.; Leimgruber, S.; Barrett, R.; Bravo-Altamirano, K.; Wipf, P.; Lazo, J. S.; Wang, Q. J. *J. Biol. Chem.* **2008**, *283*, 33516-33526.
67. LaValle, C. R.; Bravo-Altamirano, K.; Giridhar, K. V.; Chen, J.; Sharlow, E. R.; Lazo, J. S.; Wipf, P.; Wang, Q. J. *BMC Chemical Biology* **2010**, *10*.
68. (a) Raynham, T. M.; Hammonds, T. R.; Gillatt, J. H.; Charles, M. D.; Pave, G. A.; Foxton, C. H.; Carr, J. L.; Mistry, N. S. WO2007125331A2, Nov 11, 2007. (b) Raynham, T. M.; Hammonds, T. R.; Charles, M. D.; Pave, G. A.; Foxton, C. H.; Blackaby, W. P.; Stevens, A. P.; Ekwuru, C. T. WO2008074997A1, June 26, 2008. (c) Harikumar, K. B.; Kunnumakkara, A. B.; Ochi, N.; Tong, Z.; Deorukhkar, A.; Sung, B.; Kelland, L.; Jamieson, S.; Sutherland, R.; Raynham, T.; Charles, M.; Bagherzadeh, A.; Foxton, C.; Boakes, A.; Farooq, M.; Maru, D.; Diagaradjane, P.; Matsuo, Y.; Sinnott-Smith, J.; Gelovani, J.; Krishnan, S.; Aggarwal, B. B.; Rozengurt, E.; Ireson, C. R.; Guha, S. *Mol. Cancer Ther.* **2010**, *9*, 1136-1146. (d) Gamber, G. G.; Meredith, E.; Zhu, Q.; Yan, W.; Rao, C.; Capparelli, M.; Burgis, R.; Enyedy, I.; Zhang, J.-H.; Soldermann, N.; Beattie, K.; Rozhitskaya, O.; Koch, K. A.; Pagratis, N.; Hosagrahara, V.; Vega, R. B.; McKinsey,

- T. A.; Monovich, L. *Bioorg. Med. Chem. Lett.* **2011**, *21*, 1447-1451. (e) Meredith, E. L.; Ardayfio, O.; Beattie, K.; Dobler, M. R.; Enyedy, I.; Gaul, C.; Hosagrahara, V.; Jewell, C.; Koch, K.; Lee, W.; Lehmann, H.; McKinsey, T. A.; Miranda, K.; Pagratis, N.; Pancost, M.; Patnaik, A.; Phan, D.; Plato, C.; Qian, M.; Rajaraman, V.; Rao, C.; Rozhitskaya, O.; Ruppen, T.; Shi, J.; Siska, S. J.; Springer, C.; van Eis, M.; Vega, R. B.; von Matt, A.; Yang, L.; Yoon, T.; Zhang, J.-H.; Zhu, N.; Monovich, L. G. *J. Med. Chem.* **2010**, *53*, 5400-5421. (f) Meredith, E. L.; Beattie, K.; Burgis, R.; Capparelli, M.; Chapo, J.; DiPietro, L.; Gamber, G.; Enyedy, I.; Hood, D. B.; Hosagrahara, V.; Jewell, C.; Koch, K. A.; Lee, W.; Lemon, D. D.; McKinsey, T. A.; Miranda, K.; Pagratis, N.; Phan, D.; Plato, C.; Rao, C.; Rozhitskaya, O.; Soldermann, N.; Springer, C.; van Eis, M.; Vega, R. B.; Yan, W.; Zhu, Q.; Monovich, L. G. *J. Med. Chem.* **2010**, *53*, 5422-5438.
69. Evans, I. M.; Bagherzadeh, A.; Charles, M.; Raynham, T.; Ireson, C.; Boakes, A.; Kelland, L.; Zachary, I. C. *Biochem. J.* **2010**, *429*, 565-572.
70. Torres-Marquez, E.; Sinnett-Smith, J.; Guha, S.; Kui, R.; Waldron, R. T.; Rey, O.; Rozengurt, E. *Biochem. Biophys. Res. Commun.* **2010**, *391*, 63-68.
71. (a) Bravo-Altamirano, K.; George, K. M.; Frantz, M.-C.; LaValle, C. R.; Tandon, M.; Leimgruber, S.; Sharlow, E. R.; Lazo, J. S.; Wang, Q. J.; Wipf, P. *ACS Med. Chem. Lett.* **2010**, *2*, 154-159. (b) George, K. M.; Frantz, M.-C.; Bravo-Altamirano, K.; LaValle, C. R.; Tandon, M.; Leimgruber, S.; Sharlow, E. R.; Lazo, J. S.; Wang, Q. J.; Wipf, P. *Pharmaceutics* **2011**, *3*, 186-228.
72. Guo, J.; Clausen, D.; Beumer, J.; Parise, R.; Egorin, M.; Bravo-Altamirano, K.; Wipf, P.; Sharlow, E.; Wang, Q.; Eiseman, J. *Cancer Chemother. Pharmacol.* **2013**, *71*, 331-344.

73. (a) Meanwell, N. A. *J. Med. Chem.* **2011**, *54*, 2529-2591. (b) St. Jean, D. J.; Fotsch, C. J. *Med. Chem.* **2012**, *55*, 6002-6020.
74. Wang, T.; Yin, Z.; Zhang, Z.; Bender, J. A.; Yang, Z.; Johnson, G.; Yang, Z.; Zadjura, L. M.; D'Arienzo, C. J.; DiGiugno Parker, D.; Gesenberg, C.; Yamanaka, G. A.; Gong, Y.-F.; Ho, H.-T.; Fang, H.; Zhou, N.; McAuliffe, B. V.; Eggers, B. J.; Fan, L.; Nowicka-Sans, B.; Dicker, I. B.; Gao, Q.; Colonno, R. J.; Lin, P.-F.; Meanwell, N. A.; Kadow, J. F. *J. Med. Chem.* **2009**, *52*, 7778-7787.
75. Babu, S.; Cheng, Z.; Reynolds, M. E.; Savage, S. J.; Tian, Q.; Yajima, H. WO 2009/055730, April 30, 2009.
76. Zhang, Y.-M.; Gu, M.; Ma, H.; Tang, J.; Lu, W.; Nan, F.-J. *Chin. J. Chem.* **2008**, *26*, 962-964.
77. (a) Ple, N.; Turck, A.; Couture, K.; Queguiner, G. *J. Org. Chem.* **1995**, *60*, 3781-3786. (b) Turck, A.; Plé, N.; Mongin, F.; Quéguiner, G. *Tetrahedron* **2001**, *57*, 4489-4505. (c) Eicher, T.; Hauptmann, S.; Speicher, A., *The Chemistry of Heterocycles*. 2nd ed.; WILEY-VCH Verlag: Weinheim, 2004.
78. (a) Mosrin, M.; Knochel, P. *Org. Lett.* **2008**, *10*, 2497-2500. (b) Piller, F. M.; Knochel, P. *Org. Lett.* **2008**, *11*, 445-448. (c) Mosrin, M.; Knochel, P. *Chem. Eur. J.* **2009**, *15*, 1468-1477. (d) Rohbogner, C. J.; Wunderlich, S. H.; Clososki, G. C.; Knochel, P. *Eur. J. Org. Chem.* **2009**, 1781-1795.
79. Thrash, T.; Cabell, L. A.; Lohse, D.; Budde, R. J. A. US 2006/0004002 A1, Jan 5, 2006.
80. Gacek, M.; Ongstad, L.; Undheim, K. *Acta Chem. Scand.* **1979**, *B33*, 150-151.
81. (a) Meth-Cohn, O.; Narine, B. *Synthesis* **1980**, 133-135. (b) Meth-Cohn, O.; Narine, B.; Tarnowski, B. *J. Chem. Soc., Perkin Trans. 1* **1981**, 1531-1536.

82. Huang, K.; Merced, F. G.; Ortiz-Marciales, M.; Meléndez, H. J.; Correa, W.; De Jesús, M. *J. Org. Chem.* **2008**, *73*, 4017-4026.
83. Beckmann, E. *Chem. Ber.* **1886**, *19*, 988-993.
84. Vilsmeier, A.; Haack, A. *Chem. Ber.* **1927**, *60*, 119-122.
85. (a) Childs, M. E.; Weber, W. P. *J. Org. Chem.* **1976**, *41*, 3486-3487. (b) Mander, L. N.; Sethi, S. P. *Tetrahedron Lett.* **1983**, *24*, 5425-5428.
86. George Rosenker, K. M.; Tandon, M.; Wang, Q. J.; Wipf, P. *Unpublished results*.
87. Ajitha, M.; Rajnarayana, K. *Int. J. Pharma Bio Sci.* **2011**, *2*, 81-90.
88. Shirasaka, T.; Kunitake, T.; Tsuneyoshi, I. *Brain Res.* **2009**, *1300*, 105-113.
89. Kato, Y.; Ebiike, H.; Achiwa, K.; Ashizawa, N.; Kurihara, T.; Kobayashi, F. *Chem. Pharm. Bull.* **1990**, *38*, 2060-2062.
90. (a) Ito, S.; Hirata, Y.; Nagatomi, Y.; Satoh, A.; Suzuki, G.; Kimura, T.; Satow, A.; Maehara, S.; Hikichi, H.; Hata, M.; Ohta, H.; Kawamoto, H. *Bioorg. Med. Chem. Lett.* **2009**, *19*, 5310-5313. (b) Favor, D. A.; Powers, J. J.; White, A. D.; Fitzgerald, L. W.; Groppi, V.; Serpa, K. A. *Bioorg. Med. Chem. Lett.* **2010**, *20*, 5666-5669.
91. Hardcastle, I. R.; Liu, J.; Valeur, E.; Watson, A.; Ahmed, S. U.; Blackburn, T. J.; Bennaceur, K.; Clegg, W.; Drummond, C.; Endicott, J. A.; Golding, B. T.; Griffin, R. J.; Gruber, J.; Haggerty, K.; Harrington, R. W.; Hutton, C.; Kemp, S.; Lu, X.; McDonnell, J. M.; Newell, D. R.; Noble, M. E. M.; Payne, S. L.; Revill, C. H.; Riedinger, C.; Xu, Q.; Lunec, J. *J. Med. Chem.* **2011**, *54*, 1233-1243.
92. Valencia, E.; Fajardo, V.; Freyer, A. J.; Shamma, M. *Tetrahedron Lett.* **1985**, *26*, 993-996.

93. Valencia, E.; Freyer, A. J.; Shamma, M.; Fajardo, V. *Tetrahedron Lett.* **1984**, 25, 599-602.
94. Yoo, K. D.; Park, E. S.; Lim, Y.; Kang, S. I.; Yoo, S. H.; Won, H. H.; Kim, Y. H.; Yoo, I. D.; Yoo, H. S.; Hong, J. T.; Yun, Y. P. *J. Pharmacol. Sci.* **2012**, 118, 171-177.
95. Sorbera, L. A.; Leeson, P. A.; Silvestre, J.; Castaner, J. *Drugs Future* **2001**, 26, 651-657.
96. (a) Yang, G.; Zhang, W. *Org. Lett.* **2012**, 14, 268-271. (b) Eastwood, P.; González, J.; Gómez, E.; Caturla, F.; Aguilar, N.; Mir, M.; Aiguadé, J.; Matassa, V.; Balagué, C.; Orellana, A.; Domínguez, M. *Bioorg. Med. Chem. Lett.* **2011**, 21, 6253-6257. (c) Luo, Y.; Xiao, F.; Qian, S.; He, Q.; Lu, W.; Yang, B. *Med. Chem. Commun.* **2011**, 2, 1054-1057. (d) Zou, H.; Zhang, L.; Ouyang, J.; Giulianotti, M. A.; Yu, Y. *Eur. J. Med. Chem.* **2011**, 46, 5970-5977. (e) Kilikli, A. A.; Dengiz, C.; Özcan, S.; Balci, M. *Synthesis* **2011**, 3697-3705. (f) Augner, D.; Gerbino, D. C.; Slavov, N.; Neudörfl, J. M.; Schmalz, H. G. *Org. Lett.* **2011**, 13, 5374-5377. (g) Zhu, C.; Falck, J. R. *Org. Lett.* **2011**, 13, 1214-1217. (h) Angelin, M.; Rahm, M.; Fischer, A.; Brinck, T.; Ramström, O. *J. Org. Chem.* **2010**, 75, 5882-5887.
97. Pierce, J. G.; Waller, D. L.; Wipf, P. *J. Organomet. Chem.* **2007**, 692, 4618-4629.
98. Miller, B.; Mao, S.; Rosenker, K. M. G.; Pierce, J. G.; Wipf, P. *Beilstein J. Org. Chem.* **2012**, 8, 1091-1097.
99. Wipf, P.; Nunes, R. L. *Tetrahedron* **2004**, 60, 1269-1279.
100. (a) Fürstner, A.; Langemann, K. *J. Am. Chem. Soc.* **1997**, 119, 9130-9136. (b) Ghosh, A. K.; Cappiello, J.; Shin, D. *Tetrahedron Lett.* **1998**, 39, 4651-4654.
101. (a) Zhan, Z. Y. WO Patent 2007003135, Jan 11, 2007. (b) Rix, D.; Caijo, F.; Laurent, I.; Boeda, F.; Clavier, H.; Nolan, S. P.; Mauduit, M. *J. Org. Chem.* **2008**, 73, 4225-4228.

102. (a) Joe, D.; Overman, L. E. *Tetrahedron Lett.* **1997**, *38*, 8635-8638. (b) Bourgeois, D.; Pancrazi, A.; Nolan, S. P.; Prunet, J. *J. Organomet. Chem.* **2002**, *643-644*, 247-252. (c) Schmidt, B. *Eur. J. Org. Chem.* **2004**, 1865-1880.
103. (a) Gimeno, N.; Formentín, P.; Steinke, J. H. G.; Vilar, R. *Eur. J. Org. Chem.* **2007**, 918-924. (b) Hong, S. H.; Sanders, D. P.; Lee, C. W.; Grubbs, R. H. *J. Am. Chem. Soc.* **2005**, *127*, 17160-17161. (c) Schmidt, B. *J. Mol. Catal. A: Chem.* **2006**, *254*, 53-57.
104. (a) Ulman, M.; Grubbs, R. H. *The Journal of Organic Chemistry* **1999**, *64*, 7202-7207. (b) Maynard, H. D.; Grubbs, R. H. *Tetrahedron Lett.* **1999**, *40*, 4137-4140. (c) Bourgeois, D.; Pancrazi, A.; Ricard, L.; Prunet, J. *Angew. Chem., Int. Ed.* **2000**, *39*, 725-728.
105. (a) Brem, B.; Seger, C.; Pacher, T.; Hofer, O.; Vajrodaya, S.; Greger, H. *J. Agric. Food Chem.* **2002**, *50*, 6383-6388. (b) Greger, H. *Planta Med.* **2006**, *72*, 99-113.
106. (a) Aloise Pilli, R.; de Oliveira, M. C. F. *Nat. Prod. Rep.* **2000**, *17*, 117-127. (b) Pilli, R. A.; Rosso, G. B.; de Oliveira, M. C. F. *Nat. Prod. Rep.* **2010**, *27*, 1908-1937. (c) Kongkiatpaiboon, S.; Schinnerl, J.; Felsing, S.; Keeratinijakal, V.; Vajrodaya, S.; Gritsanapan, W.; Brecker, L.; Greger, H. *J. Nat. Prod.* **2011**, *74*, 1931-1938.
107. Williams, D. R.; Brown, D. L.; Benbow, J. W. *J. Am. Chem. Soc.* **1989**, *111*, 1923-1925.
108. (a) Götz, M.; Strunz, G. M., *Alkaloids*. Butterworths: London, 1975; Vol. 9. (b) Pilli, R. A.; Rosso, G. B.; de Oliveira, M. C. F., The Stemona Alkaloids. In *The Alkaloids: Chemistry and Biology*, Cordell, G. A., Ed. Academic Press: 2005; Vol. 62, pp 77-173. (c) Alibés, R.; Figueredo, M. *Eur. J. Org. Chem.* **2009**, 2421-2435.
109. (a) Wipf, P.; Kim, Y. *Tetrahedron Lett.* **1992**, *33*, 5477-5480. (b) Wipf, P.; Kim, Y.; Goldstein, D. M. *J. Am. Chem. Soc.* **1995**, *117*, 11106-11112. (c) Goldstein, D. M.; Wipf, P. *Tetrahedron Lett.* **1996**, *37*, 739-742. (d) Wipf, P.; Li, W. *J. Org. Chem.* **1999**, *64*,

- 4576-4577. (e) Wipf, P.; Mareska, D. A. *Tetrahedron Lett.* **2000**, *41*, 4723-4727. (f) Wipf, P.; Spencer, S. R. *J. Am. Chem. Soc.* **2005**, *127*, 225-235. (g) Hoye, A. T.; Wipf, P. *Org. Lett.* **2011**, *13*, 2634-2637.
110. Wipf, P.; Rector, S. R.; Takahashi, H. *J. Am. Chem. Soc.* **2002**, *124*, 14848-14849.
111. Kakuta, D.; Hitotsuyanagi, Y.; Matsuura, N.; Fukaya, H.; Takeya, K. *Tetrahedron* **2003**, *59*, 7779-7786.
112. (a) Hitotsuyanagi, Y.; Hikita, M.; Oda, T.; Kakuta, D.; Fukaya, H.; Takeya, K. *Tetrahedron* **2007**, *63*, 1008-1013. (b) Hitotsuyanagi, Y.; Takeda, E.; Fukaya, H.; Takeya, K. *Tetrahedron Lett.* **2008**, *49*, 7376-7379.
113. Lin, W.; Xu, R.; Zhong, Q. *Huaxue Xuebao* **1991**, *49*, 927-931.
114. (a) Claisen, L. *Ber. Dtsch. Chem. Ges.* **1912**, *45*, 3157-3166. (b) Wipf, P., Claisen Rearrangements. In *Comprehensive Organic Synthesis*, Barry, M. T.; Ian, F., Eds. Pergamon: Oxford, 1991; pp 827-873.
115. (a) Wei, Z. Y.; Knaus, E. *Synlett* **1993**, 295-296. (b) Wei, Z. Y.; Knaus, E. *Tetrahedron* **1994**, *50*, 5569-5578. (c) Napoletano, M.; Della Bella, D.; Fraire, C.; Grancini, G.; Masotto, C.; Ricciardi, S.; Zambon, C. *Bioorg. Med. Chem. Lett.* **1995**, *5*, 589-592. (d) Gheorghe, A.; Schulte, M.; Reiser, O. *J. Org. Chem.* **2006**, *71*, 2173-2176. (e) Mo, F.; Li, F.; Qiu, D.; Wang, J. *Tetrahedron* **2010**, *66*, 1274.
116. (a) Ghosh, A. K.; Kulkarni, S. *Org. Lett.* **2008**, *10*, 3907-3909. (b) Ghosh, A. K.; Yuan, H. *Tetrahedron Lett.* **2009**, *50*, 1416-1418. (c) Vrielynck, S.; Vandewalle, M. *Tetrahedron Lett.* **1995**, *36*, 9023-9026.
117. Fukuyama, T.; Lin, S. C.; Li, L. *J. Am. Chem. Soc.* **1990**, *112*, 7050-7051.
118. Bassetti, M.; D'Annibale, A.; Fanfoni, A.; Minissi, F. *Org. Lett.* **2005**, *7*, 1805-1808.

119. (a) Tuo, S.-C.; Ye, J.-L.; Wang, A.-E.; Huang, S.-Y.; Huang, P.-Q. *Org. Lett.* **2011**, *13*, 5270-5273. (b) Liu, X.-K.; Ye, J.-L.; Ruan, Y.-P.; Li, Y.-X.; Huang, P.-Q. *J. Org. Chem.* **2013**, *78*, 35-41. (c) Tuo, S.; Liu, X.; Huang, P. *Chin. J. Chem.* **2013**, *31*, 55-62.
120. Huang, P.-Q. *Synlett* **2006**, 1133-1149.
121. Mannich, C.; Krösche, W. *Arch. Pharm.* **1912**, *250*, 647-667.
122. (a) Hanessian, S.; McNaughton-Smith, G. *Bioorg. Med. Chem. Lett.* **1996**, *6*, 1567-1572. (b) Rassu, G.; Carta, P.; Pinna, L.; Battistini, L.; Zanardi, F.; Acquotti, D.; Casiraghi, G. *Eur. J. Org. Chem.* **1999**, 1395-1400.
123. Corey, E. J.; Zheng, G. Z. *Tetrahedron Lett.* **1997**, *38*, 2045-2048.
124. Mitsunobu, O.; Yamada, M. *Bull. Chem. Soc. Jpn.* **1967**, *40*, 2380-2382.
125. (a) Mukaiyama, T.; Banno, K.; Narasaka, K. *J. Am. Chem. Soc.* **1974**, *96*, 7503-7509. (b) Mukaiyama, T.; Izawa, T.; Saigo, K. *Chem. Lett.* **1974**, *3*, 323-326.
126. (a) Carreira, E. M.; Singer, R. A.; Lee, W. *J. Am. Chem. Soc.* **1994**, *116*, 8837-8838. (b) Singer, R. A.; Carreira, E. M. *Tetrahedron Lett.* **1997**, *38*, 927-930. (c) Singer, R. A.; Brock, J. R.; Carreira, E. M. *Helv. Chim. Acta* **2003**, *86*, 1040-1044.
127. (a) Oisaki, K.; Suto, Y.; Kanai, M.; Shibasaki, M. *J. Am. Chem. Soc.* **2003**, *125*, 5644-5645. (b) Ding, K.; Wang, Y.; Yun, H.; Liu, J.; Wu, Y.; Terada, M.; Okubo, Y.; Mikami, K. *Chem. Eur. J.* **1999**, *5*, 1734-1737.
128. Fournier, L.; Kocienski, P.; Pons, J.-M. *Tetrahedron* **2004**, *60*, 1659-1663.
129. (a) Wakabayashi, T.; Saito, M. *Tetrahedron Lett.* **1977**, *18*, 93-96. (b) Sadovoy, A. V.; Kovrov, A. E.; Golubeva, G. A.; Sviridova, L. A. *Chem. Heterocycl. Comp.* **2011**, *46*, 1215-1223.

130. (a) Butters, M.; Davies, C. D.; Elliott, M. C.; Hill-Cousins, J.; Kariuki, B. M.; Ooi, L.-l.; Wood, J. L.; Wordingham, S. V. *Org. Biomol. Chem.* **2009**, *7*, 5001-5009. (b) Polniaszek, R. P.; Belmont, S. E. *J. Org. Chem.* **1991**, *56*, 4868-4874.
131. Baussanne, I.; Chiaroni, A.; Royer, J. *Tetrahedron: Asymmetry* **2001**, *12*, 1219-1224.
132. (a) Illuminati, G.; Mandolini, L. *Acc. Chem. Res.* **1981**, *14*, 95-102. (b) Galli, C.; Mandolini, L. *Eur. J. Org. Chem.* **2000**, 3117-3125.
133. Nubbemeyer, U., Synthesis of Medium-Sized Ring Lactams. In *Stereoselective Heterocyclic Synthesis III*, Metz, P., Ed. Springer Berlin Heidelberg: 2001; Vol. 216, pp 125-196.
134. Staudinger, H.; Meyer, J. *Helv. Chim. Acta* **1919**, *2*, 635-646.
135. (a) Barnes, C. L.; McGuffey, F. A.; van der Helm, D. *Acta Cryst.* **1985**, *C41*, 92-95. (b) Zelder, C.; Schürmann, M.; Preut, H.; Krause, N. *Acta Crystallographica Section E* **2001**, *57*, o216-o217.
136. Chen, S.; Xu, J. *Tetrahedron Lett.* **1991**, *32*, 6711-6714.
137. Carpino, L. A. *J. Am. Chem. Soc.* **1993**, *115*, 4397-4398.
138. Yao, T.; Larock, R. C. *J. Org. Chem.* **2005**, *70*, 1432-1437.
139. Cherry, K.; Duchêne, A.; Thibonnet, J.; Parrain, J.-L.; Anselmi, E.; Abarbri, M. *Synthesis* **2009**, 257-270.
140. Godoi, B.; Schumacher, R. F.; Zeni, G. *Chem. Rev.* **2011**, *111*, 2937-2980.
141. Barluenga, J.; Trincado, M.; Rubio, E.; González, J. M. *Angew. Chem.* **2003**, *115*, 2508-2511.
142. Sperger, C. A.; Fiksdahl, A. *J. Org. Chem.* **2010**, *75*, 4542-4553.

143. (a) Koseki, Y.; Kusano, S.; Ichi, D.; Yoshida, K.; Nagasaka, T. *Tetrahedron* **2000**, *56*, 8855-8865. (b) Gilmore, K.; Alabugin, I. V. *Chem. Rev.* **2011**, *111*, 6513-6556.
144. *The Merck Index: An Encyclopedia of Chemicals, Drugs, and Biologicals*. 14th ed.; Merck: Whitehouse Station, NJ, 2006; p 1638.
145. Takacs, J. M.; Weidner, J. J. *J. Org. Chem.* **1994**, *59*, 6480-6483.
146. Allin, S. M.; James, S. L.; Martin, W. P.; Smith, T. A. D.; Elsegood, M. R. J. *J. Chem. Soc., Perkin Trans. 1* **2001**, 3029-3036.